

SERI/TR-332-416  
VOLUME 2 OF TWO VOLUMES  
UC CATEGORY: UC-61

REVIEW OF THERMALLY REGENERATIVE  
ELECTROCHEMICAL SYSTEMS

VOLUME 2

HELENA L. CHUM  
SOLAR ENERGY RESEARCH INSTITUTE

ROBERT A. OSTERYOUNG  
STATE UNIVERSITY OF NEW YORK AT BUFFALO  
BUFFALO, NEW YORK

APRIL 1981

PREPARED UNDER TASK NO. 3356.50

**Solar Energy Research Institute**

A Division of Midwest Research Institute

1617 Cole Boulevard  
Golden, Colorado 80401

Prepared for the  
U.S. Department of Energy  
Contract No. EG-77-C-01-4042

## PREFACE

This review was prepared by R. A. Osteryoung, formerly with Colorado State University and now with the State University of New York at Buffalo, and by H. L. Chum, formerly with Colorado State University and presently on the SERI staff. Work was performed largely under Contract No. AM-9-8078-1 and SERI Task 3356.10. Compiled in two volumes, the review covers the technical background of thermally regenerative electrochemical systems and presents recommendations for further work. For the reader interested in a general overview, Volume 1, Synopsis and Executive Summary, is a condensed version of Volume 2. Volume 2, which discusses the thermally regenerative electrochemical systems in more detail, is intended for researchers in chemical and electrochemical areas and for engineers (although detailed coverage of the fields of engineering, corrosion, and materials problems is outside the scope of this report).

The authors wish to acknowledge T. A. Milne for the suggestion of the subject of this report and for helpful discussions. During the course of this review, discussion took place with a number of people involved in research and development of fuel cells and/or regenerative electrochemical systems. Among these were J. Appleby, B. Baker, M. Breiter, E. Cairns, T. Cole, G. Elliot, E. Findl, A. Fischer, F. Gibbard, L. Heredy, J. Huff, T. Hunt, C. Johnson, R. Kerr, M. Klein, K. Kordesch, F. Ludwig, J. McBreen, L. Nanis, W. O'Grady, J. Plambeck, H. Shimotake, H. Silverman, R. Snow, S. Srinivasan, C. Tobias, R. Weaver, N. Weber, and E. Yeager. These discussions were very helpful. Special thanks are due to J. H. Christie for profitable discussions and careful editing of the manuscript. The technical support of the Colorado State University Library and the Solar Energy Information Center is gratefully appreciated.



---

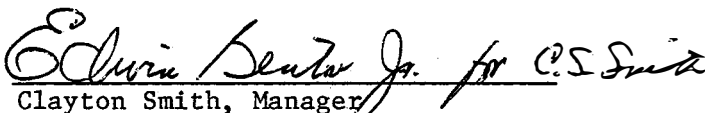
Helena L. Chum  
Senior Electrochemist

Approved for  
SOLAR ENERGY RESEARCH INSTITUTE



---

Thomas A. Milne, Chief  
Biomass Thermal Conversion & Exploratory  
Research Branch



---

Clayton Smith, Manager  
Chemical and Biological Division

## SYNOPSIS

## OBJECTIVE

Thermally regenerative electrochemical systems (TRES) are closed systems that convert heat into electricity in an electrochemical heat engine that is Carnot cycle limited in efficiency.

In this report, past and present work on TRES is reviewed and classified. Two broad classes of TRES can be identified according to the type of energy input required to regenerate the electrochemical cell reactants: thermal input alone (Section I and II) or the coupling of thermal and electrolytic energy inputs (Sections III-V). To facilitate the discussion, these two broad categories are further divided into seven types of TRES (Types 1-3 for thermal regeneration; Types 4-7 for coupled thermal and electrolytic regeneration). The subdivision was made according to significant differences in either the electrochemical cells or in the regenerators.

## DISCUSSION

In Type 1 TRES, compound CA is formed from C and A in an electrochemical cell at temperature  $T_1$  with concomitant production of electrical work in the external load. Compound CA is sent to a regenerator unit at  $T_2$  through a heat exchanger. In the regenerator, compound CA is decomposed into C and A, which are separated and redirected to the electrochemical cell via a heat exchanger, thus closing the cycle. The thermodynamic requirements for the electrochemical reaction are  $\Delta G < 0$ ,  $\Delta S < 0$ , and  $\Delta C_p$  as close to zero as possible. This type of TRES is equivalent to a primary battery, in which electrodes A and C are consumed. By coupling the battery with a regenerator unit, the electrode materials are regenerated. The classes of compounds that were investigated or proposed for this type are metal hydrides, halides, oxides, and chalcogenides. One of the most thoroughly investigated systems is the lithium hydride system ( $T_1 \sim 500^\circ\text{C}$ ,  $T_2 \sim 900^\circ\text{C}$ ). The advantage of this system is that lithium hydride decomposes into liquid lithium and gaseous hydrogen, enabling relatively simple separation. The power delivered by this system was low. Problems were encountered in the gas electrode, in the rate of decomposition of lithium hydride, and in materials. The best conditions for the electrochemical cell and for the regenerator were never realized in a practical system. A considerable fraction of the compounds investigated or proposed had  $T_2 \sim 800^\circ\text{C}$ - $900^\circ\text{C}$ . Nuclear reactors were the heat source envisioned for that temperature range. Some materials decomposing at lower temperatures were tried. An example is antimony pentachloride, which decomposes at  $\sim 300^\circ\text{C}$  into liquid antimony trichloride and gaseous chlorine; however, the performance of the electrochemical cell was very poor. All of the above systems had one electrochemical reaction product and the regeneration was accomplished in a one-step process. An interesting example of a system in which two electrochemical reaction products are regenerated in one step has long been known. It involves the oxidation of tin and the reduction of chromium (III) species at a graphite electrode in the electrochemical cell generating power. The regeneration is accomplished by lowering the temperature when the spontaneous reverse reaction takes place. This is a periodic power source.

Type 2 is similar to Type 1, but the products C and E of the electrochemical cell reaction  $A + D \rightarrow C + E$  are regenerated in a two-step process ( $C \rightarrow A + B$ ;  $E + B \rightarrow D$ ). It involves more complex plumbing and two regenerator units. The systems attempted include metal halides or oxides; for example, A = tin (II) or tellurium (II) chloride and D = antimony (V) or copper (II) chloride with B = gaseous chlorine. If at the regeneration temperatures A is also in the gaseous state, the separation of A and B is the major obstacle to successful operation of this type of system. To date, no complete electrochemical cell coupled with the regenerator has been demonstrated to be feasible.

Type 3 is also similar to Type 1 and involves a one-step regeneration. Liquid metal electrodes are composed of one electroactive metal C and one electroinactive metal B. C and B form alloys C(B) or bimetallic compounds  $C_xB_y$ . The anode and the cathode have, respectively, high and low concentrations of the electroactive metal in the liquid electrode. The cells are concentration cells. The regeneration is accomplished by sending the electrode materials (combined or individually) to a distillation unit where the C+B mixture is separated into C-rich and C-poor components, which are returned to the anode and cathode compartments, respectively. Examples include C = sodium or potassium and B = mercury or lead. These are the systems for which the feasibility of the thermal regeneration coupled to the battery was demonstrated. The performance of the demonstrated systems was poor, due in part to constraints imposed by the space applications envisioned. The performance of this type of system can be improved.

In Type 4 systems, compound CA, formed in the electrochemical cell at temperature  $T_1$ , is sent to a regenerator, which is an electrolysis cell at temperature  $T_2$ . In the regenerator, reactions opposite to those occurring at  $T_1$  regenerate C and A by using two energy inputs--electric and thermal. The electrolysis cell uses a fraction of the voltage produced by the battery at  $T_1$  (the additional energy is supplied as heat) and the remaining voltage is used to perform work in the external load. These systems are analogous to, and have the same requirements as, secondary (rechargeable) batteries. A few systems have been investigated; for example, CA = sodium chloride, lead iodide, cadmium iodide, lithium iodide. If C and A are in the gaseous state (for instance, hydrogen and oxygen), the electrochemical cell is a fuel cell; the regeneration is performed by water electrolysis at high temperature. To date, no complete demonstration of the feasibility of these systems has been performed. In addition to the above-mentioned examples of high temperature electrolysis, very few systems operating at lower temperature were explored in this mode of regeneration.

Type 5 systems are a particular case of Type 4, in which the electrolysis is performed at low pressure. They include systems in which one of the electroactive species is in the gaseous state. The battery and the electrolysis cell operate at the same temperature, and the pressure of the electroactive species is varied in these two cells by physical means, e.g., by the coupling of the cells with cold fingers. The operation is periodic. Examples include gaseous iodine as the working electroactive fluid in lithium/molten iodide/iodine cells. Low voltages are expected from these devices as well as mass transfer problems. However, these systems have energy storage capability.

In Type 6 systems, or thermogalvanic or nonisothermal cells, the two electrodes are at different temperatures and the cell temperature is not uniform. The electrodes can be metallic, liquid, or gaseous (with inert electrodes). The electrolyte can be solid or liquid, homogeneous or heterogeneous. During the passage of current through the thermogalvanic cell, matter is transferred from one electrode to the other as a result of the electrochemical reactions at the electrode/electrolyte interface and ionic transport in the electrolyte. In some types of cells the transfer of matter is permanent, and therefore a mechanical means to reverse the temperature of the electrodes must be provided for continuous operation of the engine as a power source. In these cells the thermal and electrolytic paths are not separated. Examples include copper electrodes immersed in a variety of copper salt solutions and gaseous chlorine in solid electrolyte or molten salt media. Most data for these cells refer to scientific information (e.g., irreversible thermodynamics) and not to power generation. The systems generate low power outputs but can be made much more cheaply than their solid-state analogs.

Type 7 engines are based on pressure differences of the working electroactive fluid across an isothermal electrolyte (solid or liquid). The pressure difference is maintained by using the changes in the vapor pressure with the temperature of the working electroactive fluid. The work performed is equivalent to the isothermal expansion of the working electroactive fluid from the high to the low pressure zone at  $T_2$  through the electrolyte and its interfaces. After expansion, the working fluid is condensed in a cold reservoir and can be recycled to the high temperature, high pressure zone of the cell by means of a pump. The cells are concentration cells. Because the working fluid does not undergo chemical changes, no regeneration and separation steps are necessary. Examples include iodine vapor expanded through isothermal liquid lead iodide and sodium vapor expanded through isothermal solid beta-alumina electrolyte. In the first example, the major difficulty is maintenance of the liquid electrolyte integrity when it is subjected to a pressure gradient. In the second example ( $T_1 \sim 200^\circ\text{--}300^\circ\text{C}$ ,  $T_2 \sim 800^\circ\text{--}900^\circ\text{C}$ ), this problem is avoided by using a solid superionic conductor electrolyte. The highest power outputs in TRES to date have been obtained with this type of engine. The present non-availability of other superionic conductors limits the extension of this concept to other practical energy converters.

## CONCLUSIONS AND RECOMMENDATIONS

TRES cover temperature ranges from near room temperature to about  $1200^\circ\text{C}$ . To date, power outputs of  $0.1 \text{ mW/cm}^2$  to about  $1 \text{ W/cm}^2$  have been achieved. The majority of the systems reported utilized molten salt electrolytes and high regeneration temperatures. In addition, several promising energy converters employed solid electrolytes, which are superionic conductors. Much less explored are lower-temperature media--aqueous, nonaqueous, or molten salt. Little effort was expended on the use of catalysts to improve the rates of thermal decomposition. General problems included engineering and materials problems. A considerable fraction of the research and development of these engines was performed around 15 to 20 years ago in connection with the production of secondary space power sources to utilize heat from nuclear reactors.

In this report we recommend areas of research in either science or engineering that would have long-range benefit to a TRES program. These areas include molten salt chemistry and electrochemistry, solid-state chemistry, materials sciences, aqueous systems and electrochemistry under extreme conditions, electrochemical engineering, and systems analysis. It should be pointed out that because solar-derived heat covers a very wide range of temperatures ( $\sim 80^{\circ}$ - $1000^{\circ}\text{C}$ ), more TRES can be brought into consideration.

TABLE OF CONTENTS

	<u>Page</u>
Introduction.....	1
Objective.....	1
Background.....	1
Types of Thermally Regenerative Electrochemical Systems.....	2
I Thermal Regeneration: Metal Hydrides, Halides, Oxides, and Chalcogenides.....	15
I.1 Single or Multiple Electrochemical Reaction Products and Single-Step Regeneration.....	26
I.1.1 Metal Hydride Systems: Lithium Hydride.....	26
I.1.2 Halide-Containing Systems.....	47
I.1.3 Oxide-Containing Systems and Other Systems....	53
I.1.4 Summary and Discussion of TRES Type 1.....	56
I.2 Multiple Electrochemical Reaction Products and Multiple- Step Regeneration.....	57
I.2.1 Metal Halides.....	58
I.2.2 Metal Oxides.....	66
I.2.3 Discussion of TRES Type 2.....	66
II Thermal Regeneration: Alloys or Bimetallic Systems.....	69
II.1 Amalgam and Thallium Cells.....	76
II.1.1 The Potassium-Mercury System.....	76
II.1.2 The Sodium-Mercury System.....	85
II.1.3 The Potassium-Thallium and Analogous Systems..	97
II.2 Bimetallic Cells.....	100
II.2.1 Sodium-Containing Systems.....	100
II.2.2 Lithium-Containing Systems.....	109
II.3 Summary of the Performance and Discussion of Thermally Regenerative Alloys or Bimetallic Systems.....	112
III Thermogalvanic or Nonisothermal Cells.....	115
III.1 Molten Salt Thermogalvanic Cells.....	121
III.1.1 Solid or Liquid Electrodes.....	121
III.1.2 Gaseous Electrodes.....	127
III.1.3 The Bismuth-Bismuth Iodide System.....	130
III.2 Thermogalvanic Cells with Solid Electrolytes.....	132
III.3 Thermogalvanic Cells in Aqueous and Nonaqueous Solvents	140
III.4 Discussion of TRES Type 6.....	148

TABLE OF CONTENTS (concluded)

	<u>Page</u>
IV Coupled Thermal and Electrolytic Regeneration Based on Pressure Differences of the Working Electroactive Fluid.....	149
IV.1 Single Cells.....	149
IV.1.1 Continuous Gas Concentration Cells.....	150
IV.1.2 The Sodium Heat Engine.....	154
IV.2 Multiple Cells.....	161
IV.3 Summary and Discussion of TRES Types 5 and 7.....	167
V Coupled Thermal and Electrolytic Regeneration: General.....	169
V.1 High Temperature Electrolysis.....	173
V.1.1 Molten Salt Media.....	173
V.1.2 Aqueous Media.....	177
V.1.3 Hydrogen-Oxygen Fuel Cell Coupled with High Temperature Water Electrolysis and Related Systems.....	180
V.2 Fluorides of Uranium(VI) or Cerium(IV) and Arsenium(III): Spontaneous Charge Reaction.....	182
V.3 Thermocell Regenerators.....	184
V.4 Discussion of TRES Type 4.....	187
VI Conclusions and Recommendations.....	189
VII References.....	193



## LIST OF FIGURES

	<u>Page</u>
S-1 Thermal Regeneration: Type 1.....	5
S-2 Thermal Regeneration: Type 2.....	6
S-3 Thermal Regeneration: Type 3.....	7
S-4 Coupled Thermal and Electrolytic Regeneration: Type 4.....	8
S-5 Coupled Thermal and Electrolytic Regeneration: Type 5.....	9
S-6 Coupled Thermal and Electrolytic Regeneration: Type 6.....	10
S-7 Coupled Thermal and Electrolytic Regeneration: Type 7.....	11
I-1 General Scheme for a Thermally Regenerative Electrochemical System.....	16
I-2 Theoretical Standard Cell Potentials As a Function of Temperature for Various Metal Hydrides.....	30
I-3 Lithium Hydride Regenerative Cell.....	32
I-4 Lithium Hydride Regenerative Fuel Cell with a Cold-Salt Seal Flange.....	33
I-5 Batch Lithium-Hydrogen Cell.....	36
I-6 Permeation Isobars of Hydrogen on Vanadium and Armco Iron Foils 0.0254 cm Thick at 1 atm.....	40
I-7 Calculated Equilibrium Hydrogen Pressure for LiH-LiCl Mixtures....	43
I-8 Voltage-Current Curve for a Lithium Hydride Cell with a 0.025-cm Vanadium Diaphragm at 525°C.....	45
I-9 Voltage-Current Curve for a Lithium Hydride Cell with a 0.005-cm Vanadium Diaphragm at 425°C.....	45
I-10 Scheme of Thermally Regenerative Electrochemical System Proposed by McCully et al.....	60
I-11 Tafel Plots for the Electrochemical Oxidation of Te(II) (16 Mole % in AlCl <sub>3</sub> ) at 200°C.....	62

LIST OF FIGURES (continued)

	<u>Page</u>
I-12 Tafel Plots for the Electrochemical Reduction of Cu(II) (4 Mole % in 3:1 Molar Ratio AlCl <sub>3</sub> :KCl) at 200°C.....	62
I-13 Potentials of the TeCl <sub>2</sub> (Anode)/CuCl <sub>2</sub> (Cathode) Galvanic Cells in Molten AlCl <sub>3</sub> .....	64
I-14 Discharge Curves for TeCl <sub>2</sub> (Anode)/CuCl <sub>2</sub> (Cathode) Cells under 50- and 100-Ohm Loads.....	64
II-1 Schematic Representation of a Thermally Regenerative Alloy System (a) for Amalgam Cells C = Na, K; B = Hg; and (b) for Bimetallic Cells.....	70
II-2 (a) Constant-Pressure Phase Diagram for a Generic Bimetallic System C/B; (b) Three-Dimensional Phase Diagram for a Two-Component System; and (c) Phase Diagram Showing Equilibrium between Vapor and Solid in the V-CB Region Resulting from Overlap of V-L and L-CB Regions.....	72
II-3 Ternary Phase Diagram of KOH-KBr-KI and Properties of the Ternary Eutectic.....	78
II-4 EMF of K/K <sup>+</sup> glass/K(Hg) Cells at 136°C.....	79
II-5 Voltage-Time Plot of Cycling Differential Density Potassium-Mercury Cells.....	81
II-6 Potassium-Mercury Liquid Metal Cell (LMC).....	81
II-7 Phase Diagram of Hg-K at 1 atm.....	83
II-8 Open-Circuit Potentials of Sodium-Sodium-Mercury Galvanic Cells at 500°C.....	88
II-9 Cross Section of Static Electrode TRAC Cell.....	88
II-10 Discharge Characteristics of a Static TRAC Cell.....	89
II-11 Cross Section of the Flowing Electrode TRAC Cell.....	91
II-12 Vapor/Liquid Equilibrium Compositions of the Na/Hg System at 5.8 atm.....	93
II-13 TRAC Test Loop Flow Diagram.....	95
II-14 Solid/Liquid Equilibrium Compositions of the Potassium-Thallium System.....	99

LIST OF FIGURES (continued)

	<u>Page</u>
II-15 Thermally Regenerative Sodium-Tin System.....	103
II-16 Thermally Regenerative Sodium-Lead System Operated for 100 Hours.....	105
II-17 Voltage-Current Density Plot for the Sodium-Lead Galvanic Cell Operating under Thermal Regeneration.....	107
II-18 Improved Thermal Regenerator for the Sodium-Lead System Operated Continuously for 1000 Hours.....	107
II-19 EMF-Temperature-Composition Characteristics of the Cell $\text{Li}(\ell)   \text{LiCl-LiF}(\ell)   \text{Li}_x\text{Sn}$ .....	111
II-20 Pressure-Composition Diagram for the Li-Sn System at 1200°C.....	111
II-21 Voltage vs. Current Density of the Lithium-Containing Bimetallic Cells with the LiCl-KCl Electrolyte.....	113
III-1 Weininger's $\text{I}_2   \alpha\text{-AgI}   \text{I}_2$ Thermocell.....	139
III-2 Diagram of the Sulfuric Acid Concentration Thermocell and Current-Voltage Curves for the Cell.....	146
IV-1 Laboratory Continuous Gas Concentration Cell.....	151
IV-2 Advanced Continuous Gas Concentration Cell.....	153
IV-3 Schematic Diagram of the Sodium Heat Engine.....	155
IV-4 Calculated Power-Efficiency Performance of the Sodium Heat Engine for Various Values of $T_2$ .....	159
IV-5 Experimental and Calculated (Eq. IV-5) Voltage-Current Curves for the Sodium Heat Engine as a Function of $T_2$ .....	159
IV-6 Schematic Diagram of the Sodium Heat Engine Cells with $\beta''$ -Alumina Tubes.....	160
IV-7 Low-Pressure Electrolysis Apparatus.....	163
IV-8 Laboratory Cell $\text{Li}/\text{I}_2$ .....	165
IV-9 Multiple-Cell Electrochemical Heat Engine.....	165
V-1 Generic Scheme for Electrothermal Regeneration.....	172

LIST OF FIGURES (continued)

	<u>Page</u>
V-2 OCV of Cells Composed of $AsF_3$ and $UF_6$ or $CeF_4$ Separated by the Solid Electrolyte $PbF_4$ .....	185
V-3 Regenerative, Molten Salt, Thermoelectric Fuel Cell Schematic Diagram.....	185
V-4 Laboratory Cell Scheme for a Thermocell Regenerator Coupled with the Galvanic Cell.....	186

## LIST OF TABLES

	<u>Page</u>
S-1	Examples of the Thermally Regenerative Electrochemical Systems..... 12
I-1	Thermodynamically Suitable Compounds for Thermal Dissociation in Thermally Regenerative Fuel Cells..... 20
I-2	Compounds Selected as Possible Candidates for Thermal Regeneration..... 25
I-3	Summary of Galvanic Cell Performance..... 48
I-4	Cell Voltages Obtained in the Reactions of Metal Halides.... 59
I-5	Summary of Experimental Regenerator Operation..... 65
I-6	Thermally Reversible Oxides..... 67
I-7	Characteristics of Oxide Cells..... 67
II-1	Operation of the Na/Pb Thermally Regenerative System..... 104
III-1	Summary of Thermoelectric Powers in Ag Molten Salt Ag Thermocells..... 123
III-2	Summary of Initial Thermoelectric Powers in Metal Molten Salt Metal Thermocells..... 125
III-3	Summary of Transported Entropies ( $\bar{S}_M^{n+}$ ), Partial Molal Entropies ( $\bar{S}_M^{n+}$ ), and Entropies of Transfer ( $S_M^{*n+}$ ) for Molten Salt Thermocells..... 126
III-4	Summary of Thermoelectric Powers in Thermocells $X_2$  Molten Salt (l)  $X_2$ ..... 128
III-5	Summary of Thermoelectric Powers of Solid-Electrolyte Thermocells..... 133
III-6	Summary of Thermoelectric Powers of Some Ionic Salts..... 135
III-7	Summary of Transported Entropies ( $\bar{S}_M^{n+}$ ) for Solid Electrolytes of Ordered Structure and Summary of Overall Transported Entropies for Solids of the $\alpha$ -AgI Type and AgI-Ag Oxysalts (75-80 Mole % AgI)..... 136
III-8	Performance of the Iodine Cell..... 140

## LIST OF TABLES (continued)

		<u>Page</u>
III-9	Thermoelectric Powers of the Cu Electrolyte Cu Cells in Aqueous and Nonaqueous Solvents.....	142
III-10	Thermoelectric Powers for Some Selected Thermogalvanic Cells in Aqueous Media.....	144
IV-1	Voltage Characteristics of the $I_2(T_2) PbI_2(\ell) I_2(T_1)$ Cell with Ni Electrodes.....	152
IV-2	Characteristics of Continuous Gas Concentration Cells with Several Working Fluid/Electrolyte Systems.....	154
V-1	Cell Potentials and Resistances as a Function of Temperature for the $Fe(CN)_6^{4-} Fe(CN)_6^{3-}$ and $Cu(NH_2)_4^{2+} Cu(NH_3)_2^+$ Systems...	179
V-2	Ideal Efficiency for $H_2-O_2$ Thermochemical Power Cycle.....	181
V-3	Ideal Efficiency for $H_2-O_2-HCl_{(aq)}$ Thermochemical Power Cycle.....	183

## INTRODUCTION

### OBJECTIVE

This review of thermally regenerative electrochemical systems (TRES) was written upon request of T. A. Milne of the Chemical and Biological Division of the Solar Energy Research Institute. The bulk of the information contained in this report was collected from February to October 1979. The information comes from literature searches and from visits to the laboratories of, and discussions with, technical personnel involved with this type of research. Work on TRES has been classified and analyzed, with emphasis on the operation of the electrochemical systems. It is important to emphasize, however, that TRES involve the merging of several disciplines in addition to electrochemistry: thermal conversion, engineering, materials science, etc. The purpose of this review is to aid evaluations of the electrochemical technique of direct thermal-to-electrical conversion.

The majority of the systems published in the open literature or patented are reviewed. Because this area was developed from the late fifties to the late sixties with the utilization of heat from nuclear reactors as a major mission, most of the systems operated at high temperatures. Our review covers these systems and a variety of others developed or proposed, which operate under a wide variety of conditions. A cross-comparison, or ranking, of systems for different missions, at different stages of development, and at different operating conditions is not feasible for this review.

The systems investigated in the past are reviewed in detail in Vol. 2 and more briefly in the Executive Summary. It is our purpose to suggest areas of research (in either science or engineering) that would benefit from a long-range TRES program, rather than to propose specific systems for further device exploration. In the past, most of the funding and expectations were device oriented in short-term programs. The systems for which there existed a better understanding of the chemical, electrochemical, engineering, and materials problems were pursued in relatively long-term and research-oriented projects.

The Executive Summary has the same structure as Vol. 2, so that references and further technical background can be located easily.

### BACKGROUND

Regenerative electrochemical systems were one of a variety of complex methods of energy conversion investigated during the period from 1958 to 1968. In these systems the working substance produced in an electrochemical cell (fuel cell, battery, galvanic system, emf cell) is regenerated by the appropriate input of energy (thermal, light, atomic, electrical, or chemical), thereby defining the thermal, photo-, nuclear, electrolytic, or redox regenerative electrochemical systems [1]. The major heat source envisioned during this period was nuclear reactor heat. Direct use of sunlight for photoregeneration also was attempted, as well as use of nuclear radiation. The electrolytically regenerative systems are essentially indistinguishable from secondary batteries and were explored chiefly for their possible utilization in load leveling,

for their storage capability, and for space-flight application. The redox systems appeared particularly attractive because of their energy storage capability [2].

Austin [3] critically reviewed the government-sponsored fuel cell research from 1950 to 1964, including regenerative types, for possible space power application or for silent and portable electric generators. Kerr [4] reviewed work up to 1967, comparing the different types of regeneration for space power application. Nuclear, photo-, and redox systems were eliminated from consideration due to weight, complexity, and low efficiency. The proceedings of a symposium on regenerative emf cells [5], published in 1967, includes discussion of most types of regenerative systems.

Because of the low overall efficiencies [3,4,5] of the regenerative systems due to Carnot cycle limitations (thermal), problems of pumping, plumbing and separation (thermal and nuclear), and low quantum yields (photo-), research after 1968 was concerned primarily with electrolytic regenerative [6] and redox [2] systems. However, because thermal energy can be obtained by harnessing the sun's rays, it is possible to envision TRES operating under conditions that differ markedly from those offered by nuclear reactors. It is therefore conceivable, as pointed out by Kerr [4], that the problems of TRES for some applications are surmountable. In this report, we classify thermally regenerative electrochemical systems as systems regenerated by the input of thermal or coupled thermal and electrolytic energy. Because the seven types of TRES have unique features, a general introduction is not given at this point.

#### TYPES OF THERMALLY REGENERATIVE ELECTROCHEMICAL SYSTEMS

Thermally regenerative electrochemical systems are closed systems that convert heat into electricity in an electrochemical heat engine that is Carnot-cycle limited in efficiency. In this report the TRES have been classified into two broad classes: systems regenerated thermally and systems regenerated by a coupling of thermal and electrolytic inputs. To facilitate discussion, the types of TRES within these two broad classes have been designated according to significant differences in either the electrochemical cells or regenerators.

Sections I and II concern thermal regeneration, and the following three types of TRES are defined:

##### Type 1.

Figure S-1 illustrates this type of system. The electrochemical reaction product CA is formed from C and A in an electrochemical cell at  $T_1$ , with concomitant production of electrical work in the external load. For such a production of electricity to be continuous, compound CA must be easily decomposed into C and A. Thus, compound CA is sent to a regenerator at  $T_2$  via a heat exchanger. In the regenerator, the thermal decomposition reaction takes place spontaneously. Compounds C and A formed in the regenerator at  $T_2$  are separated by physical (or chemical) means, and the isolated compounds C and A are returned to the electrochemical cell after being returned to temperature  $T_1$  through the heat exchanger, thus completing the



cycle. The most favorable thermodynamic properties of the electrochemical reaction for a thermally regenerative electrochemical system are:  $\Delta G < 0$ ,  $\Delta S < 0$ , and  $\Delta C_p$  as close to zero as possible.

#### Type 2.

Figure S-2 illustrates this type of system. In this case, a more complex set of galvanic cell reactions occurs at  $T_1$ . Two or more products are formed in the electrochemical reaction; therefore, the regeneration of the anode and cathode materials (A and D) must be performed separately at  $T_2$  and  $T_3$ , as indicated in Fig. S-2. It is a more complex scheme, requiring more plumbing, heat exchangers, and regenerator chambers than the simple system of Type 1.

#### Type 3.

Figure S-3 illustrates this type of system. In principle, this scheme is identical to that of Type 1. However, it applies to specific cases in which the electrochemical cell reaction involves only one electroactive couple  $C^+/C$  in a concentration cell at  $T_1$ .  $C(B)$  represents, for instance, an alloy or a bimetallic compound.

Sections III, IV, and V concern coupled thermal and electrolytic regeneration, and the following four types of TRES are defined:

#### Type 4.

As illustrated in Fig. S-4, compound CA formed in the galvanic cell at  $T_1$  is sent to a regenerator at  $T_2$  via a heat exchanger, where it is electrolytically decomposed into C and A. The requirements for this type of regeneration are that the cell reactions  $C \rightleftharpoons C^+ + e^-$  and  $A + e^- \rightleftharpoons A^-$  are reversible and of high coulombic efficiency and high exchange current. In addition, the voltage  $V(T_1)$  must be larger than  $V(T_2)$ . The cells are connected in electrical opposition and the electrolysis takes place consuming  $V(T_2)$ . The remaining voltage can be used to perform useful work in the external load. The separation is inherent in this type of regeneration. Compounds C and A are returned to the galvanic cell via heat exchangers, and the loop is closed. If at a temperature  $T_x$  the reverse reactions of reactions in the galvanic cell take place spontaneously, then the regeneration produces an additive voltage  $V(T_x)$  while regenerating C and A at  $T_x$ .

#### Type 5.

This type is illustrated in Fig. S-5. Two galvanic cells at the same temperature are arranged so that the activity of one of the electroactive species can be varied by some physical means. In the example shown, a cold finger reduces the pressure of the gaseous working electroactive fluid A. The galvanic cells are connected back to back. The galvanic cells are concentration cells in the  $A/A^-$  species. As cell 1 discharges, cell 2 charges and work is performed in the external load proportional to the differences in activities of A in the two cells. The operation is interrupted as A-rich material is consumed. The switch reaction corresponds to heating the cold finger associated with cell 2 and cooling that associated with cell 1. The roles of the two cells are now reversed

and the system can again perform electrical work in the external load. This scheme is equivalent to an electrolysis performed at reduced pressure. Mass transfer could be the major limitation to this type of TRES.

#### Type 6.

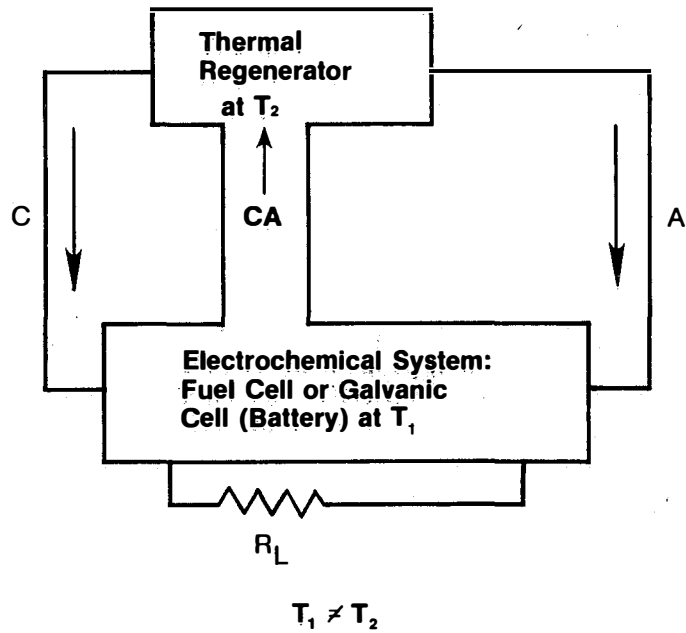
This type of TRES is illustrated in Fig. S-6. The thermal and electrolytic paths are not separated. Two or more electrodes are at different temperatures. These electrodes (not necessarily chemically identical or reversible) are in contact with the electrolyte (liquid or solid, not necessarily homogeneous in composition, and with or without permeable membranes interposed in the electrolyte), in which a temperature gradient exists. These TRES are called thermogalvanic or nonisothermal cells. During the passage of current in the cells, matter is transferred from one electrode to the other as a result of the electrochemical reactions at the electrolyte/electrode interfaces and ionic conduction.

If the transfer of matter is permanent, as occurs with electroactive metal electrodes, the electrodes must have their temperatures reversed periodically for continuous operation of the engine as a power source. This temperature reversal operation can be avoided if gas electrodes, or redox soluble couples, are used. These thermogalvanic cells are the electrochemical analogs of thermoelectric devices. The efficiency in these devices is related to the Carnot efficiency. The upper limit is determined by the use of expressions developed for solid-state, thermoelectric devices. These equations take into account the Carnot efficiency, the thermal and electrical conductivities, and the thermoelectric power ( $dE/dT$ ) of the system, but they do not take into account electrode polarization effects characteristic of the electrochemical reactions.

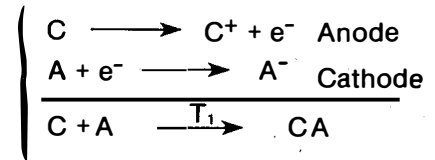
#### Type 7.

In this type, illustrated in Fig. S-7, the thermal and electrolytic paths are separated. An isothermal electrolyte (solid or liquid) separates the working electroactive fluid from two pressure regions. The work performed in these engines is equivalent to the isothermal expansion of the fluid from the high pressure, high temperature zone ( $P_H, T_H$ ) to a low pressure zone ( $P_L, T_H$ ) separated by the electrolyte and created by cooling one end of the engine. The element C undergoes oxidation, the electrons traverse the external circuit, and ions  $C^+$  cross the electrolyte as a result of the pressure differential across the electrolyte. The  $C^+$  ions are reduced at the electrode attached to the bottom of the electrolyte, at a lower pressure. At the cold trap, C is condensed. To produce electricity continuously with these engines,  $C(P_L, T_L)$  must be pumped to  $C(P_H, T_H)$ . These engines do not need a chemical separation step.

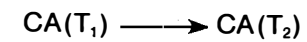
Table S-1 presents a summary of typical examples of all seven types of TRES. Inspection of the table shows that these systems can cover various ranges of temperatures from near room temperature to 1000°C. In the systems studied to date, powers of 0.1 mW/cm<sup>2</sup> to 1 W/cm<sup>2</sup> have been achieved. Emphasis in past work was placed on systems regenerated at high temperatures.



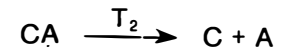
**Electrochemical Cell Reactions**



**Heat Exchange**



**Thermal Regenerator**



**Heat Exchange**

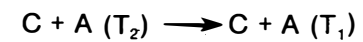
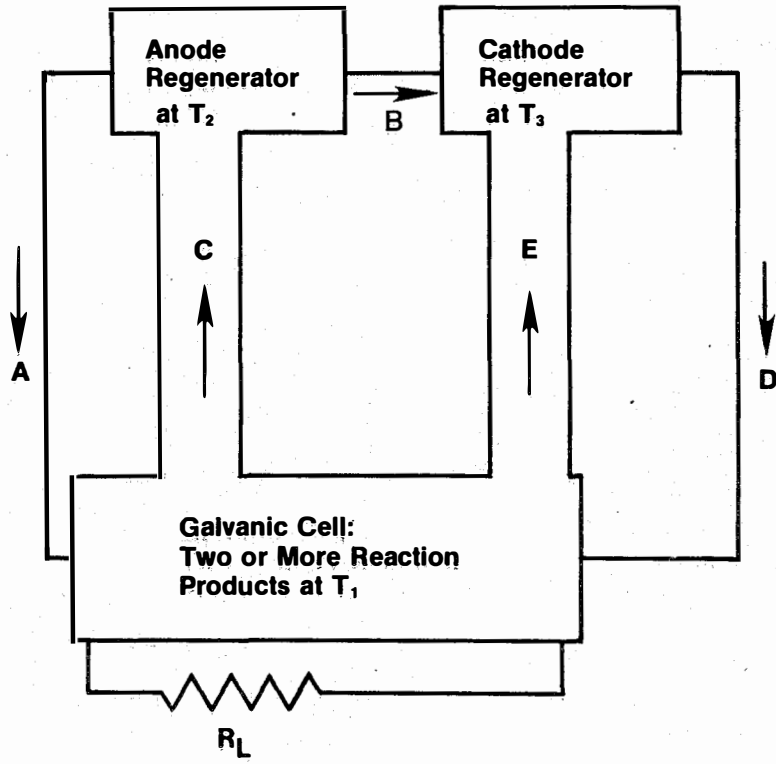
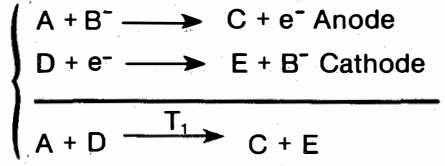


**Figure S-1. Thermal Regeneration: Type 1**

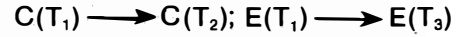


$$T_1 \neq T_2 \neq T_3$$

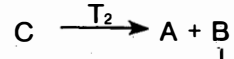
Galvanic Cell Reactions



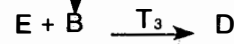
Heat Exchange



Anode Regeneration



Cathode Regeneration



Heat Exchange

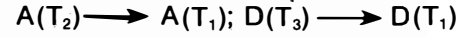
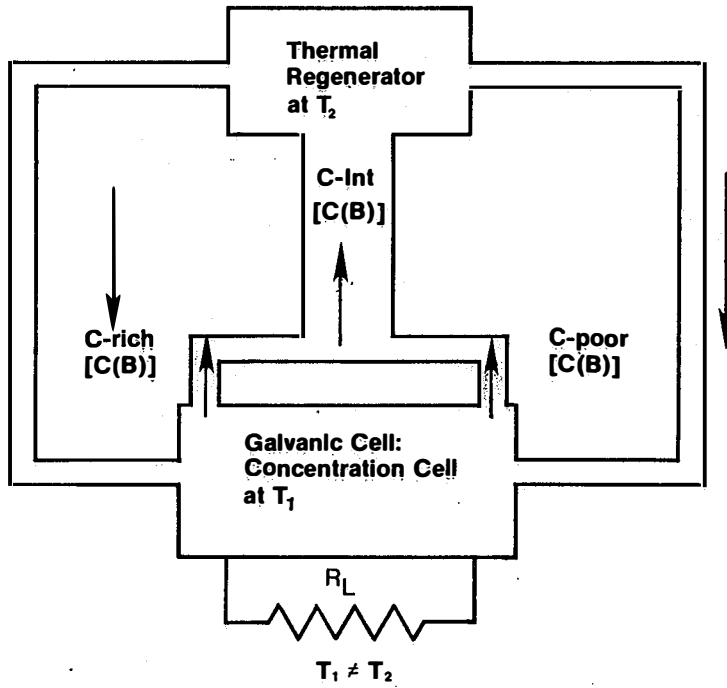
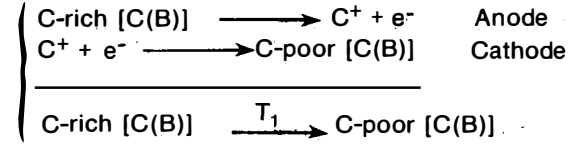


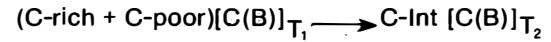
Figure S-2. Thermal Regeneration: Type 2



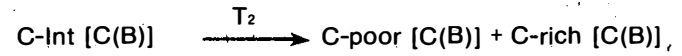
**Electrochemical Cell Reactions**



**Heat Exchange**



**Thermal Regenerator**



**Heat Exchange**

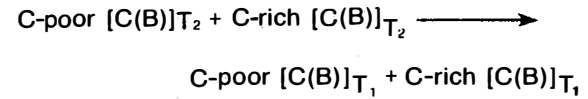


**Figure S-3. Thermal Regeneration: Type 3**

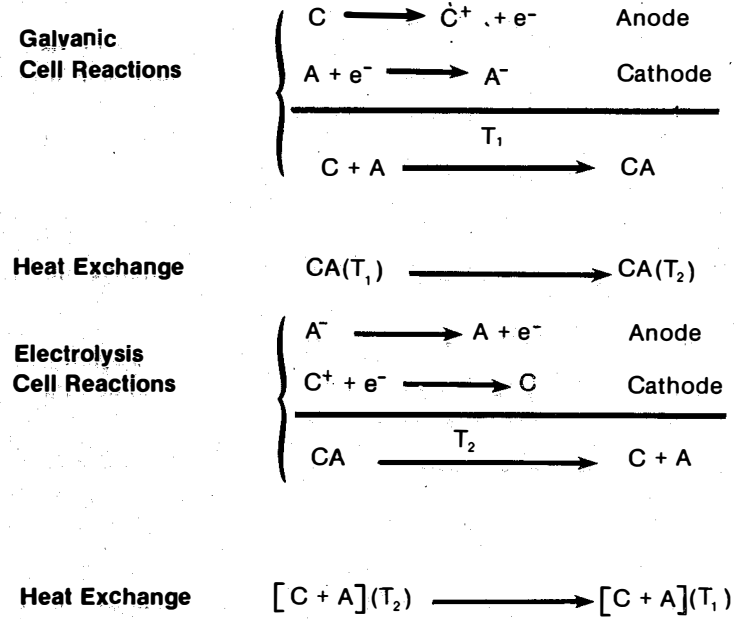
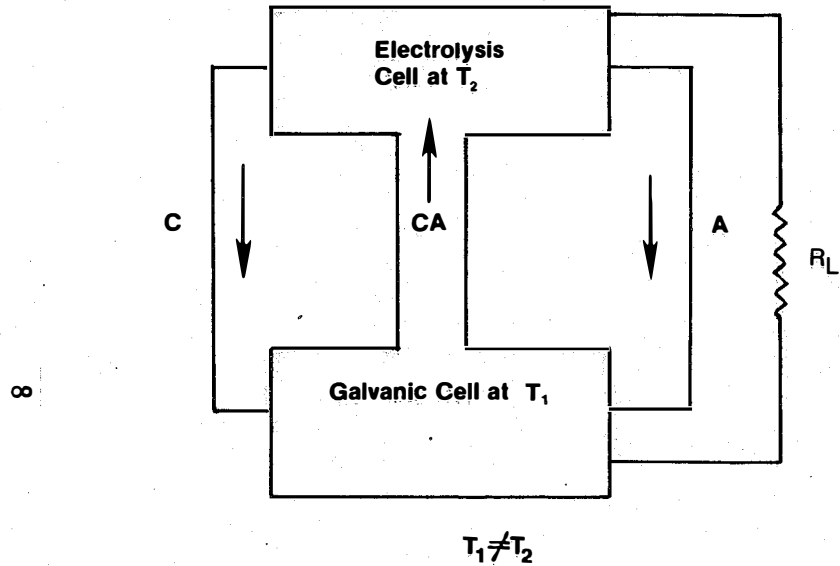
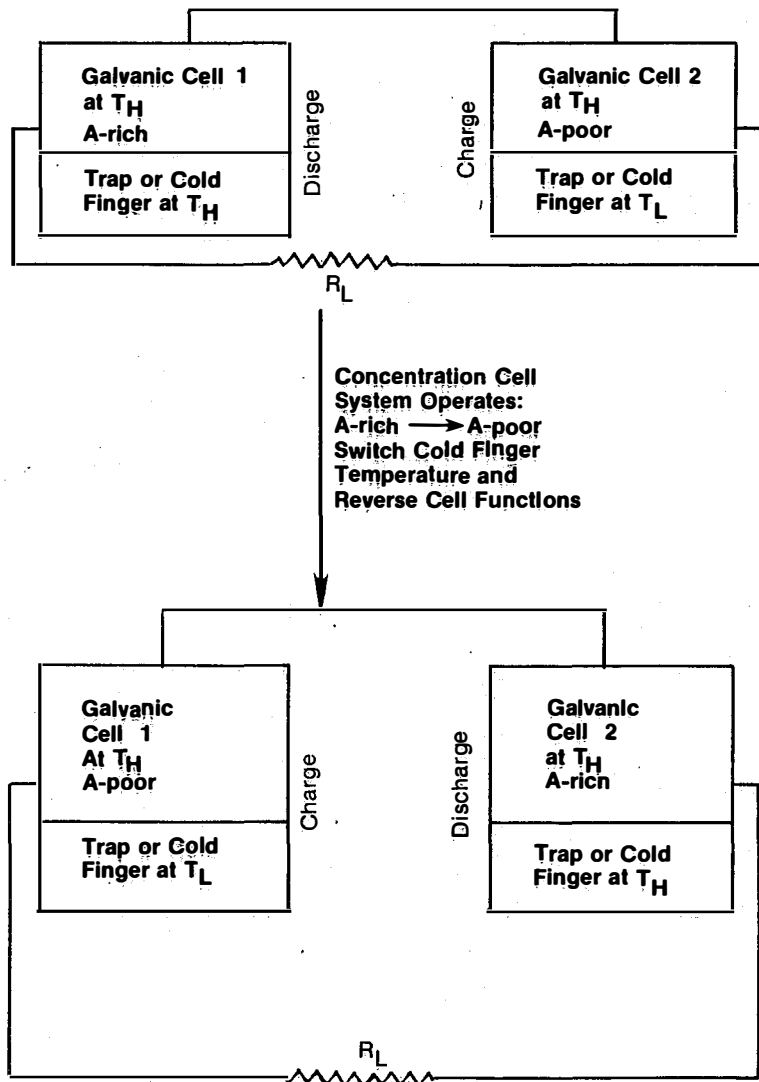
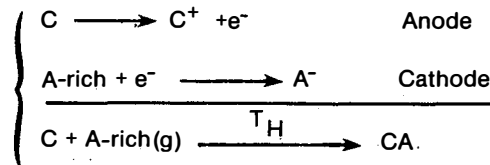


**Figure S-4. Coupled Thermal and Electrolytic Regeneration: Type 4**

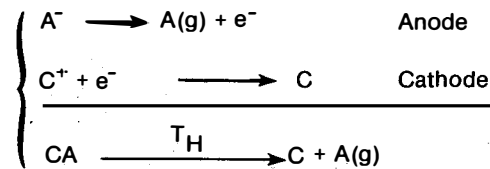


Electrolysis at Low Pressure

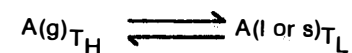
Electrochemical Cell 1 Reactions (Discharge)



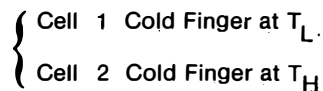
Electrochemical Cell (2) Reactions (Charge)



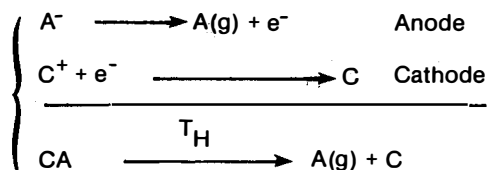
Cold Finger



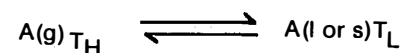
Switch Reaction (No Power to External Circuit)



Electrochemical Cell 1 Reactions (Charge)



Cold Finger



Electrochemical Cell 2 Reactions (Discharge)

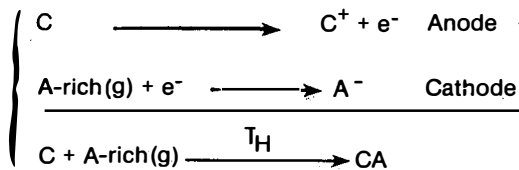
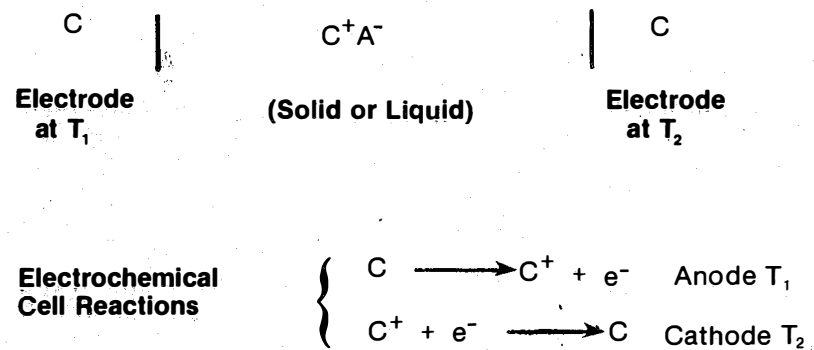
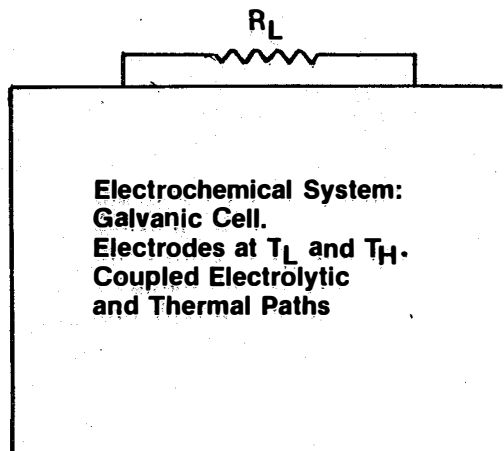


Figure S-5. Coupled Thermal and Electrolytic Regeneration: Type 5



If  $C = \text{Metal}$ , the roles of electrodes at  $T_1$  and  $T_2$  have to be reversed periodically.

**Figure S-6. Coupled Thermal and Electrolytic Regeneration: Type 6**



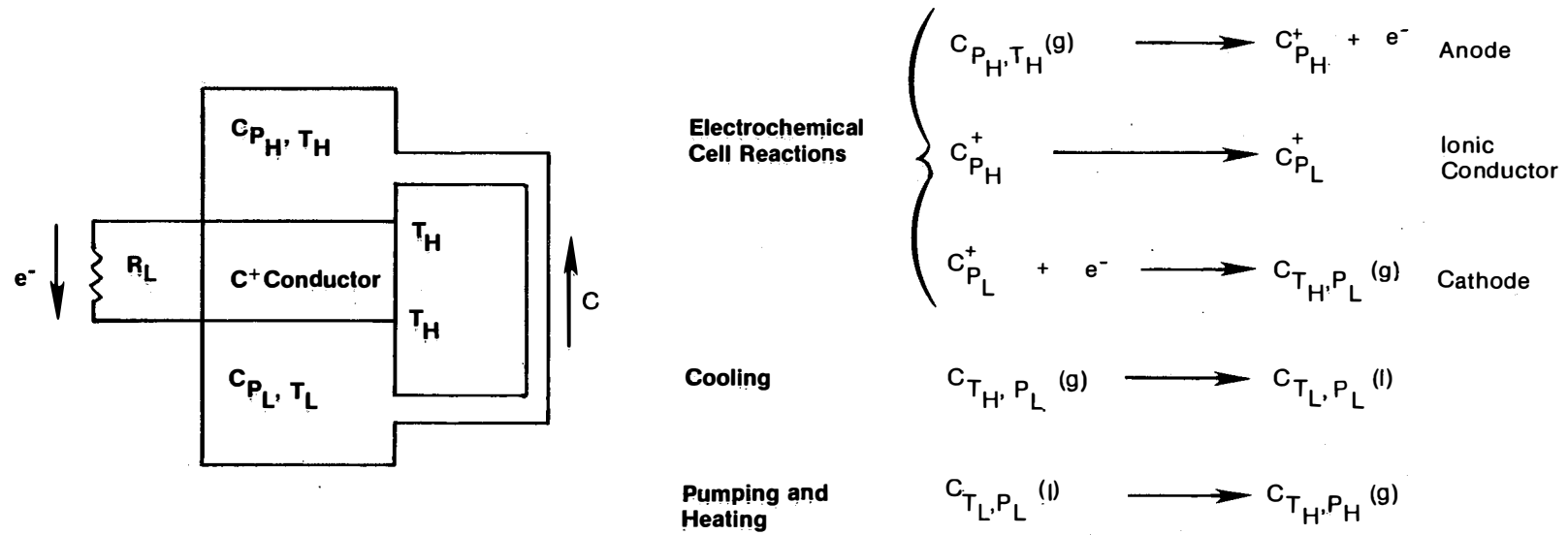


Figure S-7. Coupled Thermal and Electrolytic Regeneration: Type 7

Table S-1. EXAMPLES OF THE THERMALLY REGENERATIVE ELECTROCHEMICAL SYSTEMS

Type of Regeneration	System	Electrolyte	T <sub>2</sub> (°C)	T <sub>1</sub> (°C)	P (atm)	Carnot Efficiency (%)	Projected <sup>d</sup> Efficiency (%)	Performance (cells at T <sub>1</sub> )			Comments
								Open Circuit Voltage (V)	Voltage at Current Density		
									V (V)	I (mA/cm <sup>2</sup> )	
Type 1	LiH	eutectic molten, LiH-LiCl-LiF	900	530	1	32	-	0.6	0.3	200	Static cell; 0.025-cm vanadium diaphragm as H <sub>2</sub> electrode. Closed-loop system not tested.
Type 3 T <sub>2</sub> >T <sub>1</sub>	Na Hg	molten NaCN:NaI:NaF 58:30:12 mol %	~685	~495	9	~20	~6	0.32	0.2	25	High resistivity of alumina matrix impregnated with electrolyte; total 1200-h operation of which 750 h were closed-loop operation.
Type 3	Na Pb	molten NaF:NaCl:NaI 15.2:31.6:53.2 mol %	875	575	8/760	26	9-12	0.39	0.18	100	Complete system operated ~100 h. Regenerator only operated 1000 h.
Type 1 or 4 T <sub>2</sub> <T <sub>1</sub>	Sn+Sn <sup>2+</sup> +2e <sup>-</sup> 2Cr(III)+2e <sup>-</sup> +2Cr(II)	aqueous, excess Cl <sup>-</sup>	20	80	-	-	-	~0.1	0.06	3 <sup>a</sup>	Periodical power source.
Type 3 or 4	K Tl	molten KCl	175	335	-	-	-	0.6	-	-	Regeneration by cooling and separating the two phases (liquid and solid).
Type 4 T <sub>2</sub> >T <sub>1</sub>	Na NaCl Cl <sub>2</sub>	molten NaCl	-	827	-	-	-	3.24	1 up to 4.3 A/cm <sup>2</sup> with IR drop only	-	Low coulombic efficiencies (40% Na utilization). Low electrode polarization on discharge at ~1000°C.
Type 4	Li LiI I <sub>2</sub>	molten LiI	1170	500	-	50.6	~18	2.50	1.5	320	Closed-loop system not tested. Two mol % dissolved in LiI.
Type 4 T <sub>2</sub> >T <sub>1</sub> ; ΔG <sub>T<sub>2</sub></sub> <0	2UF <sub>6</sub> +2UF <sub>6</sub> +2e <sup>-</sup> +2F <sup>-</sup> AsF <sub>3</sub> +2e <sup>-</sup> +2F <sup>-</sup> +AsF <sub>5</sub>	solid electrolyte PbF <sub>2</sub> (KF doped)	>900	25	-	-	-	-0.5(25°C) +0.3(900°C)	-	-	No voltage-current data.

Table S-1. EXAMPLES OF THE THERMALLY REGENERATIVE ELECTROCHEMICAL SYSTEMS (Concluded)

Type of Regeneration	System	Electrolyte	T <sub>2</sub> (°C)	T <sub>1</sub> (°C)	P (atm)	Carnot Efficiency (%)	Projected <sup>d</sup> Efficiency (%)	Performance (cells at T <sub>1</sub> )			Comments
								Open Circuit Voltage (V)	Voltage at Current Density		
									V (V)	I (mA/cm <sup>2</sup> )	
Type 5	I <sub>2</sub>  molten alkali I <sub>2</sub> metal iodides	molten electrolyte	350	350		-	~30	0.29	0.23	100	Cold finger at 25°C. Mass transfer problems.
Type 6	I <sub>2</sub> (T <sub>1</sub> ) α-AgI I <sub>2</sub> (T <sub>2</sub> )	solid electrolyte α-AgI	340	184		25	~5 <sup>b</sup>	0.2	0.1	1.4 <sup>a</sup>	Internal resistance ~70 ohms; expected practical efficiency 1%-2%.
Type 6	Cu(T <sub>1</sub> ) CuSO <sub>4</sub>  Cu(T <sub>2</sub> )	aqueous acid	100	20		21	-	~0.09	0.03	8	Saturated solutions at each temperature.
Type 6	Pt Fe(CN) <sub>6</sub> <sup>4-</sup> , Fe(CN) <sub>6</sub> <sup>3-</sup>  Pt	aqueous	80	30		14	-	0.08	-	-	Maximum power estimated <0.1 mW/cm <sup>2</sup> .
Type 7	Na β"-Al <sub>2</sub> O <sub>3</sub>  Na	solid electrolyte	800-900	100-200		~60	~25	~1.2	0.7	1000	Voltage losses due to interfacial polarization and thickness of β" alumina electrolyte.
Type 7	I <sub>2</sub>  PbI <sub>2</sub> (x) I <sub>2</sub>	molten PbI <sub>2</sub>	170-400	20-100		-	-	0.17 <sup>c</sup>	-	6.2 <sup>a,c</sup>	Liquid electrolyte integrity difficult to maintain due to the pressure gradient.

<sup>a</sup>Current in mA.

<sup>b</sup>For T<sub>2</sub> = 500°C and T<sub>1</sub> = 200°C.

<sup>c</sup>T<sub>2</sub> enough to give 1 atm iodine; 24.5-ohm load; electrolyte temperature of 540°C.

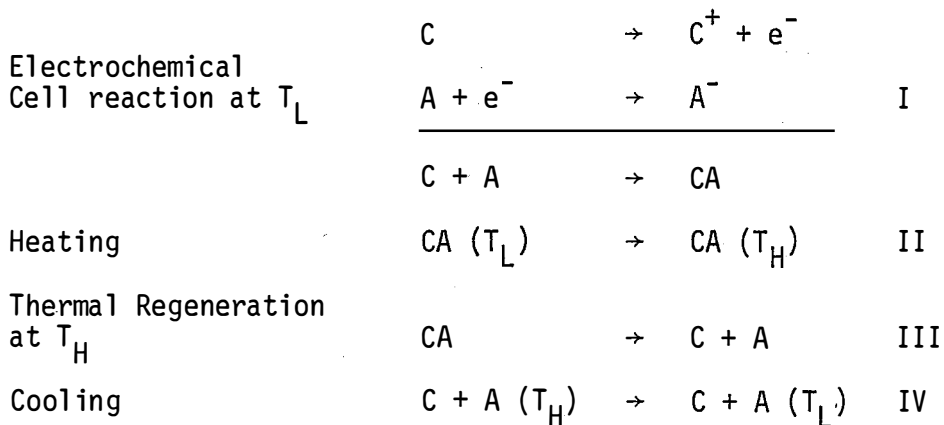
<sup>d</sup>Some of the numbers in this column were obtained from a minimum amount of experimental data.

**SERIO** 

SECTION I

THERMAL REGENERATION: METAL HYDRIDES, HALIDES, OXIDES, AND CHALCOGENIDES

The general scheme for a thermally regenerative electrochemical system (TRES) of Type 1 is shown in Fig. I-1. It consists of an electrochemical cell in which substance CA is formed electrochemically from C and A at temperature  $T_L$  with production of electrical energy. The working substance CA is then heated and fed to the regenerator at temperature  $T_H$  where it undergoes thermal decomposition into A and C. A cooling step completes the cycle, thus regenerating C and A at the lower temperature  $T_L$ .



This cycle can be considered a heat engine which converts part of the energy absorbed at a high temperature into useful work and rejects the remainder as heat at the lower temperature. The study of TRES was suggested by Yeager [7] in 1958.

Liebhafsky [8] has shown that though the efficiency of the fuel cell escapes the Carnot cycle limitation, the combination fuel cell heat source in TRES does not, having a maximum theoretical efficiency

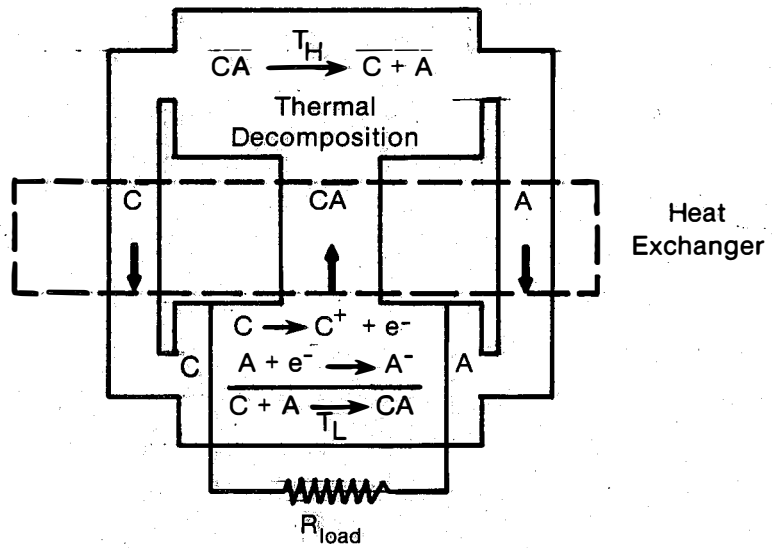


**Figure I-1. General Scheme for a Thermally Regenerative Electrochemical System**

for reversible steps I and III and  $\Delta C_p = 0$  ( $C_{CA} = C_C + C_A$ ) of

$$\frac{\text{electrical work}}{\text{heat input}} = \frac{T_H - T_L}{T_H} \quad \text{I-1}$$

The open-circuit voltage of the cell is

$$E = \frac{\Delta H_1}{nF} \frac{T_H - T_L}{T_H} \quad \text{I-2}$$

where  $\Delta H_1$  is the enthalpy of dissociation of CA into C and A at  $T_L$ . One of the chief sources of irreversibility in these cells is the heat exchanged during heating (II) and cooling (IV). This can be minimized by having  $\Delta C_p$  as close to zero as possible. The desirable thermodynamic properties for a regenerative fuel cell reaction are  $\Delta G_I < 0$ ;  $\Delta S_I < 0$ , and  $\Delta C_p$  as close to zero as possible [9].

In practice the cell irreversibilities prevent the working voltages from attaining the reversible potentials (Eq. I-2) when the cell is operating at useful loads [10]. From a practical point of view it is important that CA decompose at reasonable temperatures and that C and A can be easily separated, preferably by being in different physical states. More elaborate thermodynamic treatment of these systems were given by deBethune [9] and Friauf [11].

Henderson, Agruss, and Caple [12] presented a practical approach to the determination of efficiencies of TRES and to the thermodynamic selection of candidate systems. In their derivation of efficiencies, they assumed that the compound CA leaves the heat exchanger to go to the regenerator at a temperature  $T_E$ , and that the compounds C and A, after being cooled through the radiator, leave this heat exchanger at a temperature  $T_R$ . The temperatures of the regenerator and of the fuel

cell are respectively  $T_H$  and  $T_L$ . The efficiency of the heat exchangers is assumed to be 95%. The cell irreversibilities (polarization and ohmic losses) are represented by  $E_{loss}$ , which is the cell operating voltage ( $E$ ) less the reversible cell potential ( $E_R$ ).

The efficiency expression for  $\Delta C_p = 0$  with the inclusion of cell irreversibilities and heat exchanger losses is

$$\eta = \frac{T_H - T_L - \frac{nFE_{loss}}{\Delta S_H}}{T_H + 0.05 \frac{C_{CA}}{\Delta S_H} (T_H - T_L)} \quad \text{I-3}$$

which reduces to the Carnot expression for an ideal and reversible system operation.

In practice, few systems present  $\Delta C_p = 0$ , but  $C_{CA}$  can be larger or smaller than  $C_C + C_A$ . The efficiency of the system with  $C_{CA} > C_C + C_A$ , for which the heat content of C and A is not enough to raise the temperature of CA from  $T_L$  to  $T_H$ , is expressed by

$$\eta = \frac{[-T_H \Delta S_H + T_L \Delta S_L - C_{CA}(T_H - T_E) - 0.05(C_C + C_A)(T_H - T_L) - nFE_{loss}]}{[-T_H \Delta S_H + C_{CA}(T_H - T_E)]} \quad \text{I-4}$$

If  $C_{CA}$  is less than  $C_C + C_A$ , the heat contained in C and A is sufficient to raise the temperature of CA from  $T_L$  to  $T_H$ , and if larger, the excess will have to be radiated away. The efficiency expression for this case is

$$\eta = \frac{[-T_H \Delta S_H + T_L \Delta S_L - 0.05C_{CA}(T_H - T_L) - (C_C + C_A)(T_R - T_H) - nFE_{loss}]}{[-T_H \Delta S_H + 0.05C_{CA}(T_H - T_L)]} \quad \text{I-5}$$

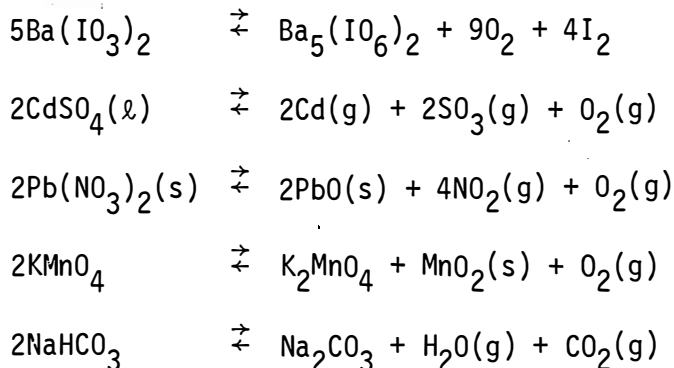


The survey of thermodynamically feasible systems for TRES conducted at the Allison Division of General Motors by Henderson et al. [12] reviewed over 900 compounds, of which only 20 (see Table I-1) were considered suitable for further evaluation as thermally regenerative electrochemical systems. The criteria to exclude the remaining compounds and some examples of excluded systems are the following:

- (1) More than two products are formed after or during decomposition.

If several compounds result from the thermal decomposition of CA, the separation of the intermediates is necessary before these compounds can be recombined in the electrochemical cell. The separation of various products is a problem for both terrestrial and space applications. The electrode reactions for such an operation would be highly complex.

The following are examples of compounds exhibiting multiproduct dissociation.



- (2) Two gaseous decomposition products are formed.

Gas separation is extremely difficult. An exception is hydrogen, due to the possibility of separation by diffusion through metal foils. The systems in which one of the gases formed was hydrogen were not


 TABLE I-1. THERMODYNAMICALLY SUITABLE COMPOUNDS FOR THERMAL DISSOCIATION  
 IN THERMALLY REGENERATIVE FUEL CELLS [12]<sup>a</sup>

HYDRIDES			
2LiH(l)	↔	2Li(l)	+ H <sub>2</sub> (g)
2KH(l)	↔	2K(l)	+ H <sub>2</sub> (g)
2CsH	↔	2Cs(l)	+ H <sub>2</sub> (g)
2RbH	↔	2Rb(l)	+ H <sub>2</sub> (g)
Ga <sub>2</sub> H <sub>6</sub>	↔	2Ga(l)	+ 3H <sub>2</sub> (g)
CHLORIDES AND OXYCHLORIDES			
2CuCl <sub>2</sub> (l)	↔	2CuCl(l)	+ Cl <sub>2</sub> (g)
2CuOCl <sub>2</sub> (l)	↔	2CuCl <sub>2</sub> (l)	+ O <sub>2</sub> (g)
BROMIDES			
2CuBr <sub>2</sub> (l)	↔	Cu <sub>2</sub> Br <sub>2</sub> (l)	+ Br <sub>2</sub> (g)
2HBr	↔	H <sub>2</sub> (g)	+ Br <sub>2</sub> (g)
PbBr <sub>2</sub> (l)	↔	Pb(l)	+ Br <sub>2</sub> (g)
2TiBr <sub>3</sub>	↔	TiBr <sub>2</sub> (l)	+ TiBr <sub>4</sub> (g)
IODIDES			
2HI(g)	↔	H <sub>2</sub> (g)	+ I <sub>2</sub> (g) <sup>b</sup>
PbI <sub>2</sub> (l)	↔	Pb(l)	+ I <sub>2</sub> (g) <sup>c</sup>
SULFIDES			
2Bi <sub>2</sub> S <sub>3</sub> (l)	↔	4Bi(l)	+ 3S <sub>2</sub> (g or l)
2Bi	↔	2Bi(l)	+ S <sub>2</sub> (g or l)
4CeS(l)	↔	Ce(g)	+ Ce <sub>3</sub> S <sub>4</sub> (l)
H <sub>2</sub> S	↔	H <sub>2</sub> (g)	+ S(l or g)
PEROXIDES			
2H <sub>2</sub> O <sub>2</sub>	↔	2H <sub>2</sub> O(l or g)	+ O <sub>2</sub> (g)
CARBONATES			
Tl <sub>2</sub> CO <sub>3</sub> (l)	↔	Tl <sub>2</sub> O(l)	+ CO <sub>2</sub> (g) <sup>d</sup>

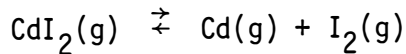
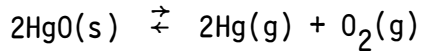
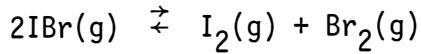
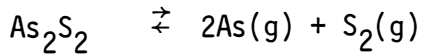
<sup>a</sup> See text for criteria employed in the selection of these compounds.

<sup>b</sup> At 283°C, 18% of HI is dissociated.

<sup>c</sup> At 750°C, log P<sub>I<sub>2</sub></sub> (atm) = -3.22.

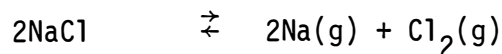
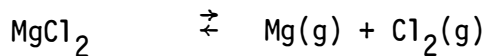
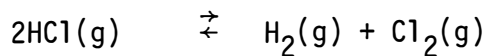
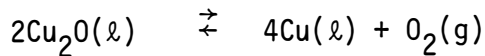
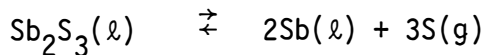
<sup>d</sup> At 353°C, P<sub>CO<sub>2</sub></sub> is 470 torr.

excluded. If techniques for separation of gases are improved, additional systems can be evaluated. Typical examples are:



(3) Decomposition takes place above 1000°C.

The arbitrary limit of 1000°C as a maximum allowable temperature was chosen considering the severity of materials problems above this temperature. Many compounds were found in this class, for instance:



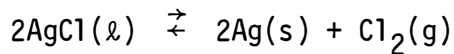
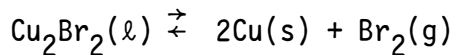
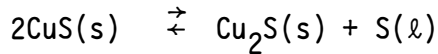
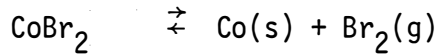
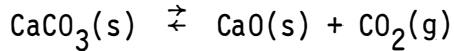
(4) Decomposition is explosive or exothermic.

Only a few compounds were found in this category, e.g.,  $\text{NH}_4\text{IO}_4$ ,  $\text{NH}_4\text{MnO}_4$ ,  $\text{Cl}_2\text{O}$ .

(5) Solid is present among the decomposition products.

This restriction was imposed by the space application envisioned at the time. For terrestrial application these systems could be recon-

sidered from a thermodynamic point of view. Some examples of this class are:



The criteria for selection of the compounds listed in Table I-1 are:

- (a) appreciable decomposition at or below 1000°C;
- (b) no solids present;
- (c) compound decomposes into only two products;
- (d) only one product gaseous;
- (e) compound and one product are liquid at the decomposition temperature; and
- (f) products remain liquid at fuel cell temperature.

King, Ludwig, and Rowlette [13] have analyzed twelve thermodynamic models, which treated the effects of reversible and irreversible conditions and finite specific heat differences to obtain the thermodynamic efficiencies of the systems. The twelve models are based on:

(1) Dissociation occurs only at  $T_H$ . Equilibrium attained at the re-generator outlet but not at the inlet. Four models are possible:

- (a) reversible cycle with  $\Delta C_p = 0$ ;

- (b) Irreversible cycle with  $\Delta C_p = 0$ ;
- (c) reversible cycle with  $\Delta C_p \neq 0$ ; and
- (d) irreversible cycle with  $\Delta C_p \neq 0$ .

(2) Dissociation and equilibrium are achieved at all temperatures between  $T_L$  and  $T_H$ . Two models are possible:

- (e)  $\Delta C_p = 0$ ; and
- (f)  $\Delta C_p \neq 0$ .

(3) If the equilibrium is not attained at the regenerator outlet, six models (g through l) are possible, equivalent to those in (1) and (2).

The efficiencies for these models are:

$$\eta_a = \frac{T_H - T_L}{T_H} = \frac{\Delta G_L}{\Delta H_L} \tag{I-6}$$

$$\eta_b = \frac{T_H - T_L}{T_H} \left[ 1 + \frac{\ln \frac{[CA]_L}{[CA]_H}}{\ln \frac{K_H}{K_L}} \right] \tag{I-7}$$

$$\eta_c = \frac{T_H - T_L}{T_H} - \frac{\Delta C_p}{\Delta H_{15}} \left( T_L \ln \frac{T_H}{T_L} - T_H + T_L \right) \tag{I-8}$$

$$\eta_d \approx \eta_f \approx \eta_{g-1} \approx \eta_b \times \frac{\eta_c}{\eta_{Carnot}} \tag{I-9}$$

where  $K_H$  and  $K_L$  are the equilibrium constants for the dissociation reaction at  $T_H$  and  $T_L$  and  $\Delta H_{15}$  is the extra heat to be rejected by the material as it cools since it cannot be exchanged totally in the heat exchanger.

The calculations performed by King et al. [13] are based on the

analysis of the term  $\Delta G_L/\Delta H_L$  in Eq. 1-6.  $\Delta H$  was assumed to be independent of temperature between  $T_L$  and  $T_H$ . If  $\Delta G_L/\Delta H_L$  was too low, the efficiency was low; if it was too high (close to 1), the ratio  $T_H/T_L$  was high, meaning that the regenerator temperatures would be too high to be feasible. Table I-2 shows the compounds considered feasible for thermal regeneration based on these calculations. It is important to notice that all these values assume that no phase changes occur between  $T_L$  and  $T_H$ . Phase changes do occur in several cases, making the simplified calculations incorrect. In these cases, the systems may not be thermally regenerable. One example is the  $CdI_2$  system. The melting points of Cd and  $CdI_2$  are 594 K and 660 K, respectively. At 700 K, the ratio  $\Delta G/\Delta H$  is 0.63. Thus, the regenerator temperature at which the  $I_2$  vapor pressure is 1 atm, as calculated from Eq. 1-6, is  $T_H = 700 / (1 - 0.63) = 1890$  K. At this temperature, the  $CdI_2$  would be vaporized. The assumption of constant  $\Delta H$  is no longer applicable, and the new  $\Delta H$  is much lower. The system  $CdI_2$  is, therefore, unlikely to be feasible for thermal regeneration (see Section I.1.2.1 and Refs. 3 and 10).

In this section the metal hydrides, halides, oxides, and chalcogenides which have been studied are described. Due to the considerable effort directed towards the investigation of the system lithium hydride, a separate summary and conclusion are included. The remaining systems in this section have not been thoroughly investigated. Some metal halides were proposed as thermodynamically feasible but the models were very rudimentary and the practical experience has shown no thermal decomposition. The two major divisions of this section are based on the

TABLE I-2. COMPOUNDS SELECTED AS POSSIBLE CANDIDATES FOR THERMAL REGENERATION [12]<sup>a</sup>

Compound	mp C (K)	mp CA (K)	$\Delta H_{\text{fus}}$ C ( $\frac{\text{kcal}}{\text{mole}}$ )	$\Delta H_{\text{fus}}$ CA ( $\frac{\text{kcal}}{\text{mole}}$ )	$\Delta G^{\circ}_{298}$ ( $\frac{\text{kcal}}{\text{mole}}$ )	$\Delta H^{\circ}_{298}$ ( $\frac{\text{kcal}}{\text{mole}}$ )	$\Delta S^{\circ}_{298}$ ( $\frac{\text{cal}}{\text{deg mole}}$ )	$\frac{\Delta G^{\circ}}{\Delta H^{\circ}}$ at 298. K	$\Delta G^{\circ}_{700}$ ( $\frac{\text{kcal}}{\text{mole}}$ )	$\Delta H^{\circ}_{700}$ ( $\frac{\text{kcal}}{\text{mole}}$ )	$\frac{\Delta G^{\circ}}{\Delta H^{\circ}}$ at 700 K
LiH	459	957	1.6	7.0	-16.7	-21.3	-15.5	0.78	-10.0	-15.9	0.63
AlBr <sub>3</sub>	932	371	2.6	2.7	-124	-138	-46	0.86	-108.3	-137.9	0.79
TiCl <sub>2</sub>	2000	950	4.6	6.0	-96	-144	-35	0.84	-90.5	-113.6	0.80
WCl <sub>6</sub>	3650	548	8.4	5.7	-74	-96.9	-93	0.76	-33.3	-99.6	0.33
CoI <sub>2</sub>	1766	790	3.7	6.0	-26	-36	-32	0.72	-13.6	-33.7	0.40
ZnCl <sub>2</sub>	693	566	1.6	5.5	-88.3	-99.4	-37.4	0.83	-74.8	-95.7	0.78
CdI <sub>2</sub>	594	660	1.5	3.6	-53.3	-63.3	-35.1	0.84	-38.6	-61.2	0.63
GaI <sub>3</sub>	303	485	1.3	3.9	-58	-73	-49	0.80	-38.3	-70.5	0.54
SnCl <sub>2</sub>	505	520	1.7	3.0	-72.2	-83.6	-32	0.86	-59.2	-79.8	0.74
BiCl <sub>3</sub>	544	505	2.6	2.6	-76.3	-90.6	-47.8	0.84	-57.4	-90.6	0.63
AsI <sub>3</sub>	1087	415	6.6	2.2	-21.9	-35.9	-47	0.61	-4.5	-40.3	0.11
TeCl <sub>4</sub>	723	497	4.3	4.5	-58.3	-77.4	-64	0.75	-64	-77.2	0.45

<sup>a</sup>For selection criteria see text.

number of products formed in the electrochemical reaction and of regeneration steps. Section I.1 deals with systems which present one or more electrochemical reaction products which use one-step regeneration (TRES, Type 1). In Section I.2, the systems in which two or more compounds are formed in the galvanic cell reaction are explained in detail. In these systems the regeneration of each galvanic cell component is performed independently, and therefore these TRES require a multiple-step generation (TRES, Type 2). These systems have been selected based on thermodynamic calculations by Snow [14]. Thermochemical data for 58 families of halides and oxides were compiled. The metals chosen existed in more than one valence state. The heats of formation and transition, transition temperatures, coefficients in heat capacity equations, and free energies of formation were tabulated. The temperature range over which these calculations were performed was 25-1200°C. The temperatures at which these compounds could be generated were also given [14]. Section I.2 includes the systems investigated as a result of these calculations.

## I.1 SINGLE OR MULTIPLE ELECTROCHEMICAL REACTION PRODUCTS AND SINGLE-STEP REGENERATION

Such cells are commonly referred to as thermally regenerative fuel cells (TRFC) or thermally regenerative galvanic cells (TRGC).

### I.1.1 Metal Hydride Systems: Lithium Hydride

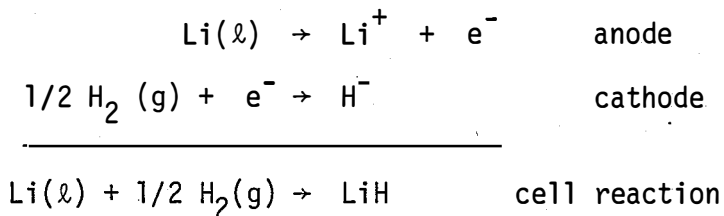
#### I.1.1.1 Summary

The metal hydride systems were proposed as thermally regenerative



electrochemical systems in 1958 as a result of the research performed at Mine Safety Appliance Research Corporation (MSA) [16-23]. This research continued through 1961 at MSA and also at the TAPCO division of Thompson-Ramo-Wooldridge, Inc. (TRW) [24-31]. From 1961 to 1967, the Chemical Engineering Division of Argonne National Laboratory (ANL) [33-46] performed research on the lithium hydride system at a more basic level. Parallel and earlier pertinent research efforts were made at the Wright Patterson Air Force Base [32] and at Tufts University [47-49].

The lithium hydride system was the first to be envisioned as a practical TRES. The electrochemical cell reactions are:



This system is appealing because pure LiH decomposes at 900°C into easily separable liquid lithium and gaseous hydrogen. At this temperature the pressure of the hydrogen gas is about 760 torr. The gas can be easily separated from the lithium at this temperature because it diffuses very rapidly through metals, e.g., iron foil.

For scientific and practical reasons, however, this system poses problems. First, both lithium and the hydride are susceptible to reaction with normal atmospheric components (oxygen, nitrogen, water), and therefore an inert atmosphere is necessary. Second, a solvent is required that dissolves the LiH but not the lithium metal, is thermodynamically stable to lithium metal at the regeneration temperature,

and preferably has a low vapor pressure at this temperature. Molten salt systems meet most of these requirements and some research was devoted to the search for suitable electrolytes. Third, it was necessary to develop lithium anodes and hydrogen gas cathodes operable in the molten salt medium. Certainly the most difficult problem is the gas electrode.

In the 10 years which followed the initial work on the metal hydride regenerative systems, emphasis was first placed on the porous gas electrodes. Since the electron transfer takes place in the vicinity of the electrode surface, three-phase contact sites must exist to achieve practical current densities. A frequent problem with this type of electrode is the absorption of liquids by capillary action, which causes the electrolyte-electrode interface to retreat within the electrode. Thus, flooding of the electrode with either the electrolyte or gas can occur. Catalysts are often needed for fast heterogeneous reaction rates at the porous electrode. The porous electrodes tested were not stable in the presence of the highly corrosive molten salt media at the working temperatures (above 400°C).

It was then recognized that this system provided an unusual opportunity to avoid the use of porous electrodes by using solid, thin foils of metals that are permeable to hydrogen gas at these elevated temperatures. Thus, hydrogen can be transferred by interatomic diffusion to the metal/molten salt electrolyte interface. However, the temperature has to be high for the hydrogen to diffuse through the metal foil at an appreciable rate. This diminishes the efficiency of the system.

The regeneration step in the presence of the molten salt medium also proved less than straightforward. Low hydrogen partial pressures (100-200 torr) for most of the molten salts tested forces the use of pumps to bring the hydrogen pressure to the 1 atm required for better performance of the gas electrode. This further decreased the cycle efficiency.

The separation steps were complicated by the presence of LiH in the hydrogen exit line. The LiH was formed in the reaction of Li vapor and hydrogen at the regenerator temperature. A further complication was the need to perform the separation under the zero-gravity conditions imposed by the space power application envisioned at that time. The engineering and materials problems due to corrosion were formidable [3,4,35].

#### I.1.1.2 Detailed Review

In 1958 Shearer and Werner [16] reported the first investigation of schemes for the continuous regeneration of a galvanic system by thermal energy based on the formation and decomposition of alkali and alkaline-earth metal hydrides in molten halide electrolytes. Figure I-2 shows theoretical cell output potential as a function of temperature, calculated assuming that all the chemicals are in their standard states at the various temperatures [17]. This is only a guide, since the actual cells would operate under different conditions. From Fig. I-2, the lower the fuel cell operating temperatures are, the higher the open-circuit voltages are. On the other hand, increasing temperatures will decrease the polarization at the hydrogen electrode and increase the solubility of the ionic hydride, therefore facilitating the continuous

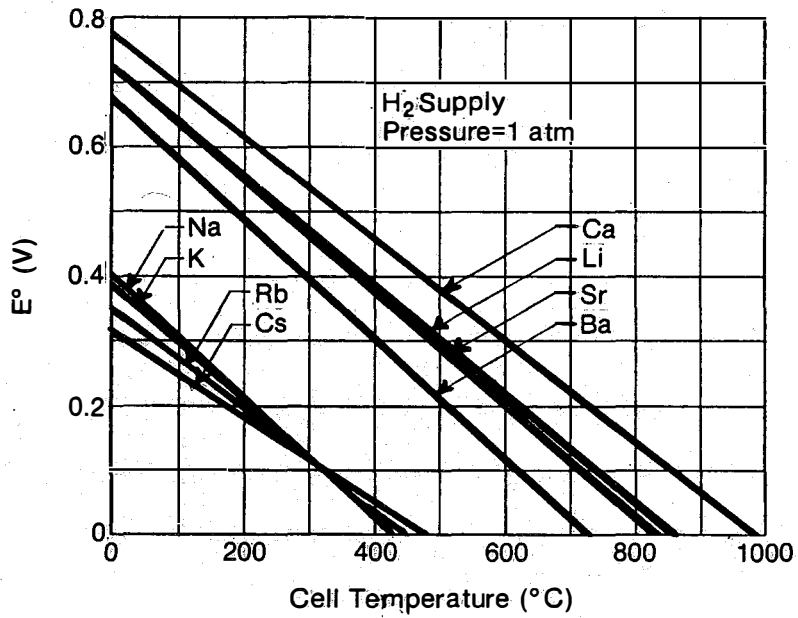


**Figure I-2. Theoretical Standard Cell Potentials As a Function of Temperature for Various Metal Hydrides [20]**

regeneration operation [16-21].

Experimental work by MSA [16-23] included cell studies of Li, Na, K, and Ca electrodes with the following molten salt solutions as electrolytes: (a) LiCl-LiF (570°C); (b) LiCl-KCl (357°C); and (c) LiCl-NaCl-RbCl-CsCl (285°C) [20,23]. Other electrolyte systems were also investigated (KBr-KF-KI; LiCl-LiF-LiI; LiBH<sub>4</sub>-KBH<sub>4</sub>; LiI-LiBr-KI-KBr) [23]. Cells were operated most successfully on a batch basis with external supply of hydrogen and liquid metal. Continuous regeneration was attempted using cells of the type shown in Fig. I-3 [17], which exhibited severe materials and leakage problems [3]. Better seals and electrical insulation were obtained by using a flange system with a cold-salt seal (Fig.I-4) [23]. For all the cell configurations and electrolyte systems used, the current densities did not exceed 65 mA/cm<sup>2</sup> at very low working voltages (~0.1 V) [16-23]. One exception was a batch operation in which a current density of 250 mA/cm<sup>2</sup> at 0.3 V under steady-state conditions was obtained employing a liquid lithium anode, the LiF-LiCl molten eutectic electrolyte at 570°C, and a stainless steel cathode (screen or porous micrometallic). No details about experiment duration or other conditions were given [17,23].

In general, due to the elevated temperatures employed, the porous electrodes tested by MSA (nickel, platinum, palladium, and carbon) exhibited variable catalytic activity at the surface of the frits, flooding of the frits with either hydrogen gas or fused electrolyte, concentration polarization, and severe corrosion. The diffusion membrane (Pd-Ag) corroded rapidly. For reasonable continuous regeneration

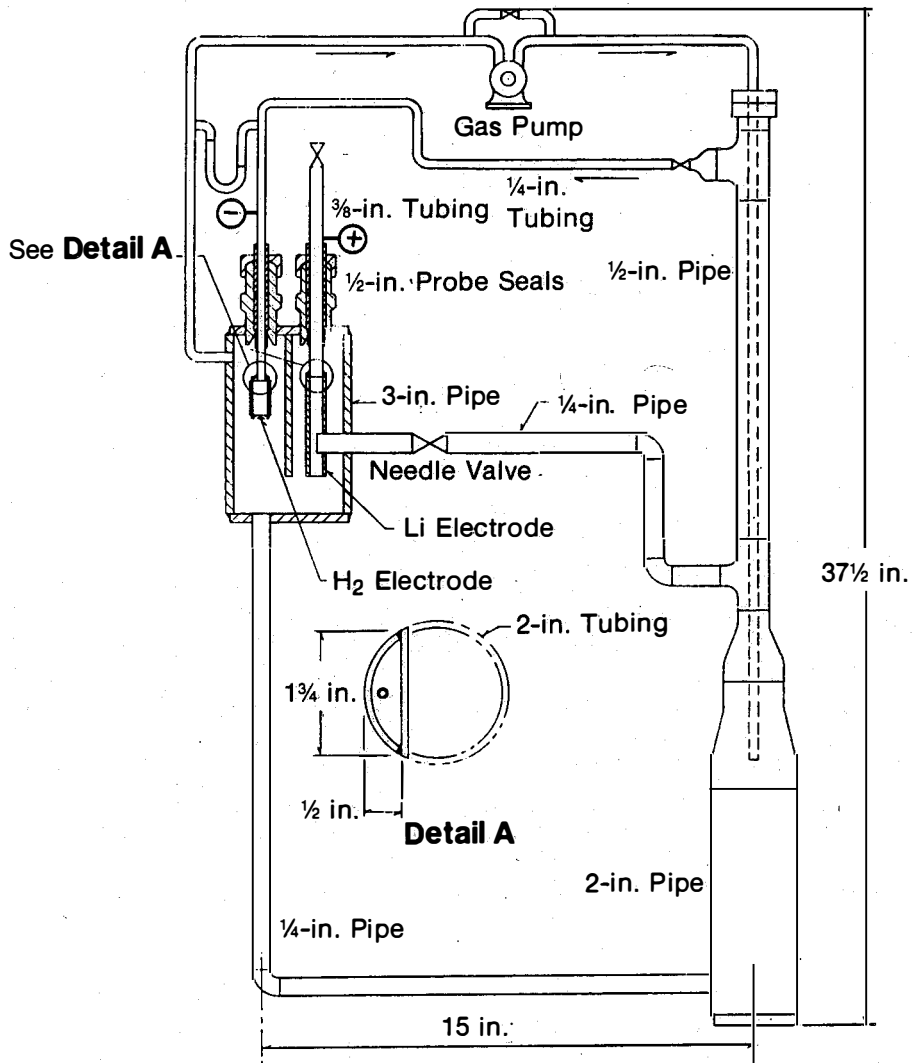
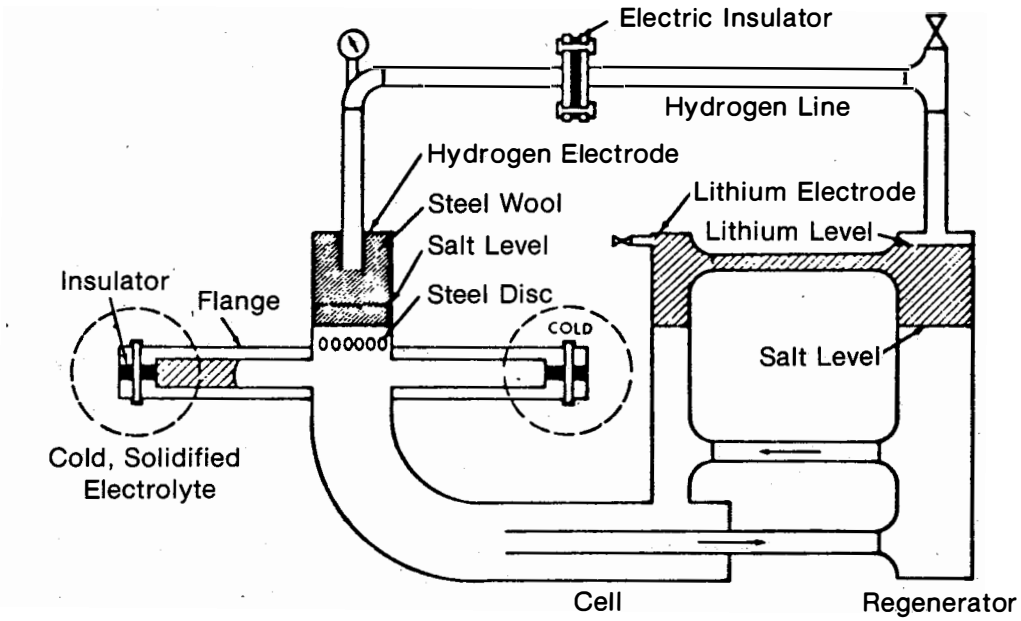


Figure I-3. Lithium Hydride Regenerative Cell [20]



**Figure I-4. Lithium Hydride Regenerative Fuel Cell with a Cold-Salt Seal Flange [23]**

operation, the hydrogen pressure must be about 1 atm; however, the closed-loop cells tested at the regeneration temperatures of 800-1100°C, and at the lithium hydride compositions of 0.35-0.42 w/w %, exhibited low (20-300 torr) partial hydrogen pressures [17,23]. The hydrogen was circulated by pumping argon, which was recirculated from the cell to the regenerator. The metal and the electrolyte were circulated by natural convection.

The plausible coupling of this system with nuclear reactors was envisioned [20], as well as the potential application for thermal energy conversion and storage of solar energy [21].

All experimental work carried out at MSA was of an exploratory nature, searching for possible electrolytes and electrodes but at the same time device oriented. The work carried out at TRW [24-31], principally on the lithium hydride systems, was also device oriented. Due to the state of the art of TRES at the time, Austin [3] questioned the validity of the stated objective to "develop a thermally regenerative lithium hydride fuel cell suitable for use under zero-gravity conditions with a nuclear heat source" [24].

Fuscoe, Carlton, and Laverty performed the initial studies at TRW [24] with lithium and hydrogen reactants and the eutectic electrolyte mixture of LiCl-LiF (79:21 w/w %) at 510°C and 1 atm. An open-circuit voltage (OCV) of 0.5 V was observed, and  $6 \text{ mA/cm}^2$  could be obtained with a 50% polarization loss. The cells were constructed of 316 stainless steel, with a stainless steel bell-shaped lithium anode, and a metal foil diaphragm cathode (iron, 0.005 cm) replacing the porous



electrodes. This replacement eliminated the need for a catalyst and minimized the electrolyte interface and separation problems, but the foil electrodes behaved properly only at elevated temperatures. Major problems related to the purity of the melt, electrode and cell materials, and gases (argon and hydrogen) were encountered leading to high spurious open-circuit voltages (which decayed) and irreproducible results. The major impurities were water, oxygen, and nitrogen; the stainless steel contact welded to the cathode material corroded. Niobium foil was also tested as a cathode material but the niobium oxide, formed at the surface or present in the metal, was not removed under the treatment given to the electrode; iron was more successful since the iron oxides formed were reduced by hydrogen gas [24,25,26]. The regenerator, separators, and radiation effects were also studied [24].

The equilibrium pressure of hydrogen on the LiCl-LiF eutectic containing 5-10 mole % of LiH was investigated at 880°C. At this temperature, appreciable vapor pressure of Li, insoluble in the melt, led to the recombination of evolved hydrogen and lithium, thereby forming LiH in the exit line. Under these conditions LiCl is present in the vapor phase as well. The dissociation of LiH in the presence of LiCl was also studied [24].

An improved batch cell design [25] is shown in Fig. I-5, where high purity iron was used to contain the melt, eliminating some of the spurious high initial voltage. A steady OCV of 0.38-0.58 V was obtained. The cathode was a 0.010-cm, high purity, iron foil. As expected, the cell voltage and current density decreased with decreased hydrogen pressure. At low pressure (<200 torr) the observed current densities

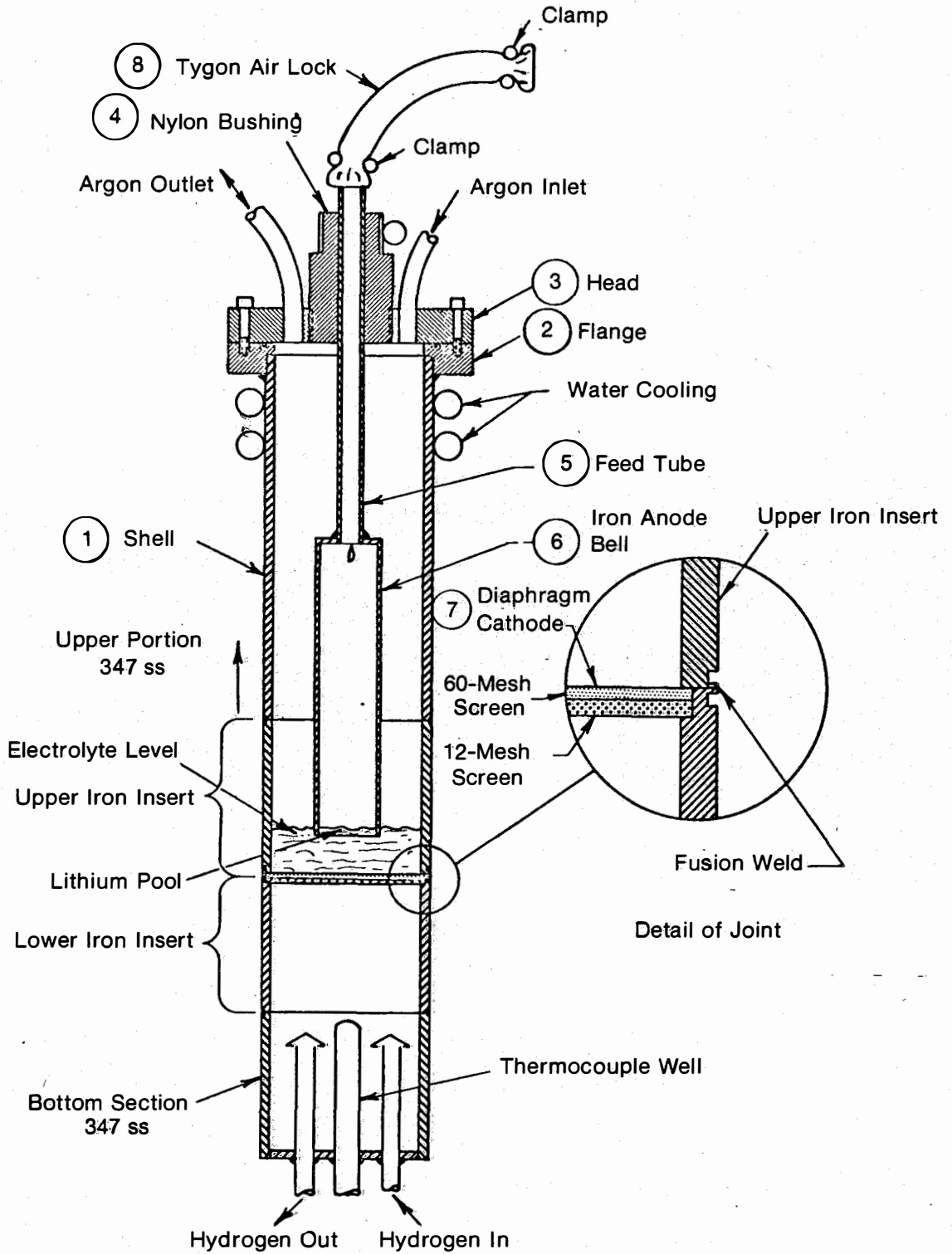


Figure I-5. Batch Lithium-Hydrogen Cell [25]

agreed with calculated values (based on the rate of diffusion of H<sub>2</sub> through the iron foil) and were found to be proportional to the square root of the pressure of the hydrogen at the electrode (assuming the partial pressure of hydrogen on the electrolyte side of the foil to be zero). The rate of diffusion and the permeability of hydrogen on the iron foil were low:  $3.75 \times 10^{-4}$  cm<sup>2</sup>/s and  $2.6 \times 10^{-5}$  ml/(cm<sup>2</sup>/s), respectively, at 550°C and 760 torr [25].

Other materials studied included rhenium, nickel, zirconium, beryllium, tantalum, palladium, niobium, vanadium, rhodium, titanium, and thorium. Theoretical calculations of the permeability, based on literature data, indicated that corrosion-resistant niobium, tantalum, and vanadium had higher permeability to hydrogen than did iron, and that niobium had a 1000 times greater permeability. Very preliminary experiments indicated a permeability for niobium only 20 times larger than that of iron [25].

A continuous thermal regeneration unit for a normal gravity environment was designed, fabricated, and tested with different pumping systems. The degree of regeneration achieved was lower than expected [25,29,30].

More extensive studies of the niobium foil cathode were carried out by Carlton [26,27]. Thorough purification schemes were developed for the melt, gases, and electrode materials, as well as the manufacture of an all-niobium cell of a configuration inverse to that shown in Fig. I-5 (anode on the bottom; gases fed from the top). Niobium turnings were used to getter oxygen from the melt and a 0.016% oxygen content was achieved. A new lithium anode on porous niobium was developed. As a

result of the elaborate purification procedure used during this project, the single cell tested showed no high spurious voltage. The cell potential rose to a steady 0.45-V OCV value. Due to the small amount of lithium available in the anode, the run lasted 45 min. Electrode polarization studies were carried out and indicated low cathodic and low anodic polarization. In these studies current densities as high as 1500 mA/cm<sup>2</sup> at half of the OCV were achieved on a 0.012-cm foil cathode. Under load (2 ohms) current densities of 125 mA/cm<sup>2</sup> were obtained at 0.12 V. The current density was later questioned by Johnson and Heinrich [33], who contended that the permeation would not support current densities of that magnitude.

The separation of the hydrogen gas from the liquid metal/electrolyte mixture was examined at TRW [28] using a compact gas/liquid separator. The liquid/gas mixture was introduced tangentially at high velocity. Beneath the cylindrical section was a conical chamber. The gas was removed from the base of the cone, the heavier liquid from the side, and the lighter liquid from the apex.

Problems with the lithium hydride systems included the operation of the separators in space [28,32], electrical isolation of the cells, life of the pumps, and materials problems [3,4,35].

From 1961 to 1967, the Chemical Engineering Division of Argonne National Laboratory [33-46] continued the research efforts on the lithium hydride TRES at a more basic level than that previously described. No attempt to develop a practical continuous regeneration cell was made, but guidelines for practical cell design were suggested [33].

The techniques employed were similar to previous work. An inert-

atmosphere dry box was developed in which purified helium was circulated [34]. The performance of iron cells similar in design to that shown in Fig. I-5 was tested in KCl-LiCl (41:59 mole %, 357°C) with an iron foil diffusion cathode. Again spurious high voltages were also found. The polarization of the lithium anode was found to be small using a lithium reference electrode. In agreement with TRW results [25], iron foils were found to support current densities less than  $100 \text{ mA/cm}^2$  [36].

Considerable effort was expended by Heinrich, Johnson, and Crouthamel [36,37,38] in measuring diffusion rates through iron, iron-molybdenum alloys, vanadium, niobium, and tantalum [36]. Quantitative permeation studies of Armco iron and iron-molybdenum alloys [37] confirmed that currents in excess of  $100 \text{ mA/cm}^2$  cannot be obtained with these diaphragms. However, permeation studies on pure vanadium [38], a more reasonable material than niobium [4] from an economical and engineering point of view, showed that practical current densities could be sustained by these electrodes. Figure I-6 compares the current densities obtainable with Armco iron and vanadium. The disadvantage of the vanadium (or niobium) diaphragm is that the foil is poisoned by oxide formation, resulting in a time-dependent performance of the electrodes.

The permeation studies suggest that initially hydrogen gas is adsorbed at the metal surface in a moderately fast reversible step. This is followed by diffusion of the gas atoms into the metal, the rate determining step which controls the rate of saturation of the metal and also the rate at which the equilibrium potentials in the cell are attainable (slow for vanadium and niobium; fast for iron). Finally, the atomic hydrogen at the surface accepts an electron and migrates into the solution.

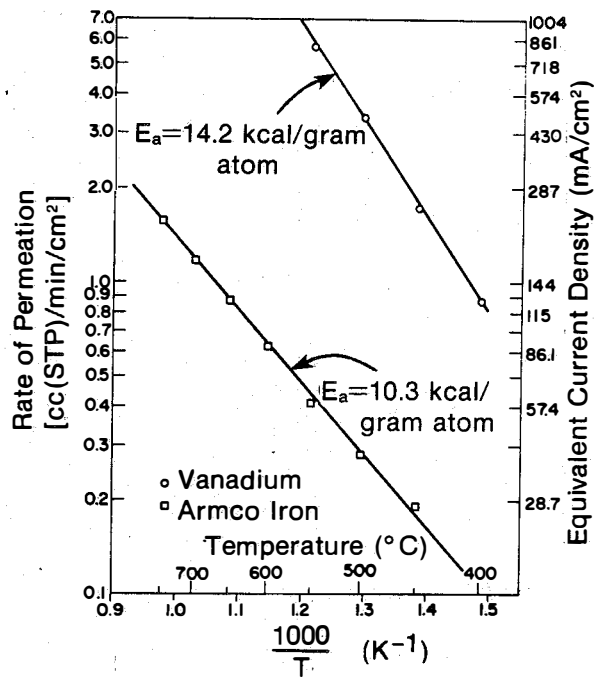


Figure I-6. Permeation Isobars of Hydrogen on Vanadium and Armco Iron Foils 0.0254 cm Thick at 1 atm [33]

In addition, Plambeck, Elder, and Laitinen [39] investigated the kinetics of the electrode reaction on an iron or tungsten flag electrode in the KCl-LiCl melt at 375°C by using steady-state voltammetric and chronopotentiometric measurements. Whereas the anodic oxidation of hydride ions to hydrogen was found to be a diffusion-controlled, one-electron process, the reverse process, of interest in the lithium hydride cell, was found to be monoelectronic but rather complex and slower, with a transfer coefficient  $\alpha = 0.4$  and an exchange current density of about  $1 \text{ mA/cm}^2$ , based on chronopotentiometric data at low cathodic overvoltages [39].

The lithium anodes employed were retained on sintered metal fiber sponge (SS-430) [33]. The interfacial tension of the liquid lithium in the sponge ensured that the metal was retained in place below the surface of the electrolyte, as long as the density of the electrolyte was not very high [33,36].

The search for suitable molten electrolytes led to determination of the phase diagrams of the lithium-hydride/alkali-metal-halide-based binary [40-42] and ternary [43,44] systems, complementing the existing literature up to 1961 [33]. Two electrolytes were selected for practical cell use because of their lower liquidus temperatures: LiH-LiCl-LiF, predominantly a solid solution with a minimum at 456°C, and LiH-LiCl-LiI, a ternary eutectic with a melting point of 330°C [44].

From EMF data on the lithium hydride/lithium halide binary melts in the 400-600°C range, the thermodynamic properties of lithium hydride were determined by Johnson, Heinrich, and Crouthamel [45]. Derived values of the standard free energy, enthalpy, and entropy of formation

at 527°C are  $\Delta G_f^\circ = -6.74$  kcal/mole,  $\Delta H_f^\circ = -20.9$  kcal/mole, and  $\Delta S_f^\circ = -17.7$  cal/degree mole [45]. The Nernst equation,  $E = E^\circ - (RT/nF)\ln[A_{\text{LiH}}/(A_{\text{Li}}/a_{\text{H}_2}^{1/2})]$ , for the reaction  $\text{Li}(\ell) + 1/2 \text{H}_2(\text{g}) \rightarrow \text{LiH}(\text{s})$  reduces to the EMF being identical to the standard EMF since the activities of the solid, liquid, and gas (1 atm) are unity in saturated solutions. The temperature dependence of the standard EMF is  $E^\circ = 0.908 - (7.70 \times 10^{-4}) T$  [45].

The extension of EMF studies as a function of temperature gave information on the regeneration characteristics of the system [33,36]. The EMF dependence on lithium hydride concentration in unsaturated solutions and the value for  $E^\circ$  led to the determination of the lithium hydride activity. With the activity of lithium hydride and the Nernst equation (above) indirect data were obtained for the hydrogen equilibrium pressure at each temperature and composition (see Fig. I-7) [33,36]. These data are in agreement with direct hydrogen partial pressure measurements carried out by Fuscoe, Carlton, and Laverty [24] at TRW.

Studies of the hydrogen diffusion through the diaphragm showed that the quantity of hydrogen diffusing through the metal is proportional to the difference in the square roots of the hydrogen pressures on each side [33,36], in agreement with earlier studies at TRW [24]. The larger the pressure at the cell, the higher is the output voltage [33,36]. Therefore, if the hydrogen pressures at the regenerator are low (see Fig. I-7), an increase to 1 atm or more by means of a pump is needed to improve the performance of the fuel cell and the efficiency of the system. Johnson et al. [33,36] pointed out that, in principle, if the ternary eutectic (LiH-LiCl-LiI) were used as the working electrolyte, at



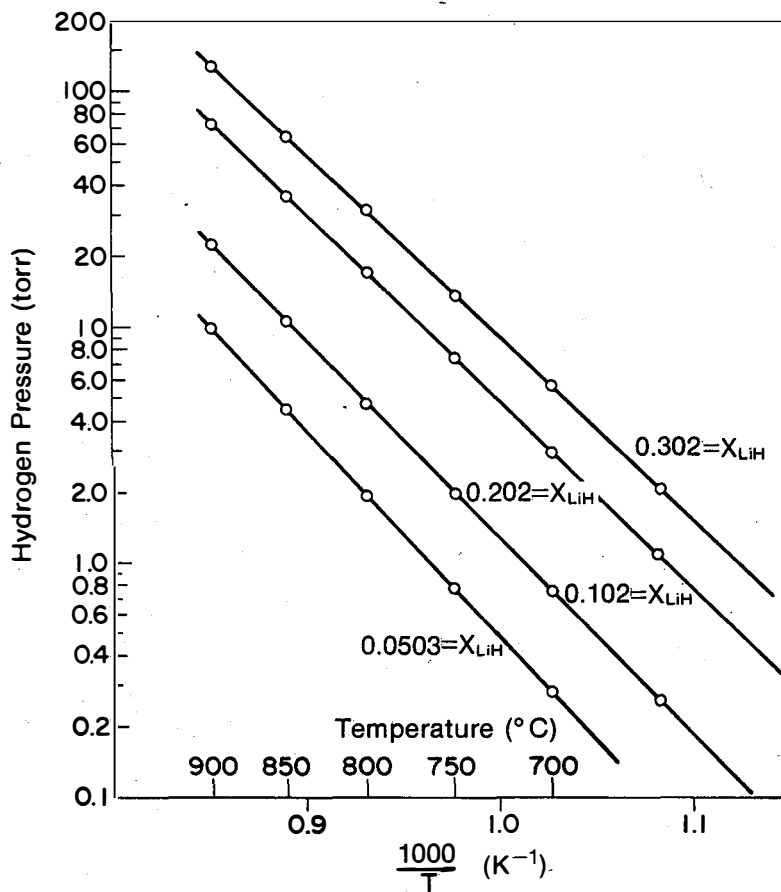


Figure I-7. Calculated Equilibrium Hydrogen Pressure for LiH-LiCl Mixtures [36]

or near saturation with respect to LiH at 330°C (or above), the regeneration pressure could be significantly increased by sending to the regenerator a mixture richer in LiH (90-95 mole % LiH). The pumping requirements would be substantially smaller, and, therefore, the efficiency of the system higher. Johnson et al. [33,35] also studied the voltage losses across the vanadium diaphragms.

At Argonne National Lab. a practical batch cell was tested for 540 hours at 535°C, giving current densities in excess of 200 mA/cm<sup>2</sup> at half the OCV (0.3 V) [36]. This cell used a nontreated 0.025-cm-thick vanadium diaphragm and LiH-LiCl-LiF molten salt. Figure I-8 shows the current-voltage characteristics of this cell [36]. The OCV followed the Nernst equation. A plot of  $p_{H_2}^{1/2}$  as a function of the OCV is linear with the slope corresponding to a reversible H<sub>2</sub>/H<sup>-</sup> couple at the vanadium electrode.

Preliminary practical cells were also tested with the eutectic LiH-LiCl-LiI, which has a lower melting point than LiH-LiCl-LiF. Larger Carnot cycle efficiencies, due to the lower operating temperatures, and possibly more effective regeneration can be expected (see above). Figure I-9 shows two experiments with this melt using 0.005-cm-thick vanadium diaphragms. These experiments differ in internal cell resistance by a factor of four. This difference was attributed to the different pretreatments of the diaphragms, yielding materials with different oxide content. This gave variable voltage losses probably associated with the overvoltage at the hydrogen electrode.

Hesson and Shimotake [46] have discussed in detail the thermodynamics and thermal efficiencies of the lithium hydride systems.

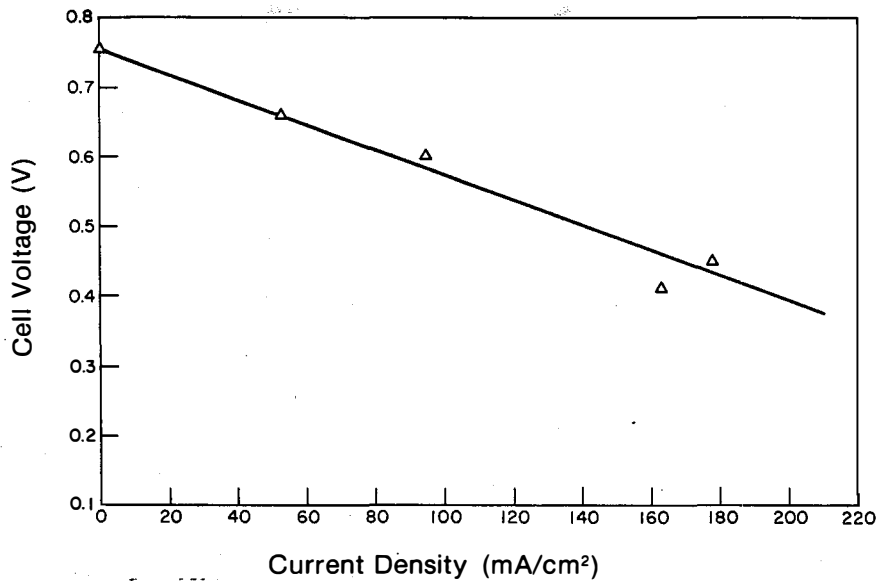


**Figure I-8. Voltage-Current Curve for a Lithium Hydride Cell with a 0.025-cm Vanadium Diaphragm at 525° C [36]**

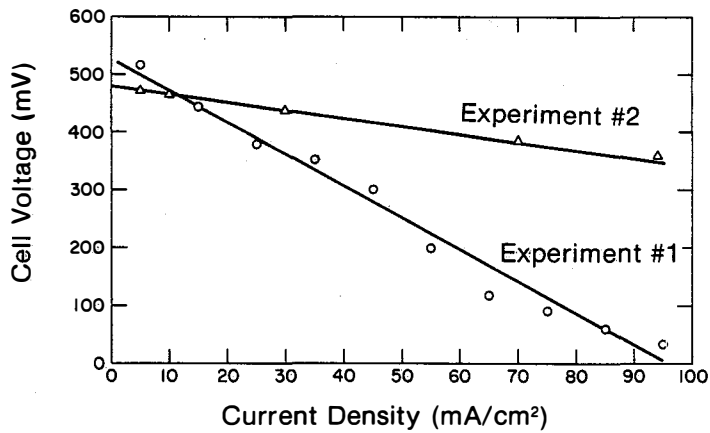


**Figure I-9. Voltage-Current Curve for a Lithium Hydride Cell with a 0.005-cm Vanadium Diaphragm at 425° C [36]**

### I.1.1.3 Conclusions

In almost 10 years (1958-1967) of research on lithium hydride thermally regenerative systems, no practical cell was developed under defined conditions in a continuous regeneration mode. Cells for batch operation showed the possibility of obtaining practical current densities ( $\sim 200 \text{ mA/cm}^2$ ) at relatively low working voltages ( $\sim 0.3 \text{ V}$ ). Most of the initial effort was largely empirical, and even the more basic work lacked reproducibility because of the difficulty in obtaining thin metal diaphragms of oxide-free vanadium.

A practical lithium hydride cell should operate at the lowest possible temperature to take advantage of the higher voltage and higher Carnot cycle efficiency thus obtained. There are still two key issues unresolved: the gas electrode and engineering problems.

With respect to the gas electrode there are again two approaches to be investigated. If thin films are used as cathode materials, modern surface spectroscopic techniques can facilitate the definition of oxide content and impurities to ensure reproducibility of the foils. More reproducible surfaces can be obtained with more adequate pretreatment of the foils. Melts operating at lower temperatures permit renewed consideration of the abandoned porous electrodes as cathodes, particularly in view of recent technological advances.

The regeneration step is not simple due to the low partial pressure of hydrogen obtained in most cases and the slow rate of hydrogen formation. Perhaps the use of the ternary eutectic  $\text{LiH-LiCl-LiI}$  would effectively raise the hydrogen equilibrium pressure in practice.

However, even for the most promising molten salt systems ( $\text{LiH-LiCl-LiF}$  and  $\text{LiH-LiCl-LiI}$ ) the engineering problems continue - circulation

and separation of the liquid/solid mixtures (e.g., solid LiH in LiH-LiCl-LiI); the presence of LiH, LiCl, and LiI in the hydrogen exit line (this problem can be minimized by taking advantage of the fast diffusion of hydrogen through metals at these regenerator temperatures); and corrosion, principally by LiH.

### I.1.2 Halide-Containing Systems

In 1959, when Werner and Shearer [19] proposed their patent on metal hydride thermally regenerative systems, they also suggested metal halides as potentially interesting TRES. In aqueous solution, a galvanic cell with a cuprous bromide paste anode and a bromine gas electrode formed  $\text{CuBr}_2$  electrochemically, with an OCV of 0.66 V. They proposed that the regeneration could be achieved by heating and driving off water and bromine and returning the cuprous bromide to the cell anode. Molten salt media were also suggested but not tested, and these cells were not pursued further.

Most of the halide-containing systems investigated and described in this section did not operate successfully. Some halide-containing systems which used two different halide compounds as anode and cathode will be described in Section I.2.1.

#### I.1.2.1 Metal Iodides

Systems based on  $\text{SnI}_2$ ,  $\text{PbI}_2$ , and  $\text{CdI}_2$  were proposed by Lockheed Aircraft Corp. [50,51] as potential TRES. The initial work was devoted to testing the performance of cells of metal|molten iodide|iodine gas. The results are summarized in Table I-3. When regeneration was attempted at temperatures up to  $1000^\circ\text{C}$ , no decomposition was observed. Misleading kinetic arguments [3] (cf. Ref. 9, 12) were used to explain the lack of

decomposition, but later it was realized that these iodides are thermodynamically stable and therefore unlikely to be thermally decomposed at this temperature [50,51,9]. The  $\text{BiI}_3$  cycle was examined in the thermal regeneration mode by Aerojet General Corp. [52], but later a thermogalvanic type of operation (see Section III) was preferred. Later, the iodide systems were employed more successfully under a different mode of operation, the coupling of electrical and thermal regeneration [51] (see Sections IV and V).

 Table I-3. SUMMARY OF GALVANIC CELL PERFORMANCE [50]<sup>a</sup>

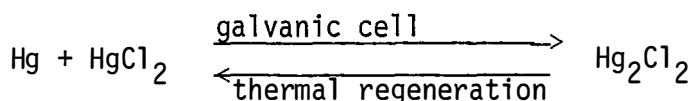
System	Cell Temperature (°C)	OCV (V)		Performance (V)		Comments
		calcd.	expt.	$I_2$ (mA/cm <sup>2</sup> )		
Sn/I <sub>2</sub>	not given	0.8	0.4	--	--	electrolyte solidified
Pb/I <sub>2</sub>	450	--	0.63	55	0.3	ohmic polarization only
Cd/I <sub>2</sub>	370	--	0.87	55	0.35	ohmic polarization only
	470	--	0.83	55	0.65	--

<sup>a</sup>The cell consisted of a porcelain beaker containing molten salt floating on a molten metal anode and a porous carbon electrode as the iodine vapor cathode (500 torr above atmospheric pressure).

#### I.1.2.2 Mercury Halides and Systems Regenerated by Thermal Disproportionation Reactions

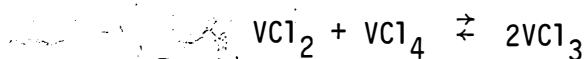
Another system proposed by Lockheed [50] was the cell:  $\text{Hg}|\text{HgBr}_2:\text{KBr}$  (50:50 mole %)| $\text{Br}_2$  at 260°C. A calculated OCV of 0.61 V was expected, but under these conditions solid  $\text{Hg}_2\text{Br}_2$  was formed due to the reaction  $\text{Hg}(\ell) + \text{HgBr}_2(\ell) \rightarrow \text{Hg}_2\text{Br}_2(\text{s})$ . Increased temperatures sublimed the  $\text{Hg}_2\text{Br}_2$ .

An analogous system, using the disproportionation reaction of mercury(I) chloride as the thermal regeneration step, was proposed by the Illinois Institute of Technology Research Institute (IITRI) [53] as a result of thermodynamic calculations [14]:



Preliminary galvanic cell measurements with a cell cathode containing  $\text{HgCl}_2:\text{AlCl}_3$  (0.33:0.67 mole fraction) and an anode of pure mercury gave an OCV of 0.73 V at 205°C, and 0.22 V with a 100- $\Omega$  load [53]. Preliminary studies of the regeneration encountered problems in separating mercury vapor from gaseous  $\text{HgCl}_2$  [54]. Diffusion of mercury vapor through a gold foil was attempted as well as the preferred, but not very effective, separation by preferential absorption of  $\text{HgCl}_2$  in NaCl-KCl melts [54].

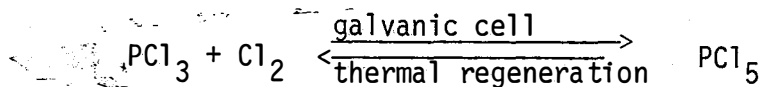
A similar system was recently proposed by IITRI [55]:



The projected OCV is 1.5 V at 175°C; the regeneration is to be performed at 700°C.

### I.1.2.3 Phosphorus Pentachloride

The following system was proposed [56,57] as thermally regenerative in organic solvents of high dielectric constant:



The conductivity of the solutions was attributed to the  $\text{PCl}_4^+$  and  $\text{PCl}_6^-$  ions [57]. Several solvents were tested: acetonitrile, dimethylformamide, dimethylsulfoxide (violent reaction in contact with the phosphorous

compounds), methylthiocyanate (reacted with  $\text{PCl}_5$ ), and nitromethane (decomposition reactions occurred with time). The supporting electrolyte was  $\text{LiNO}_3$  [57,58]. The  $E^\circ$  for the cell was 0.28 V at 15°C. A cell was built but no significant results were reported.

Some electrode kinetics studies were carried out by chronopotentiometry of the chlorides of P, Sb, and W in dimethylformamide at 25°C on platinum working electrodes [59,60].

#### I.1.2.4 Antimony Pentachloride

This is one of the halide systems tested by IITRI [61,62] from 1960-1967, as a result of theoretical thermodynamic calculations [14] in a device-oriented project. This compound was selected because of its easy dissociation into liquid antimony trichloride and gaseous chlorine at relatively low temperatures.

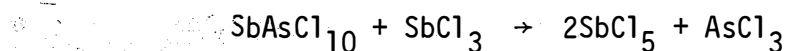
The drawback of this system is the expected poor ionic conductivity of the antimony chlorides, which can be improved slightly to about  $10^{-3} \text{ ohm}^{-1} \text{ cm}^{-1}$  by addition of arsenium trichloride and minor amounts of aluminum chloride. Cells constructed with  $\text{SbCl}_3$  anodes and chlorine cathodes containing  $\text{SbCl}_5$  gave about 0.3 V and the mixture  $\text{SbCl}_3:\text{AsCl}_3$  (1:1) gave about 0.4-0.5 V, but the cell resistance was still very high [63]. A solid electrolyte ( $\text{PbCl}_2$  doped with KCl) was used in a small cell with some success. The conductivities were studied, as a function of temperature, of several other solid electrolytes based on  $\text{PbCl}_2$ ,  $\text{PbF}_2$ ,  $\text{BiCl}_3$ , and ion exchange polymers (silicates, sodium phosphotungstates, and sodium polyphosphates), but none exhibited behavior which would be suitable for this type of cell [63].

The dissociation reaction  $\text{SbCl}_5(\ell) \rightarrow \text{SbCl}_3(\ell) + \text{Cl}_2(\text{g})$  was studied



in detail. The regeneration was demonstrated satisfactorily (80-90% dissociation of  $\text{SbCl}_5$ ) over a wide range of temperatures (250-350°C) and pressures (1-25 atm), producing liquid  $\text{SbCl}_3$  and gaseous chlorine [61, 62].

The work with mixtures of antimony, arsenic, and aluminum chlorides was largely empirical with respect to the species present in solution. Plots of EMF as a function of the ratio of  $\text{SbCl}_5$  to  $\text{SbCl}_3$  in  $\text{AsCl}_3$  solvent show a variation of about 300 mV when the ratio is changed by a factor of 10 at low  $\text{SbCl}_5$  content (70°C). From ratios of 1:1 to 100:1, the EMF is essentially independent of the composition and equal to  $\sim 0.65$  V. It was proposed that mixtures of Sb and As chlorides can be oxidized by free chlorine-forming species containing As(V) which could participate in the electrode reactions. McCully and coworkers [61,62] suggested the following total cell reaction:



A unit of 500-W formal power was built with 10 cells connected in series with  $\sim 0.3$ -cm spacing between anode and cathode compartments. The compartments were separated by the solid electrolyte (woven glass cloth impregnated with doped  $\text{PbCl}_2$ ). The anode and cathode compartment compositions were  $\text{SbCl}_3$ :  $\text{AsCl}_3$  (2:1 mole ratio) and  $\text{SbCl}_5$ : $\text{AsCl}_3$  (4:1 mole ratio), respectively, both containing 4 w/w %  $\text{AlCl}_3$ . The cell had a heat exchanger between the batteries and the regenerator unit. The regenerator worked successfully but the cell performance was very poor. The system could be charged to an output potential of 1.4 V, which decreased very rapidly without appreciable load. It was verified that, under pressure, cracks in the electrolyte allowed the mixing of the

anode and cathode compartments [61,62].

The use of solid electrolytes was discouraged for this system. It was proposed that research should be continued in the direction of improving the conductivity of the antimony chloride solutions [62], since the regeneration in this system can be accomplished easily, with minor corrosion problems [63].

#### 1.1.2.5 Hydrogen Halides and Other Halides

Rightmire and Callahan [64] described a hydrogen iodide thermally regenerative system in 1963. The fuel cell operated at 120°C with two porous platinized electrodes sandwiching the electrolyte, an aqueous solution of HI. The fuel cell reactions were hydrogen gas oxidation at the anode and iodine reduction at the cathode. Regeneration was performed by flowing the electrolyte through a heat exchanger for pre-heating and then catalytically decomposing it in a reactor at 1000°C (using a Pt catalyst supported on alumina or a natural clay base). The total pressure of the closed system was 6-7 atm. The equilibrium mixture  $2\text{HI}(\text{g}) \xrightleftharpoons{\text{H}_2\text{O}(\text{g})} \text{H}_2(\text{g}) + \text{I}_2(\text{g})$  was then cooled. Iodine dissolved in HI as  $\text{I}_3^-$  (condensed) and the solution  $[\text{H}_2\text{O}, \text{HI}, \text{I}_2(\text{I}_3^-)]$  was fed to the cathode. The hydrogen gas separated from the condensed liquid and was fed to the anode compartment of the fuel cell. When 43%  $\text{H}_2\text{O}$  and 57% HI were used as electrolyte at 120°C, the OCV was 0.5 V. The authors claim that a power output of 0.03-0.08  $\text{W}/\text{cm}^3$  at 75% thermal efficiency (the Carnot efficiency was 91%) can be obtained in this system with current densities as high as 100  $\text{mA}/\text{cm}^2$ . The authors suggested that hydrogen bromide would also be suitable for thermal regeneration.

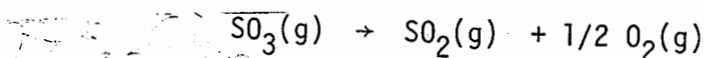
Proposals by Rowlette and others [3,13] to use the iodine mono-

bromide system and other metal halide systems are based on thermodynamic and kinetic data. The melting point of IBr is 42°C and its boiling point is 116°C. The conductivity is low but can be increased by addition of KBr. At 300°C, IBr is 20% decomposed, whereas at room temperature ca. 8% is decomposed. The system thus seems feasible for thermal regeneration but no further experimental studies were carried out.

### 1.1.3 Oxide-Containing Systems and Other Systems

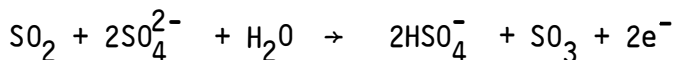
#### 1.1.3.1 Sulfur dioxide-trioxide

In 1961-1962, Kumm [65] investigated the system in which the regeneration reaction is

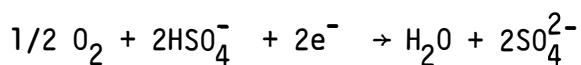


and the cell  $\text{SO}_2|\text{electrolyte}|\text{O}_2$ . Thermodynamic studies of the regeneration steps indicated that at about 1000°C the sulfur trioxide is largely decomposed. Kumm [65] presented equilibrium data over a wide range of temperatures. To separate the two gases formed, two methods were suggested: absorption of  $\text{SO}_2$  by water, or condensation of  $\text{SO}_3$  to act as a scrubber for  $\text{SO}_2$ . The first method is not feasible due to the high vapor pressures of water at temperatures at which  $\text{SO}_2$  can be distilled from water.

The galvanic cell reactions



and



were expected in the two media tested: molten eutectic  $\text{LiHSO}_4$ - $\text{KHSO}_4$  at

$\sim 150^{\circ}\text{C}$ , and dimethyl sulfate saturated with  $\text{LiHSO}_4\text{-KHSO}_4$ . For the first medium at  $\sim 180^{\circ}\text{C}$  an OCV of  $\sim 0.1$  V was found and for the second at  $\sim 95^{\circ}\text{C}$  an OCV of  $\sim 0.17$  V was obtained. Current densities were very low and it was concluded that a thermally regenerative electrochemical system based on  $\text{SO}_2/\text{SO}_3$  was not feasible.

More recently, Wentworth [66] has been investigating the  $\text{SO}_2/\text{SO}_3$  system in an alkaline medium. An OCV of about 1 V is expected. In his prior studies the molten salt  $\text{NH}_4\text{HSO}_4$  has been shown to undergo decomposition in two steps which can regenerate  $\text{SO}_2$ . In the first step at about  $400^{\circ}\text{C}$ ,  $\text{NH}_4\text{HSO}_4$  is decomposed into  $\text{NH}_3(\text{g})$ ,  $\text{H}_2\text{O}(\text{g})$ , and  $\text{SO}_3(\text{g})$  in a reaction which stores solar thermal energy. After the three gases have been separated the  $\text{SO}_3$  can be decomposed into  $\text{SO}_2(\text{g})$  and  $\text{O}_2$  at a higher temperature ( $950^{\circ}\text{C}$ ) in a catalyzed reaction. Studies of the system are underway. So far, low current densities and voltages have been obtained [66].

#### I.1.3.2 Metal Oxides

From thermodynamic considerations but without experimental data Lyons [67] proposed metal oxide fuel cells in which lower-valent metal oxides are oxidized in alkaline fuel cells to the higher-valent metal oxides. The latter are reconverted to the lower-valent oxides by heat or chemical reduction. The oxides proposed in this patent are of copper, cobalt, manganese, lead, and iron.

Again from thermodynamic considerations, McKenzie and Howe [68] proposed cells with oxides or oxyanions of rare earths, and group VIA or VIB metals, e.g.,  $\text{UO}_3/\text{U}_3\text{O}_8$ .

### 1.1.3.3 Other Compounds and the Sn|Sn(II), Cr(III), Cr(II)|C System

Werner and Shearer [19] tested the system of an iron(II) sulfide anode in molten sodium polysulfide (110°C) and a sulfur cathode. A 0.25-V OCV was obtained and iron disulfide produced. Since the standard free energy of formation of iron disulfide from ferrous sulfide and sulfur is zero at 700°C, the authors suggested that at this temperature the cathode and anode regeneration could be accomplished. They also suggested lithium nitride formation as a possible TRES, though of very low cell potential ( $\sim 0.1$  V).

### 1.1.3.4 The Sn|Sn(II),Cr(III),Cr(II)|C System

In 1886, Case [69] reported what appears to be the first thermally regenerative system described in the literature. It produced electrical energy periodically if a periodical temperature change was applied to the system. Thus, at a temperature of 90-100°C the system delivered electrical energy and at 15-20°C it was spontaneously chemically regenerated. Case's system is based on the galvanic cell composed of a tin anode and an inert cathode (e.g., porous graphite) reversible to the soluble species Cr(II) and Cr(III). At 90-100°C the galvanic cell operates and generates electricity. When the reactants are exhausted, the regeneration is performed by disconnecting the electrical circuit and letting Cr(II) ions reduce chemically the Sn(II) ions to Sn metal, which deposits on the anode. In 1895, Skinner improved the anode by replacing pure tin with tin amalgam [70; 128, p. 348].

A continuous regeneration operation might be obtained by flowing the electrolyte enriched with Sn(II) and Cr(II) ions to a lower-temperature compartment, and by returning the precipitated tin to the

anode and the Cr(II)-enriched solution to the cell (cf. with Section II.1.3).

Almost a century later, Case's system has been reinvestigated by Vedel, Soubeyrand, and LeQuan [71]. The temperature dependence of the EMF of the cell  $\text{Sn}|\text{Sn(II)}||\text{Cr(III),Cr(II)}|\text{C}$  was measured at various electrolyte compositions ( $\text{HCl}:\text{CaCl}_2$ ) and changed sign between 25°C and 95°C. These authors obtained a temperature coefficient for the cell of 1.42 mV/°C. By choosing the electrolyte composition, the inversion of the sign can be made to occur at any temperature within the given range. Low voltages, -60 to +60 mV, and low currents, ~3 mA, were obtained.

#### I.1.4 Summary and Discussion of TRES Type 1

Table S-2 represents a summary of the thermally regenerative electrochemical systems investigated or proposed in the literature covered by Sec. I.1.

The majority of the systems reported in Sec. I.1 utilized molten salt electrolyte systems and high regeneration temperatures (500 - 1000°C). Several halide systems were shown not to decompose appreciably within the temperature range investigated. In some cases slow kinetics was responsible for the low decomposition yields. Catalytic decomposition was attempted only in the HI system. With the use of suitable catalysts, other systems may deserve renewed consideration. Very little experimental work has been done in oxide systems.

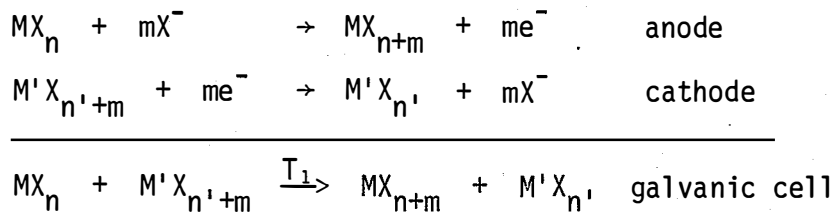
Aqueous and nonaqueous systems have received far less attention than molten salt media--principally because of the lower operating temperatures, which would not be suitable for coupling with nuclear heat sources but which certainly would be adequate for solar applications.

Systems operating at lower temperatures [analogous to Sn|Sn(II), Cr(III),Cr(II)|C], discovered by Case in the 19th century, have not been thoroughly investigated. This is an area in which existing thermodynamic data or new experimental data may indicate systems of better performance than Case's system.

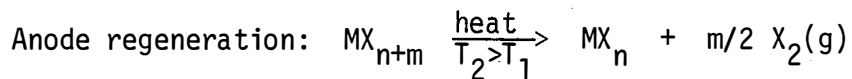
I.2 MULTIPLE ELECTROCHEMICAL REACTION PRODUCTS AND MULTIPLE-STEP REGENERATION

A more complex galvanic cell was devised in which there are two electrochemical products (See Type 2, in the Introduction). The anode and cathode are composed of different compounds, e.g., metal halides or oxides. The anode and cathode are regenerated separately, generally at different temperatures [72]. The general scheme of such a system for metal halides is:

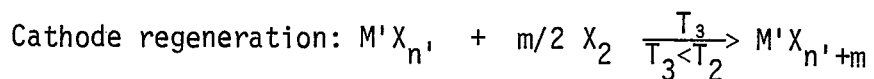
Galvanic Cell Reactions



Regeneration Reactions



After separation of  $MX_n$  and  $X_2$ ,  $MX_n$  is returned to the anode and  $X_2$  is allowed to react with  $M'X_{n'}$ , thus regenerating the cathode.



These systems are clearly much more complex than those described in

Section I.1. A general problem arises when the anode regeneration step produces two products in the same physical state. For instance, if  $\text{SnCl}_4$  or  $\text{TeCl}_4$  are the result of the anodic processes, at the thermal decomposition temperatures the two products  $\text{SnCl}_2$  or  $\text{TeCl}_2$  and  $\text{Cl}_2$  are in the gaseous state, and the difficult separation constitutes a very severe limitation to the practical application of this type of system [61,62]. If  $\text{SbCl}_5$  or  $\text{CuCl}_2$  are formed as a result of the anodic reaction, the regeneration yields  $\text{SbCl}_3(\ell)$  or  $\text{CuCl}(\ell)$  and  $\text{Cl}_2(\text{g})$ , which can be separated by a relatively simple process (see Section I.1.2.4 on  $\text{SbCl}_5$ ). Self-discharge processes pose additional difficulties to the utilization of cells of this type.

This approach to thermally regenerative galvanic cells was proposed and researched from 1960 to 1969 at IITRI (formerly Armour Research Foundation) by McCully, Rymarz, and Snow, among others. Thermochemical and thermodynamic calculations disclosed several chemical compounds as potentially suitable for thermal regeneration and galvanic cell operation [14]. Sections I.1.2.2 and I.1.2.4 describe the  $\text{SbCl}_5$  and  $\text{HgCl}_2$  systems, which composed part of the research effort at IITRI on simpler halide systems. Sections I.2.1 and I.2.2 deal with the more complex cell concept.

### I.2.1 Metal Halides

The reactions of metal halides studied at IITRI during the 1960-1967 period are summarized in Table I-4, in which selected galvanic cell results are assembled. The proposed diagram for this type of system, including the cell, the regenerators, and the heat exchangers, is shown in Fig. I-10.



Table I-4. CELL VOLTAGES OBTAINED IN THE REACTIONS OF METAL HALIDES [52,73]

Reaction <sup>a</sup>	Composition		Temperature (°C)	Open-Circuit Voltage (V)	Voltage Under 100-ohm Load (V)	Comments
	Anode	Cathode				
$\text{SnCl}_2 + \text{SbCl}_5 \rightarrow \text{SnCl}_4 + \text{SbCl}_3$	$\text{SnCl}_2:\text{AlCl}_3$ 50 w/w %	$\text{SbCl}_5:\text{SbCl}_3$ <sup>b</sup>	150	0.47	0.3 <sup>b</sup>	Stable performance for over 2 weeks
$\text{SnBr}_2 + \text{SbBr}_5 \rightarrow \text{SnBr}_4 + \text{SbBr}_3$	$\text{SnBr}_2$	$\text{SbBr}_2 + \text{Br}_2$ <sup>c</sup>	not given	0.15	--	Expected OCV of 0.54 V; low $\text{Br}_2$ concentration responsible for low OCV
	Mole Fraction in $\text{AlCl}_3$					
$\text{SnCl}_2 + 2\text{CuCl}_2 \rightarrow \text{SnCl}_4 + 2\text{CuCl}$	0.23	0.25	205	0.70	0.29	Platinum electrodes
	0.32	0.25	205	0.85	0.30 <sup>d</sup>	
	0.41	0.25	205	0.97	0.32	
$\text{CuCl} + \text{CuCl}_2 \rightarrow \text{CuCl}_2 + \text{CuCl}$	0.31	0.25	253	0.25	0.11	Platinum electrodes
$\text{TeCl}_2 + 2\text{CuCl}_2 \rightarrow \text{TeCl}_4 + 2\text{CuCl}$	1	0.25	205	0.92	0.51 <sup>f</sup>	Platinum electrodes
	0.40	0.25	205	0.58	0.20	
	0.06 <sup>e</sup>	0.1 <sup>e</sup>	195	0.46	--	
$\text{HgCl} + \text{CuCl}_2 \rightarrow \text{HgCl}_2 + \text{CuCl}$	0.40	0.25	200	0.75	0.26	Platinum electrode Graphite electrode- Cathode disintegrated Tungsten electrodes Tantalum electrodes
	0.40	0.25	200	--	--	
	0.40	0.25	230	0.71	0.29	
	0.40	0.25	210	0.66	--	

<sup>a</sup>1st reactant: anode; 2nd reactant: cathode.

<sup>b</sup>Electrolyte:  $\text{AlCl}_3:\text{KCl}$  eutectic; load: 10,000 ohms; current density: 50  $\text{mA}/\text{cm}^2$ .

<sup>c</sup>Electrolyte:  $\text{AlBr}_3:\text{KBr}$  eutectic.

<sup>d</sup>Current densities: 13  $\text{mA}/\text{cm}^2$  for 9-mm electrolyte thickness; 50  $\text{mA}/\text{cm}^2$  for 3-mm thickness and stationary operation; and 60  $\text{mA}/\text{cm}^2$  for flow operation.

<sup>e</sup>In  $\text{AlCl}_3:\text{KCl}$  eutectic.

<sup>f</sup>Current density: 22  $\text{mA}/\text{cm}^2$  for 9-mm electrolyte thickness; current density increases with decreased electrolyte thickness.

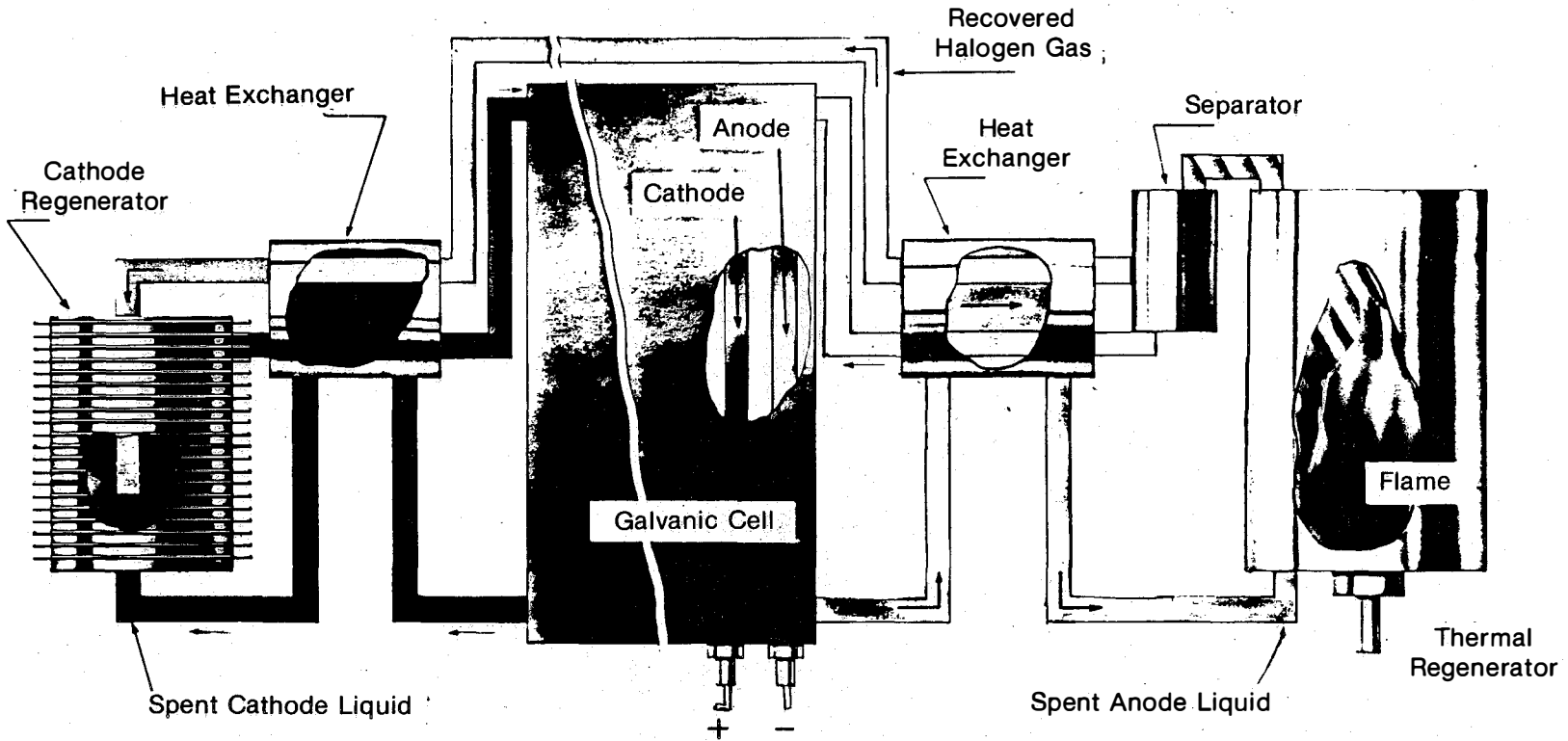


**Figure I-10. Scheme of Thermally Regenerative Electrochemical System Proposed by McCully et al. [72,73]**

The research on systems containing tin halides was abandoned due to high decomposition temperatures of  $\text{SnCl}_4$  ( $>1700^\circ\text{C}$ ) and the severe corrosion problems associated with  $\text{SnCl}_2(\text{g})$  and  $\text{Cl}_2(\text{g})$  at this temperature, in addition to the problems of separating the two gaseous products [53,54]. The anode regeneration in  $\text{CuCl}$  systems did not appear very difficult [ $\text{CuCl}_2(\text{l}) \rightarrow \text{CuCl}(\text{l}) + 1/2 \text{Cl}_2(\text{g})$ ] at temperatures below the melting point of  $\text{CuCl}$  ( $1365^\circ\text{C}$ ), but the galvanic cell performance [ $\text{CuCl}$  (anode)| $\text{CuCl}_2$  (cathode)] was poorer than that of other systems (see Table I-4).

The  $\text{TeCl}_2(\text{anode})|\text{CuCl}_2(\text{cathode})$  system was considered the most promising based on the galvanic cell performance (see Table I-4). Therefore, a more detailed analysis of the electrode kinetics of both electrodes was performed [70]. The electrochemical oxidation reaction  $\text{Te(II)} \rightarrow \text{Te(IV)} + 2\text{e}^-$  was found to be faster on Pt electrodes than on Ta electrodes. On Pt electrodes an exchange current of about  $100 \text{ mA/cm}^2$  (16 mole %  $\text{TeCl}_2$  in  $\text{AlCl}_3$ ) was found. Tafel curves for this oxidation on Ta and Pt are shown in Fig. I-11. The electrode reaction  $\text{Cu(II)} + \text{e}^- \rightarrow \text{Cu(I)}$  was found to be much slower than the corresponding  $\text{Te(II)}$  oxidation. Tantalum electrodes were found to catalyze this reduction reaction. Tafel curves for the reduction on Pt and Ta are shown in Fig. I-12. The cupric chloride cathode showed poorer performance than the  $\text{TeCl}_2$  anode. Current densities of about  $35 \text{ mA/cm}^2$  were obtained at 0.1-V polarization (IR-free).

Cells four inches in diameter were constructed and tested which produced current densities of about  $20 \text{ mA/cm}^2$ . Based on the electrode kinetics studies, using platinum anodes and tantalum cathodes and 0.1-

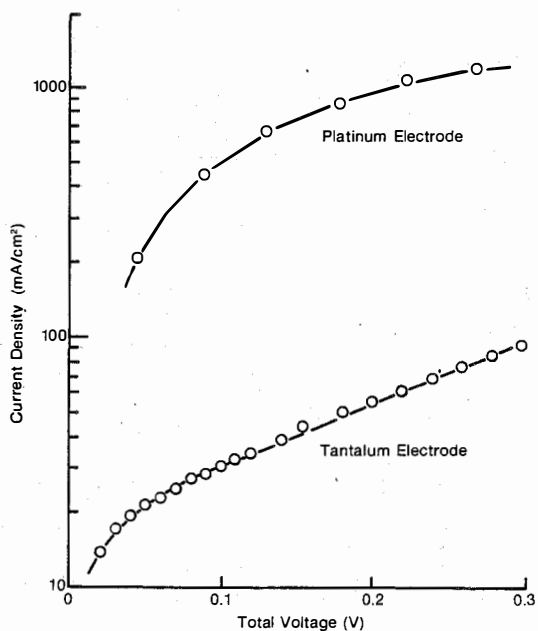


Figure I-11. Tafel Plots for the Electrochemical Oxidation of Te(II) (16 Mole % in AlCl<sub>3</sub>) at 200° C

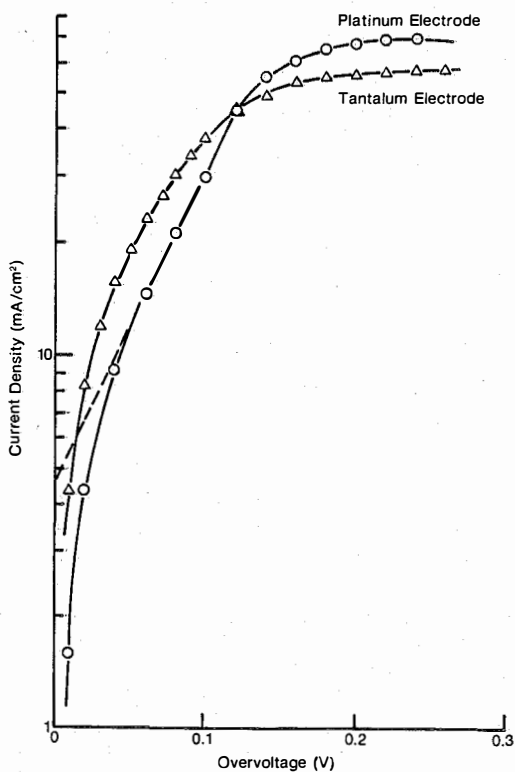


Figure I-12. Tafel Plots for the Electrochemical Reduction of Cu(II) (4 Mole % in 3:1 Molar Ratio AlCl<sub>3</sub>:KCl) at 200° C. [74]

cm interelectrode spacing, performance improvements of a factor of 10 were projected [62]. This optimistic [4] estimate increased by another factor of 2.5 by increasing the  $\text{TeCl}_2$  concentration in the anode. A unit of formal 5-kW power based on this concept, was built and operated for about 30 minutes, after which leakages resulted in cell shutdown [55,62].

The effect of the presence of  $\text{AlCl}_3$  in the compartment, in which  $\text{TeCl}_2$  and  $\text{TeCl}_4$  were also present, is shown in Fig. I-13. The data referred to as "high Te" were obtained from cells in which the Te/Al mole ratio was greater than unity, whereas the "low Te" data refer to ratios of 0.02-0.35. The experimental lines obtained were consistent with the theoretical Nernst slopes [61]. The large effect of the Te/Al mole ratio suggested that there was an appreciable interaction between the two chlorides [61]. Species characterization studies were not performed. Data on tellurium species in chloroaluminate melts are available in the literature [75]. More recent studies of electrode processes as a function of chloroaluminate melt acidity are also available [76].

Examples of discharge curves for  $\text{TeCl}_2|\text{CuCl}_2$  cells are shown in Fig. I-14. The voltage under load was maintained for a period of about 20 hours at a current efficiency level of 75% (50-ohm load) [61].

Though the galvanic cell studies indicated the feasibility of a  $\text{TeCl}_2|\text{CuCl}_2$  cell, the ability of this system to undergo thermal regeneration was not successfully demonstrated. At the regeneration temperatures ( $>550^\circ\text{C}$ ),  $\text{TeCl}_4$  decomposes into gaseous  $\text{TeCl}_2$  and  $\text{Cl}_2$ , and several years of research were spent in trying to devise a suitable and efficient separation method [70,77,78].

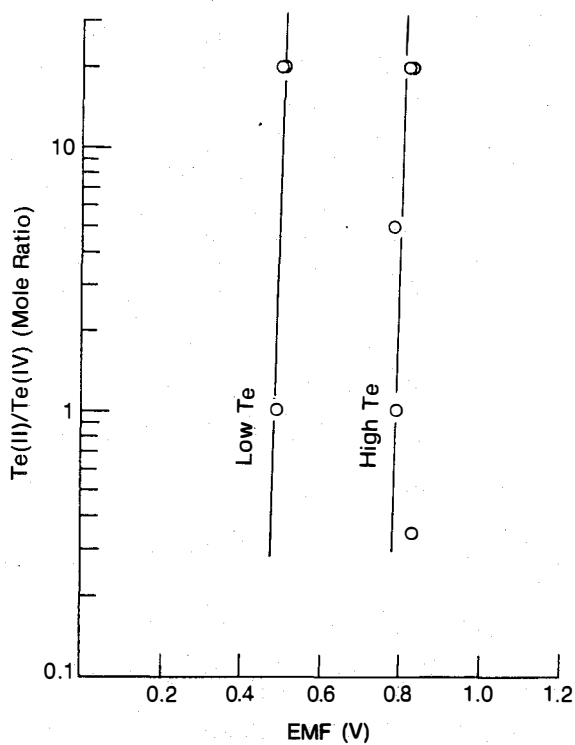


Figure I-13. Potentials of the  $\text{TeCl}_2$ (Anode)/ $\text{CuCl}_2$  (Cathode) Galvanic Cells in Molten  $\text{AlCl}_3$  [61]

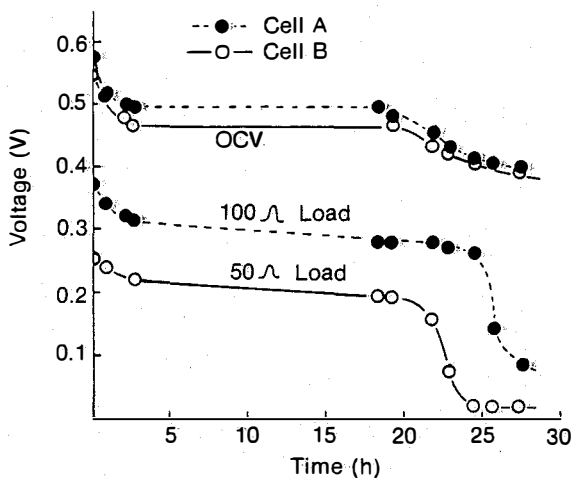


Figure I-14. Discharge Curves for  $\text{TeCl}_2$ (Anode)/ $\text{CuCl}_2$ (Cathode) Cells under 50- and 100-Ohm Loads [61]

A successful but energy-inefficient separation was achieved by rapidly quenching the gaseous mixture at the liquid nitrogen temperature, producing solid  $\text{TeCl}_2$ . Measurements of the rate of recombination of  $\text{TeCl}_2$  and  $\text{Cl}_2$  indicated that at  $500^\circ\text{C}$  the recombination was complete within 20 ms [61].

A second approach to separate  $\text{TeCl}_2$  from  $\text{Cl}_2$  was to keep the  $\text{TeCl}_2$  in the liquid phase by forming a coordination complex with one of the chlorides of group IIIB of the periodic chart:  $(\text{Al, Ga, Te}) \text{TeCl}_4 \cdot \text{complex}(\ell) \xrightarrow{\text{heat}} \text{TeCl}_2 \cdot \text{complex}(\ell) + \text{Cl}_2(\text{g})$ . Extensive phase diagram, thermal analysis, and conductometric studies were carried out [77,78]. Table I-5 summarizes the regeneration study results. The best regeneration yields were on the order of 2% with  $\text{TeCl}_4 \cdot 2\text{AlCl}_3 \cdot \text{KCl}$ . It is not very clear whether a large improvement in the regeneration of this system can be achieved.

Table I-5. SUMMARY OF EXPERIMENTAL REGENERATOR OPERATION [74,77,78]

System	% Regeneration (single pass)	Operating Pressure (atm abs)	Temperature( $^\circ\text{C}$ )
$\text{TeCl}_4 \cdot \text{TlCl}$	0.1 <sup>a</sup>	15	500
$\text{TeCl}_4 \cdot \text{GaCl}_3$	0.6	18	650
$\text{TeCl}_4 \cdot \text{AlCl}_3$	0.7	10	572
$\text{TeCl}_4 \cdot \text{AlCl}_3$	0.9	11	608
$\text{TeCl}_4 \cdot 2\text{AlCl}_3$	0.4 <sup>b</sup>	20	230
$\text{TeCl}_4 \cdot 2\text{AlCl}_3 \cdot \text{KCl}$	1.8	18	548

<sup>a</sup>In the presence of  $\text{Cl}_2$ ,  $\text{TlCl}$  is oxidized to  $\text{TlCl}_3$ , which at this temperature and pressure seems to decompose, yielding ca. 20%  $\text{Cl}_2$  [77].

<sup>b</sup> $\text{AlCl}_3$  sublimes under these conditions.

### I.2.2 Metal Oxides

The thermochemical and thermodynamic calculations by Snow [14] indicated that the oxides listed in Table I-6 are thermally reversible compounds [62]. Some of these oxides were selected for practical cell tests in 1960. Test cells were cylindrical pellets having three layers - anode|electrolyte|cathode - obtained by pressing dry powdered materials [62,79]. The electrolyte layer (70-90% inert  $ZrO_2$  mixed with an electrolyte of  $Na_2CO_3:Li_2CO_3$  eutectic) was pressed first and then the anode and cathode layers were pressed at opposite ends. The cells were placed between platinum electrodes, and galvanic cell tests were conducted.

Typical galvanic cell results with selected oxides are shown in Table I-7 [79]. The conductivity of the cells improved upon addition of graphite. However, this material was obviously incompatible with the anode regeneration step due to the formation of carbon oxides and reduction of the metal oxides to metal. The work on oxides was abandoned in favor of the halide systems, which seemed more promising (see Section I.2.1) [62,69].

### I.2.3 Discussion of TRES Type 2

This approach of multiple electrochemical reaction products and multiple-step regeneration (see Fig. S-2) is far more complex than the remaining types of TRES. To date, none of the systems investigated displayed both good cell performance and good regeneration performance. It is clear that most of the systems promising from an electrochemical point of view had a very poor regenerator performance if two gases were the result of the thermal regeneration. It is our feeling that systems of this type should be investigated only if the thermal decomposition



products are in different physical states, or if major breakthroughs in the separation of gases are made in the near future.

Table I-6. THERMALLY REVERSIBLE OXIDES [62]

Reaction	Calculated Reversal Temperature(°C)
$3\text{MnO}_2 \rightleftharpoons \text{Mn}_3\text{O}_4 + \text{O}_2$	652
$2\text{Mn}_3\text{O}_4 \rightleftharpoons 6\text{MnO} + \text{O}_2$	1427
$2\text{Ag}_2\text{O} \rightleftharpoons 4\text{Ag} + \text{O}_2$	127
$4\text{CuO} \rightleftharpoons 2\text{Cu}_2\text{O} + \text{O}_2$	1127
$2\text{Sb}_2\text{O}_5 \rightleftharpoons 2\text{Sb}_2\text{O}_4 + \text{O}_2$	527
$2\text{Sb}_2\text{O}_4 \rightleftharpoons 2\text{Sb}_2\text{O}_3 + \text{O}_2$	927
$\text{Tl}_2\text{O}_3 \rightleftharpoons \text{Tl}_2\text{O} + \text{O}_2$	677
$2\text{PbO}_2 \rightleftharpoons 2\text{PbO} + \text{O}_2$	362
$6\text{UO}_3 \rightleftharpoons 2\text{U}_3\text{O}_8 + \text{O}_2$	1327
$\text{U}_3\text{O}_8 \rightleftharpoons 3\text{UO}_2 + \text{O}_2$	1827
$2\text{Rb}_2\text{O}_3 \rightleftharpoons 4\text{RbO} + \text{O}_2$	527
$4\text{RbO} \rightleftharpoons 2\text{Rb}_2\text{O} + \text{O}_2$	777
$\text{Rb}_2\text{O}_3 \rightleftharpoons \text{Rb}_2\text{O} + \text{O}_2$	652

Table 1-7. CHARACTERISTICS OF OXIDE CELLS [79]

Cell	Composition in Molten Eutectic $\text{Li}_2\text{CO}_3:\text{Na}_2\text{CO}_3^a$		EMF (V)		Resistance (ohm)
	Anode	Cathode	Calcd.	Measured	
$\text{MnO} \text{CO}_3^{2-} \text{Sb}_2\text{O}_5$	80 wt % MnO	80 wt % $\text{Sb}_2\text{O}_5$	0.29	0.17	2800
$\text{MnO} \text{CO}_3^{2-} \text{Sb}_2\text{O}_5$	same as above with 30 vol % graphite added		0.29	0.27	29
$\text{Cu}_2\text{O} \text{CO}_3^{2-} \text{Sb}_2\text{O}_5$	graphite added		0.30	0.23	2000

<sup>a</sup>Electrolyte: 80 wt %  $\text{ZrO}_2$ ; 20 wt % eutectic  $\text{Li}_2\text{CO}_3:\text{Na}_2\text{CO}_3$ .

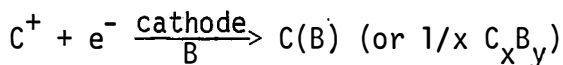
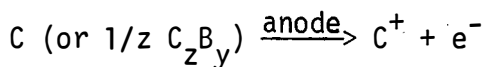
**SERIO** 

## SECTION II

## THERMAL REGENERATION: ALLOYS OR BIMETALLIC SYSTEMS

A schematic representation of a thermally regenerative alloy system is shown in Fig. II-1 (see Type 3 above in the Introduction). Liquid metal C is oxidized to the respective  $C^+$  ions at the anode. These ions migrate into the  $C^+$  conducting electrolyte and undergo reduction and solubilization in B or alloy formation [ $C(B)$  or  $C_xB_y$ ] at the cathode. This alloy, alone or combined with anode material, is pumped (e.g., electromagnetically) or flows to a boiler where it is heated above the boiling point of the metal of lower boiling point. In a separator the vapor phase, richer (not necessarily pure) in the more volatile component, is separated from the liquid phase, richer in the less volatile metal, and the two streams are individually returned to the galvanic cell. Therefore, the electrochemical reaction product is a liquid metal alloy [ $C(B)$ ] or an intermetallic compound ( $C_xB_y$ ) in a concentration cell with respect to the electroactive species  $C^+/C$ .

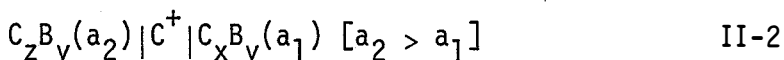
The electrode reactions are essentially identical in opposite directions:



Such cells can be represented schematically as



or



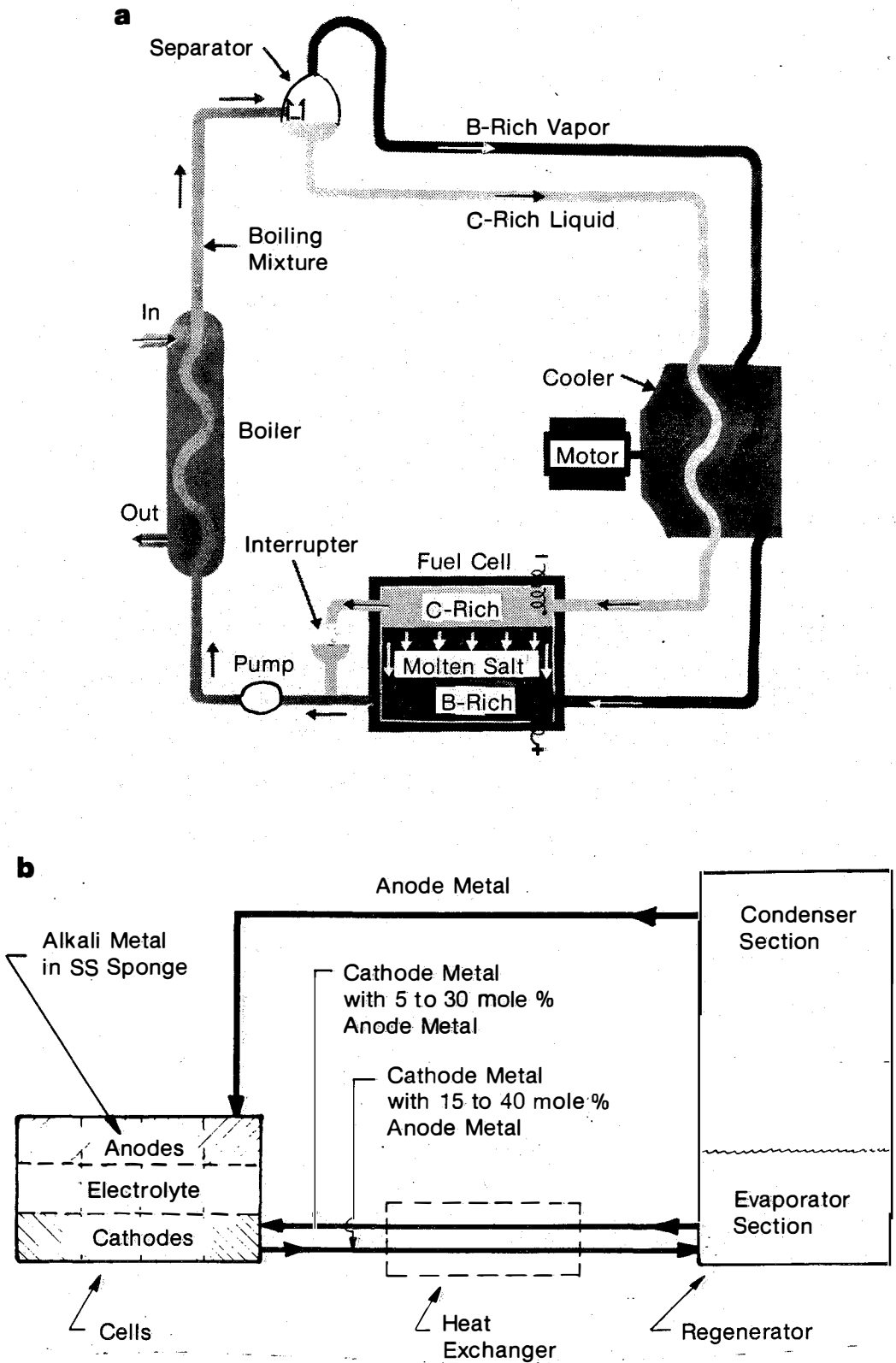


**Figure II-1. Schematic Representation of a Thermally Regenerative Alloy System (a) for Amalgam Cells C = Na, K; B = Hg; and (b) for Bimetallic Cells**

in which C and B represent a variety of metals (e.g., C = Li, Na, K, Rb, Cs, Mg, Ca; and B = Hg, Cd, Zn, TlP, In, Ga, Pb, Sn, Bi, P) and  $a_i$  represents the activity of metal C in each electrode. The cell potential can be expressed as a function of the activities of C as follows:

$$E = - \frac{RT}{nF} \ln \frac{a_1}{a_0} = - \frac{RT}{nF} \ln a_1 \quad (\text{if } a_0 = 1, \text{ pure metal}) \quad \text{II-3}$$

or

$$E = - \frac{RT}{nF} \ln \frac{a_1}{a_2} \quad \text{II-4}$$

The potential decreases with increasing activity of C in the alloy formed at the cathode. The more negative the free energy of formation of the intermetallic compound or alloy, the more thermodynamically stable it is and the larger the cell potential is that will be obtained due to the low activity of C in the compound or alloy.

The electrolytes for most of these cells are molten salts because of the high conductivity of these media ( $\sim 10^{-1} - 10 \text{ ohm}^{-1} \text{ cm}^{-1}$ ) compared to that of aqueous electrolyte solutions ( $\sim 10^{-4} - 10^{-2} \text{ ohm}^{-1} \text{ cm}^{-1}$ ) and because of the high exchange currents obtained at metal electrodes due to small activation polarization [80]. The major voltage losses in this type of cell are ohmic.

Many of the important parameters in selecting a bimetallic system for feasible thermal regeneration are implicit in the phase diagram of the system. An approximate analysis of the system can be made by considering just the CB binary diagram (e.g., Fig. II-2) though in actual operation, the presence of the electrolyte components, soluble to some extent in the anode and cathode material, complicates the regeneration analysis. C and B are chosen such that they have an appreciable dif-

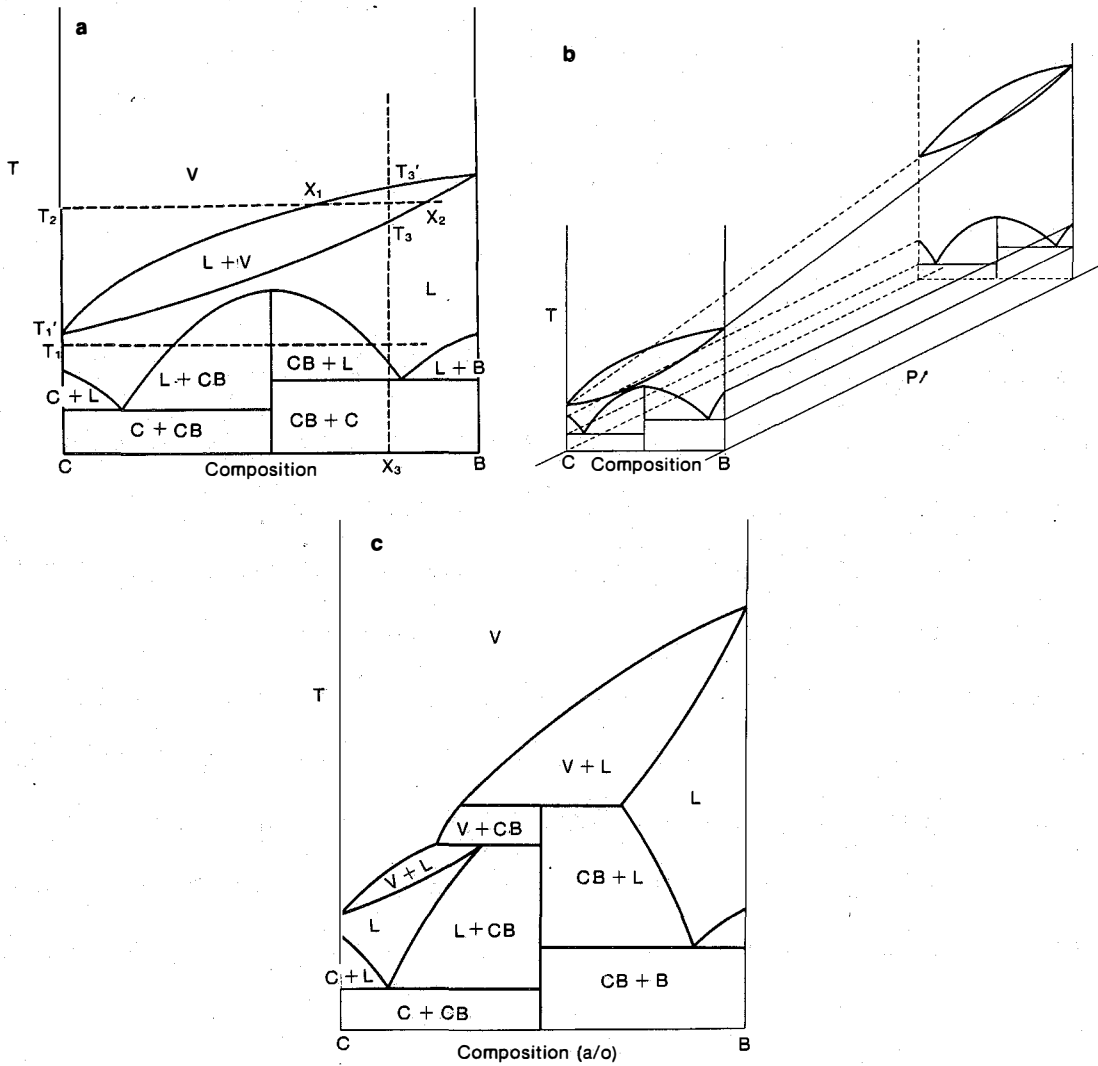


**Figure II-2. (a) Constant-Pressure Phase Diagram for a Generic Bimetallic System C/B;**  
**(b) Three-Dimensional Phase Diagram for a Two-Component System; and**  
**(c) Phase Diagram Showing Equilibrium between Vapor and Solid in the V-CB Region Resulting from Overlap of V-L and L-CB Regions [104]**

ference in boiling points. The equilibrium pressure of the cell system is determined by the condensation temperature in the radiator of the regenerator system [ $T_1$  in Fig. II-2(a);  $T_1$  can be equal to  $T_1$ , the galvanic cell operating temperature]. This pressure fixes the applicable T vs. composition phase diagram and will determine whether the liquid/vapor loop is separated from the solid/liquid equilibrium regions [Fig. II-2(b) illustrates the effect of pressure on the diagram of Fig. II-2(a), and Fig. II-2(c) illustrates a case in which the two loops interact and present a solid/vapor equilibrium region]. The compositions of the streams returning to the anode and cathode are determined by the temperature of the boiler of the regenerator [ $T_2$  in Fig. II-2(a)], and the anode and cathode streams have compositions  $x_1$  and  $x_2$ , respectively, provided the boiler is fed with a stream of composition  $x_3$ . If the stream returning to the anode is not enriched enough in C, fractionation can be considered. Since the net composition of C and B in the cell should be kept constant, the rate of distillation of the C-enriched stream is directly related to the current-generating capacity of the cell. In other words, the rate of circulation of the streams enriched in C and B is directly proportional to the rate at which coulombs of electricity are generated (current density).

Compound formation in the cell is desirable to lower the activity of C in the cathode and thus increase the obtainable voltage; however, for thermal regeneration, the melting point of the compound should not be so high that separation of the vapor/liquid and liquid/solid regions cannot be achieved at a practical operating pressure. The practical problem of a diagram such as Fig. II-2(c) is that the solid phase CB

will be present in the condenser, allowing the buildup of solid materials, eventually altering the anode composition, and constituting a serious engineering problem. Azeotrope formation can also be encountered in the liquid/vapor diagram. It must be emphasized that the above considerations assume equilibrium pressures and will not accurately represent all conditions in an operating cell, but they allow one to draw certain conclusions which are generally valid and helpful in evaluating the systems and predicting best theoretical operating conditions. Fisher [104] presents a comprehensive review of phase diagram considerations applied to bimetallic systems.

For electrical regeneration, i.e., operation as a rechargeable secondary battery, it is necessary that the electrochemical reactions be reversible, with negligible polarization, low self-discharge, and high power densities. To minimize self-discharge and coulombic inefficiency, the mutual solubilities of C and B in the electrolyte must be as low as possible under operating conditions.

Section II.1 describes in detail the liquid metal cells with  $B = \text{Hg}$  and  $C = \text{K, Na}$ ; i.e., amalgam cells with the boiling points of  $B < C$ . Regeneration is performed by distillation [see Fig. II-1(a)] of the combined cathode and anode materials, which yields streams of solvent(Hg)-rich distillate and solvent-poor residue to be returned to the cathode and anode, respectively. The thallium-potassium system, in which the regeneration is obtained by partial solidification, is also described in this section. These systems operated reasonably well in the thermal decomposition mode or as secondary batteries and can be operated in the electrothermal regeneration mode.



Section II.2 discusses the remaining bimetallic systems, in which regeneration is performed by distillation [see Fig. II-1(b)] of the alloy formed in the cathode. The distillate is the electroactive metal-rich phase (the anode metal) of a composition determined by the phase diagram characteristics and operating temperature and pressure conditions of the system; it is returned to the anode. The residue is the electroactive metal-poor phase, which returns to the cathode. The majority of the bimetallic systems intended for use in a thermal regenerative mode employed lithium or sodium metal as anodes, but most of these cells did not operate successfully in the thermal regeneration mode. However, the cells operated more successfully in the electrical regeneration mode, as secondary batteries, and operation in the electrothermal regeneration mode should be possible.

The groups involved in the major research efforts on these systems were: General Motors Corporation (Allison and Delco-Remy Divisions), which proposed the systems Na/Sn [81-84], K/Hg [84-88], and K/Tl [89]; North American Aviation, Inc. (Atomics International), which developed the sodium-mercury thermally regenerative alloy cell (TRAC) [93-101]; and Argonne National Laboratory (Chemical Engineering Division), which investigated several bimetallic systems (Na/Pb; Na/Bi; Li/Bi; Li/Te; Li/Sn; Li/Cd; Li/Pb; Li/Zn) in a research effort parallel to that on the lithium hydride system (see Section I.1) [36,46,104]. The physico-chemical investigation of the bimetallic systems was very thorough and careful, aiming at thermal or electrical regeneration. Few of the systems were found suitable for thermal regeneration. The search for couples exhibiting good electrical regeneration properties (secondary

batteries) was fruitful and is being continued [105]. Since this review involves only the thermally and coupled thermally-electrolytically regenerable systems, the work at Argonne aimed at secondary storage batteries (pure electrolytic regeneration) is not reviewed here.

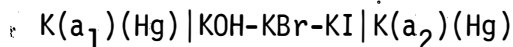
To place these activities in perspective, it must be realized that at the time of these investigations (1960-1966) the research was aimed at providing space power sources utilizing waste heat from a nuclear reactor. Therefore, the operating temperatures were dictated by the characteristics of the reactor and its cooling system. In addition, zero gravity resulted in the expenditure of only a small amount of energy for pumping the heavy fluid.

An added advantage of thermally regenerative systems employing alloy cells is the capability of storage of electrical energy, since, in principle, these systems could be rather compact secondary batteries.

## II.1 AMALGAM AND THALLIUM CELLS

### II.1.1 The Potassium-Mercury System

The electrochemical and regenerative feasibility of the K/Hg system was investigated at the Allison Division of General Motors Corp. by Agruss, Henderson, Karas, Wright, and Mangus [84-88]. The liquid metal cell employed was

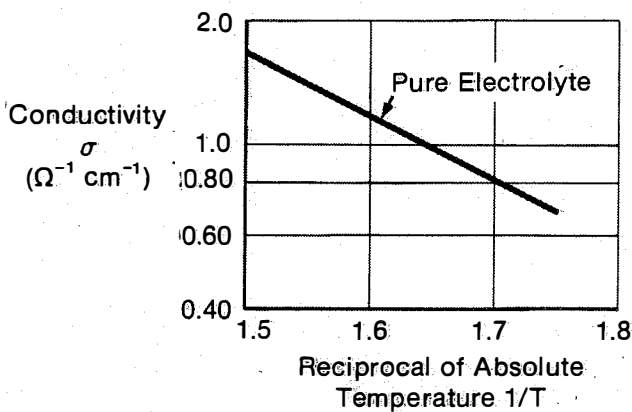
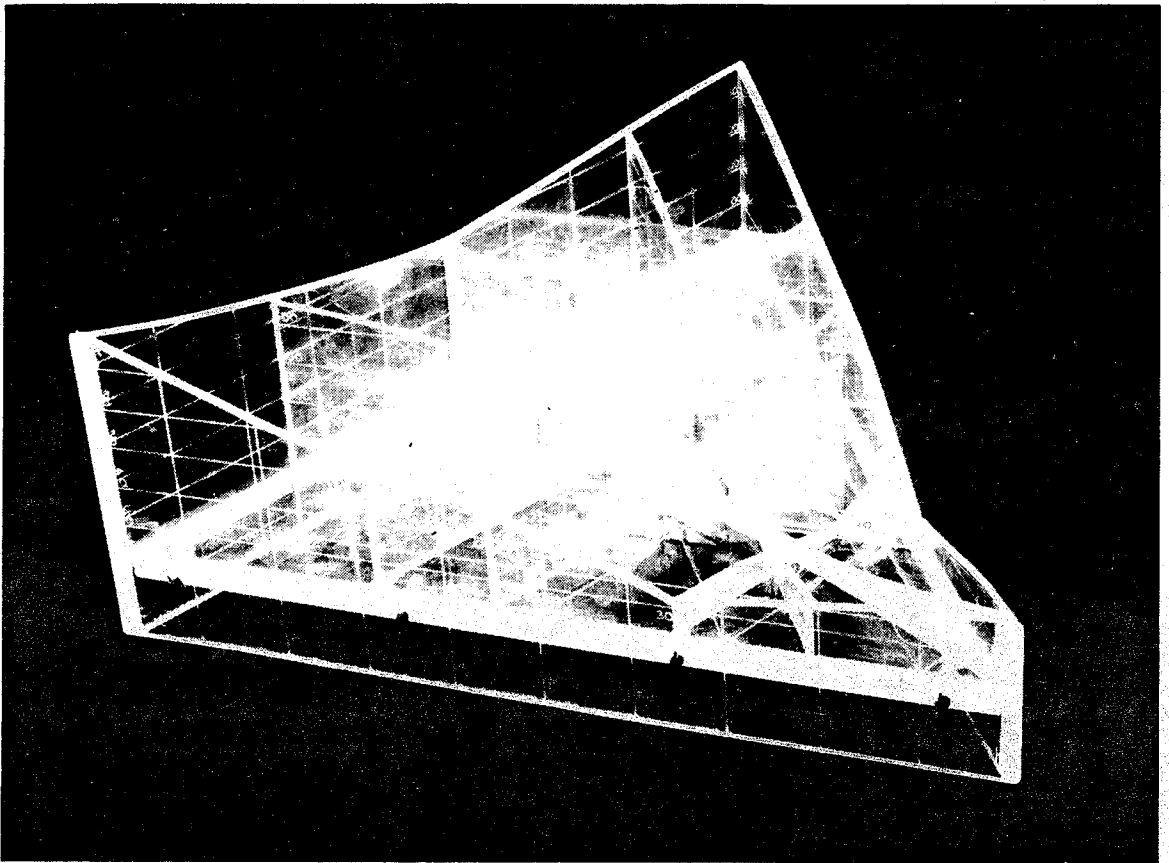


where the electrolyte composition was 70:15:15 mole % in KOH:KBr:KI, which is molten at 250°C. Some binary eutectics, such as KOH-KBr and KOH-KI, were also studied but were discarded because they presented

more serious corrosion problems. Some of the physical properties of the ternary eutectic, as well as the phase diagram for the KOH-KBr-KI system, are shown in Fig. II-3 [84]. The electrolyte conductivity increases with temperature, and therefore temperatures higher than 300°C were chosen for cell operation to minimize ohmic losses. The mutual solubility of potassium is greater than that of mercury in the ternary eutectic (see Fig. II-2), giving rise to self-discharge and only 90-95% coulombic efficiency in this system.

Potentials of cells  $K|K_{\text{glass}}^+|K(\text{Hg})$  obtained by Lantratov and Tsarenko [90] are shown in Fig. II-4 (136°C). Additional measurements at operating conditions were made by LaMantia and Bonilla [91], who also performed a more thorough thermodynamic investigation of the system. Curves calculated according to Eq. II-3 agree well with experimental data; the slight deviation is related to compound formation [84-86]. Reference 92 presents some aspects of the thermodynamics of this system.

Several cell configurations were employed by the General Motors researchers. For batch operation a differential density cell [84-86,88] held within a ceramic crucible was built with the K/Hg amalgam on the bottom, the ternary melt ( $d = 2.4 \text{ g/cm}^3$ ) floating on top of the amalgam layer, and finally, a layer of molten potassium ( $d = 0.78 \text{ g/cm}^3$ ) floating on top of the electrolyte. Leads were introduced into the K/Hg and K layers by iron wires surrounded by alumina tubes. A flowing system of this type was also made by the addition of suitable inlets and outlets, using a stainless steel body, but was not successful. Batch differential density cells were operated in an electrical regeneration mode undergoing charge/discharge cycling (12 minutes of charge and



70% KOH, 15% KI, 15% KBr  
 $\rho = 2.1 \text{ g/ml at } 300^\circ\text{C}$   
 $m p = 225^\circ\text{C}$   
 Mutual solubility with Hg — none  
 Mutual solubility with K — 2 mol %  
 K saturates eutectic at  $300^\circ\text{C}$   
 .1 mol% eutectic saturates K at  $300^\circ\text{C}$

Figure II-3. Ternary Phase Diagram of KOH-KBr-KI and Properties of the Ternary Eutectic [84]

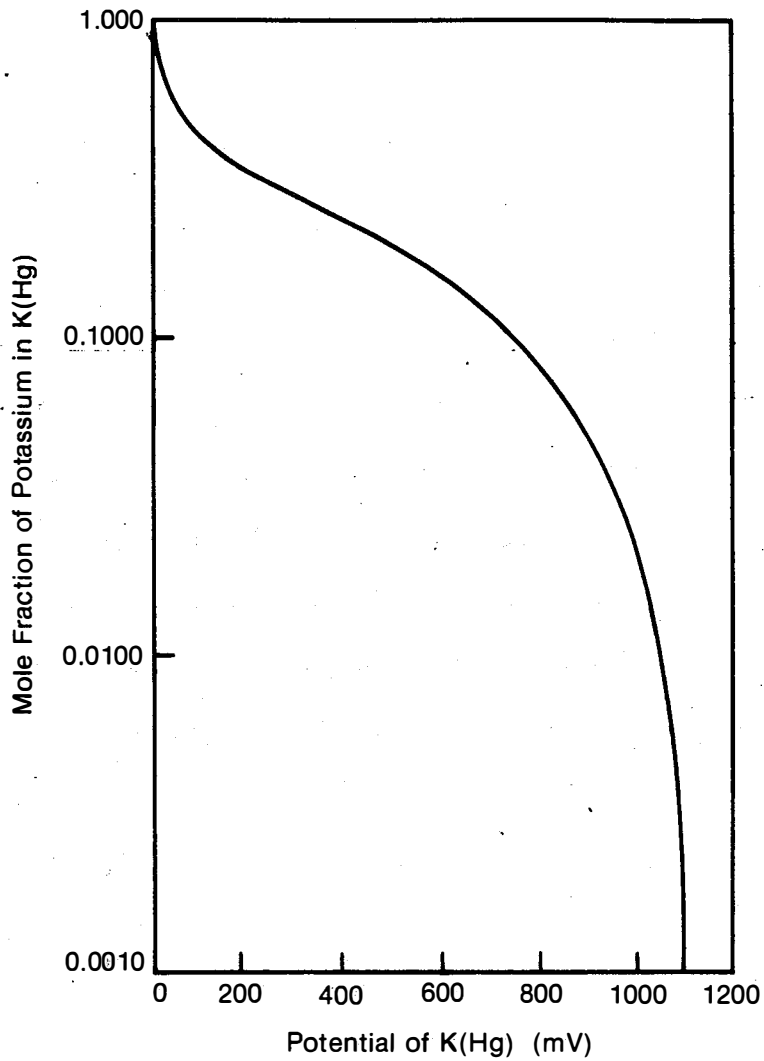
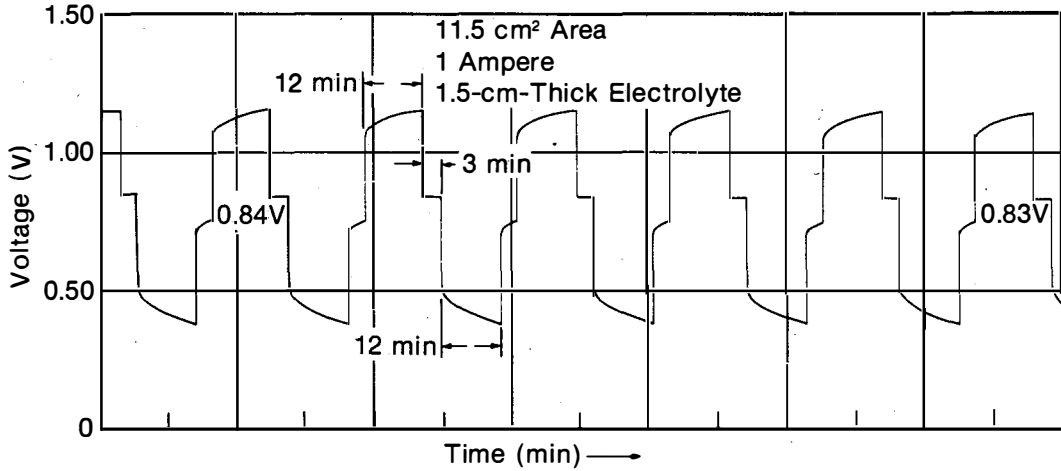


Figure II-4. EMF of  $K/K_{glass}^+/K(Hg)$  Cells at 136°C [90]

discharge at a current density of  $\sim 90 \text{ mA/cm}^2$  interrupted by a 3-minute open-circuit rest period). Some results of the cycling tests are shown in Fig. II-5 [84]. The shapes of the curves for charge and discharge indicate concentration polarization [84,88]. From the decrease in OCV at the successive rest periods, a coulombic efficiency of 90-95% was estimated [84]. Cells of this type operated continuously for over 700 hours with no deterioration in performance [85].

Wright [87] studied diffusion properties of potassium amalgams and found a smaller diffusion coefficient for K in dilute amalgams than in concentrated amalgams. This explains why concentration polarization begins at a lower current density during charge than during discharge, at the same bulk electrode composition. At a given current density and bulk concentration, the differential potassium concentration (surface to bulk) in the amalgam will be lower on discharge than on charge. This corresponds to a lower concentration polarization on discharge.

A better cell for flow operation was built by holding the electrolyte in place by impregnating it in a porous, sintered MgO matrix [84,85]. However, the problems of matrix strength and resistivity and of seals able to withstand pressure remained unsolved, principally for high current density and operation of long duration. Cracks in the matrix allowed mixing of the anode and cathode materials, leading to an internal short. Figure II-6 shows an exploded view of the liquid metal cell in which a matrix sandwich configuration was used, which allows electrolyte feed after cell assembly. Two ribbed insulators "coined" into the Kovar metal cell halves sealed the three liquid streams from each other and the outside of the cell [84,88]. Some progress in



**Figure II-5. Voltage-Time Plot of Cycling Differential Density Potassium-Mercury Cells [84]**

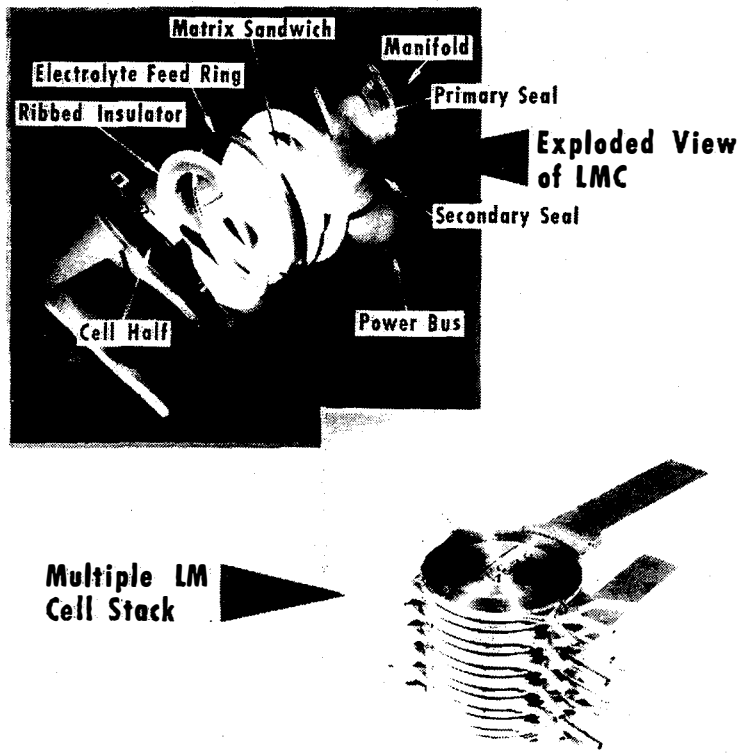


**Figure II-6. Potassium-Mercury Liquid Metal Cell (LMC) [84]**

reducing the resistance of the electrolyte-impregnated matrix was achieved by reducing the matrix thickness and improving the preparation of the paste electrolyte. However, the final resistance achieved was still rather large for high current density operation (see Ref. 3).

Data for the liquid/vapor equilibrium at 1 atm pressure (the Hg vapor pressure at  $\sim 350^\circ\text{C}$  is  $\sim 1$  atm) are shown in Fig. II-7 [84,86]. As indicated by the phase diagram, separation appears feasible at the operating temperatures, with the composition of the mixture fed to the boiler and the regenerator temperature and pressure dictating the composition of the streams to be returned to the anode and cathode. In the tests performed at the Allison Division of General Motors Corp., the mode of operation of the flow cells was not fully thermally regenerative, since the liquid potassium was fed from a tank. The potassium-enriched mercury from the boiler was stored and the mercury-enriched vapor from the boiler was condensed and fed to the cathode. Fresh mercury supply was furnished from time to time [88,3].

The performance of the single cell shown in Fig. II-6 was tested for about 430 hours with continuous discharges up to 32 hours, producing power output of 50-100  $\text{mW}/\text{cm}^2$ . During ca. 75 hours of the test, mercury was flowing through the cell in order to maintain voltage and power. A three-cell stack, also shown in Fig. II-6, was operated a total of 104 hours with discharges totalling 64 hours, producing 50  $\text{mW}/\text{cm}^2$  and with mercury flow during 60% of the operating time [84,88].

A mathematical analysis of the K/Hg system was performed, with the cell shown in Fig. II-6 divided into segments and with countercurrent liquid metal flow [84,88]. Changes in voltage, concentration, dif-



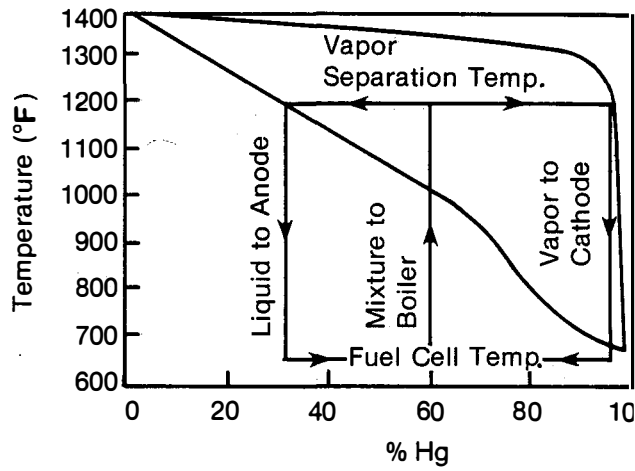


Figure II-7. Phase Diagram of Hg-K at 1 atm [84]

fusion layer, and current density were calculated for each segment and then integrated for the cell. Results were obtained after incorporating data for the concentrations of potassium leaving and entering the cell, as fixed by the phase diagram. These compositions also fix changes in heat capacity, vaporization, and thermal energy for a given electrical output. From these calculations [88] and experiments [84,88], the K/Hg thermally regenerative system was judged competitive with other regenerative systems (even those involving Rankine cycle mercury turbines) in the 1-50 kW range [84].

These results show that the K/Hg system is electrochemically simple and possibly capable of generating current densities of the order of  $100 \text{ mA/cm}^2$  at ca. 0.5 V with relatively low self-discharge rates. The concentration polarization, which leads to a buildup of a diffusion-controlled layer at the cathode, can be minimized by using thinner cathode streams. Ohmic losses can be decreased by improving the conductivity of the electrolyte matrix. Some mechanical problems of the cell were: leakage through the seals; electrolyte leakage out of the matrix due to pressure differences between anode and cathode compartments (e.g., if the K in the anode compartment is starved of feed); and cracking of the matrix. One advantage of the liquid metal cell for high current density operation, when the temperature inside the cell can rise appreciably, is the ease of heat management in the system due to the flow operating conditions and the inherent excellent heat transfer capabilities of these metals. Closed-loop operation, however, has not been demonstrated.

### II.1.2 The Sodium-Mercury System

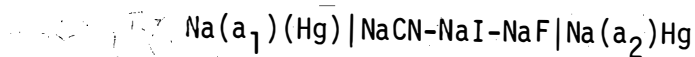
The Thermally Regenerative Alloy Cell (TRAC) system was developed at Atomics International, a Division of North American Aviation, Inc. (presently Rockwell Intl.) by Recht, Iverson, Heredy, and Oldenkamp, among others [93-101]. The mission of the program was to investigate the feasibility of closed-cycle, static devices for converting heat into electricity based on liquid metal amalgam cells with the sodium-mercury system. At the time, major emphasis was placed on the use of waste heat from nuclear reactors for the production of electricity in compact, lightweight space power plants with no moving parts [Systems for Nuclear Auxilliary Power (SNAP)]. As a result, most of the research aimed at devices with high power output/weight ratios and not at the highest possible efficiency of the systems. Moreover, a reactor source at  $\sim 700^{\circ}\text{C}$  (SNAP 8) and the constraint of minimum radiator area imposed certain operating temperatures (cell:  $\sim 460\text{-}510^{\circ}\text{C}$ ; regenerator:  $670\text{-}700^{\circ}\text{C}$ ), thus allowing a maximum Carnot efficiency of the order of 20%. The efficiency was reduced to about half of that value due to irreversibilities and was reduced further by weight constraints to about 30% of the Carnot efficiency [96]. Performance analysis of a 3-kW isotope-powered system, in which the regeneration was performed in a two-stage distillation process ( $900^{\circ}\text{C}$  and  $700^{\circ}\text{C}$ ), showed improved performance of the cell and higher Carnot efficiency (34%) (net efficiency estimated as 11%), but this system had trade-offs in the need for two separators, two pumps, and three heat transfer stages [93].

The TRAC program demonstrated the feasibility of the closed-loop operation in the Na/Hg system (cf. Section II.1.1). The program devel-

oped static cells [94] to furnish the proper background for the closed-loop operation [95], as well as the liquid/vapor equilibrium diagram [94] under operating conditions. Section II.1.2.1 describes the batch cells and Section II.1.2.2 the closed-loop operation.

#### II.1.2.1 Batch Cells [94]

The sodium-mercury amalgam cell



employed by Atomics International contained amalgams of different sodium activities in the anode and cathode compartments, which were separated by a porous (40-50% porosity) beryllium oxide matrix [98] impregnated with the ternary salt mixture of eutectic composition 58:30:12 mole % of NaCN:NaI:NaF, which is molten at 477°C. Other electrolytes were also investigated and found suitable: ternary or quaternary mixtures of anhydrous sodium salts of the halide anions ( $\text{I}^-$ ,  $\text{F}^-$ ), cyanide, and carbonate. The compositions and properties of these electrolytes are described in a patent [99]. These molten salts are thermally stable at the projected cell operating temperatures ( $\sim 500^\circ\text{C}$ ), have low resistivity ( $< 1 \text{ ohm cm}$ ), have low electrolyte/sodium amalgam mutual solubility [ $\sim 0.2 \text{ wt } \%$  solubility of sodium in the above ternary electrolyte was found, and Hg was found to be insoluble; the mutual solubility of Na in its salts is smaller than that of K in its salts], and are chemically inert in the presence of cell components, seals, matrices, etc. The BeO matrices did not show attack by sodium amalgam after about 1200 hours at 480-530°C.

EMF studies of sodium/sodium amalgams were carried out [94,101] in

cells  $\text{Na}(\ell) | \text{Na}^+_{\text{glass}} | \text{Na}(\text{Hg})(\ell)$  in the 350-400°C range, extending available literature data [102]. At higher temperatures open-circuit voltages of the static cells as a function of electrode composition were used. Figure II-8 shows an example at 500°C. The OCV values agreed within 10-15 mV with those calculated from Eq. II-4. The diagram of the static cell used in these measurements is shown in Fig. II-9. This cell was also used for studies of cell resistance, electrode polarization, and electrolyte matrix configurations as functions of temperature. Since at the operating temperature ( $\sim 500^\circ\text{C}$ ) the vapor pressure of mercury is 5.8-9.5 atm, the cell was contained in a stainless steel pressure vessel under argon atmosphere at 9.5-12 atm total pressure.

Batch cells of this type were operated for a period of  $\sim 180$  hours and the tests were terminated voluntarily. An example of the discharge characteristics of a static cell with a BeO matrix (0.25-cm thick, 11.4-cm<sup>2</sup> effective area), impregnated with the ternary electrolyte at 500°C, and containing initial amalgam concentrations of 37.6 and 2.9 atom %, respectively, in the anode and cathode compartments is shown in Fig. II-10. Cells were recharged electrically after discharge periods of 5-15 hours. Figure II-10 shows discharges at various current densities (upper numbers) and the corresponding cell resistivities (lower numbers). Up to about 200 mA/cm<sup>2</sup>, no appreciable concentration polarization was observed, as indicated by the approximately constant values of the calculated cell resistivities. The magnitude of the concentration polarization is a function of the cell voltage. For instance, for an OCV of  $\sim 0.48$  V (higher sodium concentration at the anode), appreciable concentration polarization was found only at 300-360 mA/cm<sup>2</sup>. During the

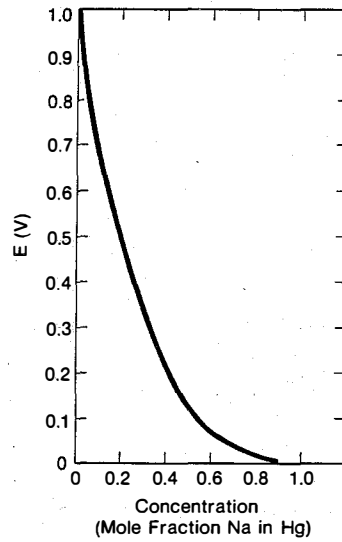


**Figure II-8. Open-Circuit Potentials of Sodium-Sodium-Mercury Galvanic Cells at 500°C [93]**

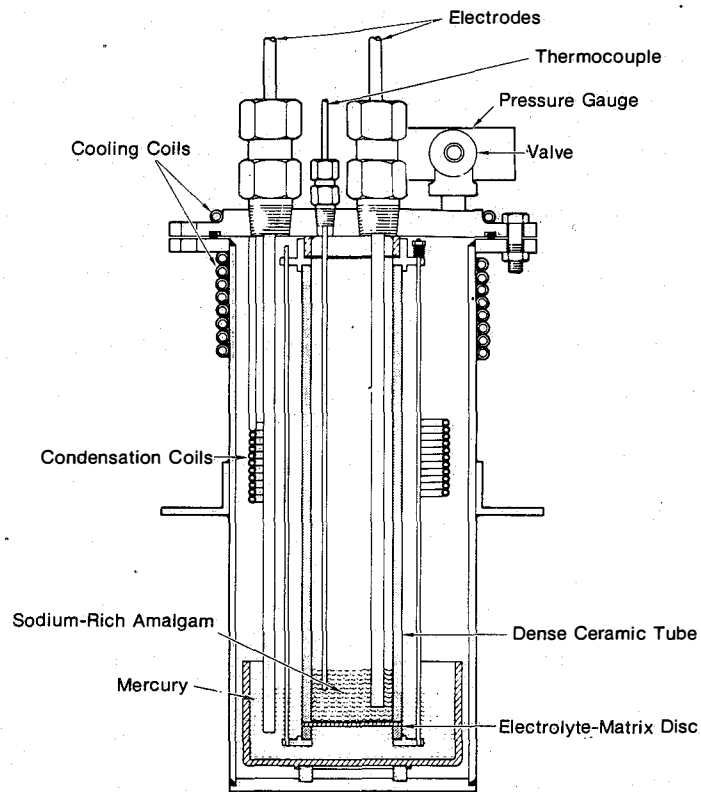


**Figure II-9. Cross Section of Static Electrode TRAC Cell [94]**

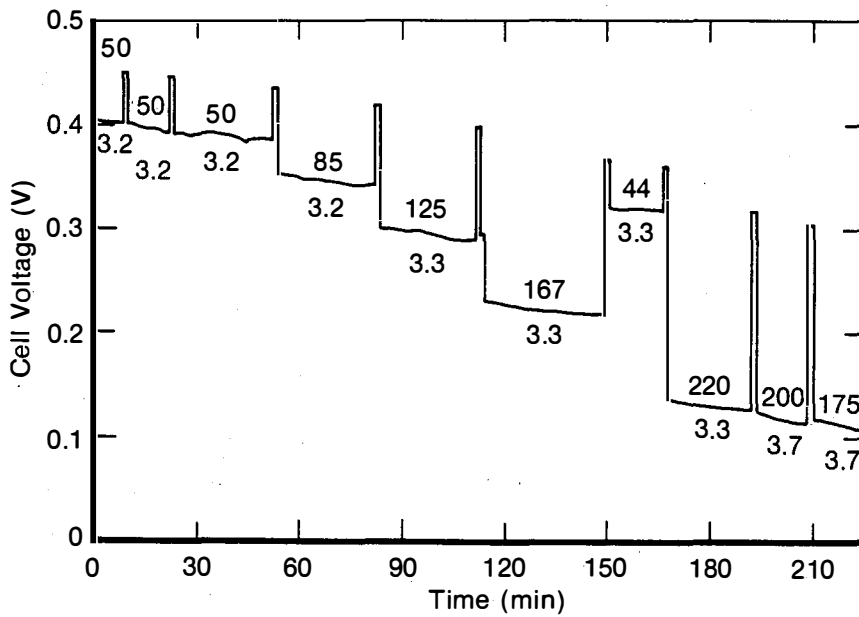


**Figure II-10. Discharge Characteristics of a Static TRAC Cell [94]**

Initial anode and cathode sodium concentrations: 37.6 and 2.9 atom %.

Figures above curve are current densities (mA/cm<sup>2</sup>) and below curve are calculated resistivities (ohm cm).

recharging period a larger concentration polarization was observed, in agreement with Wright's observations on the K/Hg system [87].

The onset of concentration polarization was shown to be a function of the quality of the matrix. The resistivity of the matrix electrolyte is greater by a factor of at least six than that of the pure electrolyte ( $\sim 0.5$  ohm cm). Improvements in the porous matrices with respect to their structural characteristics could lead to better cell performance.

#### II.1.2.2 Flowing Electrode Cell and Closed-Loop Operation [95]

The cross-section sketch of the flowing electrode TRAC cell is shown in Fig. II-11. The ceramic matrix containing the electrolyte in this cell is a porous tube of high purity alumina, held between two dense ceramic end pieces within the cylindrical ceramic cell body. The end pieces, in turn, are held between the cell flanges by iron knife-edge gaskets, which seal off the inside of the cell from the air. This seal was designed for easy testing but not for advanced cells (see Ref. 100 for the practical cell design proposed). A thermocouple well passes through the center of the alumina tube. The two liquid metal streams are pumped through the cell countercurrently, the mercury flowing upwards in the annulus (cathode compartment) between the cylindrical ceramic cell body and the outside of the matrix electrolyte, and the amalgam flowing downward inside the porous alumina tube (anode compartment). A tubular stainless steel structure holds the ceramic parts. The entire cell was mounted inside a constant-temperature oven for testing. This cell was tested for a few days in an electrical regeneration mode, using reservoirs for the reactants and products and using



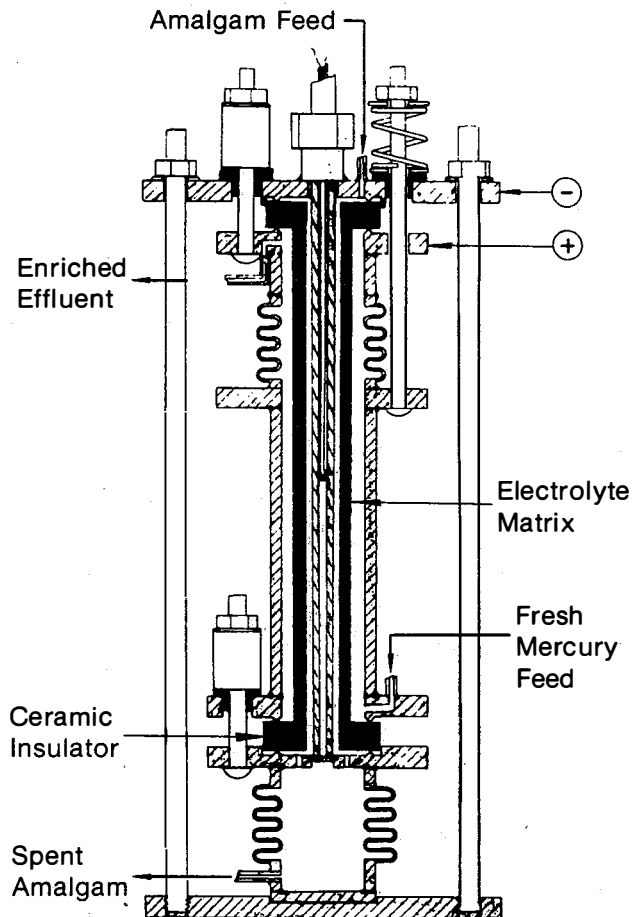


Figure II-11. Cross Section of the Flowing Electrode TRAC Cell [93]

argon gas pressure to circulate the metal streams. Current densities of 50-100 mA/cm<sup>2</sup> were maintained and a power of 35 mW/cm<sup>2</sup> was achieved with an electrode flow of 0.5-2.5 cm/min. The resistivity of the electrolyte matrix was two to four times higher (6-12 ohm cm) than that obtained for the porous discs used in the static cell.

The coupling of the flowing electrode cell with the regeneration loop is shown schematically for a liquid metal cell in Fig. II-1(b). The liquid stream from the condensing radiator is nearly pure mercury, which enters the cell under its own vapor pressure at the radiator exit temperature. This fixes the system pressure at about 5.8 atm if the radiator is at 485°C. The pressure in the separator will be very nearly the same as the cell inlet pressure. With the pressure and temperature at the separator fixed, the sodium content in the liquid and vapor phases is determined by the equilibrium values under these conditions. The separator was designed as a centrifugal cyclone. Mercury vapor and liquid amalgam enter the separator tangentially, where their velocities cause them to spin around the inside wall, forcing the vapor to flow out the top. Provided that the boiling material reaches the separator well mixed, equilibrium between liquid and vapor is approached in the separator and a one-theoretical-plate separation should occur (this was verified under operating conditions). Figure II-12 shows the liquid/vapor equilibrium diagram for sodium amalgams at 5.8 atm. From these data one can conclude that at 685°C (~1300°F) the vapor phase is nearly pure mercury with 0.1-1 atom % sodium (cathode stream) whereas the liquid phase is approximately 36 atom % sodium (anode stream).

If the regeneration can be performed at a higher temperature, e.g.,

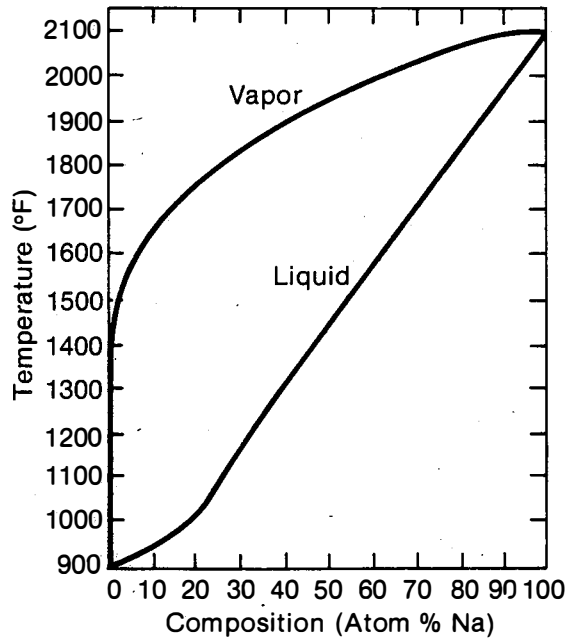


Figure II-12. Vapor/Liquid Equilibrium Compositions of the Na/Hg System at 5.8 atm [95]

815°C ( $\sim$ 1500°F), a more significant sodium concentration will appear in the vapor phase, which could be partially condensed at about 485°C, and the condensed phase could be returned to the boiler. Under these conditions the anode stream will be essentially 60 atom % sodium and the cathode stream will be very low in sodium [93].

A schematic of the test loop is shown in Fig. II-13. A more complete description of the closed-loop assembly is given in Ref. 95. The regeneration system test loop was made of a 5-kW (thermal) electrically heated boiler, a cyclone-type separator, a water-cooled condenser, two reservoirs, an electromagnetic pump, and connecting tubing assembled in a loop, coupled to the flowing electrode cell (Fig. II-11), as shown in Fig. II-13. These parts were designed for operation in a free-fall environment.

In the first test of the combined cell/regeneration system, the matrix was impregnated with electrolyte after the cell was assembled and connected to the system. After the matrix was impregnated and the excess electrolyte was drained out, the regeneration loop was loaded with 14 atom % amalgam and started up. The loop was operated for a short time to generate a supply of mercury and concentrated amalgam in the reservoirs. After this the cell was filled, and the cell and the regeneration loop were operated continuously for 118 hours and then shut down for disassembly. During this test, it was found that since the cell temperature was higher than expected (to maintain the coolest part of the cell oven at 485°C), the system pressure essentially doubled and reduced the separation that could be achieved. A maximum OCV of about 0.25 V was developed, but the system operated satisfactorily, with the

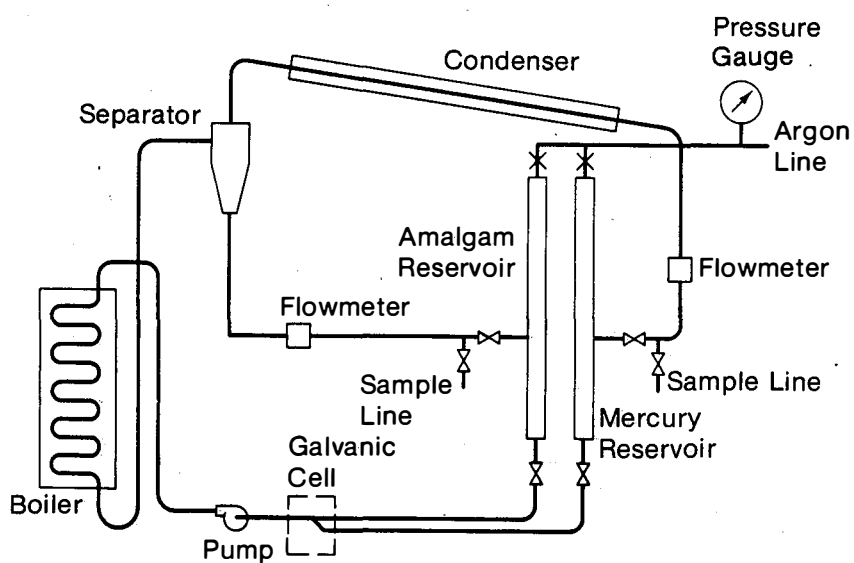


Figure II-13. TRAC Test Loop Flow Diagram [95]

cell internal resistance remaining essentially constant. The loop performance was steady but the pressure drop across the loop increased at the end of the test. The matrix was intact (dark colored) but excess electrolyte was found in the cell. The sealing gaskets had been corroded by atmospheric oxygen. The loop contained loose black material which was found to be iron. The buildup of materials in the loop and the excess electrolyte were believed responsible for the pressure drop increase during the test.

The second test was continued until the system failed. The matrix electrolyte impregnation was carried out in a separate apparatus and the iron gaskets were prevented from contact with atmospheric oxygen by a nitrogen flow system installed in the cell oven. The test was performed similarly to the previous one. The cell temperature was maintained at  $\sim 495^{\circ}\text{C}$  and the system pressure was maintained at 9.2 atm. A better separation was obtained which allowed a maximum steady OCV of 0.32 V. After a period of about 625 hours the loop portion was shut down for about 440 hours to replace leaking valves, and the cell remained in operation in an electrically rechargeable mode. The regeneration loop was then restarted and the whole system operated for an additional 130 hours. The test was terminated when the bottom iron gasket of the cell began to leak due to a failure in the nitrogen purge system. The cell operated continuously for about 1200 hours, during which the cell internal resistance remained constant. The maximum power density generated was  $5 \text{ mW/cm}^2$  from  $25 \text{ mA/cm}^2$  at 0.2 V. The power and current densities were low as a result of a high resistivity of the electrolyte matrix (54 ohm cm), caused by the low porosity (15%) of the alumina tube employed.

These tests demonstrated the compatibility of the alumina matrix with the sodium amalgam, though beryllium oxide was found to be a better material [100], presenting higher resistance to alkali metals and their amalgams, and having higher thermal conductivity than magnesia or alumina. No detectable amount of electrolyte leached out of the matrix during about 500 hours. Cell materials do not seem to pose a problem for long-lived devices.

A performance analysis of a 42-kW TRAC plant was carried out [96] coupled with a SNAP 8 reactor [600 kW (thermal)], assuming a rather small resistivity of the ceramic tubes ( $\sim 3$  ohm cm), and 120 cells, using the regenerator at 693°C and 6.1 atm pressure and, therefore, anode and cathode sodium concentrations of 38.5 and 0.2 atom %. The pumping requirements were estimated as 2 kW for an overall 42-kW net power output, corresponding to a net efficiency of 7%. Details of this analysis are given in Ref. 96. A detailed analysis of a 3-W (electrical) isotope system with a two-step regeneration, the two-stage TRAC cell, was performed [93]. Due to the higher regeneration temperature the overall efficiency was estimated as 11%.

### II.1.3 The Potassium-Thallium and Analogous Systems

A different approach for regeneration in the alloy systems has been suggested in the literature (cf. Ref. 86, p. 808, and Ref. 89). A galvanic cell of the type described in Section II.1 ( $A_zB_y | A^+ | A_xB_y$ ) operates at a temperature above the melting point of the alloys. The streams of the alloys from the anode and cathode are combined, well mixed, and cooled down to a definite temperature at which the mixture partially solidifies, forming a C-rich phase and a C-poor phase, one of which will

be in the solid state and the other in the liquid state. These two phases can be mechanically separated by conventional methods and the two separated streams of regenerated anode and cathode materials individually reheated to the cell temperature and returned to the galvanic cell.

A system which seems suitable for this type of regeneration has been proposed by Agruss, Hietbrink, and Nagey [89]: the potassium-thallium system. Figure II-14 shows the solid/liquid phase diagram for this system obtained by Kurnakow and Puschen [103]. The galvanic cell  $K(Tl)a_1 | K^+ | K(Tl)a_2$  consists of a molten K-Tl solution rich in K as anode and a molten K-Tl solution rich in Tl as cathode, separated by a porous matrix impregnated with molten KCl at an operating temperature higher than 335°C. The combined streams of the anode and cathode materials are taken to a container in which the mixture, containing 0.75 mole fraction of thallium, is cooled down to 173°C via cooling coils. From Fig. II-14 one can conclude that at this temperature a solid phase containing 0.5 mole fraction of Tl is in equilibrium with a liquid phase containing 0.84 mole fraction of Tl. The two phases are separated, individually reheated to the cell temperature, and returned to the anode and cathode. Approximately 0.6 V has been obtained with cells of this type [89].

A process for continuous transfer of the solutions from the cell to the separator and for continuously reconveying the separated, less dense solid phase, floating on top of the liquid phase, is described in Ref. 89. A mesh-type conveyor belt transfers the solid to a melting pot where it is heated by heating coils to the cell temperature and returned to the anode. The system is made continuous simply by feeding cell effluent to the settling container and removing an equal amount of



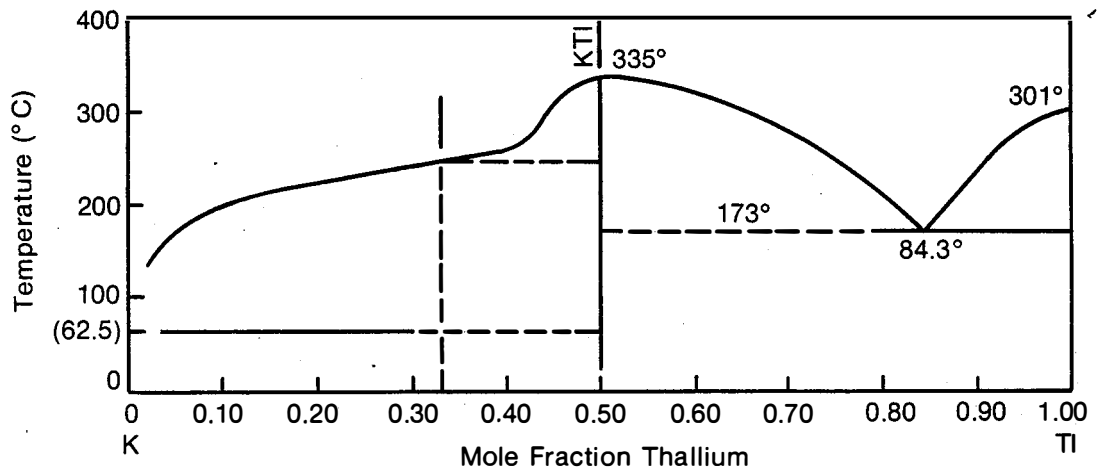


**Figure II-14. Solid/Liquid Equilibrium Compositions of the Potassium-Thallium System [103]**

separated solid and liquid.

Agruss, Hietbrink, and Nagey [89] suggest that this same type of regeneration can be applied to various systems and mention the following specifically in their patent: Al/Se; Al/Te; Bi/Ca; Bi/K; Bi/Na; Ca/Hg; Ga/Na; Hg/Mg; K/Sn; Li/Pb; Mg/Sn; Te/Tl; Bi/Li; Bi/Te; Ca/Pb; Hg/K; Hg/Na; K/Se; Li/Sn; Na/Sb; Mg/Sb; Bi/Mg; Bi/Tl; Ca/Sb; Li/Tl; and Sn/Te.

From the thermodynamic data for the K/Hg system [91], Bonilla (in Ref. 86) concludes that very low voltages ( $\sim 0.1$  V) would be obtained in this mode of operation. The same conclusion appears to hold for Na/Bi and Li/Bi systems (cf. Ref. 116, 36, and 46 for phase diagrams and EMF data).

## II.2 BIMETALLIC CELLS

### II.2.1 Sodium-Containing Systems

#### II.2.1.1 The Sodium-Tin System

Laboratory cells of the type  $\text{Na}|\text{Na}^+\text{glass}|\text{Na}_x\text{Sn}$  were operated in batch mode, in the 500-700°C range, by Agruss [81]. The cathode composition was varied between 15-30 mole % of sodium and the resulting OCV were 0.42-0.36 V (500°C) and 0.43-0.33 V (700°C) [81,84]. These results agreed with previous EMF data obtained by Weaver et al. [82] using  $\text{Na}|\text{NaI-NaCl}|\text{Na}_x\text{Sn}$  cells at 625°C, with the eutectic electrolyte of composition 62.5:37.5 mole % NaI:NaCl, molten at 562°C, in the static mode (differential density cells) and with flowing electrodes (using a flame-sprayed alumina H-cell).

The static and flowing cells were used to study charge/discharge

behavior of these cells. One static cell showed ability to undergo cycling tests on a 20-minute charge/discharge cycle for about a month. The average discharge current was  $\sim 50 \text{ mA/cm}^2$ . Due to an improper sealing of the cell there was loss of sodium during the test, thus explaining the low coulombic efficiency. The real coulombic efficiency in this system should approach 95%. No concentration polarization effects were found in these studies. Flooding of the porous alumina matrix with sodium caused short circuits in the flowing cells. Projections based on a less porous matrix impregnated with the molten eutectic indicate a maximum OCV of 0.5 V and  $\sim 700 \text{ mA/cm}^2$  at 0.25 V. These cells should operate satisfactorily in an electrothermal regeneration mode [82].

Agruss [81] investigated the ability of this system to undergo thermal regeneration up to temperatures of  $\sim 1000^\circ\text{C}$ . Since the measured activities of Na in the alloy (from EMF data) correlated linearly with the inverse of the absolute temperature in the  $500\text{--}700^\circ\text{C}$  range, the activity data extrapolated to the  $900\text{--}1000^\circ\text{C}$  range were used to provide estimates of the sodium vapor pressure over the alloy solution (15-30 mole % Na) in the desired regeneration temperature range. The EMF can be related to the activity of sodium in the alloy, which is equal to the ratio of sodium partial pressure over the alloy solution ( $p$ ) and the partial pressure of pure sodium ( $P_0$ ) at that temperature, provided Raoult's law is obeyed:  $E = -(RT/nF)\ln(p/P_0)$ . It was found that only above  $1100^\circ\text{C}$  could 200-400 torr sodium vapor pressure be obtained, which would facilitate the thermal regeneration. Separate distillation experiments in the  $900\text{--}1000^\circ\text{C}$  range showed that the distillation was

very slow. One attempt was made to run in a regenerative mode with the system shown in Fig. II-15, using the cell  $\text{Na}|\text{NaI-NaCl}$  impregnated alumina $|\text{Na}_x\text{Sn}$  at 625-650°C and the regenerator at 1000°C. The cathode was filled with 30 mole % Na/Sn alloy, with no pure sodium in the anode cup. The regenerator was operated for about 10 minutes to generate enough sodium to start the cell operation. Power was drawn from the cell for about 15 minutes at 0.3 V and 100 mA until the metal-to-ceramic seals were corroded by hot sodium vapor and started to leak [81,84]. Since regeneration under 1000°C was not feasible, the Allison Division of General Motors Corp. started investigating the potassium-mercury system described in Section II.1.1.

#### II.2.1.2 The Sodium-Lead System [36]

The galvanic cell  $\text{Na}|\text{NaF-NaCl-NaI}|\text{Na}_x\text{Pb}$  was chosen by Argonne National Laboratory [36] as a possible thermally regenerable system, with the eutectic electrolyte of composition 15.2:31.6:53.2 mole % of NaF:NaCl:NaI, molten at 530°C. Phase diagrams for this ternary system [106] as well as for binary sodium halide electrolytes were investigated [36]. The ternary eutectic was chosen for the investigation of sodium-containing cells because of its low melting point. EMF data for  $\text{Na}|\text{Na}^+$  glass ( $\text{Na}_2\text{O}$ ) $|\text{Na}_x\text{Pb}$  had been determined by Hauffe and Vierk [107], by Lantratov [108], and also by Porter and Feinleib [109] using as electrolyte alumina impregnated with sodium carbonate. These results agreed with values calculated from the vapor pressure of sodium over sodium lead alloy (40 atom %), which are about 8 mV higher than the direct EMF measurements [36,110]. The vapor pressure data were successfully

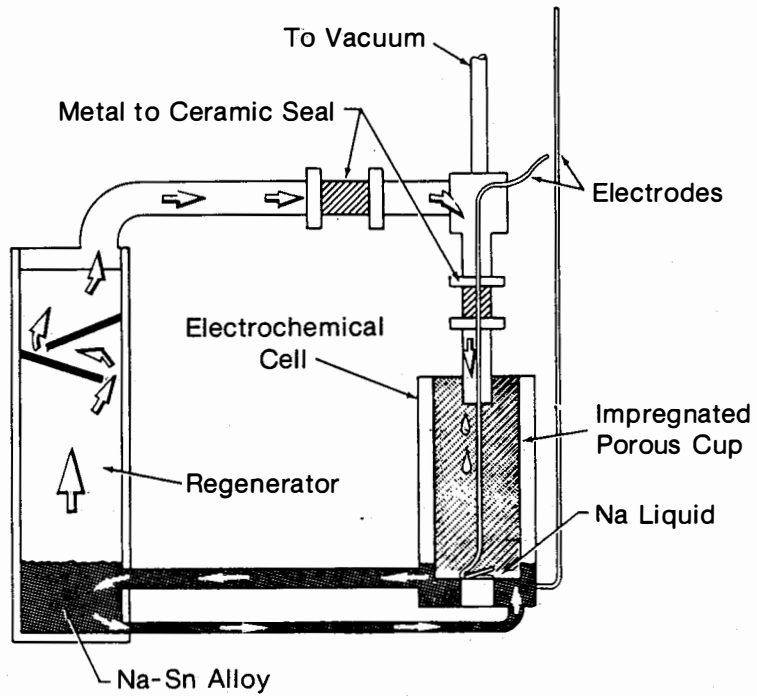


**Figure II-15. Thermally Regenerative Sodium-Tin System [81]**

analyzed by a quasi-ideal solution treatment (previously utilized in the analysis of the sodium-bismuth system [115]), in which the major intermetallic species were assumed to be NaPb, NaPb<sub>3</sub>, and Na<sub>3</sub>Pb [111].

The phase diagram studies [36] indicate that this system does not present problems of overlap of the liquid/vapor and solid/liquid equilibrium regions. In fact, the highest melting point of any compound in the system is 400°C. At this temperature the vapor pressure of pure sodium is 0.35 torr, and at this pressure the boiling point of lead is ~900°C. Higher operating pressure (6-10 torr) and high regeneration temperature (~900°C or higher) should allow regeneration of this system.

The EMF of sodium-lead cells is 0.3-0.5 V (alloy composition ~10-40 atom % sodium). One complete cell and regenerator system was operated for approximately 100 hours. The apparatus employed is shown schematically in Fig. II-16. The cell was loaded with the ternary electrolyte and with 30:70 atom % Na:Pb alloy in the cathode. The regenerator was operated to distill sodium for the anode, to be consumed in the cell. Eleven runs of 2-7 hours, for a total operating time of 45 hours, with the cell at 545-600°C and 5.7-9 torr pressure, were performed. The electrode area was 45 cm<sup>2</sup> and the interelectrode separation 1.9 cm. Table II-1 shows the continuous operating current obtained at three temperature and pressure conditions of the regenerator.

Table II-1. OPERATION OF THE Na/Pb THERMALLY REGENERATIVE SYSTEM [36]

Regenerator Temperature (°C)	Regenerator Pressure (torr)	Cell Current (A)
875	8	7.5
850	7	5.0
825	6	2.5

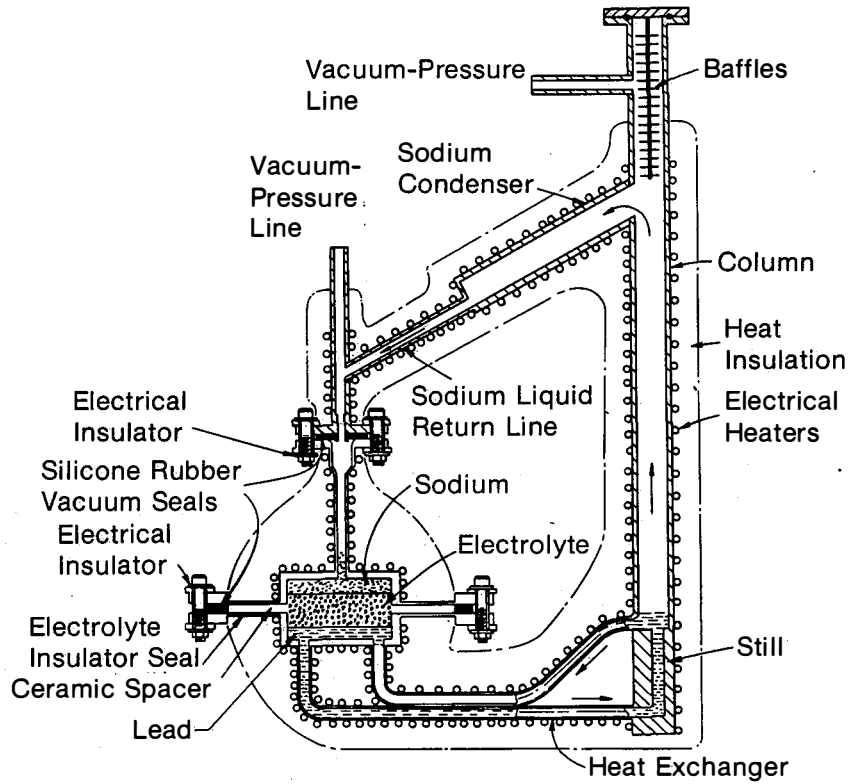


**Figure II-16. Thermally Regenerative Sodium-Lead System Operated for 100 Hours [36]**

Cell OCV as high as 0.41 V at 575°C were recorded, indicating that the regenerator had reduced the cathode sodium concentration from 30 to 18 atom %. One example of the cell performance at this temperature is shown in Fig. II-17. An OCV of 0.39 V and a current density of 100 mA/cm<sup>2</sup> at 0.18 V were obtained with the regenerator at 875°C and 8 torr.

The regenerator shown in Fig. II-16 led to erratic sodium-lead circulation. Since the pressure of the system was shown to be an important parameter in the liquid circulation, a better regeneration system was designed, providing a hydrostatic head to improve circulation (see Fig. II-18). No major problems of corrosion were encountered in approximately 1000 hours. The initial liquid circulation (first 3 days) was erratic but improved with better degassing of the system.

The differential density cell (cf. Fig. II-15) was considered as an initial design but cells with immobilized electrolytes (cf. Sections II.1.1., II.1.2., and II.2.1.1) were judged superior. Several design concepts were proposed, including designs for multicell operation. Due to the low voltages obtained per cell, a practical device would have to connect many cells in series to achieve useful voltages. The efficiency of this system should be 9-12%. Therefore, the Na/Pb system was not considered attractive for a practical device by Argonne National Laboratory investigators [36].

#### II.2.1.3 The Sodium-Bismuth System

The cell Na|NaF-NaCl-NaI|Na<sub>x</sub>Bi was also investigated at Argonne National Laboratory [36] with the ternary eutectic electrolyte described



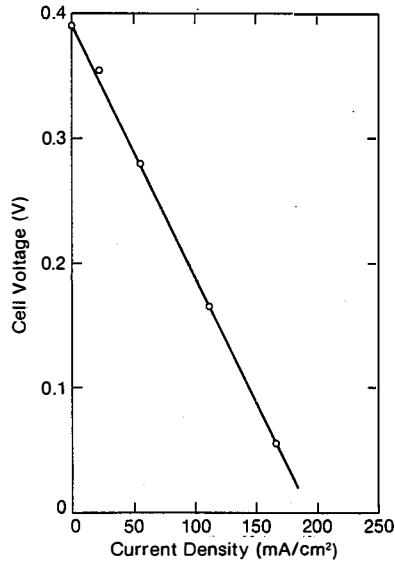


**Figure II-17. Voltage-Current Density Plot for the Sodium-Lead Galvanic Cell Operating under Thermal Regeneration [36]**

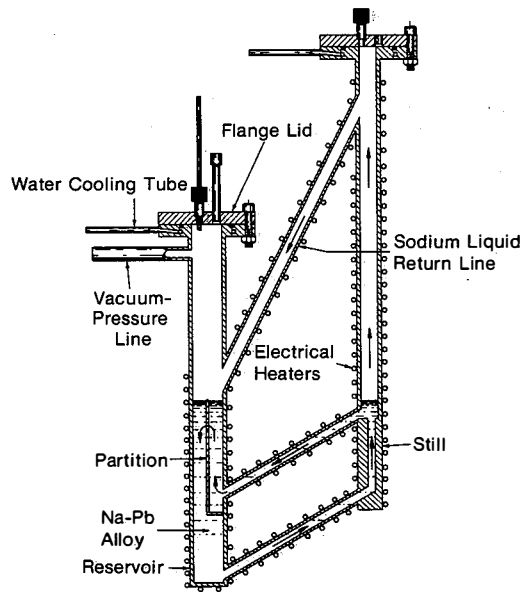


**Figure II-18. Improved Thermal Regenerator for the Sodium-Lead System Operated Continuously for 1000 Hours [36]**

for the Na/Pb system (Section II.2.1.2). The sodium-bismuth cell has an EMF in the 0.55-0.75 V range, ca. 0.2 V higher than the Na/Pb cells, thus promising better performance. The EMF decreases with increased sodium content in the cathode but between 20-40 atom % sodium the decrease is slow (approximately 0.6-0.5 V). At about 55 atom % sodium, a sodium-saturated solution is found and the EMF is approximately 0.4 V [36,46]. A closed cell of the differential density type, similar to the bottom half of that employed in the study of the Na/Pb system using the still (see Fig. II-16) as a simple reservoir for charging sodium and bismuth, was operated in charge and discharge cycles for a period of 17-18 months at 550°C without deterioration of performance. The OCV of this cell was 0.7 V (20 atom % sodium in the cathode) and current densities on discharge of 90 and 110 mA/cm<sup>2</sup> were obtained at 0.5 and 0.45 V, respectively. The electrode area was 45 cm<sup>2</sup> and the calculated internal resistance was 0.05 ohm. No decomposition of the molten salt was observed and minimum corrosion was detected after this period. An improved cell design using a sodium retainer/current collector in the form of a stainless steel spiral, mounted in the anode compartment, maintained a uniform current distribution throughout the anode area. This cell could be charged and discharged at currents up to 50 A (1.1 A/cm<sup>2</sup>) over 50 times and at various temperatures, with no deterioration. The combined charge/discharge efficiency was approximately 80% for a current density of 665 mA/cm<sup>2</sup> at 565°C [36,112].

One drawback of these cells is the relatively fast self-discharge, associated partly with the large solubility of the intermetallic compounds (e.g., Na<sub>3</sub>Bi) in the molten salt system, which increases with

temperature [113]. Foster [114] presents an interesting account of the bimetallic cells with regard to the solubilities of the intermetallic compounds and species characterization in the molten salt media.

Thermodynamic and phase diagram studies of the sodium-bismuth system were performed [115,116]. In this system, the solid/liquid and liquid/vapor equilibrium regions overlap at low pressures. The total pressure curves indicate the appearance of a three-phase equilibrium ( $\text{Na}_3\text{Bi}$  solid, of melting point  $842^\circ\text{C}$ , in equilibrium with liquid and vapor) below a pressure of approximately 240 torr. Therefore, the operational pressure of a regenerative sodium-bismuth system must be  $\geq 240$  torr. In order to collect pure sodium at this pressure, a condenser temperature of approximately  $770^\circ\text{C}$  is required, which would raise the galvanic cell operating temperature about  $270^\circ\text{C}$ . Another consequence of operating at 240 torr pressure is that in order to obtain a reasonable cathode composition, the regeneration temperature should be  $1200\text{-}1300^\circ\text{C}$ . At this temperature, materials problems and dynamic corrosion by Na/Bi could be very difficult to overcome. The vapor obtained would still contain several atom % Bi [115], thus necessitating fractionation (refluxing), which reduces the overall efficiency.

### II.2.2 Lithium-Containing Systems

The systems Li/Sn [117], Li/Bi [118], Li/Te [119], Li/Cd [36], Li/Zn [36], and Li/Pb [36] were investigated at Argonne National Laboratory in the 1961-1967 period, from the electrically or thermally regenerative point of view [36]. EMF data for these systems [36,117-119] were obtained using as an electrolyte the binary eutectic LiF-LiCl or

LiCl-KCl molten salts at approximately 500°C. Figure II-19 shows the EMF-temperature-composition plot obtained for the Li/Sn system; higher EMFs were obtained for the Bi and Te systems. For thermally regenerative operation, both the Li/Bi and Li/Te systems were found inadequate due to the high vapor pressure of Bi and Te over their respective lithium alloys. In the Li/Bi systems, the same problems encountered for Na/Bi that resulted from the overlap in the phase diagrams can be foreseen [36,116]. The compound  $\text{Li}_3\text{Bi}$  has a melting point of approximately 1150°C [116]. The only attractive system for thermally regenerative operation is the Li/Sn system, due to the very low tin vapor pressures over lithium-tin alloys even at very high temperatures (e.g., 1200°C) [120].

The phase diagram for the Li/Sn system shows a region of liquid/solid coexistence including the compound  $\text{Li}_7\text{Sn}_2$  with a melting point of 783°C [36]. The liquid/vapor diagram at 1200°C is shown in Fig. II-20. At this temperature the solid/liquid and liquid/vapor equilibrium regions do not overlap. The lithium vapor pressure over a reasonable cathode composition (e.g., 30 atom % lithium) is of the order of 2 torr. The regeneration at this low pressure (cf. 6-10 torr for the Na/Pb system; see Section II.2.1.2) may pose problems of heat, mass, and momentum transfer, in addition to the materials and corrosion problems of operating the thermal regeneration at 1200°C. However, since the cell could operate with a ternary eutectic LiCl-LiF-LiI [106] of melting point <350°C, the expected Carnot efficiency for this system could be 58%, and a much higher net efficiency could be expected (25-30%) [4] if the materials problems can be overcome.

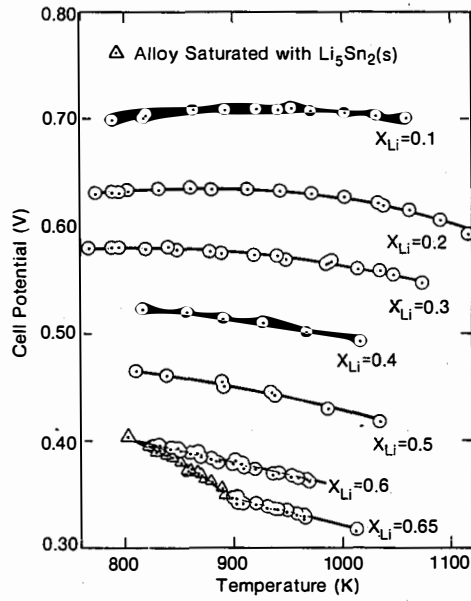


Figure II-19. EMF-Temperature-Composition Characteristics of the Cell  $\text{Li}(l)/\text{LiCl-LiF}(l)/\text{Li}_x\text{Sn}$  [36]

$X_{\text{Li}}$  = atom fraction lithium

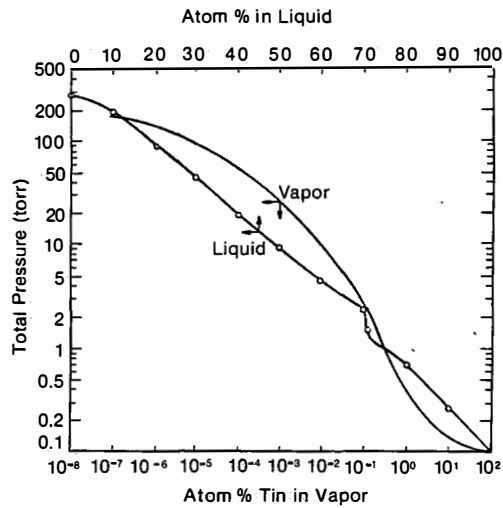
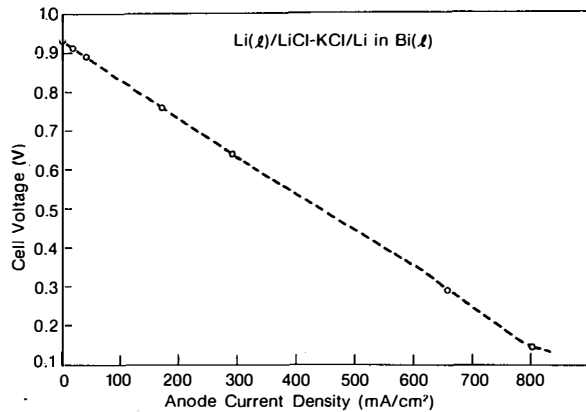
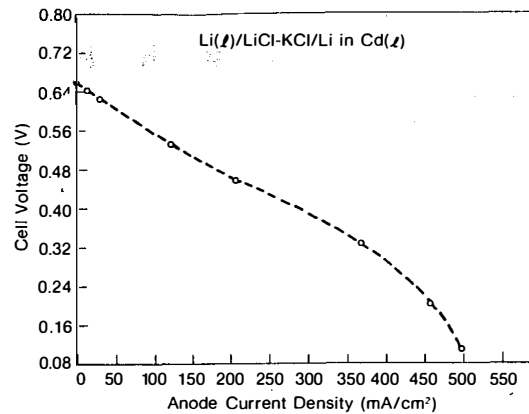
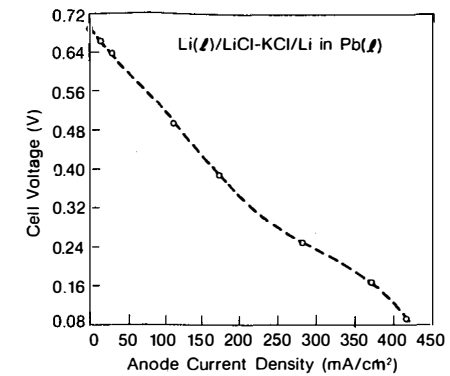
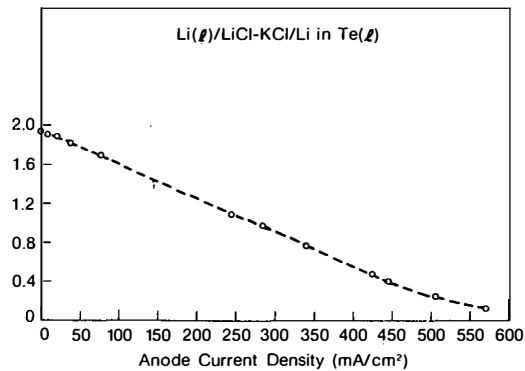
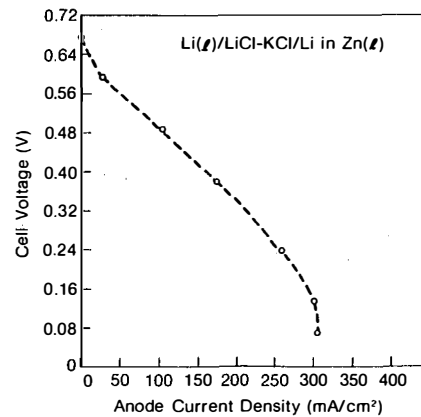
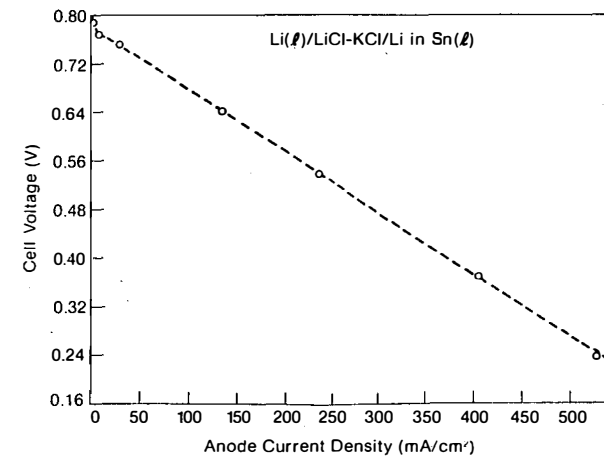


Figure II-20. Pressure-Composition Diagram for the Li-Sn System at  $1200^\circ\text{C}$  [120]

The other bimetallic systems with lithium anodes were investigated as possible secondary batteries. Figure II-21 shows examples of the discharge characteristics of these systems [36]. Most of these systems produced high current densities at reasonable voltages (especially Li/Te and Li/Se) and exhibited good cycling capabilities. Due to these characteristics, the subsequent investigations at Argonne continued to explore the secondary battery and electrical energy storage application of high temperature galvanic cells with Li or Li/Al anodes using immobilized electrodes with molten salt electrolytes.

### II.3 SUMMARY OF THE PERFORMANCE AND DISCUSSION OF THERMALLY REGENERATIVE ALLOYS OR BIMETALLIC SYSTEMS

Table S-5 assembles results for the alloy and bimetallic systems reported in our review. It is fair to state that the electrochemical cell performances listed in the table are low limits. These systems exhibited better cell performance in batch cells tested. They are also good storage battery systems. The coupling of the electrochemical cell and regenerator system were successful in the Na|Hg and Na|Pb systems. The operating temperatures were very high because of the application envisioned at the time. One can safely state that these systems were closer to success in the thermal regeneration mode than those described in Secs. I.1 and I.2, when compared for regeneration in the  $>500^{\circ}\text{C}$  temperature range. Since the cell reactions  $\text{C} \rightleftharpoons \text{C}^+ + \text{e}^-$  are reversible, the systems of high coulombic efficiency (e.g., Na|Hg and Na|Pb) should be suitable for operation in the coupled thermal and electrolytic regeneration mode. A more detailed integral systems analysis could be

(a) Lithium-Bismuth,  $T = 489 \pm 2^\circ\text{C}$ (b) Lithium-Cadmium,  $T = 493 \pm 20^\circ\text{C}$ (c) Lithium-Lead,  $T = 483 \pm 9^\circ\text{C}$ (d) Lithium-Tellurium,  $T = 496 \pm 5^\circ\text{C}$ (e) Lithium-Zinc,  $T = 486 \pm 6^\circ\text{C}$ (f) Lithium-Tin,  $T = 496 \pm 2^\circ\text{C}$ 

**Figure II-21. Voltage vs. Current Density of the Lithium-Containing Bimetallic Cells with the LiCl-KCl Electrolyte [36]**

performed to suggest suitable systems to reinvestigate once a solar-derived, high temperature source is identified. This analysis is particularly important in view of the large quantities of materials pumped.

At this point it should be emphasized that past investigation of concentration cells for power generation purposes in media other than molten salts is rather limited. The reasons are the generally slow electrode kinetics in other media and high ohmic losses due to lower conductivity. Molten salts with lower melting points and other media could be the basis for the investigation of other thermal or coupled thermal and electrolytic regeneration systems.



### SECTION III

#### THERMOGALVANIC OR NONISOTHERMAL CELLS

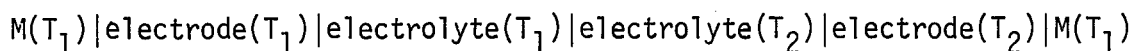
Thermogalvanic cells can be defined as galvanic cells in which the temperature is not uniform. They are the electrochemical equivalent of thermoelectric devices, which convert heat into electricity. In these cells two or more electrodes are at different temperatures. These electrodes, not necessarily chemically identical or reversible, are in contact with an electrolyte, solid or liquid, not necessarily homogeneous in composition, and with or without permeable membranes interposed in the electrolyte. During the passage of current through the thermogalvanic cells, matter is transferred from one electrode to the other as a result of the electrochemical reactions at the electrode/electrolyte interface and ionic transport in the electrolyte. In this respect, the thermogalvanic cell differs from metallic thermocouples, or thermoelectric devices in general, in which no net transfer of material occurs and the state of the conductor remains unchanged with the passage of current. In fact, thermoelectric effects in the metallic leads from the electrodes in the thermogalvanic cells contribute to the observed EMF of these cells [121-125]. The names "thermal cell," "thermocell," "electrochemical thermocouple," "nonisothermal cell," "galvanic thermocouples," and "galvanic thermocells" have been employed for thermogalvanic cells, and expressions such as "thermogalvanic energy conversion" and "ionic thermoelectric conversion" are used. These cells are designated as Type 6 in the Introduction.

Thermocells have been investigated since 1879 (see Ref. 121) and

have been the subject of several reviews; e.g., deBethune, Licht, and Swendeman [121]; deBethune [122]; Agar [123]; and Wagner [124]. Much of the work has involved studies of the temperature dependence of reference electrodes in aqueous solution [121,123,123] and also in molten salt media and solid electrolytes [123,123,124]. The research has focused on thermodynamic aspects, principally on the application of irreversible thermodynamics to these systems. Some papers have also dealt with more practical applications [125], e.g., thermogalvanic corrosion [121] and power generation [125]. Sundheim [126] considered molten salt thermocells for specific power generation uses in 1960 and Christy [127] examined the possibility of employing ionic solids in thermoelectric devices.

The EMF of a thermogalvanic cell in its initial state arises from three factors: (1) the differences in electrode temperature, (2) the thermal liquid junction potential, and (3) the metallic thermocouple effect. In general, the EMF arising from (1) and (2) is about two orders of magnitude larger than the EMF from (3), which arises at the junction in the external circuit between two electrode metals at different temperatures (the Seebeck effect). With the passage of time, a thermal cell is subject to thermal diffusion in the electrolyte (Soret effect), which tends to concentrate the electrolytes in the cold region. The concentration gradient further changes the two electrode potentials, and the cell reaches a new stationary state (final EMF). The formation of the concentration gradient can be avoided by stirring or convection (as long as the thermal gradient is not destroyed) and is not present in cells with solid electrolytes in which only one kind of ion is mobile [128].

The thermogalvanic cell can be written as:



where  $T_2 > T_1$ . The electrodes can be metals or gases with inert electrodes [121,122]. The electrolyte can be an aqueous solution, a fused salt, or a solid. Temperature  $T_1$  is fixed and  $T_2$  is varied. The most widely used sign convention for thermogalvanic cells is that the EMF ( $E$ ) is positive when the terminal connected to the electrode at  $T_2$  is positive with respect to that connected to the cold electrode. Therefore, the hot electrode is the cathode, and the  $(dE/dT_2)_{T_1}$  constant is positive. This coefficient,  $(dE/dT)_{\text{thermal}}$ , is the thermoelectric power, sometimes also designated the "Seebeck coefficient" in analogy with the nomenclature used in thermoelectric phenomena [129]. The thermoelectric power is obtained from measurements at open circuit ( $I = 0$ ).

The thermoelectric power can be described as the sum of a heterogeneous term (due to the electrode temperature effect) and a homogeneous part (thermal liquid junction potential for solutions or the thermoelectric effect on solid or liquid ionic conductors) [125,127,130]. The driving force for the thermogalvanic cell is the transport of entropy from the high temperature reservoir (at  $T_2$ ) to the low temperature sink (at  $T_1$ ), as is the case for any heat engine. References 121-123 and 131 give thermodynamic treatments of thermogalvanic cells and cite the various important papers in this field. References 121 and 122 are particularly oriented to aqueous solutions and give a comprehensive treatment of the subject [122], as well as values for  $(dE/dT)_{\text{thermal}}$  and

$(dE/dT)_{\text{isothermal}}$  [for cells SHE||electrolyte|electrode, where SHE is the standard hydrogen electrode and  $(dE/dT)_{\text{isothermal}}$  is the derivative  $dE/dT$  of the EMF (E) of the isothermal cell] for ca. 300 electrodes at 25°C [121]. Reference 123 presents a comprehensive treatment of the subject for all three media and in particular includes a review of the confusing thermodynamic nomenclature encountered in this subject. Reference 124 reviews the literature up to 1972 on the thermoelectric power of ionic solids and melts. In the following brief description of the thermogalvanic cells, the nomenclature of Agar and Breck [132] is used.

For a thermocell, for instance with pure metal electrodes and a simple electrolyte  $MX_n$ , solid or fused, the EMF of the cell is the electrical potential of a wire attached to the hot electrode minus the potential of a similar wire attached to the cold electrode. The electrical work for  $n$  equivalents of electricity is determined by the entropy absorbed from the heat reservoir surrounding the hot electrode when positive electricity passes through the cell from the cold to the hot electrode [131]. This entropy is identical to the sum of the entropy absorbed in the electrode reaction [in this case,  $S_M$  (molar entropy of the metal) -  $\bar{S}_M n + (\text{partial molar entropy of } M^{n+}) - n\bar{S}_{e^-}(M)$  (partial molar entropy of the electron in M)] and the entropy transported away from the hot electrode [in this case,  $-S_M^* n + (\text{entropy of transfer of } M^{n+}) - nS_{e^-}^*(M)$  (entropy of transfer of  $e^-$ )] [123,131]. The entropies of transfer result from heat effects attributable to the movement of electrons and ions through a thermal gradient under the influence of a voltage drop. Since  $\bar{S} + S^* = \bar{\bar{S}}$  (total transported entropy),

one can write

$$nF \frac{dE}{dT} = S_M - \bar{S}_M^{n+} - n\bar{S}_{e^-}^{(M)} \quad \text{III-1}$$

Expression III-1 also holds for aqueous thermocells after the Soret equilibrium is reached (final EMF) [121]. For the initial EMF of such aqueous thermocells (uniform electrolyte distribution) the term  $t_-(S_M^{*n+} + nS_X^{*-})$ , where  $t_-$  is the transference number of the anion, must be added to Eq. III-1. This sum of ionic entropies of transfer governs the Soret equilibrium. In a pure salt (solid or liquid) the transfer of both ions in the same direction is the gross linear movement of the salt, with no net entropy of transfer:  $(S_M^{*n+} + nS_X^{*-})_{\text{pure salt}} = 0$  [131]. The entropies of transfer for metal ions in fused salts are sufficiently small that the expression

$$nF \left( \frac{dE}{dT} \right)_{I=0} = \Delta S_{\Delta T=0} \quad \text{III-2}$$

can be deduced from Eq. III-1 if the transfer terms are neglected (as has been found experimentally for several molten salt thermocells with pure ionic fused salts). The term  $(dE/dT)_{\text{thermal}}$  is then equal to  $(dE/dT)_{\text{isothermal}}$ .

The thermoelectric power,  $(dE/dT)_{\text{thermal}}$ , measured at  $I = 0$  or calculated from the appropriate equation has been used to calculate the figure of merit,  $Z$ , of the thermocell [121-123,131], in analogy to that used for thermoelectric devices [133]:

$$Z = \frac{(dE/dT)_{I=0}^2}{\rho\kappa} \quad \text{in } K^{-1} \quad \text{III-3}$$

where  $\rho$  = specific resistivity in ohm cm,  $\kappa$  is the specific thermal conductivity in  $W \text{ cm}^{-1} K^{-1}$ , and  $dE/dT$  is in  $V K^{-1}$ . Ionic conductors were found to have figures of merit of approximately  $10^{-3} K^{-1}$ , which are of the order of magnitude of the semiconducting thermoelectric devices [125,128,133]. The conversion efficiencies are Carnot cycle limited for both the thermoelectric and thermogalvanic cells. However, anticipated practical figures of merit would be consistently less than those obtained from  $I = 0$ .

The expression of Telkes [134] for solid-state device efficiencies  $\eta$  has been applied to thermogalvanic cells:

$$\eta = \frac{1}{\frac{2T_2}{T_2 - T_1} + \frac{4 \kappa \rho}{(dE/dT)_{I=0}^2 (T_2 - T_1)}} \times 100\% \quad \text{III-4}$$

where the first term in the denominator is related to the Carnot efficiency and the second is related to the figure of merit. Wartanowitz [135] has expressed the efficiency of molten salt thermogalvanic cells as

$$\eta = \frac{\eta_c M}{(M+m+1)[A(M+m+1)(B/m+1)+1] - C(m+1)} \quad \text{III-5}$$

where  $\eta_c$  = Carnot efficiency  $(T_2 - T_1/T_2)$ ;  $A = 1/ZT_2$ ;  $B = (T_2^2 - T_1^2)(L)(Z)/$

$2(T_2 - T_1)(dE/dT)^2$ ;  $C = \eta_c/2$ ;  $L =$  Lorenz number;  $m =$  electrode resistance/molten salt resistance; and  $M =$  load resistance/molten salt resistance. Wartanowicz's [136] experimental results with a  $\text{Ag}|\text{AgNO}_3(\ell)|\text{Ag}$  cell agree with Eq. III-5.

The analyses of  $Z$  and  $\eta$  above do not consider electrode polarization effects, which effectively limit the power output of such devices under current drain.

Zito [125] compares thermoelectric devices with the thermogalvanic cells, based mostly on molten salts or solid electrolytes, since the wider temperature range of these materials allows higher Carnot efficiencies to be obtained. This paper also includes pertinent comments about materials problems associated with these higher-temperature cells, fabrication techniques, and cell construction.

Since the century-old literature on thermogalvanic cells is very extensive, our review is not comprehensive but covers most of the thermocells studied for power generation in molten salt, solid electrolyte, and aqueous media, as well as the more recent papers in the field. References 121-124 contain most literature citations prior to approximately 1970 concerning principally the thermodynamics of irreversible processes, temperature effects on reference electrodes, and thermoelectric powers of solid electrolytes and melts.

### III. 1 MOLTEN SALT THERMOGALVANIC CELLS

#### III.1.1 Solid or Liquid Electrodes

The thermocell  $\text{Ag}|\text{AgNO}_3|\text{Ag}$  has been known since 1890 [Poincaré; see Ref. 137]. Since 1950 this system has been the subject of several

investigations [131]. Sundheim and Rosenstrein [137] measured initial thermoelectric powers for this system in 1953. Other determinations have been made over a wide range of temperatures with pure  $\text{AgNO}_3$  [137,138] or with molten nitrate mixtures [139,140,141,142]; some results are given in Table III-1. The measurements of Sundheim et al. [139] in  $\text{AgNO}_3:\text{NaNO}_3$  were repeated by Haase et al. [140], who also measured the  $\text{AgNO}_3:\text{LiNO}_3$  system. Haase and co-workers extended the treatment of the EMF of the thermocells [143] to binary melts and derived new general relations for the thermoelectric power of a thermocell consisting of a two-component ionic melt (three ion constituents) and two similar electrodes reversible to one of the ion constituents [140]. The relationship between the thermoelectric power and the Soret coefficient was derived. The transport quantities relevant to thermal diffusion and related phenomena in the melt are the transported entropies of the two cations and a linear combination of the heats of transport of these cations. The experimental work included new measurements of thermoelectric powers, transport numbers, and activity coefficients. Transported entropies, the difference between the two heats of transport, and the Soret coefficient were calculated from these measurements.

Connan and Dupuy [144] have measured the thermoelectric powers of mixtures of  $\text{AgNO}_3:\text{MNO}_3$  ( $M = \text{Li}, \text{K}, \text{Rb}, \text{Tl}$ ); initial thermoelectric powers of 0.38, 0.25, 0.30, 0.28 mV/degree at the 0.5:0.5 mole fraction composition were found for these mixtures. The dependence of the initial thermoelectric power on the mixture composition was investigated.

Abraham and Gauthier [141,142] extended studies on mixtures of binary molten salts ( $\text{AgNO}_3:\text{TlNO}_3$ ), which gave low thermoelectric powers



Table III-1. SUMMARY OF THERMOELECTRIC POWERS IN Ag|MOLTEN SALT|Ag THERMOCELLS

Molten Salt	Temperature (°C)	Initial (dE/dT) <sub>I=0</sub> (mV/degree)	Steady-State (dE/dT) <sub>I=0</sub> (mV/degree)	Temperature Range (°C)	Reference
<u>Nitrates</u>					
AgNO <sub>3</sub>	305	-0.344	--	240-310	137
AgNO <sub>3</sub>	250	-0.32 to -0.34	--	225-310	138
AgNO <sub>3</sub>	310	-0.319	--	--	139
AgNO <sub>3</sub> :NaNO <sub>3</sub> (0.5:0.5) <sup>a</sup>	310	-0.331	-0.248	--	139
AgNO <sub>3</sub> :NaNO <sub>3</sub> (0.05:0.95) <sup>a</sup>	310	-0.419	-0.149	--	139
AgNO <sub>3</sub> :NaNO <sub>3</sub> (0.5:0.5) <sup>a</sup>	310	-0.328	-0.354	280-340	140
AgNO <sub>3</sub> :LiNO <sub>3</sub> (0.1:0.9) <sup>a</sup>	310	-0.496	-0.549	260-340	140
AgNO <sub>3</sub> :LiNO <sub>3</sub> (0.5:0.5) <sup>a</sup>	310	-0.379	-0.405	240-340	140
AgNO <sub>3</sub> :TlNO <sub>3</sub> (0.5:0.5) <sup>a</sup>	90,180	-0.221, -0.254	--	--	142
AgNO <sub>3</sub> :(Cd,Na,K)NO <sub>3</sub> <sup>b</sup> (0.001:0.999) <sup>a</sup>	120	-0.820	--	--	142
<u>Halides</u>					
AgCl	--	-0.375	--	500-900	146
AgCl	--	-0.40	--	450-650	147
AgCl	--	-0.42	--	487-590	148
AgCl	627	-0.38	--	--	149
AgBr	477	-0.45	--	--	148
AgI	577	-0.43	--	--	131
AgI	577	-0.50	--	--	148
<u>Sulfate</u>					
Ag <sub>2</sub> SO <sub>4</sub>	--	-0.31	--	657-750	150

<sup>a</sup> Mole fraction composition.

<sup>b</sup> Eutectic composition: 0.460:0.394:0.146.

(see Table III-1), to ternary molten salts based on  $\text{Cd}(\text{NO}_3)_2$  and two other nitrates of Li, Na, K, Cs, or Tl, at eutectic and noneutectic compositions. The temperature of operation in these melts was 84-120°C. Thermoelectric powers as high as 0.82 mV/degree at much lower temperatures than those listed in Table III-1 were obtained. The melts investigated form glasses and in the supercooled region the temperature dependence of the thermopotential is represented by a straight line of different slope than that of the normal liquid range. The authors proposed measurements on thermocells as a means of studying supercooling and nucleation [145]. The presence of metal ions such as  $\text{Cd}^{2+}$  and  $\text{Tl}^+$  leads to mixed metal deposition at the cathodes; these cells are not suitable for power generation.

The molten salt thermocells  $\text{Ag}|\text{AgX}(\ell)|\text{Ag}$  ( $\text{X}^- = \text{Cl}^-, \text{Br}^-, \text{I}^-$ ) were investigated by Markov [148], Senderoff and Bretz [146], Holtan [147], and Anderson et al. [149]. The thermoelectric powers for the halide thermocells are also shown in Table III-1, as is the value for the molten cell  $\text{Ag}|\text{Ag}_2\text{SO}_4(\ell)|\text{Ag}$ .

Table III-2 summarizes the thermoelectric powers of other metal|molten salt|metal cells studied. Most of the lead cells had thermoelectric powers of a few microvolts (see Table III-2). Detig and Archer [130] used tungsten-lead contacts whereas Anderson et al. [149, see also Ref. 3] ran the molten lead discharged at the cold electrode back to the anode by gravity flow. The cell  $\text{Tl}|\text{Tl}_2\text{O}|\text{Tl}$  was also investigated but was found to be very corrosive [149].

Table III-3 summarizes some of the data on transported entropies in molten salts (see Eq. III-1) for some of the reported cells. In the

Table III-2. SUMMARY OF INITIAL THERMOELECTRIC POWERS IN METAL|MOLTEN SALT|METAL THERMOCELLS

Cell	Temperature (°C)	$(dE/dT)_{I=0}$ (mV/degree)	Reference
Cu CuCl Cu	462-588	-0.436	150
W:Pb(l) PbCl <sub>2</sub>  Pb(l)W	500-700	-0.006	138
W:Pb(l) PbBr <sub>2</sub>  Pb(l)	400-700	-0.040	138
Pb(l) PbCl <sub>2</sub>  Pb(l)	627	-0.008	149
Pb(l) PbI <sub>2</sub>  Pb(l)	627	-0.048	149
Zn ZnCl <sub>2</sub>  Zn	327	+0.13	131
Sn SnCl <sub>2</sub>  Sn	--	-0.028	149

Table III-3. SUMMARY OF TRANSPORTED ENTROPIES ( $\bar{S}_{M^{n+}}$ ), PARTIAL MOLAL ENTROPIES ( $\bar{S}_{M^{n+}}$ ), AND ENTROPIES OF TRANSFER ( $S_M^{*n+}$ ) FOR MOLTEN SALT THERMO-CELLS<sup>a</sup>

Cell	Temperature (°C)	$\bar{S}_{M^{n+}}$	$\bar{S}_{M^{n+}}$	$S_M^{*n+}$	Reference
Ag AgNO <sub>3</sub>  Ag	227	21.0	19.0	2	131
Ag AgCl Ag	527	26	22	4	131
Ag AgCl Ag	727	26.7	--	--	146
Ag AgBr Ag	477	27	22	5	131
Ag AgI Ag	577	27	24	3	131
Cu CuCl Cu	525	24.2	--	--	150
Zn ZnCl <sub>2</sub>  Zn	327	8	114	-6	131
Sn SnCl <sub>2</sub>  Sn	327	22	16	+6	131
	$\text{AgNO}_3^b$	Temperature (°C)	$\bar{S}(\text{Ag}^+)$	$\bar{S}(\text{Li}^+ \text{ or } \text{Na}^+)$	
Ag AgNO <sub>3</sub> ,NaNO <sub>3</sub>  Ag	0.3	310	22.7	16.5	140
	0.5	310	22.4	17.4	140
	1.0	310	21.8	--	140
Ag AgNO <sub>3</sub> ,LiNO <sub>3</sub>  Ag	0.3	310	24.6	16.4	140
	0.5	310	23.6	16.3	140
	1.0	310	21.8	--	140

<sup>a</sup>All entropies are given in cal/degree g ion.

<sup>b</sup>Mole fraction of AgNO<sub>3</sub>.

case of pure molten salts the transfer entropies ( $S^*$ ) were found to be small [131], of the order of 26 e.u. The partial molal entropies in the simple binary salts were calculated by

$$\bar{S}_{M^+} = \frac{1}{2} \left( S_{MX} + \frac{3}{2} R \ln \frac{M_M}{M_X} \right) \quad \text{III-6}$$

where  $M_i$  is the ionic weight [131]. Table III-3 also gives the transported entropies calculated by Haase et al. [140] for the cations in the  $\text{AgNO}_3:\text{Li}, \text{NaNO}_3$  molten salts at 3 of the 10 compositions studied.

### III.1.2 Gaseous Electrodes

The thermoelectric powers of some  $X_2(\text{g})|\text{molten electrolyte}|X_2(\text{g})$  cells with inert electrodes (e.g., graphite) are shown in Table III-4. Halogen reversible electrodes generally produce higher thermoelectric powers than those obtained with metal electrodes (compare Table III-4 with Tables III-1 and III-2). The cell  $\text{Cl}_2|\text{AgCl}(\ell)|\text{Cl}_2$  has been investigated in several laboratories [146,153,149]. Senderoff [153] patented a thermocell of this type using molten  $\text{AgCl}$ ,  $\text{KCl}:\text{LiCl}$ , or  $\text{NaAlCl}_4$  (see Table III-4). In the 500-900°C range, with molten  $\text{KCl}:\text{LiCl}$ , current densities as high as 700 mA/cm<sup>2</sup>, with very little polarization, were reported. This was achieved using a cell design consisting of two inert porous graphite current collectors, provided with suitable channels for transporting gas to their outer faces where the graphite electrodes were in contact with the molten salt electrolyte, which was sandwiched between the current collectors. Chlorine gas was fed at 500°C and 900°C countercurrently [153]. Lockheed Aircraft Corp. [149] reinvestigated this system and obtained current-voltage curves that indicated only IR

Table III-4. SUMMARY OF THERMOELECTRIC POWERS IN THERMOCELLS  
 $X_2$  | MOLTEN SALT ( $\ell$ ) |  $X_2$

Cell	Temperature (°C)	$(dE/dT)_{I=0}$ (mV/degree)	Reference
$Cl_2$   AgCl   $Cl_2^a$	727	-0.644	146
$Cl_2$   AgCl   $Cl_2^a$	500-900	-0.655	152
$Cl_2$   AgCl   $Cl_2$	500-900	-0.65	153
$Cl_2$   AgCl   $Cl_2^a$	627	-0.675	149
$Cl_2$   LiCl   $Cl_2$	627	-0.534	154
$Cl_2$   NaCl   $Cl_2$	860	-0.45	138
$Cl_2$   NaCl   $Cl_2$	850	-0.475	146
$Cl_2$   NaCl   $Cl_2$	827	-0.483	154
$Cl_2$   KCl   $Cl_2$	830-950	-0.40	138
$Cl_2$   KCl   $Cl_2$	850	-0.475	146
$Cl_2$   KCl   $Cl_2$	727	-0.504	154
$Cl_2$   $PbCl_2$   $Cl_2$	727	-0.544	154
$Cl_2$   $CsCl$   $Cl_2$	727	-0.533	154
$Cl_2$   $PbCl_2$   $Cl_2$	627	-0.579	149
$Cl_2$   KCl : LiCl   $Cl_2$ (54.5 wt % KCl)	500-900	-0.55	152
$Cl_2$   $NaAlCl_4$   $Cl_2$	--	-1.0-1.4	153
$I_2$   $PbI_2$   $I_2$	627	-0.637	149
$I_2$   LiI   $I_2$	627	-0.595	149

<sup>a</sup> One atmosphere  $Cl_2$  pressure.

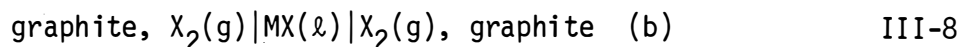
polarization to at least 300 mA/cm<sup>2</sup>. Similar results were found with the I<sub>2</sub>(g)|PbI<sub>2</sub>(ℓ)|I<sub>2</sub>(g) and I<sub>2</sub>(g)|LiI(ℓ)|I<sub>2</sub>(g) cells, although PbI<sub>2</sub> had too high a vapor pressure to be of practical use [149, see also Ref. 3]. Brodd [155] designed a closed-system, molten salt thermocell with gaseous electrodes.

Meissner et al. [152] studied the pressure dependence of thermocells of the type Cl<sub>2</sub>(g)|MCl|Cl<sub>2</sub>(g), where M = Ag, Na, K, and Li. The efficiencies of these cells were found to increase with a decrease in total vapor pressure and with an increase in the hot cell temperature. Higher temperatures and lower total vapor pressures increase the fraction of electrolyte in the vapor, which would cause electrolyte carried by chlorine gas to condense along the way to the cold electrode. Estimated efficiencies of these cells are 2-5% (1-0.1 atm; low temperature at 500°C, high temperature at 900-1300°C). A preliminary analysis based on literature data for the F<sub>2</sub>|LiF|F<sub>2</sub> thermocell gave an estimated energy conversion efficiency of 8-10% between 900-1400°C, with total pressure between 0.2-1.0 atm [152].

Senderoff and Bretz [146] as well as Anderson et al. [149] verified experimentally that the thermoelectric powers of the thermocells



and



and the temperature coefficient of the isothermal cell



can be related as follows

$$\left(\frac{dE}{dT}\right)_b - \left(\frac{dE}{dT}\right)_a = \left(\frac{dE}{dT}\right)_c - \left(\frac{dE}{dT}\right)_{\text{graphite/metal}} \quad \text{III-10}$$

Equation III-10 can also be derived from

$$F\left(\frac{dE}{dT}\right)_a = S_M - \bar{S}_{M^+} - \bar{S}_{e^-(M)} \quad \text{III-11}$$

and

$$F\left(\frac{dE}{dT}\right)_b = -\frac{1}{2} S_{Cl_2}^{\circ} + \bar{S}_{Cl^-} - S_{e^-(G)} \quad \text{III-12}$$

where the electronic transported entropies are negligible for most thermocells under consideration (note deviations from Ref. 156). Katelaar [157] has shown that the same type of correlation (Eq. III-10) cannot be used or derived for cells in which mixed molten salts are used.

### III.1.3 The Bismuth-Bismuth Iodide System

The system Bi/BiI<sub>3</sub> was studied at Aerojet-General Corp. [52,158], aiming initially at thermal regeneration which evolved into the thermogalvanic mode. A working sandwich-type cell was constructed with a porous ceramic material impregnated with BiI<sub>3</sub> (with or without additional electrolyte, e.g., ZnI<sub>2</sub>, AuCl, PtCl<sub>2</sub>, PdCl<sub>2</sub>, CdI<sub>2</sub>, HgI, KI) and sealed between conductive materials (e.g., Au). Heating one side and cooling the other produced current. Another cell contained a sandwich of two porous carbon electrodes on either side of the electrolyte. Since BiI<sub>3</sub> decomposes at 500°C, when the cells were operated with the hot side at T > 500°C (e.g., 900°C), iodine was evolved at the hot electrode and reduced at the cold electrode with mass transfer within



the cell. Preliminary work with unsealed cells gave about 0.5 V OCV and 100 mA/cm<sup>2</sup> at 0.3 V. An attempt to seal the cells gave 0.25 V at 14 mA/cm<sup>2</sup> with the hot face at 740°C. The performance was of limited duration due to the poor seal of the cell which led to oxidation of the graphite anode and of the bismuth as well as loss of both iodine and electrolyte. Sealed cells with a hot face temperature at 500°C were shown to have a life of ~230 hours with a very poor performance.

Another group of researchers at North American Aviation investigated the molten Bi/BiI<sub>3</sub> system, studying the thermoelectric powers [159], magnetic properties [160], electrical conductivities [161], and thermal diffusion [162]. Above 485°C, liquid bismuth is miscible in all proportions with BiI<sub>3</sub>. Thermoelectric powers were determined for this system between 400-500°C as a function of composition (from pure Bi to pure BiI<sub>3</sub>), and ranged from -0.053 to 0.125 mV/degree, with a maximum at about 40 mole % Bi and minima at ca. 10 and 85 mole % Bi [159]. The results were interpreted in the framework of irreversible thermodynamics and were consistent with an interpretation involving electronic conduction in metal-rich compositions and a mixture of electronic and ionic conduction in salt-rich compositions. These conclusions were supported by magnetic susceptibility data in which a deviation from simple additivity was observed at high metal concentrations [160]. It was concluded that Bi dissolves in BiI<sub>3</sub> by reacting to form Bi<sup>+</sup>, as was shown in analogous Bi/BiBr<sub>3</sub> and Bi/BiCl<sub>3</sub> systems [163]. Metals and/or free electrons were concluded to be present at high metal concentration. The electrical conductivities increased continuously from 0.32 ohm<sup>-1</sup>cm<sup>-1</sup>

(pure  $\text{BiI}_3$ ) to  $7.2 \times 10^3 \text{ ohm}^{-1}\text{cm}^{-1}$  (pure Bi) [161]. Final thermoelectric powers were also determined in this system with the cell  $\text{W}|\text{Bi-BiI}_3|\text{W}$  over the composition range of 0.01-0.90 mole fraction of Bi. From 0.30 to 0.90 mole fraction of Bi the initial and final thermoelectric powers were identical (0.097-0.015 mV/degree), whereas at lower metal concentrations the final thermoelectric powers were larger than the initial; e.g., at 0.03 mole fraction of Bi, the initial and final thermoelectric powers were 0.035 and -3.1 mV/degree, respectively [162]. Discussions of mechanisms and transported entropy data are given by Kellner [162].

### III.2 THERMOGALVANIC CELLS WITH SOLID ELECTROLYTES

The possibility of using solid electrolytes composed of ionic materials for power generation has been envisioned in batteries and in thermocells since the 1950s [125,127,164]. Examples of thermocell and galvanic cell developments using solid electrolytes were given by Weininger [165-170] and Schiraldi et al. [172-175]. The work using  $\beta$ -alumina solid electrolyte in modified thermogalvanic cells is described in Section IV. In 1972, Wagner [24] reviewed the literature on thermoelectric powers in solid electrolytes and molten salts. Most work concerning the study of thermoelectric power in solid electrolytes aimed at the investigation of the transport mechanisms and the evaluation of heats of transport of the point defects in the lattices of the systems considered [123-125,131,147,176-180].

Table III-5 lists thermoelectric powers for some thermogalvanic cells with solid electrolytes (these powers include those for the ionic salts plus the electrode temperature effect). Comparison of Tables III-5,

Table III-5. SUMMARY OF THERMOELECTRIC POWERS OF SOLID-ELECTROLYTE THERMOCELLS [125]

Cell	$(dE/dT)_{I=0}$ (mV/degree)	Temperature (°C)
Ag AgI(s) Ag	0.60	140-500
Ag  $\alpha$ -AgI Ag <sup>a</sup>	0.56-0.60	150-400
Cl <sub>2</sub>  AgCl(s) AgCl <sub>2</sub>	1.29	300-410
Cl <sub>2</sub>   $\alpha$ -AgI Cl <sub>2</sub> <sup>a</sup>	1.2-1.4	160-500
Pb PbCl <sub>2</sub> (s) Pb	0.54	200-470
Cl <sub>2</sub>  PbCl <sub>2</sub> (s) Cl <sub>2</sub>	1.28	260-400
Pb PbBr <sub>2</sub> (s) Pb	0.40	350
Br <sub>2</sub>  PbBr <sub>2</sub> (s) Br <sub>2</sub>	1.20	320

<sup>a</sup> From Ref. 168.

III-4, III-2, and III-1 indicate that for the same salt system the thermoelectric powers increase in the order:  $M|MX(\ell)|M < X_2|MX(\ell)|X_2 \approx M|MX(s)|M < X_2|MX(s)|X_2$ , thus reflecting the larger homogeneous thermoelectric powers (and obviously larger transported entropies) in the solid salts as compared to the molten salts.

Table III-6 lists thermoelectric powers for some ionic salts with ordered structure [164] (low concentration of point defects) and with disordered cationic sublattices of the  $\alpha$ -AgI structural type [164].

Recently determined thermoelectric powers of the ionic glass-like solids  $AgI-Ag_nXO_4$  (where  $X = Cr, Mo, W, S, Se, P, As$ ) and  $AgI-Ag_2Cr_2O_7$  (75-80 mole % AgI), which exhibit high ionic conductivity, are in the range of 0.5-0.6 mV/degree in the temperature range of 25-275°C [172].

Table III-7 lists values of the transported entropies ( $\bar{S}_{Mn+}$ ) for some solid electrolytes [123,131] and an overall transported entropy for  $\alpha$ -AgI and related compounds (in which chemical disorder is superimposed on the thermal disorder) and for some of the glass-type solids described above [172] (cf. Table III-3).

A few cells were made for power generation and their discharge characteristics were studied. The work of Weininger [165-170] at General Electric Co. is described in more detail in Section III.2.1. Schiraldi et al. [172-175] have reported only battery results using the silver iodide-silver oxysalts solid electrolytes at low temperature (25-60°C), but they estimate the figure of merit of their thermocell system as  $10^{-3}$ - $10^{-4}$  degree<sup>-1</sup>. The limitation imposed by mass transfer is emphasized by the authors [172]; no current-voltage curves for these thermocells have been measured.

Table III-6. SUMMARY OF THERMOELECTRIC POWERS OF SOME IONIC SALTS

Ionic Salt	$-(dE/dT)_{I=0}^a$ (mV/degree)	Temperature (°C)	Reference
NaCl	944/T - 2.295	450-750	178
NaBr	1.1	600-700	179
KCl	1.8-1.9	550-700	178
KBr	1.8-1.9	550-700	179
AgCl	1.2	300	127
AgBr	0.8	300	127
	0.6	350	177
	0.66	350	130
$\gamma$ -AgI	0.6	25-146	180
$\beta$ -AgI	1.0	146	180
$\alpha$ -AgI	0.7	148	180
$RbAg_4I_5$	93/T + 0.36	25-200	180
$KAg_4I_5$	78/T + 0.28	25-200	180
$NH_4Ag_4I_5$	58/T + 0.31	25-200	180

<sup>a</sup> T is absolute temperature.

Table III-7. SUMMARY OF TRANSPORTED ENTROPIES ( $\bar{S}_{M,n+}$ ) FOR SOLID ELECTROLYTES OF ORDERED STRUCTURE [123,131] AND SUMMARY OF OVERALL TRANSPORTED ENTROPIES FOR SOLIDS OF THE  $\alpha$ -AgI TYPE [172] and AgI-Ag OXYSALTS (75-80 MOLE % AgI) [172]

Electrolyte	Temperature (°C)	$\bar{S}_{M,n+}$ (cal/degree g ion)
AgCl	127	44
	427	31.8
AgBr	127	46
	327	32.8
$\beta$ -AgI	127	40.6
CuCl	127	33
PbCl <sub>2</sub>	227	46
PbBr <sub>2</sub>	227	40
$\alpha$ -AgI	227	26.3 <sup>a</sup>
	227	27.6 <sup>b</sup>
RbAg <sub>4</sub> I <sub>5</sub>	227	23.9
NH <sub>4</sub> Ag <sub>4</sub> I <sub>5</sub>	227	23.2
AgI·Ag <sub>2</sub> MoO <sub>4</sub>	227	27.0
AgI·Ag <sub>2</sub> SO <sub>4</sub>	227	29.0
AgI·Ag <sub>2</sub> TeO <sub>4</sub>	227	32.8

<sup>a</sup> Ref. 131.

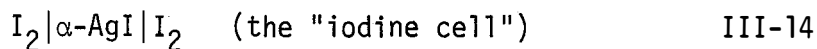
<sup>b</sup> Ref. 172.

### The $\text{Ag}|\alpha\text{-AgI}|\text{Ag}$ and $\text{I}_2|\alpha\text{-AgI}|\text{I}_2$ Thermocells

In an attempt to develop high temperature miniature batteries activated by gaseous halogens, Weininger [165,166] studied a solid electrolyte cell consisting of silver halide with Ta and Ag wires as cathode and anode. When the cathode in these cells was exposed to halogen vapor ( $\text{Br}_2$  or  $\text{I}_2$ ), a high temperature primary battery was formed. With  $\alpha\text{-AgI}$  the cells could be recharged a few times. The cell  $(\text{Ta})\text{I}_2|\alpha\text{-AgI}|\text{Ag}$ , studied in the 150-550°C temperature range, showed an OCV of 0.67 V and produced short circuit currents of 18 mA [166]. The current outputs increased with temperature [166], and improved solid electrolyte gaseous diffusion cathodes were also proposed [167]. Parallel to this battery work, thermocells were developed [168-170] involving the systems



and



Several cell configurations were tried [168] for the silver thermocell. These included (1) silver electrodes sandwiching the  $\alpha\text{-AgI}$  electrolyte (ionic resistivity of 0.38 ohm cm at 500°C and 0.47 ohm cm at 350°C) contained in a glass spacer to prevent deformation and (2) two silver electrodes sandwiching a porous  $\beta\text{-alumina}$  matrix impregnated with  $\alpha\text{-AgI}$ . During operation, silver is dissolved from the hot anode,

silver ions migrate from the hot to the cold electrode, and silver metal is deposited at the cold electrode. Dendrite formation in these cells leads to loss of contact at the electrode/electrolyte interface, loss of silver, and short circuit of the cell. The cell needs a provision for reversing the hot and cold sides for continuous operation. In the cell with a porous matrix the dendrite formation was slowed down but at the cost of increased internal resistance. Current-voltage curves were obtained for these cells. For instance, for  $\Delta T = 226^\circ\text{C}$ , a thermopotential of  $\sim 0.13$  V (OCV) was observed and at  $\sim 0.05$  V a current of 40 mA was drawn from the cell ( $R = 1.6$  ohm).

These problems of the silver cell did not appear in the iodine cell due to the gaseous electrode. In this case, the iodide ions are oxidized to iodine at the cold electrode, producing an increased iodine pressure at the cold electrode. Silver ions migrate from the cold to the hot electrode, where iodine is reduced with the formation of silver iodide. Figure III-1 shows a diagram of the iodine thermocell in which the porous iodine diffusion electrodes are made of graphite. Some of the major problems of this cell were: contraction of the AgI on heating, maintenance of the three-phase electrode/electrolyte/iodine interface, and encapsulation [168-170]. For thermodynamic expressions of the thermoelectric power taking into account the contraction of the electrolyte with temperature, see Ref. 171. The discharge characteristics of laboratory cells were studied as a function of temperature [168].

The data in Table III-8 exemplify the performance of the iodine cell. At  $\Delta T = 280^\circ\text{C}$ , electrochemical polarization limits the current drain, but at  $\Delta T < 170^\circ\text{C}$ , mostly IR polarization is observed. The



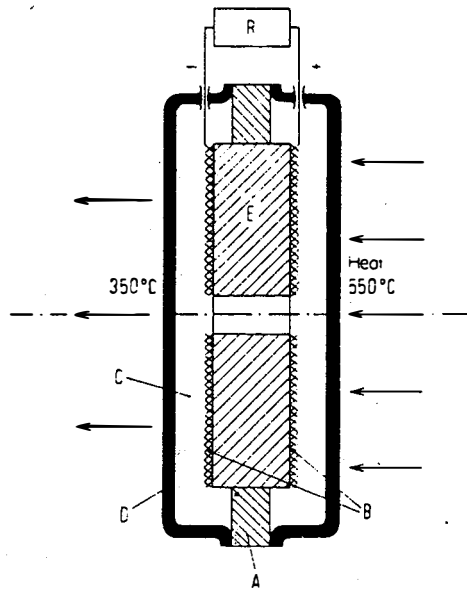


**Figure III-1. Weininger's  $I_2/\alpha\text{-AgI}/I_2$  Thermocell [168]**

**A:** annular ceramic mounting; **B:** porous diffusion gas electrodes; **C:** iodine vapor; **D:** casing; **E:** solid  $\alpha\text{-AgI}$

Table III-8. PERFORMANCE OF THE IODINE CELL [168]

$T_2$ ( $^{\circ}\text{C}$ )	$T_1$ ( $^{\circ}\text{C}$ )	$\Delta E$ (mV)	$\frac{\Delta E}{\Delta T}$ (mV/degree)	I at $\frac{\Delta E}{2}$ (mA)	$R_i$ (ohms)
342	262	95	1.10	0.6	79
340	184	208	1.33	1.4	67 <sup>a</sup>
335	165	232	1.36	1.8	61
498	218	347	1.24	1.8	91 <sup>b</sup>

<sup>a</sup>Current < 0.6 mA.

<sup>b</sup>Current > 1 mA.

coulombic capacity of the cell, limited by the geometry of the electrode, was determined: one cell had a capacity of 8.5 coulombs on a 100-ohm load. The efficiency of the iodine cell is improved by reversing the temperature gradient to avoid the advance of the solid electrolyte from the high pressure zone. The thermoelectric powers obtained, 1.2-1.4 mV/degree (see Table III-8), compare well with theoretical values, 1.3-1.5 mV/degree [see Refs. 3 and 125]. The efficiency of this system, calculated from Eq. III-4, was ~5%.

### III.3 THERMOGALVANIC CELLS IN AQUEOUS AND NONAQUEOUS SOLVENTS

The work described in this section was aimed at power generation [182,183,185,186], practical uses of thermogalvanic cells [184], or elucidation of general principles (e.g., applied to thermogalvanic corrosion) [121,187-190]. Ludwig and Rowlette [191] devised a thermogalvanic concentration cell for power generation which is described later in this section. Reference 121 lists ca. 300 temperature co-

efficients of electrode potentials (from calculations and some experimental data).

Table III-9 presents thermoelectric powers for cells  $\text{Cu}|\text{electrolyte}|\text{Cu}$  in aqueous and nonaqueous media, as well as Liebhafsky's [184] results for cells with copper electrodes sandwiching cation exchange resins which were treated with  $\text{Cu}^{2+}$  ions in aqueous solutions or mixtures of water and organic solvents. Due to the linearity of the EMF (OCV) values with  $\Delta T$ , these cells were suggested as thermogalvanic thermocouples for restricted operations [184]. Use of these cells as power generators was not suggested, but clearly large IR polarization should be expected.

Clampitt and German [182] have suggested several configurations for thermocells and have given some results for  $\text{Cu}^{2+}$  ions in aqueous and nonaqueous solvents, which are reproduced in part in Table III.9. These authors have also measured the power output and voltage of some of these cells. For  $\text{Cu}|\text{CuSO}_4$  in  $\text{H}_2\text{O}|\text{Cu}$  and  $\text{Cu}|\text{CuSO}_4$  in  $\text{H}_2\text{O} + 20\% \text{H}_2\text{SO}_4|\text{Cu}$ , the voltages attained at maximum power were 31 and 28 mV, which correspond to powers of 0.03 and 0.25  $\text{mW}/\text{cm}^2$ , respectively. For comparison, some results compiled by deBethune et al. [121] for aqueous solutions are also included in Table III-9. Due to mass transfer occurring when the cell is operating under current drain conditions, Cu is dissolved (oxidized) at the cold electrode and deposited at the hot electrode, and therefore  $\text{Cu}^{2+}$  ions are transferred from the cold to the hot electrode. To draw power continuously from the cell, it is necessary to reverse the process and heat the cold electrode and cool the hot electrode by some mechanical means (see Ref. 182). The growth of dendrites and the loss

Table III-9. THERMOELECTRIC POWERS OF THE Cu|ELECTROLYTE|Cu CELLS  
 IN AQUEOUS AND NONAQUEOUS SOLVENTS

Electrolyte	$(dE/dT)_{I=0}$ (mV/degree)	Temperature (°C)		Reference
		$t_{cold}$	$t_{hot}$	
<b>CuSO<sub>4</sub></b>				
0.08 M	0.64			
0.5 M	0.73	0-50°C		121
1.0 M	0.69-0.79			
saturated	0.9-0.97			
		$t_{cold}$	$t_{hot}$	
0.01 M; pH = 4.65	1.0	25	75	181
0.01 M; pH = 1.8-1.0	0.5-0.3	25	85	181
saturated in H <sub>2</sub> O	0.89	20	100	182
saturated in 20% H <sub>2</sub> SO <sub>4</sub> + Na <sub>2</sub> SO <sub>4</sub> ~0.4 M	1.03	20	100	182
<b>NaCl</b>				
15 w/w %	-0.35	19	100	183
15 w/w %	-0.24	19	100	183
Amberplex Cl-Cu <sup>2+</sup> form	-0.5-0.6	0	10-50	184
<b>Phenolsulfonic resin:</b>				
Cu <sup>2+</sup> form in H <sub>2</sub> O	-0.6	not specified		184
Same resin above in water/ ethylene glycol	-0.5-0.7	not specified		184
CuSO <sub>4</sub> in CH <sub>3</sub> OH <sup>a</sup>	0.68	20	68	182
CuSO <sub>4</sub> in DMSO <sup>b,a</sup>	1.19	20	152	182
CuSO <sub>4</sub> in DMF <sup>c,a</sup>	0.98	20	125	182

<sup>a</sup>Saturated solutions.

<sup>b</sup>DMSO ≡ dimethylsulfoxide.

<sup>c</sup>DMF = dimethylformamide.

of copper are the major problems anticipated for long-term operation.

Table III-10 assembles data for examples of other thermogalvanic cells studied in aqueous media. The last two examples in Table III-10, thermogalvanic cells in which the two redox species are soluble, were studied by Burrows [185,186]. In these cells the permanent mass transfer problems associated with metal deposition are not present, though, in both examples [185,186] the discharge behavior of these cells, which was studied in detail, showed that concentration polarization (the rate of mass transfer of the electroactive species —  $\text{Fe}^{3+}$ ,  $\text{Fe}^{2+}$  or  $\text{Fe}(\text{CN})_6^{4-}$ ,  $\text{Fe}(\text{CN})_6^{3-}$  — to the electrode) limits the current and therefore the power output of such devices. However, these cells did produce continuous steady-state power output (current drain) as long as the temperature gradient remained constant. The maximum power output for these systems under the experimental conditions was  $\sim 0.05 \text{ mW/cm}^2$  for the  $\text{Fe}^{2+}/\text{Fe}^{3+}$  couple [185] and  $< 0.1 \text{ mW/cm}^2$  for the  $\text{Fe}(\text{CN})_6^{4-}/\text{Fe}(\text{CN})_6^{3-}$  couple [186], which has a higher thermoelectric power than  $\text{Fe}^{2+}/\text{Fe}^{3+}$  (see Table III-10). Improvement in power output by a factor of four was obtained by forced convection of the solution adjacent to either electrode [186]. Obviously, improved mass transfer may destroy the temperature gradient in a practical device. The efficiency of conversion of 2-5% was calculated from the open-circuit data by using the solid-state thermoelectric expression (Eq. III-4) for the  $\text{Fe}^{2+}/\text{Fe}^{3+}$  couple.

References 121 and 123 give transported entropies for various metal ions in aqueous solutions.

Clampitt and German [182] and Deysher [192] describe thermogalvanic cells employing electrodes of the second kind, e.g.,  $\text{Hg}/\text{Hg}_2\text{SO}_4$ , in which

Table III-10. THERMOELECTRIC POWERS FOR SOME SELECTED THERMOGALVANIC CELLS IN AQUEOUS MEDIA

System	(dE/dT) <sub>I=0</sub> (mV/degree)	Temperature(°C)		Reference
		Cold	Hot	
Pb Pb(C <sub>2</sub> H <sub>3</sub> O <sub>2</sub> ) <sub>2</sub>  Pb <sup>a</sup>	0.2	20	100	182
Zn Zn(C <sub>2</sub> H <sub>3</sub> O <sub>2</sub> ) <sub>2</sub>  Zn <sup>a</sup>	1.1	20	100	182
Zn phenolic ion exchange resin in Zn <sup>2+</sup> form Zn	0.5	ΔT = 30		184
Pt HCl(20 w/w %) Pt	0.18	10	80	183
Pt HNO <sub>3</sub> (30 w/w %) Pt	0.30	10	90	183
Pt Fe <sup>2+</sup> , Fe <sup>3+</sup> ; 1 M HCl Pt				
[Fe <sup>2+</sup> ]=[Fe <sup>3+</sup> ] = 2 M	0.57	30	80	185
1 M	0.78	30	80	185
0.25 M	1.0	30	80	185
Pt Fe(CN) <sub>6</sub> <sup>4-</sup> , Fe(CN) <sub>6</sub> <sup>3-</sup> ; 0.5 M K <sub>2</sub> SO <sub>4</sub>  Pt				
[Fe(CN) <sub>6</sub> <sup>4-</sup> ]=[Fe(CN) <sub>6</sub> <sup>3-</sup> ] = 0.1 M	1.4	30	80	186

<sup>a</sup>Saturated solutions.

two cells are connected back to back by a metal wire and the solutions contain saturated  $\text{CuSO}_4$  and  $\text{Hg}_2\text{SO}_4$  (hot side) and  $\text{Hg}_2\text{SO}_4$  and unsaturated  $\text{CuSO}_4$  (cold side). Copper electrodes are immersed in these solutions. On the hot side,  $\text{Cu}^{2+}$  ions are reduced and the  $\text{SO}_4^{2-}$  ions precipitated as  $\text{Hg}_2\text{SO}_4$ . At the cold side, copper is oxidized and  $\text{Hg}_2\text{SO}_4(\text{s})$  dissolved. For power generation, the rate of precipitate formation and dissolution will probably limit the output of such devices. Clampitt and German [182] describe several other cells using electrodes of the second kind with more mass transfer problems than this example.

Thermoelectric powers and misleadingly high efficiencies (5-20%) given in Ref. 183 should be carefully analyzed since the authors worked in several cases with open cells, even at temperatures as high as  $120^\circ\text{C}$ . Thermoelectric powers of 4-6 mV/degree given for the system  $\text{Pb}|\text{H}_2\text{SO}_4\text{-H}_2\text{O}|\text{Pb}$  actually reflect the concentration cell formed during evaporation on the hot side. Thermoelectric powers in the temperature range of  $20\text{-}50^\circ\text{C}$  are of the order of  $<0.5$  mV/degree and compare favorably with those calculated by deBethune et al. [121].

Equations relating the thermogalvanic currents and the temperature difference between electrodes are given by Kaluzhina and co-workers [187-190] as functions of the exchange currents of the dissolution and deposition of the metal and the activation overpotentials of these processes.

### Sulfuric Acid Concentration Thermocell

Ludwig and Rowlette [191] proposed the sulfuric acid cell shown in Fig. III-2, in which the two platinum electrodes sandwich a porous, non-

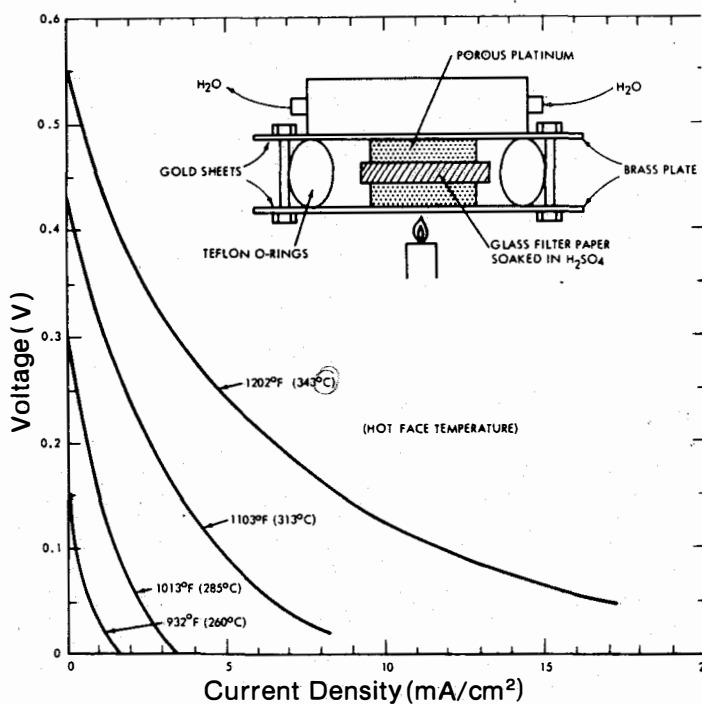
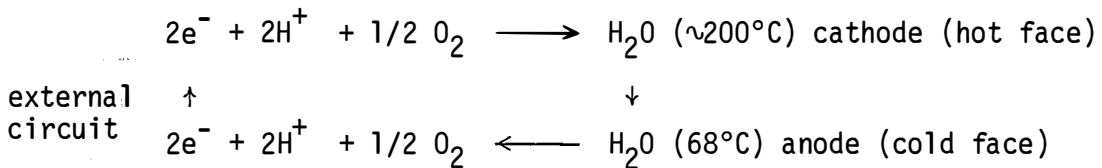


**Figure III-2. Diagram of the Sulfuric Acid Concentration Thermocell and Current- Voltage Curves for the Cell [191]**



conducting barrier. Heat is applied at the hot electrode. Water is evaporated from the heated portion and condenses at the cold electrode; therefore, the solution adjacent to the cold electrode will be more dilute than that adjacent to the hot electrode. Capillary action in the porous barrier compensates for the loss of water and sulfuric acid as the hot part dries out, so that, at equilibrium, a balance between these two processes is achieved. Since the activities of acid and water in sulfuric acid solutions vary widely with composition and temperature [193], this cell is a concentration cell on which the smaller thermogalvanic effect is superimposed. Figure III-2 also shows examples of voltage-current density curves for these cells. When oxygen gas is passed through the cell, the electrode reactions are:



OCV as high as 0.7-0.8 V were achieved and the maximum power output was 17 mA/cm<sup>2</sup> at 0.5 V [13,192]. A cell was tested continuously for 18 hours under load with no deterioration of performance. Oxygen activation overvoltages on platinum are higher than hydrogen overvoltages. Cells using hydrogen instead of oxygen were also tested but the disadvantage is that hot, concentrated sulfuric acid slowly oxidizes hydrogen.

Other cell designs were proposed with a fractionator coupled to the electrolytic cell in which the system operates solely in the thermal

regeneration mode. References 192 and 13 give detailed descriptions of these proposed cells.

#### III.4 DISCUSSION OF TRES TYPE 6

Table S-1 presents the results for some of the thermogalvanic cells developed for power generation. Molten salt thermocells can, in principle, give more power due to the higher range of liquidus in which they exist. However, some data exist for aqueous media indicating that modest powers of  $\sim 100 \mu\text{W}/\text{cm}^2$  can be achieved in these systems. In view of the availability of solar heat sources for temperatures less than  $100^\circ\text{C}$  (e.g., solar ponds), the investigation of these low-temperature, modest-power, relatively inexpensive engines should be continued. Research in this area is being performed at SERI.

## SECTION IV

## COUPLED THERMAL AND ELECTROLYTIC REGENERATION BASED ON PRESSURE DIFFERENCES OF THE WORKING ELECTROACTIVE FLUID

## IV.1 SINGLE CELLS

The electrochemical heat engines described in this section are based on a pressure difference of the working electroactive fluid across the isothermal solid or liquid electrolyte (for nonisothermal electrolytes, see Section III). The pressure difference is maintained by virtue of the change in the vapor pressure with the temperature of the working electroactive fluid. The work performed is equivalent to an isothermal expansion of the working electroactive fluid from pressure  $P_2$  to  $P_1$  at  $T_2$  through the electrolyte and its interfaces. After expansion the working fluid is condensed in a cold reservoir and can be recycled to the high temperature, high pressure part of the cell by a pump. These cells are basically concentration cells. If the temperature across the electrolyte remains constant, one of the sources of irreversibilities is minimized. One of the major advantages of this concept is that no chemical regeneration step is necessary. Because the working fluid does not undergo chemical changes, regeneration and separation steps are not necessary. These cells are discussed as Type 7 in the Introduction.

At open circuit the voltage of these engines is given by the Nernst equation as

$$E = \frac{RT_2}{nF} \ln \left( \frac{f_2}{f_1} \right) \quad \text{IV-1}$$

where  $f$  = fugacity of the working fluid at the high pressure electrode ( $f_2$ ) and at the low pressure electrode ( $f_1$ ). If the working fluid behaves as a perfect gas, the fugacities are equal to the partial pressures, which can be estimated from the Clausius-Clapeyron equation. The relationship between the open-circuit voltage and pressure is

$$\frac{dE}{d(\ln P)} = - \frac{RT_2}{nF} \left( \frac{T_2}{T_1} \right) \quad \text{IV-2}$$

where  $T_1$  is the condensation temperature and  $T_2$  is the vaporization temperature.

Section IV.1.1 describes the following continuous gas concentration cells proposed and studied by Angus [194,195]:  $I_2(g)|PbI_2(l)|I_2(g)$ ;  $Hg(g)|Hg_2Cl_2(l)|Hg(g)$ ;  $Na(g)|NaCl(l)|Na(g)$ ; and  $K(g)|KCl(l)|K(g)$ .

Section IV.1.2 describes Ford's interesting sodium heat engine  $Na(l)|\beta''-Al_2O_3(s)|Na(g)$  [196-200].

#### IV.1.1 Continuous Gas Concentration Cells

Angus [194,195] devised an electrochemical heat engine based on iodine vapor being expanded through an isothermal electrolyte,  $PbI_2(l)$ , capable of dissociating the working fluid into ions. Figure IV-1 shows the diagram of the small-scale laboratory version of the iodine cell [194]. Nickel and platinum electrodes were employed. Table IV-1 shows the voltage characteristics of the iodine cells.

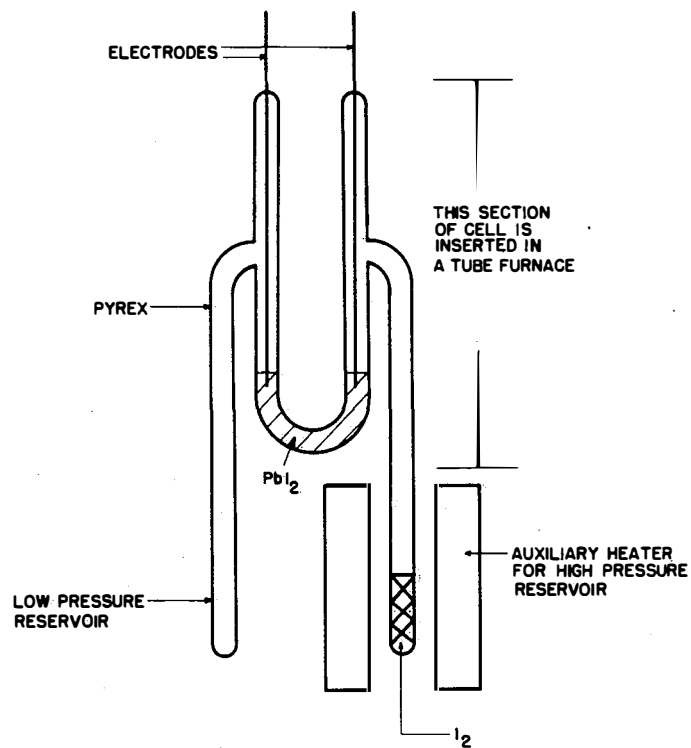


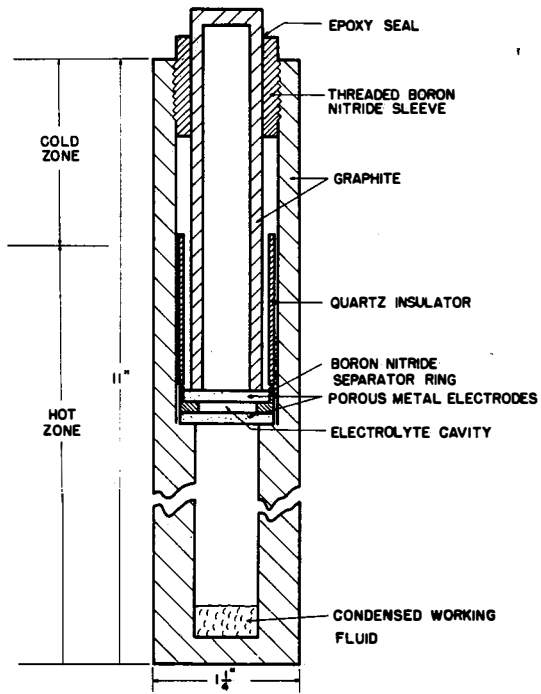
Figure IV-1. Laboratory Continuous Gas Concentration Cell [194]

Table IV-1. VOLTAGE CHARACTERISTICS OF THE  $I_2(T_2)|PbI_2(\ell)|I_2(T_1)$   
CELL WITH Ni ELECTRODES [194]

Vaporization temperature (°C)	177	193
Condensation temperature (°C)	24	24
Electrolyte temperature (°C)	538	538
Voltage (low pressure electrodes)	0.22	0.28
Predicted voltage from Eq. IV-1	0.207	0.22

Regeneration was accomplished by cooling the original hot end and vaporizing the iodine from the original cold end; the cell voltage reversed accordingly. The internal resistance of these cells was very high. Advanced cell designs were tested and the most successful is shown in Fig. IV-2. Porous nickel electrodes sandwiched the  $PbI_2(\ell)$  electrolyte. The OCV of the cell with enough  $I_2$  to give 1 atm of  $I_2$  vapor at  $T_2$  was 0.17 V ( $R_i = 2.9$  ohms). With a 24.5-ohm load, 6.2 mA were drained from the cell. However, as the cell was operated under load, its internal resistance increased continuously. It was found that the electrolyte had been forced out of the cavity into the nickel electrode from the high to low pressure zones. Corrosion of the nickel electrodes by  $I_2$  vapor was also detected, a problem avoided by the use of platinum electrodes.

Laboratory cells were also operated with the system  $Hg(g)|Hg_2Cl_2(\ell)|Hg(g)$ , with W or Pt electrodes. The  $Na(g)|NaCl(\ell)|Na(g)$  system and the corresponding potassium system were also considered as possible candidates for cells of this type. Table IV-2 assembles the characteristics of the cells with these working fluids.



**Figure IV-2. Advanced Continuous Gas Concentration Cell**

Table IV-2. CHARACTERISTICS OF CONTINUOUS GAS CONCENTRATION CELLS WITH SEVERAL WORKING FLUID/ELECTROLYTE SYSTEMS [194]

Working Fluid/ Electrolyte	$\rho$ (ohm cm)	Vaporization Temp. ( $^{\circ}\text{C}$ )	Condensation Temp. ( $^{\circ}\text{C}$ )	OCV (V)	$P_2$ (torr)	$P_1$ (torr)
$\text{I}_2/\text{PbI}_2$	2.1	410	119	0.3	31,900	93.4
$\text{Hg}/\text{Hg}_2\text{Cl}_2$	2.0	305	100	0.22	247	0.27
$\text{Na}/\text{NaCl}$	0.27	827	327	0.88	433	0.039
$\text{K}/\text{KCl}$	0.44	827	327	0.71	1408	0.64

The alkali-metal-based systems were found to display a much more favorable OCV than  $\text{I}_2$  or Hg systems. The major difficulty associated with this type of cell is the need to maintain the integrity of the liquid electrolyte when it is subjected to a pressure gradient. These pressure differences are also smaller for the alkali metal systems than those for the  $\text{I}_2$  cell (see  $P_1$  and  $P_2$  in Table IV-2).

#### IV.1.2 The Sodium Heat Engine

The sodium heat engine is similar to the cells described in Section IV.1 but does not have the problems associated with a liquid electrolyte subjected to a pressure difference. The elegant solution to these problems, advanced by Kummer and Weber [196], is to use the sodium-ion-conducting, solid electrolyte  $\beta$ "-alumina to separate the high and low pressure zones in a closed-cycle device in which fluid sodium is circulated [196-200]. The schematic diagram of this electrochemical heat engine is shown in Fig. IV-3. In the high temperature ( $T_2$ ) area of the device, fluid sodium is at a pressure  $P_2$  (upper region), higher than the



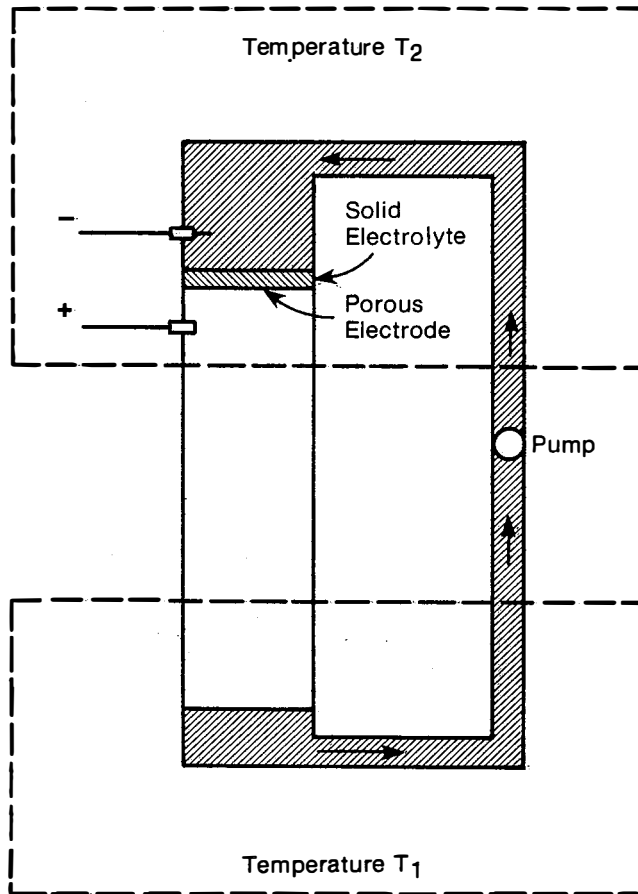


Figure IV-3. Schematic Diagram of the Sodium Heat Engine [197]

pressure  $P_1$  in the lower region. The liquid sodium is heated to  $T_2$ , and sodium is oxidized to sodium ions and electrons. The electrons leave the high pressure zone via the negative electrode (current collector). The sodium ions migrate through the solid electrolyte as a result of the pressure difference ( $P_2 - P_1$ ) across the electrolyte. At the low pressure side of the solid electrolyte, a suitable inert porous electrode (the cathode) coats the electrolyte. Sodium ions are reduced at the porous electrode by the electrons arriving through the external load, thus forming sodium metal. Neutral sodium evaporates from the porous electrode at pressure  $P_1$  and temperature  $T_2$ , passing in the gas phase to a condenser at  $T_1$  ( $T_1 < T_2$ ). Condensed liquid sodium is returned to the high pressure side by an electromagnetic pump, thus completing the cycle without the movement of mechanical parts - only circulation of fluid sodium. The work output is purely electrical but equivalent to the mechanical work of the isothermal expansion of sodium from  $P_2$  to  $P_1$  at  $T_2$  [196,197].

Weber [197] presented a theoretical analysis of the efficiencies of these devices under no load and under load, neglecting parasitic heat losses (which were included in later papers: Refs. 198,199). Current-voltage relationships were derived theoretically by using Eq. IV-1 and the rate of evaporation of the metal, since this rate is proportional to the current density. An expression of the type:

$$V = A - B \ln I - IR_0 \quad \text{IV-3}$$

was obtained, where  $R_0$  is the surface electrical resistivity of the solid electrolyte and A and B are coefficients calculated from physical constants and the empirical relation between vapor pressure and temperature

for sodium ( $A = 0.74 \text{ V}$  and  $B = 0.086 \text{ V}$  for  $T_1 = 227^\circ\text{C}$ ,  $T_2 = 727^\circ\text{C}$ ). Weber [197] analyzed the several sources of polarization and gave theoretical expressions for some of them: charge transfer (activation); overvoltage at the liquid sodium/solid electrolyte and electrolyte/porous electrode interfaces; effective ohmic resistance; and mass transfer through the porous electrode. Weber [197] also considered electrical losses resulting from the finite temperature difference needed to sustain the heat flow across the electrolyte. Heat is absorbed at the porous electrode principally from the sodium evaporation during current flow and by thermal radiation to the condenser. Equation III-1 was employed to account for these effects.

The efficiency under no load is the quotient of the net work output  $W_1$  (approximated by the isothermal expansion of sodium from  $P_2$  to  $P_1$  at  $T_2$  under quasi-equilibrium) less the work  $W_2$  necessary to circulate the liquid sodium ( $W_1 \gg W_2$ ) divided by the total heat input. The total heat input is  $W_1$  plus the latent heat  $L$  of the sodium vapor and the enthalpy difference of the liquid between  $T_2$  and  $T_1$  [ $\Delta H \approx C_p(T_2 - T_1)$ ]. Parasitic heat losses ( $Q_{1\text{loss}}$ ) should also be included in the total heat input. Thus the efficiency  $\eta$  is

$$\eta = \frac{W_1 - W_2}{W_1 + L + \Delta H + Q_{1\text{losses}}} \approx \frac{W_1}{W_1 + L + \Delta H + Q_{1\text{losses}}} \quad \text{IV-4}$$

Under load, the expression

$$\eta_L = \frac{VI}{VI + \frac{I}{F}(\Delta H + L) + Q_{1\text{losses}}} \quad \text{IV-5}$$

represents the efficiency of the system.  $Q_{1\text{losses}}$  includes radiation losses of the form  $Q_r = \sigma(T_2^4 - T_1^4)/z$ , where  $\sigma =$  Stefan-Boltzman constant,

$z$  = effective radiation resistance, and conduction losses  $Q_c = K_L \times (T_2 - T_1)$ . Figure IV-4 shows some calculated power-efficiency performance curves as a function of  $T_2$ , using an expression for efficiency of the type of Eq. IV-5 [199].

Figure IV-5 shows experimental voltage-current curves for several values of  $T_2$  as well as curves calculated from Eq. IV-5, which does not take electrode polarization into account. Interfacial polarization is responsible for most of the differences between calculated and experimental curves.

Figure IV-6 is a diagram of an operating sodium heat engine using a  $\beta''$ -alumina tube. Cells of this type as well as others with inverted geometry were used in the study of the engine performance. The initial performance (1975) was  $0.2 \text{ W/cm}^2$ , with an overall efficiency of  $\sim 10\%$  [196] and short lifetimes ( $\sim$ one week). This performance was improved to  $\sim 0.7 \text{ W/cm}^2$ , with an overall efficiency of  $\sim 20\%$ , the performance being limited mostly by interfacial polarization [197]. It appears that power outputs of  $1 \text{ W/cm}^2$  are feasible with this system [201]. For such efficiencies, these devices are very light ( $\sim 30 \text{ kW/100 lb}$ ) compared to turbines ( $30 \text{ kW/750-1000 lb}$ ) [201].

The stability of the  $\beta''$ -alumina does not seem to be a limiting factor on the future applicability of the sodium heat engine as a static and modular power source. Careful preparation and water exclusion in handling may achieve stability at temperatures as high as  $\sim 1000^\circ\text{C}$ . Tubes with thinner walls are necessary to reduce the specific surface resistivity so that larger power outputs can be drained from the system. References 202 and 203 are relevant reviews on  $\beta$ -alumina (see also

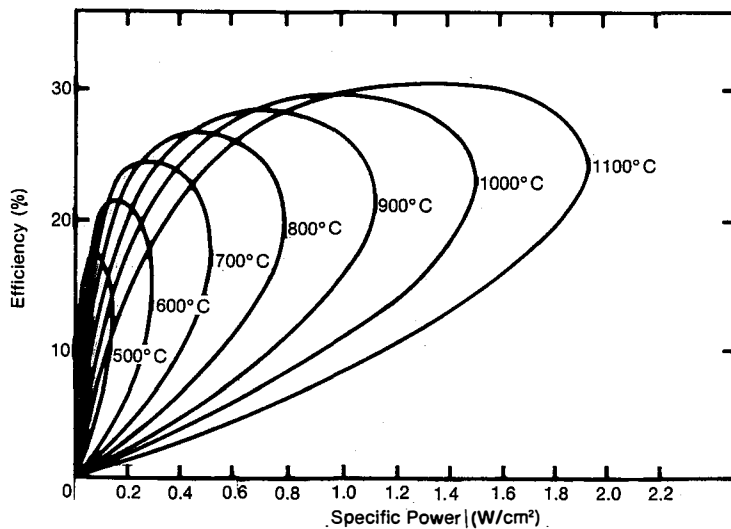


**Figure IV-4. Calculated Power-Efficiency Performance of the Sodium Heat Engine for Various Values of  $T_2$  [199]**

$R_0 = 0.18 \text{ ohm cm}^2$ ;  $T_1 = 200^\circ\text{C}$ ;  $z = 20$   
 (see Eq. IV-5)

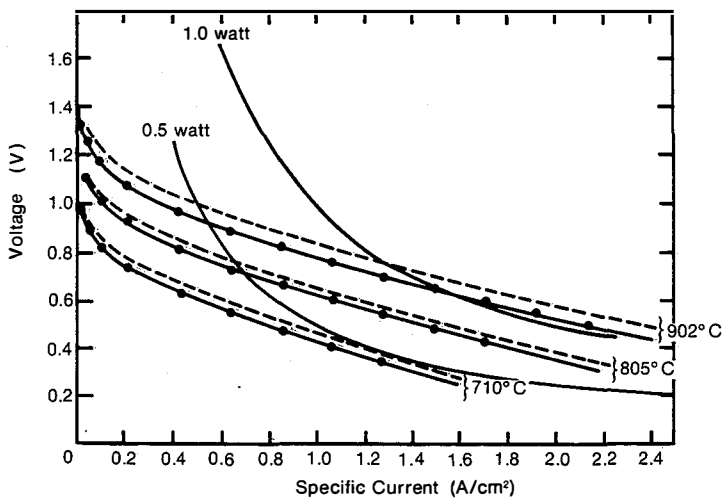


**Figure IV-5. Experimental (●) and Calculated (-) (Eq. IV-5) Voltage-Current Curves for the Sodium Heat Engine as a Function of  $T_2$  [199]**

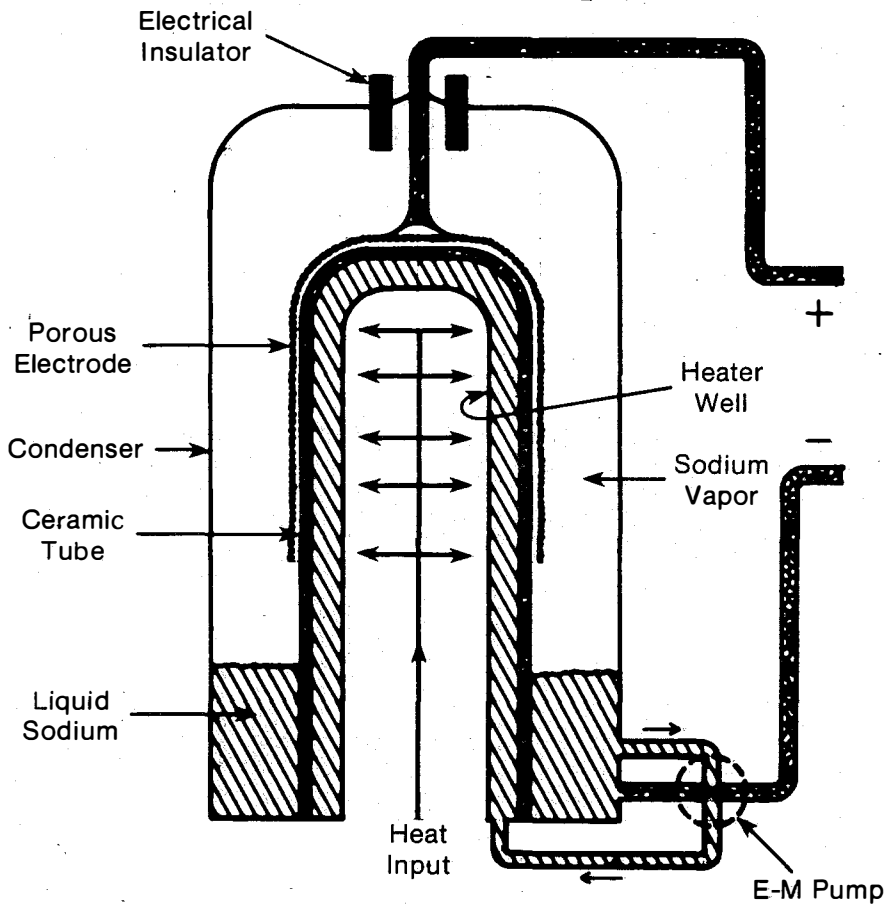


Figure IV-6. Schematic Diagram of the Sodium Heat Engine Cells with  $\beta''$ -Alumina Tubes [199]

Ref. 164). Another source of problems is the electrolyte/porous electrode interface. Molybdenum films (microns thick) can be deposited on  $\beta$ -alumina by chemical vapor deposition. These films have high in-plane electrical conductivity, good sodium vapor permeability, strong adhesion to the solid electrolyte, good high-temperature stability (tested for  $\sim 1000$  hours without deterioration), and an expansion coefficient that matches that of  $\beta$ -alumina. One of the problems of these electrodes is that recrystallization at  $900$ - $1000^\circ\text{C}$  leads to a material less permeable to sodium vapor. Cole, Weber, and Kunt [201] are investigating other methods of preparation of these electrodes (coating by sputtering). Radiation and conduction losses should be kept small if efficiencies approaching Carnot cycle are to be achieved. Neglecting heat losses and polarization at the electrodes, efficiencies as high as 46.7% are calculated when the Carnot efficiency is 50% ( $T_1 = 227^\circ\text{C}$ ,  $T_2 = 727^\circ\text{C}$ ).

#### IV.2 MULTIPLE CELLS

The electrochemical heat engines described in this section are composed of at least two closed cells operating at the same temperature (for different temperatures, see Section V) and connected in electrical opposition. These are the Type 5 cells described in the Introduction. The electrochemical reactions involve one gaseous reactant. The engine produces external work on a load when, by some mechanical means (e.g., by cooling one trap or one cold finger associated with the cells), the equilibrium partial pressure of this gaseous reactant is made to be different in both cells. This difference in partial pressure will drive the reaction of the gaseous substance and will have a minimal effect on

the condensed phases of the electrochemical cells. The net driving force of the cycle is independent of any property of the electrolyte at open circuit. If the electrode kinetics are fast, little polarization should be observed under current drain. These systems run in cycles. After discharge of one cell and consequent charge of the other, and performance of electrical work on the external circuit, it is necessary to cool down the trap (or finger) originally hot and to heat the one originally cold, thus reversing the role of the electrochemical cells. In principle, one can conceive of this type of regeneration being applicable whenever the activity of a chemical substance in one of the cells can be made different from the activity of that substance in the other cell. In fact, the type of regeneration performed in these cells is a particular case of the electrothermal regeneration detailed in Section V.

These cells were first reported by Anderson, Greenberg, and Adams [149] at Lockheed, who properly refer to this type of regeneration as electrolysis at low pressure. More recently, Elliott [204-209] at Los Alamos has extended the study of these engines with a more practical cell design (cf. Ref. 3) without mass transfer from the battery stacks.

The cell proposed by Anderson, Greenberg, and Adams [149] is shown in Fig. IV-7. The systems envisioned for this type of regeneration were  $\text{Pb}|\text{PbI}_2|\text{I}_2$  or  $\text{Cd}|\text{CdI}_2|\text{I}_2$ . The partial pressures of iodine vapor are kept different by the different temperatures in the traps, one at  $T_1$  and the other at  $T_2$ , the temperatures of the cells. Iodine is at low equilibrium partial pressure in the cold trap at  $T_1$  and, therefore, at the



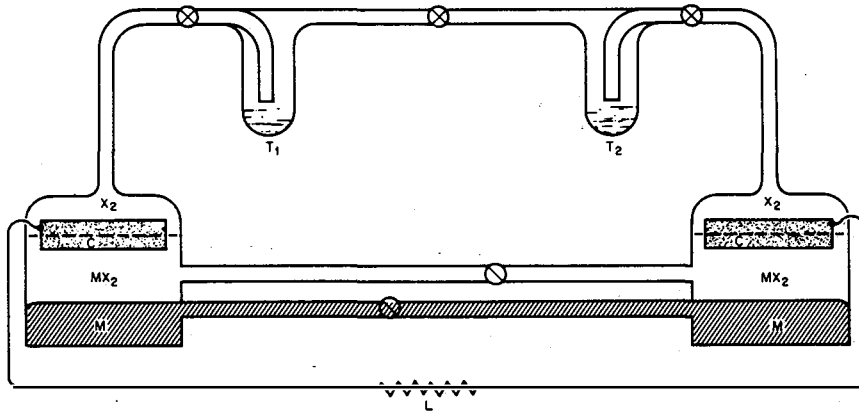


Figure IV-7. Low-Pressure Electrolysis Apparatus [149]

left-hand side of the cell, which discharges iodine vapor. The condensed iodine is transferred via a nonreturn valve to the hot trap at  $T_2$ , where it vaporizes and is ionized at the right electrode. Therefore, the system must be run in cycles, with the trap at the left being first cold, thus condensing  $I_2$ , and then heated so that the cell reverses. Electrolysis of  $CdI_2$  at  $550^\circ C$  into a liquid nitrogen trap for the iodine gave currents up to  $2 A/cm^2$  with a coarse-pore carbon electrode. However, the coulombic efficiency was low due to the high solubility of cadmium in molten cadmium iodide (30-40%). Reference 149 details the analysis of the efficiencies of these engines. One of the major limitations to a high thermodynamic efficiency is the need for a high  $T_2$  but not too high an equilibrium pressure (to avoid sealing problems). Kinetics problems at the gas electrode are likely to be a very important source of limitation of this type of cells, as well as differences in current efficiencies between the two electrochemical cells. A serious shortcoming of this type of cell, using iodine or diatomic gases, is the low voltage obtained per cell, which requires stacking of several series-connected cells to obtain practical voltages (see also Ref. 3).

The cell proposed by Elliott [204-209] is shown in Figs. IV-8 and IV-9. The single laboratory cells are made on a Pyrex cup with tungsten electrical contact (dense graphite also can be used) holding three layers of materials. The top layer is a porous graphite disc, the iodine electrode. The middle layer is zirconia felt impregnated with molten electrolyte. The middle layer supports the graphite disc and prevents contact between the gas electrode and the bottom layer of

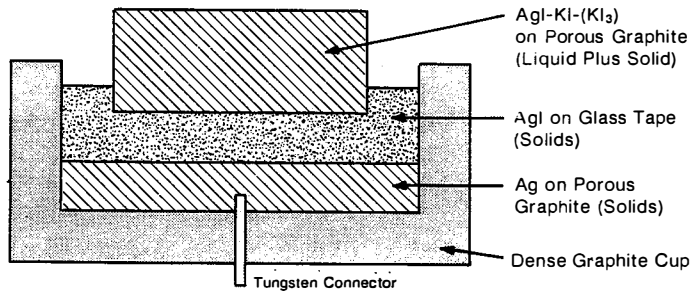


Figure IV-8. Laboratory Cell Li/I<sub>2</sub> [207]

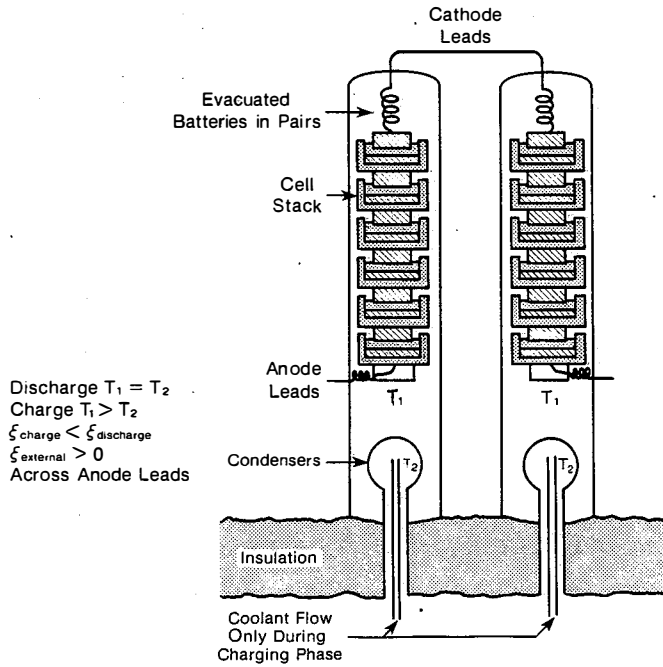


Figure IV-9. Multiple-Cell Electrochemical Heat Engine [206]

nickel felt holding the metal electrode. Preliminary studies were made for the systems  $\text{Ag}|\alpha\text{-AgI}|\text{I}_2$ ;  $\text{Ag}|\text{AgI-KI}(\text{molten eutectic})|\text{I}_2$ ; and  $\text{Li}|\text{molten alkali metal iodides}|\text{I}_2$ . A proposed multiple cell electrochemical heat engine (laboratory scale) is shown in Fig. IV-9. References 207-208 detail a proposed practical cell design for two stacks of 100 cells each.

The  $\text{Ag}|\text{I}_2$  cell with the solid electrolyte  $\alpha\text{-AgI}$  showed polarization even at small drains [204]. Therefore the solid electrolyte was replaced by the eutectic  $\text{AgI-KI}(238^\circ\text{C})$ . The electrode kinetics were faster in the molten electrolyte than in the solid electrolyte, but the internal resistances were still high (12 ohms on discharge and 36 ohms on charge).

The  $\text{Li}|\text{I}_2$  cell was also tested in the laboratory scale [206-208]. Elliott [206] reported that these cells have internal resistances of 0.3-0.8  $\text{ohm}/\text{cm}^2$ , and he indicated that these resistances remained constant from 0.25  $\text{A}/\text{cm}^2$  (discharge) to 0.80  $\text{A}/\text{cm}^2$  (charge) (with  $T_1 = 350^\circ\text{C}$  and  $T_2 = 25^\circ\text{C}$ ). The net voltage obtained at open circuit was 0.29 V. Assuming that polarization effects are small, Elliott indicated that 0.23 V could be obtained at 0.1  $\text{A}/\text{cm}^2$ . Unfortunately, he presented few experimental details or results.

Applications projected for these heat engines involve coupling energy conversion and storage, which is one of the unique qualities of these systems (as compared with systems reported in Section IV.1). These interesting applications are thoroughly described in Refs. 205-208.

Other systems proposed include additional alkali metal systems, which are supposed to give higher efficiencies but also operate at

higher temperatures. The patent literature describes the proposed systems [209].

#### IV.3 SUMMARY AND DISCUSSION OF TRES TYPES 5 AND 7

Table S-1 shows that the sodium heat engine (Type 7 engine) is the TRES of highest power demonstrated to date. In fact, this is a very interesting approach to TRES with no need for chemical regeneration steps but with a major limiting requirement--a proper solid electrolyte that is a stable superionic conductor at the desired temperature range. Most of the good solid electrolytes operate at elevated temperatures. For this reason, research of solid electrolytes for operation at lower temperatures should be strongly encouraged.

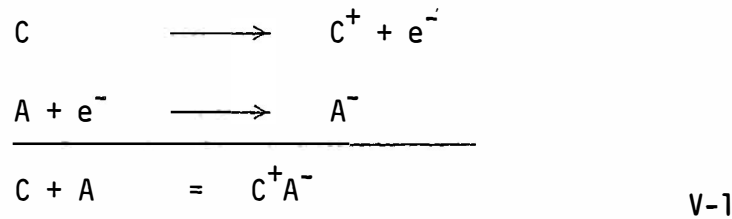
The electrolysis at reduced pressures (Type 5) has mass transfer problems. Very low power outputs have been obtained with the systems attempted to date.

**SERIO** 

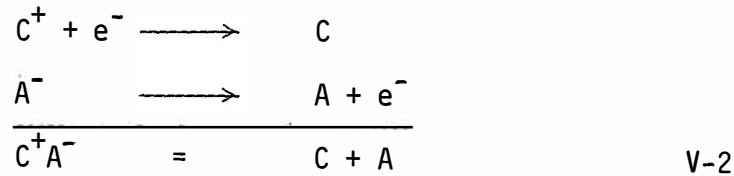
## SECTION V

## COUPLED THERMAL AND ELECTROLYTIC REGENERATION: GENERAL

In the electrothermal regeneration mode (see Fig. V-1), the electrochemical reaction products of cell 1 at  $T_1$



are regenerated by electrolysis in cell 2 at a temperature  $T_2 \neq T_1$ :



The cells are connected to oppose each other electrically (back to back). The operation of the energy converter is made continuous by sending  $C^+A^-$  (the electrolyte), formed in the galvanic cell reaction at  $T_1$  (previously taken to  $T_2$ ), to the electrolyzer. The galvanic cell reactions then drive the electrolysis of  $C^+A^-$  into C and A, which are taken to  $T_1$  and returned to the galvanic cell 1, completing the closed-cycle operation. This TRES Type 4 is discussed in the Introduction.

If  $T_1 = T_2$ , the operation is similar to that of a secondary rechargeable battery with only electrolytic regeneration taking place and with a net OCV of zero. If  $T_1 \neq T_2$ , electrothermal regeneration is operative. The basic requirement is that the cell voltage at  $T_2$  be less than that at  $T_1$  ( $V_2 < V_1$ ). Thus, a fraction of the cell voltage at

$T_1$  is used to perform the regeneration of the original reactants at  $T_2$ , and the remaining voltage is used to perform useful electrical work in the external load. If  $T_2 > T_1$ , the electrothermal regeneration is being performed by electrolysis at a higher temperature than that of the galvanic cell, and the free energy of formation of  $C^+A^-$  is less negative with increased temperature. If  $T_2 < T_1$ , the regeneration is performed by electrolysis at a lower temperature. The sign of  $(dE/dT)_p$  determines the type of regeneration. Examples in which  $T_2 > T_1$  are more common in the literature.

Another important requirement for this type of regeneration is that the electrode reactions  $C \rightleftharpoons C^+ + e^-$  and  $A + e^- \rightleftharpoons A^-$  be capable of sustaining high current densities (high exchange currents, low activation overpotentials, low electrode polarization effects in general, and low internal cell resistance) and that they present high coulombic efficiencies; i.e., the same characteristics as a secondary battery.

There is a temperature at which regeneration (reaction V-2 above) starts to take place spontaneously [ $\Delta G(T_x) = 0$ ], with no need for electrolysis (at higher or lower temperatures). An example of this type of spontaneous regeneration is Case's cell [69], described in Section I.1.3.4, in which spontaneous chemical regeneration takes place at a lower temperature than does the galvanic cell operation. McCully [210] describes another example in the opposite direction based on the reactions of the fluorides of U(VI) or Ce(IV) and  $AsF_3$ . If  $T > T_x$ , the resulting galvanic cell will generate power to the external load and regenerate the reactants of the low temperature galvanic cell (see Section V-2).



In principle, another possibility for operating electrothermally regenerative systems without transferring reactants and products from one cell to the other, as in Fig. V-1, is to reverse the operating temperatures of the two cells. After the electrolysis at  $T_2$  is completed, with the discharge of the cell at  $T_1$  (and concomitant electrical work produced in the external load) one can envision heating cell 1 to  $T_2$  and cooling cell 2 to  $T_1$ , thus reversing the roles of the two cells and obtaining work on the electrical load periodically.

In 1958, Yeager [7] suggested that the coupling of thermal and electrolytic modes of regeneration, as well as thermal regeneration alone, should be studied. Since then, several of these coupled electrolytic and thermal regeneration engines have been studied; they have been called "double thermogalvanic cell" [59,51], "electrothermally regenerative transducers" [211-213], and "electrochemical heat engines" [204-209]. Section IV.2 discusses a particular case of the electrothermal regeneration in which  $T_1$  can be identical to  $T_2$  and the work is produced by varying the partial equilibrium pressure of a gaseous working electroactive fluid by physical means.

The efficiency of the electrothermally regenerative system is also Carnot limited, as is the thermal regeneration. For a system in which  $T_2 > T_1$ , the efficiency is (for  $\Delta C_p = 0$ )

$$\eta = \frac{T_2 - T_1}{T_2} = \frac{nF(E_1 - E_2)}{Q_2} = \frac{-\Delta G_1 - \Delta G_2}{\Delta H_2 - \Delta G_2} = \frac{nF(E_1 - E_2)}{T_2 \Delta S_2} \quad V-3$$

where  $E_i$  is the thermodynamic cell potential at  $T_i$ , and  $Q_2$  is the heat per mole of reactant introduced into the dissociation unit at  $T_2$ . Hesson and Shimotake [46] analyzed the efficiency of this mode and gave ex-

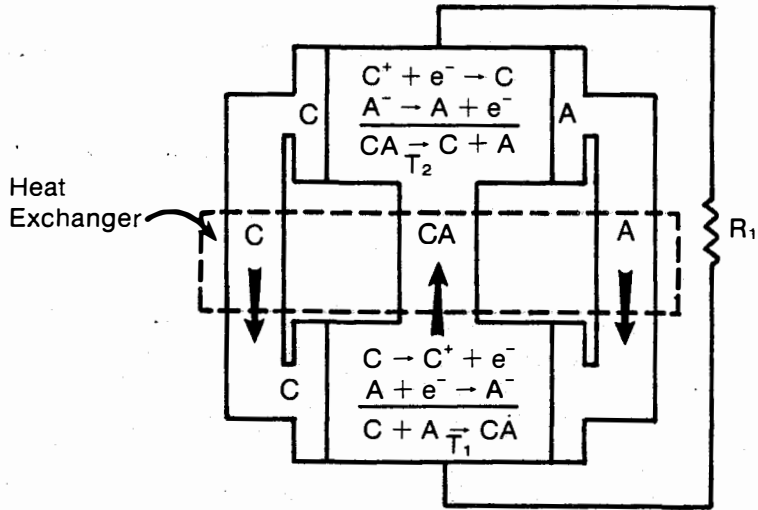


Figure V-1. Generic Scheme for Electrothermal Regeneration

pressions for the overall efficiency of the system (the product of the galvanic cell electrical efficiency and the regenerator electrical efficiency) as a function of  $E_1$ ,  $E_2$ ,  $I_1$ ,  $I_2$ , and  $(dE_2/dT)_p$ . Anderson, Greenberg, and Adams [50,51] have also analyzed efficiencies of these systems for cases in which  $\Delta C_p = 0$  and  $\Delta C_p \neq 0$ . Even when  $\Delta C_p \neq 0$  the dominant term in these efficiency expressions is still  $(T_2 - T_1)/T_2$ .

Compared to thermal regeneration, electrothermal regeneration has the advantage of an inherently simple separation of reactants. In the systems in which there is a flow of reactants and products, the complexity of the device design is similar to that encountered in thermal regeneration. Disadvantages of the electrothermal regeneration are polarization at the electrodes in the electrolyzer and possible materials problems at the higher temperatures. These disadvantages have parallels in the thermal regeneration in the slow rates of thermal decomposition and materials problems in the regenerator.

## V.1 HIGH TEMPERATURE ELECTROLYSIS

### V.1.1 Molten Salt Media

In the late fifties, two groups independently pursued the electrothermal regeneration method applied to metal|metal halide|halogen systems as illustrated by Fig. V-1; i.e., the cold galvanic cell reaction product flows to the high temperature electrolyzer(s), where the reactants of the cold galvanic cell are regenerated electrolytically, cooled down, and transferred back to the cold galvanic cell. The system  $\text{Na}(\ell)|\text{molten NaCl}|\text{Cl}_2$  was studied at the Delco-Remy Division of General Motors Corp. by Landers, Smith, and Weaver [211] in 1959 and was described

by these authors in the patent literature [2] for a satellite power system [212]. Later, Weaver [213] studied the same system more thoroughly in order to investigate the feasibility of this system as a power source for armored vehicles. The systems  $\text{Li}|\text{LiCl}(\ell)|\text{Cl}_2$  and  $\text{Li}|\text{LiI}(\ell)|\text{I}_2$  were initially investigated. Research on the  $\text{Li}|\text{LiCl}|\text{Cl}_2$  system was also independently performed at the Allison Division of General Motors by Swinkels [214,215], but the major emphasis was on the rechargeability of the battery system.

At Lockheed Aircraft Corp. the research on electrothermal regeneration described by Anderson, Greenberg, and Adams [50,51] was applied to the systems  $\text{Pb}|\text{PbI}_2|\text{I}_2$ ,  $\text{Cd}|\text{CdI}_2|\text{I}_2$ , and  $\text{Li}|\text{LiI}|\text{I}_2$ , as a continuation of the previous efforts on regenerative systems. That work started with the unsuccessful work on thermal regeneration (see Section III.1.2.1) and evolved into the thermogalvanic systems (see Section III.1.1) and then into the double thermogalvanic or electrothermal regeneration between 1959-1962 (cf. Ref. 3).

At the Delco-Remy Division [212,213] the choice of systems was based on electrolytes that exhibited a wide liquidus range and galvanic cell reactions yielding the electrolyte. This galvanic cell reaction should have a suitable decrease of OCV with increased temperatures such that the electrolyzer at a higher temperature would consume a fraction of the cell voltage produced at the lower temperature. Another requisite was the ability of the galvanic cell reaction to sustain large current densities on charge and discharge over a wide range of temperatures, with good coulombic efficiencies in both processes. The wider the liquidus range of the solvent chosen, the larger is the Carnot effici-

ency that can be expected from the system. The Na|NaCl|Cl<sub>2</sub> system (NaCl: m.p. 801°C; b.p. ~1450°C) meets most of these criteria. The cell exhibited a high OCV, e.g., 3.24 V at 827°C, which decreased with the increase in temperature, e.g., to 3.14 V at the sodium melting point (880°C) and to 2.55 V at 1220°C (a difference in OCV of 0.7 V for a 390°C temperature difference); one would anticipate a larger voltage difference at higher temperature differentials. These cells were studied on charge and on discharge in the 827-1057°C range and showed the ability to be charged and discharged at high current densities (e.g., discharge currents above 3.5 A/cm<sup>2</sup> at 827°C, with IR polarization only at current densities above 4.3 A/cm<sup>2</sup>).

The best laboratory design tested had a commercial alumina U tube as the cell body. The sodium electrode was made from an iron or nickel tube flared at the end, with a porous metal disk welded on the flare. The chlorine electrode was hollow graphitized carbon contained in one of the arms of the U tube. The cell was not sealed but kept in an argon blanket. The sodium utilization in the five cells tested averaged only 40%. Dissolution of sodium in the melt was diminished by reducing the pore size of the iron grid electrode. The faradaic efficiencies were too low to be acceptable in a practical cell. The ability of these cells to undergo charge (electrolyzer reaction) and discharge (galvanic cell reaction) over a wide temperature range was taken as a partial feasibility demonstration of the concept of the electrothermal transducer. No complete coupling of the galvanic cell and electrolyzer, with the appropriate flow of materials, was tested. Some system designs are given in Weaver's report [213]. The systems Li|LiCl|Cl<sub>2</sub> and Li|LiI|I<sub>2</sub>

were investigated. The former gave 3.52 V OCV at 650°C, good load voltages, and current densities as high as 1.9 A/cm<sup>2</sup>, with only IR polarization. Other studies of these systems were made by Swinkels [214,215]. The iodide system gave 2.42 V at 473°C. Both the lithium iodide and lithium chloride systems could be operated at lower temperatures than the sodium chloride system.

The work at Lockheed [50,51; see also Ref. 3] was performed with cells of the type described in Section I.1.2.1. For the Li|LiI|I<sub>2</sub> system at 500°C, the OCV was 2.5 V, close to the theoretical value. The current-voltage curves showed that current densities of 320 mA/cm<sup>2</sup> could be obtained at 1.5 V. About 2 mole % of lithium dissolved in the lithium iodide at 500°C, thus decreasing the coulombic efficiency. The electrolyses of CdI<sub>2</sub> (450°C) and PbI<sub>2</sub> (815°C) showed only IR polarization. However, in the case of CdI<sub>2</sub>, the solubility of cadmium was very high, leading to a high contribution of electronic conductivity, thus decreasing the coulombic efficiency. The molten PbI<sub>2</sub> did not dissolve Pb appreciably and coulombic efficiencies of 100% were achieved.

A thorough theoretical analysis of the performance of the best candidates for electrothermal regeneration, LiI and PbI<sub>2</sub> [50,51], was performed and is given in detail in Ref. 51. The Carnot efficiencies and T<sub>2</sub> for LiI and PbI<sub>2</sub> were 50.6% and 40.1%, and 1170°C and 870°C, respectively. The maximum operational efficiencies with maximum power to load at these temperatures, but without taking into account heat exchanger losses, were 18% and 15% for LiI and PbI<sub>2</sub>, respectively. In practice, lower values would obviously be obtained.

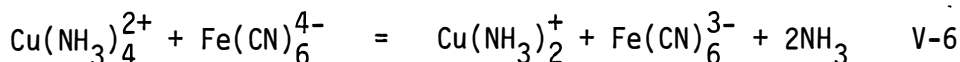
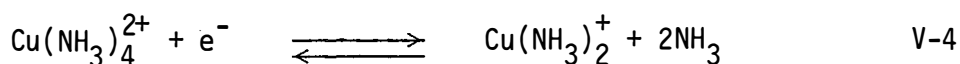
With these systems [50,51,212,213] the continuous operation as

energy converters would be achieved by sending the electrolyte, heated to  $T_2$ , to the electrolyzer at a proper rate, where the reactants of the cold galvanic cell are regenerated at  $T_2$ , cooled to  $T_1$ , and redirected to the cold galvanic cell. Heat exchanger inefficiencies lead to irreversible losses. However, easy separation of reactants and products is inherent in these systems. Since the galvanic cell is a battery, energy can be stored in these systems. The batteries can be operated temporarily for power generation, in addition to operation as energy converters. The theoretical operational efficiencies [51] are higher, in general, than the corresponding efficiencies for conventional thermoelectric devices (or thermogalvanic cells), in which the electric and thermal conduction paths cannot be separated. Most problems common to all electrochemical devices utilizing gas electrodes (plugging or flooding of the electrodes) would obviously be encountered. Finally, because the current efficiencies of the electrolyzers are lower than those of the galvanic cells, one can envision the need for more than one electrolysis cell coupled with a battery to achieve practical regeneration rates.

In principle, one can conceive a different approach to the electrothermal regeneration that does not require materials transfer from one cell to the other but only heat transfer for periodical power generation as an energy converter and also for power generation as a secondary battery, with energy storage.

#### V.1.2 Aqueous Media

Hammond and Risen [216] recently described an example of a potential electrothermally regenerative system based on the reactions:



These reactions were selected due to their large molar entropy changes ( $\Delta S = -32$  cal/degree mole for V-4 and  $\Delta S = -28$  cal/degree mole for V-5). The two half-reactions (V-4 and V-5) must be separated by semipermeable membranes. Open-circuit voltages as a function of temperature are given in Table V-1. These data were obtained with laboratory cells consisting of a beaker with rubber stoppers accommodating electrodes (working and reference), and two concentric tubes with 1-cm<sup>2</sup> windows in their sides. The windows were covered with cellophane membranes (previously exposed to Ba<sup>2+</sup> and SO<sub>4</sub><sup>2-</sup>), which are more easily permeable to singly charged ions than to multiply charged ions. Platinum electrodes (1 cm<sup>2</sup>) were set to face the membranes. The cell was placed in a constant temperature bath, and the inner and outer solutions were agitated magnetically. The middle compartment contained supporting electrolyte (NH<sub>4</sub>Cl + BaCl<sub>2</sub>). With time, a reddish-brown precipitate formed on the membrane in the side adjacent to the Fe(CN)<sub>6</sub><sup>4-</sup> solution and the resistance of the cell increased. Table V-1 also shows the resistances of the forward (+R') and reverse (-R') reactions. The studies performed encompassed the variation of OCV with temperature and a few polarization studies up to 25 mA/cm<sup>2</sup>. No current-voltage curves were given and results were interpreted in terms of IR polarization only (cf. Section III.3).



Table V-1. CELL POTENTIALS AND RESISTANCES AS A FUNCTION OF TEMPERATURE FOR THE  $\text{Fe}(\text{CN})_6^{4-}/\text{Fe}(\text{CN})_6^{3-}$  AND  $\text{Cu}(\text{NH}_2)_4^{2+}/\text{Cu}(\text{NH}_3)_2^+$  SYSTEMS [216]<sup>a</sup>

Temperature (°C)	E (V)	+R' (ohm m <sup>2</sup> x 10 <sup>4</sup> )	-R' (ohm m <sup>2</sup> x 10 <sup>4</sup> )
25	-0.518	11.6	11.4
30	-0.505	9.1	8.3
40	-0.475	7.4	7.0
60	-0.417	5.5	5.3
90	-0.330	3.4	3.4
30	-0.502	17.2	12.3

<sup>a</sup>The composition of the solution in the inner vessel is 1 M  $(\text{NH}_4)_4\text{Fe}(\text{CN})_6$ , 1.75 M  $\text{NH}_4\text{Cl}$ , and 0.05 M  $\text{K}_2\text{SO}_4$ ; it is electrolyzed to equimolar in Fe(II) and Fe(III). The composition of the solution between the outer vessel and the beaker is 0.75 M  $\text{CuCl}_2 \cdot 2\text{H}_2\text{O}$ , 2.0 M  $\text{NH}_4\text{Cl}$ , 4 M  $\text{NH}_3$ , 0.05 M  $\text{K}_2\text{SO}_4$ , and 0.25 M metal Cu (added under  $\text{N}_2$ ) to give equimolar Cu(I) and Cu(II). The interstitial solution is 2.0 M  $\text{NH}_4\text{Cl}$  and 0.5 M  $\text{BaCl}_2 \cdot 2\text{H}_2\text{O}$ .

Power output densities for these cells were calculated assuming IR polarization only, and the authors claimed that  $6.4 \text{ W/m}^2$  is feasible for operation between  $30^\circ\text{C}$  and  $90^\circ\text{C}$ . No estimates of the variation of internal cell resistance with time nor of pumping and heat exchanger requirements were made. Efficiencies of 8% were claimed (half of Carnot). Other system efficiencies were analyzed theoretically. The authors proposed coupling this type of energy converter to flat-plate solar collectors for home heating power.

### V.1.3 Hydrogen-Oxygen Fuel Cell Coupled with High Temperature Water Electrolysis and Related Systems

In this section, papers that analyze the thermodynamic feasibility of the coupling of fuel cells and electrolyzers are briefly reviewed. Literature pertinent to the present state of the art in high temperature electrolysis is cited. With current technology this coupling does not appear to be feasible.

Hsu and coworkers [217-219] and, more recently, Steinberg [220] have proposed the combination of fuel cells operating with hydrogen and oxygen at a low temperature, producing water which could be electrolyzed at a high temperature ( $>1000^\circ\text{C}$ ). Thermodynamic calculations indicate that the operation of the electrolyzer at high temperatures should require a lower voltage than that furnished by the operation of the fuel cell at lower temperatures. Table V-2 reproduces some thermodynamic results of Steinberg [220]. The ideal net voltage for operation of the electrolysis cell at  $\sim 1200^\circ\text{C}$  is  $\sim 0.4 \text{ V}$ . Polarization losses decrease this value appreciably, presenting difficulties in the utilization of this system in this regeneration mode.

Table V-2. IDEAL EFFICIENCY FOR  $H_2-O_2$  THERMOELECTROCHEMICAL POWER CYCLE [220]

Temp. t(°C)	Electrolytic Cell			Fuel Cell		Net Cell Volt. (V)	Ideal Cycle Eff. (%) $\frac{\Delta G_f + \Delta G_e}{T_e \Delta S_e}$	Carnot Eff. (%) $\frac{T_e - T_f}{T_e}$
	$T_e$ (°C)	Elec. Energy $\Delta G_e$	Heat $T_e \Delta S_e$	Temp. $T_f$ (°C)	Elec. Energy $\Delta G_f$			
25.0	298.2	+54.64	+3.16	298.2	-54.64	0.000	0.0	0.0
226.8	500	+52.36	+5.91	298.2	-54.64	0.049	38.6	40.0
726.8	1000	+46.03	+13.18	298.2	-54.64	0.187	65.3	70.2
1226.8	1500	+39.26	+20.58	298.2	-54.64	0.333	74.7	80.1
1726.8	2000	+32.31	+27.95	298.2	-54.64	0.485	80.1	85.1

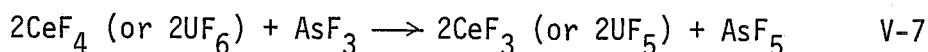
The literature on high temperature water electrolysis focuses on the production of hydrogen and on the utilization of waste heat from fusion reactors (temperatures at  $\sim 1400^\circ\text{C}$ ). The proceedings of a workshop on water electrolysis [221] presents the developments in this area up to 1975. Reference 222 contains research results regarding water electrolysis up to 1978. Reference 223 describes the status of the relevant fuel cell research in 1979. The high temperature water electrolysis utilizes solid electrolytes, e.g.,  $ZrO_2-Y_2O_3$ . The search for appropriate interconnecting materials and suitable electrocatalysts [224] is being pursued actively at several laboratories, e.g., Brookhaven National Laboratory [225] and Westinghouse Research [226]. If the research succeeds in reducing the overvoltage, IR losses, and materials problems, the coupling concept may become feasible.

Steinberg [220] also extended the thermodynamic calculations to other thermoelectrochemical cycles. One example is a  $H_2-O_2-Cl_2$  system which consists of (1) high temperature water electrolysis; (2) oxidation of aqueous HCl by the oxygen, yielding chlorine; and (3) low temperature fuel cell recombination of the  $Cl_2$  with  $H_2$ . Table V-3 presents some calculated results for this system [220].

## V.2 FLUORIDES OF URANIUM(VI) OR CERIUM(IV) AND ARSENIUM(III): SPONTANEOUS CHARGE REACTION

The patent literature [210] contains two examples of galvanic cells that can be recharged by high temperature electrolysis or, if the temperature is high enough, are transformed into the reverse galvanic cells, which also act as power generators and regenerate the original reactants of the low temperature galvanic cells. Therefore, the cell operates at one polarity at low temperature and at the opposite polarity at a higher temperature; by discharge at the higher temperature the cell is regenerated to its original electrochemical state.

These cells are based on the redox couple  $AsF_3/AsF_5$ , for which the relative stability of the two fluorides rapidly changes with increased temperature. The  $AsF_3$  is more stable at  $\sim 1200^\circ C$ . By combining this redox couple with  $UF_5/UF_6$  or  $CeF_3/CeF_4$ , which do not change relative stability with temperature, McCully [210] was able to make galvanic cells exhibiting spontaneous regeneration. At room temperature, the following discharge reaction occurs:



The reactants are separated by the solid electrolyte lead fluoride

Table V-3. IDEAL EFFICIENCY FOR  $H_2-O_2-HCl(aq)$  THERMOELECTROTHERMAL POWER CYCLE [220]<sup>a</sup>

Electrolytic Cell					Fuel Cell						
$H_2O(g) = H_2(g) + 1/2 O_2(g)$					$1/2 H_2(g) + 1/2 Cl_2(g) = 2HCl(aq)$						
t (°C)	T (K)	$\Delta G_e$	$T\Delta S_e$	Cell Voltage (V)	t(°C)	T(K)	$\Delta G$	Net $\Delta G$	Net Ideal Volt.(V)	Ideal Cycle Eff.(%)	Carnot Eff. (%)
25.0	298.2	54.64	3.16	1.185	25	298.2	-31.33 <sup>b</sup>	4.01	0.174	32.0	0.4
226.0	500	52.36	5.91	1.135	25	298.2	-31.33	5.15	0.223	37.0	40.0
726.8	1000	46.03	13.18	0.998	25	298.2	-31.33	8.32	0.360	47.4	70.2
1226.8	1500	39.26	20.58	0.851	25	298.2	-31.33	11.70	0.507	55.1	80.1
1726.8	2000	32.31	27.95	0.700	25	298.2	-31.33	15.18	0.658	60.9	85.1

<sup>a</sup>Water electrolyzers at high temperature and aqueous hydrochloric acid and fuel cell operation at low temperature.

Intermediate reaction:  $HCl(aq) + 1/4 O_2(g) = 1/2 H_2O(g) + 1/2 Cl_2(g)$ ;  $\Delta H_{298.2} = +10.95$ .

<sup>b</sup>Cell voltage = 1.359 V.

(containing KF to improve the fluoride ion conductivity) in a sandwich type of cell; the fluoride ions are transferred across the solid electrolyte and electrical work is performed on the external load. After the cell is discharged at room temperature, the battery temperature is raised to  $\sim 900^{\circ}\text{C}$ , at which temperature the reverse reaction proceeds spontaneously, generates power to the external load, and regenerates the reactants of the original cold cell. Figure V-2 shows the OCV of these cells as a function of the temperature. Current-voltage or internal cell resistance data were not given for these cells [220].

### V.3 THERMOCELL REGENERATORS

Greenberg, Thaller, and Weber [227,228] described a combination of a galvanic cell in molten salt media and a thermocell (see Section III), in which the inert electrodes are short-circuited for the regeneration of the reactants of the galvanic cell, provided that the thermopotentials developed are higher than the decomposition voltage of the salt. To avoid the accumulation of electrolysis products and, therefore, the development of a back EMF which can stop the decomposition, the decomposition products are continuously removed from the thermocell and returned to the galvanic cell. Greenberg et al. [227,228] called this type of combination a "regenerative, molten salt, thermoelectric fuel cell"; their schematic cell diagram is shown in Fig. V-3.

Laboratory cells were built as shown in Fig. V-4, one with  $\text{ZnCl}_2$  and another with  $\text{SnCl}_2$ . The cell electrodes B, C, and D were at  $400^{\circ}\text{C}$  and an auxiliary heater was employed to raise the temperature of the compartment of electrode A to  $500\text{-}600^{\circ}\text{C}$ . For the  $\text{ZnCl}_2$  cell, a thermo-

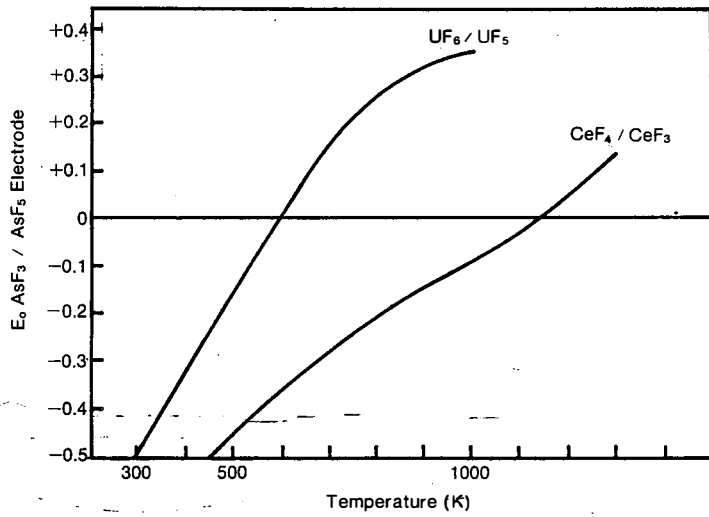


**Figure V-2. OCV of Cells Composed of  $\text{AsF}_3$  and  $\text{UF}_6$  or  $\text{CeF}_4$  Separated by the Solid Electrolyte  $\text{PbF}_4$  [210]**

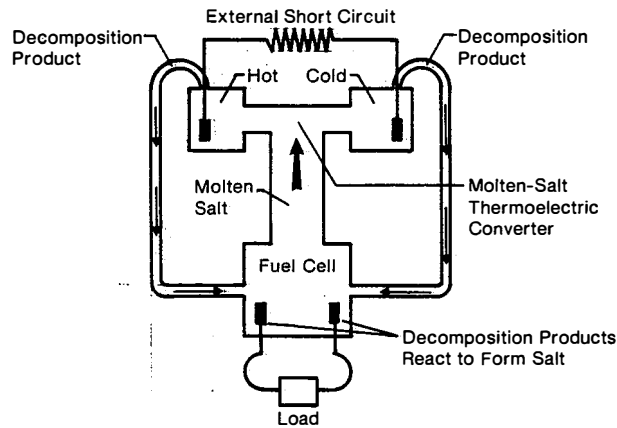


**Figure V-3. Regenerative, Molten Salt, Thermoelectric Fuel Cell Schematic Diagram [227]**

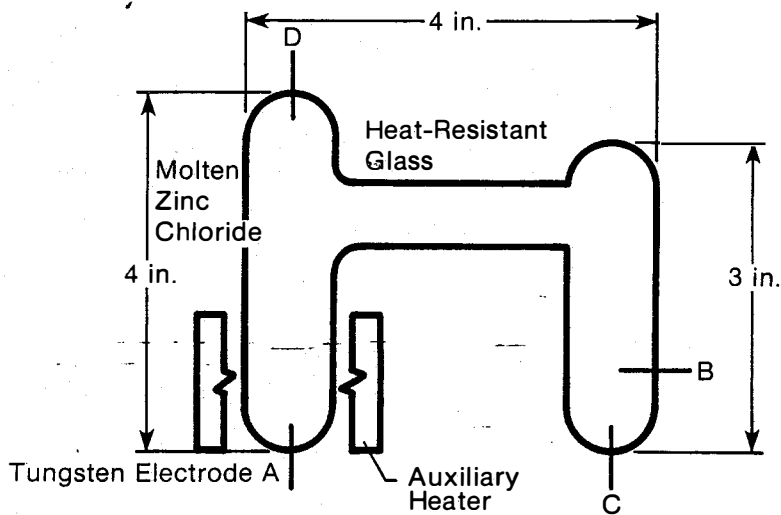
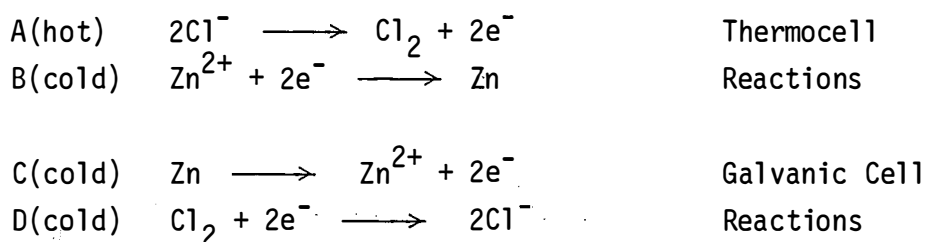


**Figure V-4. Laboratory Cell Scheme for a Thermocell Regenerator (Electrodes A, B) Coupled with the Galvanic Cell (Electrodes C, D) [227]**



galvanic potential was generated between electrodes A and C which was used to decompose the salt with currents of  $10^{-3}$ - $10^{-2}$  mA. Metallic particles were visible around electrode B, and since the metal was insoluble in the melt, it precipitated out towards electrode C. Around electrode A a yellow color was visible. The decomposition products, therefore, diffused to or precipitated at electrodes D and C, which displayed an OCV of 0.2 V. The short-circuit current between C and D was 1 mA. The half-reactions proposed are:

Electrode



The thermocells employed had very low efficiencies, which might be improved to some extent by increasing the electrode area and by using molten salts with higher thermoelectric powers (see Section III).

#### V.4 DISCUSSION OF TRES TYPE 4

Although the coupling of thermal and electrolytic regeneration was suggested in 1958, very few systems have been attempted. The very high temperature systems that were tried exhibited materials problems and low coulombic efficiencies. The systems described in Sec. II and some of Sec. I can conceivably operate in this regeneration mode. This type of regeneration has been explored to a lesser extent than thermal or electrolytic regeneration alone, but it can perhaps broaden the nature of the systems to be investigated. Media operating at lower temperatures should be investigated.

**SERIO** 

## SECTION VI

## CONCLUSIONS AND RECOMMENDATIONS

Most of the technical activities described in this review were either performed or originated many years ago and, most importantly, with specific applied objectives. Most of the work was aimed at the use of nuclear heat sources, and much of it had as its ultimate goal the development of space power systems, for which weight and zero gravitational operation were vital considerations.

It appears to us that as a result of significant time constraints imposed by the proposed space utilization timetable, much of the work involved certain preliminary experiments followed by a perhaps premature selection of a particular system for development. In certain instances, devices were fabricated and tested prior to the availability of basic chemical and/or electrochemical system information. In some cases (e.g., the thermogalvanic cells described in Sec. III), primarily scientific information was sought. In some instances, albeit far fewer (we felt), devices were fabricated based upon a known and determined scientific base.

It is worth pointing out that the reactor heat source utilization, which was one of the driving forces behind much of this work, was based on regeneration at a high temperature--usually 800°C or higher. Desire for high current efficiency tended to result in a system capable of operating over a several-hundred-degree temperature gradient. Systems operating at much lower temperatures have not been thoroughly investigated but may well be relevant to matching with solar heat sources. Our recommendations do not constitute an official position on the part of the Solar Energy Research Institute. These recommendations are intended to suggest areas for which research in either science or engineering would have long-range benefit to a TRES program. They are not intended as indications of proposed or intended development programs of a specific nature. In making these recommendations, we have not engaged in engineering or system evaluation of particular concepts and, in fact, have

purposely avoided doing so. Our recommendations attempt to assess whether past research may be worthy of renewed investigation because of the availability of new information or tools and techniques and because of the very significant changes in perspective posed by a terrestrial, solar heat source. We hope the report and subsequent evaluation of both it and our recommendations will result in new consideration of the science involved in TRES systems.

For terrestrial applications using solar heat sources, some general recommendations concerning thermally regenerative electrochemical systems can be made:

- Systems operating at lower temperatures should be investigated more thoroughly.
- The search for possible new types of TRES should be continued. Most of the obvious candidate systems for TRES have been tried; however, the development of new concepts is possible.

Our recommendations of areas of research to pursue that are related to TRES are very broad generalizations (as opposed to specific system decisions). Our assessment of the work reported and evaluated in this document convinces us this is the most reasonable approach, given the constraints discussed above.

- Molten Salt Chemistry and Electrochemistry

A broad view of the TRES area indicates the significant attempts to employ a wide variety of molten salt systems. Research in this area is rather limited at this time in the United States. New classes of molten salts have been developed in the past years, but detailed understanding of these systems is lacking. Pertinent questions have not been addressed, such as "Are electrode processes intrinsically fast at elevated temperatures, simply by virtue of the higher temperature?" Recent developments involving considerations of transport and structure in molten salts suggest that important, germane scientific information now exists (or can be obtained) that may not have been known or recognized when much of the work reported here was performed. While a good deal of the work reported here had a research component, the major thrust of most of it was developmental. Hence, additional

understanding of molten salt systems--and we might well include even concentrated electrolytes and hydrate melts--is important to this area. Structural, transport, electrochemical, and general physical properties, including valid thermodynamic data, are areas where research would be applicable to TRES development.

- Solid-State Chemistry

In a number of instances one can observe the need for either new materials (particularly stable, superionic conductors) or a better understanding of existing materials, such as stabilized zirconia or beta-alumina. Research efforts in these areas are very limited, particularly with regard to high temperature materials, except for oxide transport. In a number of cases, materials employed as ionic conductors in work reported here were used because they existed and were readily available, not because they were optimal. Kinetics and mechanisms of electrochemical reactions taking place at the solid electrolyte/electroactive material/current collector interface also constitute an area of interest. The recent development of a large number of surface spectroscopic techniques provides tools that would result in new understanding.

As a subset of this area, it appears that gas permeation through metals could be studied, again making use of recently developed surface techniques to obtain basic information of benefit to an embryonic TRES program.

- Materials Science

A quick glance through the body of this report makes obvious the materials problems--containment, bonding, corrosion--that plagued numerous activities; and, obviously, the higher the temperature, the greater the problem. A broad program in supporting materials research is recommended.

- Aqueous Systems and Electrochemistry under Extreme Conditions

While the properties of aqueous systems at room temperature are well studied, activities related to TRES suggest that one may seek to employ aqueous electrolyte systems at unusually high temperatures and

pressures. Chemical and electrochemical research in aqueous systems at much over 100°C is not a well-studied area, but it is one which would be of broad interest to this and other solar programs.

- Electrochemical Engineering

The development of any low voltage source--and all TRES are inherently low voltage--ultimately would require electrochemical engineering support in such areas as transport and battery formation. Electrochemical engineering does not appear to have paid much attention to the high temperature area except for certain specific process work, and general consideration of this problem area would be most useful. It is our opinion that such input is required for useful systems analysis.

- System Analysis

To our knowledge, no integral system analysis has been performed to assess the practicality of a complete TRES. In fact, such an analysis may not be possible at this time, based on available literature data. For example, it is not clear whether sufficient and significant polarization data for cells can be found. Nevertheless, it may be worth considering this approach for one or more of the systems reviewed, keeping firmly in mind that no electrochemical system (i.e., series arrangement of cells) has been investigated and even cell data is meager in most cases. We are unable to address the ultimate use of a TRES (i.e., central- or dispersed-power application), but clearly this consideration is important to an integral system analysis.

## SECTION VII

## REFERENCES

1. H. A. Liebhafsky, "Regenerative electrochemical systems: an introduction," in Regenerative EMF cells, C. E. Crouthamel and H. L. Recht, eds., Advances in Chemistry Series, 64, 1-10, American Chemical Society, Washington, D.C. (1967).
2. Examples of redox regenerative systems:
  - (a) "Redox flow cell development and demonstration project - calendar year 1977," Report No. NASA-TM-79067 prepared under Interagency agreement E(49-28)-1002 (1979).
  - (b) G. Ciprios, W. Erskine, and P. G. Grimes, "Redox bulk energy storage system study," vols. 1 and 2, Final Reports, N 77-33608 and N 77-33609 (1967).
  - (c) S. Asimura and Y. Miyaki, "Redox-type fuel cell. VII. Polarization characteristics of the redox-type fuel cell anode at flow-through porous carbon electrodes," Denki Kagaku, 40, 50-54 (1972).
3. L. G. Austin, "Fuel cells: a review of government sponsored research, 1950-1964," NASA-SP-120, pp. 153-203.
4. R. L. Kerr, "Regenerative Fuel Cells," Proc. Performance Forecast Selected Static Energy Conversion Devices Meet. AGARD, Propulsion and Energetics Panel, 29th, Liege, Belgium 1967 G. W. Sherman and L. Devol, eds., pp. 658-711 (1968).
5. Regenerative EMF Cells, C. E. Crouthamel and H. L. Recht, eds., Advances in Chemistry Series, 64, American Chemical Society, Washington, D. C. (1967).
6. Examples of electrolytically regenerative systems:
  - (a) J. McBreen, R. S. Yeo, A. Beaufrere, and S. Srinivasan, "Hydrogen-chlorine energy storage system," Report BNL-23 670 (1977).
  - (b) L. Swette and G. L. Holleck, "Hydrogen-nickel regenerative fuel cells," Final Report No. 339, contract F33615-73-C-2057 (1974).
  - (c) B. M. Wilner, H. A. Frank, E. Findl, and M. Klein, "Electrolytically regenerative hydrogen-oxygen fuel cells," U.S. Patent 3,507,704 (1970).
7. E. Yeager, "Fuel cells: basic considerations," Proc. 12th Ann. Battery Research and Development Conf., ed. by Power Source Division, U.S. Army Signal Research and Development Laboratory, Fort Monmouth, New Jersey, pp. 2-4 (1958).

8. H. A. Liebhafsky, "The fuel cell and the Carnot cycle," J. Electrochem. Soc., 106, 1068-71 (1959).
9. A. J. deBethune, "Fuel cell thermodynamics," J. Electrochem. Soc., 107, 937-9 (1960).
10. L. G. Austin in "Handbook of fuel cell technology," C. Berger, ed., Prentice Hall, Inc., New Jersey, pp. 36-41 (1968).
11. J. B. Friauf, "Thermodynamics of thermally regenerated fuel cells," J. Appl. Phys., 32, 616-20 (1961).
12. R. E. Henderson, B. Agruss, and W. G. Caple, "Resume of thermally regenerative fuel cells," Progr. in Astronaut. Rocketry, 3, 411-23 (1961).
13. J. King, Jr., F. A. Ludwig, and J. J. Rowlette, "General evaluation of chemicals for regenerative fuel cells," Progr. in Astronaut Rocketry, 3, 387-40 (1961).
14. R. H. Snow, "Thermochemical and thermodynamic data on selected compounds for the chemical conversion of waste heat to electrical energy," Report No. AD 265-376L, Illinois Institute of Technology Research Institute, Chicago, Illinois, under contract N0w-60-0760-c (1961).
15. G. Wurtzbacher, "Thermally regenerable fuel cells for conversion of heat to electrical energy," Chem. Ingr.-Tech, 37, 532-8 (1965).
16. R. E. Shearer and R. C. Werner, "Thermally regenerative ionic hydride galvanic cell," J. Electrochem. Soc., 105, 693 (1958).
17. R. C. Werner, R. E. Shearer, and T. A. Ciarlariello, "Fuel cell batteries - regenerative type," Proc. 13th Annual Power Sources Conf., PSC Publications Committee, Red Bank, New Jersey, p. 122 (1959).  
R. E. Shearer, J. W. Mausteller, T. A. Ciarlariello, and R. C. Werner, "Regenerative metal hydride system," Proc. 14th Annual Power Sources Conference, Red Bank, New Jersey, PSC Publications Committee pp. 76-7 (1960).
18. T. A. Ciarlariello, "Self-continuing hydride cells," U.S. Patent 3,014,084 (1961).
19. R. C. Werner and R. E. Shearer, "Fuel cells," U.S. Patent 3,031,058 (1962).
20. T. A. Ciarlariello and R. C. Werner, "Fuel cell based on nuclear reactors," Chem. Eng. Progr., 57, 42-5 (1961).
21. R. C. Werner and T. A. Ciarlariello, "Metal hydride fuel cells as energy storage devices," Proc. U.N. Conf. New Sources Energy, Rome, 1961, 2, 213-218 (1963).



22. R. E. Shearer, "Study of energy conversion devices," Reports No. 1 (AD 230 503; 1959), 2 (AD 234482, 1959), 3 (AD 238235, 1960), and 4 (AD 250695, 1960).
23. R. E. Shearer, "Study of Energy Conversion Devices," Final Report No. 7 (7/59-5/61), DA-36-039-SC-78955, USAERDL/NJ.
24. J. M. Fuscoe, S. S. Carlton, and D. P. Laverty, "Regenerative fuel cell system investigation," WADD Technical Report 60-442, Thompson-Ramo-Wooldridge, Inc., Cleveland, Ohio, contract AF33(600)-39574 (May 1960).
25. H. J. Schwartz, S. S. Carlton, and J. M. Fuscoe, "Regenerative fuel cell system," Final Report No. ASD-TDR-62-18, Thompson-Ramo-Wooldridge, Inc., Cleveland, Ohio, contract AF33(600)-39573 (April 1962).
26. S. S. Carlton, "Electrode development program," Final Report ASD-TDR-62-241, Thompson-Ramo-Wooldridge, Inc., Cleveland, Ohio, contract AF33(600)-42449 (June 1962).
27. S. S. Carlton, "Fuel cell construction," U.S. Patent 3,110,631 (1966).
28. A. J. Stromquist, "Zero gravity separator development for regenerative fuel cell," Final Report No. ASD-TDR-62-240, Thompson-Ramo-Wooldridge, Inc., Cleveland, Ohio, contract AF33(600)-42449 (June 1962).
29. D. R. Snoke and J. M. Fuscoe, "Lithium hydrogen fuel cell seen feasible," SAE J., 69(6), 68-69 (1961).
30. D. R. Snoke, J. M. Fuscoe, and S. S. Carlton, "Extended-life fuel cells for space," National Aerospace Electronics Conference of Institute of Radio Engineers, Dayton, Ohio, May 8, 1961.
31. M. A. Del Duca, J. M. Fuscoe, and T. A. Johnson, "Fuel cells for space vehicles," *Astronautics*, 5, 36-44 (1960).
32. R. L. Kerr, "Low-gravity separator investigation," Report No. ASD-TDR-62-776 (1962).
33. C. E. Johnson and R. R. Heinrich, "Thermodynamics of the lithium hydride regenerative cell," in *Regenerative EMF Cells*, C. E. Crouthamel and H. L. Recht, eds., *Advances in Chemistry Series*, 64, 105-120, American Chemical Society, Washington, D.C. (1967).
34. M. S. Foster, C. E. Johnson, and C. E. Crouthamel, "Purification unit for high purity inert atmosphere boxes," USAEC-ANL-6652, Argonne National Laboratory (1962).  
C. E. Johnson, M. S. Foster, and M. L. Kyle, "Purification of inert atmospheres," *Nuclear Applications*, 3, 563-7 (1967).

35. H. Shimotake and J. C. Hesson, "Corrosion by fused salts and heavy liquid metals - a survey," in Regenerative EMF Cells, C. E. Crouthamel and H. L. Recht, eds., Advances in Chemistry Series, 64, 149-185, American Chemical Society, Washington, D.C. (1967).
36. E. J. Cairns, C. E. Crouthamel, A. K. Fisher, M. S. Foster, J. C. Hesson, C. E. Johnson, H. Shimotake, and A. D. Tevebaugh, "Galvanic cells with fused salt electrolytes," Chemical Engineering Division, Report No. ANL-7316 (November 1967). This final report contains summaries of all partial reports "Thermally regenerative fuel cells" (ANL-6379, 6413, 6477, 6543, 6569, 6596, 6648, 6687, 6766, 6725, 6800, 6875; covering 1961-1964) and "Energy conversion" (ANL-6900, 6925, 7055, 7125, 7255, 7325; covering 1964-1966) from Argonne National Laboratories germane to TRES, both LiH and bimetallic systems.
37. R. R. Heinrich, C. E. Johnson, and C. E. Crouthamel, "Hydrogen permeation studies. I. Armco iron and iron-molybdenum alloys," J. Electrochem. Soc., 112, 1067-70 (1965).
38. R. R. Heinrich, C. E. Johnson, and C. E. Crouthamel, "Hydrogen permeation studies. II. Vanadium as a hydrogen electrode in a lithium hydride cell," J. Electrochem. Soc., 112, 1071-3 (1965).
39. J. A. Plambeck, J. P. Elder, and H. A. Laitinen, "Electrochemistry of the lithium hydride cell," J. Electrochem. Soc., 113, 931-7(1966).
40. C. E. Johnson, S. E. Wood, and C. E. Crouthamel, "Studies of lithium hydride systems. I. Solid-liquid equilibrium in the lithium hydride-lithium chloride system," J. Inorg. Chem., 3, 1487 (1964).
41. C. E. Johnson, S. E. Wood, and C. E. Crouthamel, "Studies of lithium hydride systems. II. Solid-liquid equilibrium in the sodium chloride-lithium hydride system," J. Chem. Phys., 44, 880-3 (1966).
42. C. E. Johnson, S. E. Wood, and C. E. Crouthamel, "Studies of lithium hydride systems. III. Solid-liquid equilibrium in the lithium bromide-lithium hydride and lithium iodide-lithium hydride systems," J. Chem. Phys. 44, 884-9 (1966).
43. C. E. Johnson, E. Hathaway, and C. E. Crouthamel, "Lithium hydride systems. Solid-liquid phase equilibria for the ternary lithium hydride-lithium chloride-lithium fluoride system." J. Chem. Eng. Data, 11, 372-4 (1966).
44. C. E. Johnson and E. J. Hathaway, "Lithium hydride systems: Solid-liquid equilibria for the ternary lithium hydride-lithium chloride-lithium iodide systems." J. Chem. Eng. Data, 14, 174-5 (1969).
45. C. E. Johnson, R. R. Heinrich, and C. E. Crouthamel, "Thermodynamic properties of lithium hydride by an electromotive force method," J. Phys. Chem., 70, 242-6 (1966).

46. J.C. Hesson and H. Shimotake, "Thermodynamics and thermal efficiencies of thermally regenerative bimetallic and hydride EMF cell systems," in Regenerative EMF cells, C. E. Crouthamel and H. L. Recht, eds., Advances in Chemistry Series, 64, 82-104, American Chemical Society, Washington, D.C. (1967).
47. C.E. Messer, "A survey report on lithium hydride," USAEC-NYO-9470 (October 1960).
48. C. E. Messer and J. Mellor, "The system lithium hydride-lithium fluoride," J. Phys. Chem., 64, 503-4 (1960).
49. C. E. Messer, E. B. Damon, D. C. Maybury, J. Mellor, and R. A. Seales, "Solid-liquid equilibrium in the lithium-lithium hydride system," J. Phys. Chem., 62, 220-2 (1958).
50. L. B. Anderson, E. V. Ballou, and S. A. Greenberg, "Solar Regenerative Systems," Final Report AD 289294, Lockheed Aircraft Corp., Missile and Space Division, California, contract DA-36-039 SC-85245 (1962).
51. L. B. Anderson, S. A. Greenberg, and G. B. Adams, "Thermally and photo-chemically regenerative electrochemical systems," in Regenerative EMF cells, C. E. Crouthamel and H. L. Recht, eds., Advances in Chemistry Series, 64, 2133-276, American Chemical Society, Washington, D.C. (1967).
52. R. F. Fogle and H. E. Lawson, "Investigation of an energy conversion device," Final Report AD285667, Aerojet-General Corp., California, contract DA36-039 SC87229 (1962).
53. T. M. Rymarz et al., "Chemical conversion of waste heat to electrical energy," Quarterly Report No. 4, ARF-3182-4, Armour Research Foundation of Illinois Institute of Technology, contract N0w 60-0760-c (1961).
54. T. M. Rymarz et al., "Chemical conversion of waste heat to electrical energy," Quarterly Report No. 5, ARF 3182-6 (1961).
55. Conversation with M. J. Klein and R. H. Snow (H. L. Chum and R. A. Osteryoung), Feb. 22, 1979, Chicago, Illinois.
56. J. L. Reger and L. Schieler, "Regenerable fuel cell design," U.S. Patent 3,236,691 (1966).
57. F. D. Hess and L. Schieler, "Energy conversion research program," Semiannual Tech. Report. AD 27621, Aerospace Corp., California, contract AFO 4(647)-930 (1961).
58. F. D. Hess and L. Schieler, "Energy conversion research program," Semi-annual Tech. Report, Report No. TDR-69(2220-30)TR-2 (1962) AD 285084; contract AFO 4(695)-69 (1962).
59. S. W. Mayer and W. E. Brown, Jr., "Chronopotentiometric measurements of electrode kinetics for chlorides of W, Sb, P and group IVA," Report No. TD-R69(2220-30)TM1(1962) AD 282902, Aerospace Corp., California, contract AF04(695)-69 (1962).

60. S. W. Mayer and W. E. Brown, Jr., "Electrode kinetics for chlorides of tungsten, antimony, and phosphorus," *J. Electrochem. Soc.*, 110, 306-11 (1963).
61. C. R. McCully, T. M. Rymarz, and S. B. Nicholson, "Regenerative chloride systems for conversion of heat to electrical energy," in *Regenerative EMF cells*, C. E. Crouthamel and H. L. Recht, eds., *Advances in Chemistry Series*, 64, 198-212, American Chemical Society, Washington, D.C. (1967).
62. C. R. McCully and T. M. Rymarz, "Chemical conversion of waste heat to electrical energy," Final Report No. IITR-3182-10, Illinois Institute of Technology Research Institute, contract NOW 60-0760c (1962).
63. T. M. Rymarz et al., "Chemical conversion of waste heat to electrical energy," *Quarterly Report No. 8* No. ARF-3182-9, Illinois Institute of Technology Research Institute, contract NOW 60-7060-c (1962). C. R. McCully, "Electrochemical power supply regenerated by heat," U.S. Patent 3,523,829 (1970).
64. R. A. Rightmire and J. L. Callahan, "Energy conversion system," U.S. Patent 3,088,990 (1968).
65. E. L. Kumm, "SO<sub>2</sub>-SO<sub>3</sub> regenerative fuel cell research," NASA Doc. N62-17,308 (1962).
66. W. E. Wentworth and E. Chen, "Simple thermal decomposition reactions for storage of solar thermal energy," *Solar Energy*, 18, 205-11 (1976). Phone call with W. E. Wentworth (H. L. Chum), April 15, 1979.
67. E. H. Lyons, Jr., "Metal oxide fuel cells," U.S. Patent 3,100,163 (1963).
68. D. E. McKenzie and J. P. Howe, "Electrochemical conversion of heat to electricity," U.S. Patent 3,368,921 (1968).
69. W. E. Case, "Apparatus for converting heat energy into electrical energy," U.S. Patent 344,345 (1886). W. E. Case, *Jb. d. Electrochemie*, 2, 56(1896).
70. S. Skinner, "The tin-chromic chloride cell," *Proc. Physic. Soc. London*, 13, 477-81 (1895); "The tin-chromic chloride cell," *Phil. Mag.*, 39, 444-7 (1895).
71. J. Vedel, M. Soubeyrand, and H. Le Quan, "The conversion of thermal energy into electrical energy using cells having a reversal of potential with temperature," *J. Appl. Electrochemistry*, 9, 475-81(1979).
72. C. R. McCully, "The chemical conversion of solar energy to electrical energy," *Proc. U.N. Conf. New Sources of Energy*, Rome, 1961, 2, 196-202 (1963).
73. C. R. McCully et al., "Chemical conversion of waste heat to electrical energy," *Quarterly Report No. 3*, ARF-3182-3, Armour Research Foundation of Illinois Institute of Technology, contract NOW 60-0760-c (1961).

74. C. R. McCully, "Chemical conversion of heat to electrical energy," Report No. IITRI-C-6006-10, Final, Illinois Institute of Technology Research Institute, contract NOW 60-0512-c (1967).
75. N. Bjerrum, "Electrochemical and spectroscopic studies of the chalcogens in chloroaluminate melts," in *Characterization of Solutes in Non-Aqueous Solvents*, G. Mamantov, ed., Plenum Press, New York, pp. 251-271 and references therein (1976).  
T. W. Couch, D. A. Lokken, and J. D. Corbett, "The crystal structure of tetratellurium (2+) tetrachloroaluminate and heptachlorodialuminate,  $\text{Te}_4(\text{AlCl}_4)_2$  and  $\text{Te}_4(\text{Al}_4\text{Cl}_7)_2$ ," *Inorg. Chem.*, 11, 357-9 (1972).  
N. J. Bjerrum and G. P. Smith, "Tellurium in the formal electropositive oxidation state one-half in acidic chloride media," *J. Am. Chem. Soc.*, 90, 4472 (1968).  
D. J. Prince, J. D. Corbett, and B. Garbisch, "Diatomic cations of tellurium and selenium in chloroaluminate melts," *Inorg. Chem.*, 9, 2731 (1970).  
R. Fehrman, N. J. Bjerrum, and M. A. Andreasen, "Lower oxidation states of tellurium 4  $\text{Te}_4^{2+}$ ,  $\text{Te}_6^{2+}$ ,  $\text{Te}_8^{2+}$  in chloroaluminate melts," *Inorg. Chem.*, 15, 2187 (1976).  
F. W. Paulsen, N. J. Bjerrum, and D. R. Nielsen, "Chlorocomplexes in molten salts. III. Raman study of chloro complexes found in the molten  $\text{KCl-AlCl}_3\text{TeCl}_4$  system," *Inorg. Chem.*, 13, 2693 (1974).
76. J. Robinson and R. A. Osteryoung, "The electrochemical behavior of Te(IV) in sodium tetrachloroaluminate melts," *J. Electrochem. Soc.*, 125, 1784 (1978).
77. T. M. Rymarz, "Tellurium chloride thermoregenerative galvanic cell," Final Report No. IITRI-c 6069-5, contract NOW-65-0431-c (1967).
78. D. E. Anthes, "Tellurium chloride thermoregenerative galvanic cell," Final Report No. IITRI-c 6142-5, contract NOW 19-68-C-0361 (1969).
79. C. R. McCully et al., "Chemical conversion of waste heat to electrical energy," Quarterly Report ARF-3182-2, Armour Research Foundation of Illinois Institute of Technology, contract NOW-60-0760-c (1961).
80. Iu. K. Delimarski and B. F. Markov, *Electrochemistry in Fused Salts*, The Sigma Press, Washington, D.C. (1961).
81. B. Agruss, "The thermally regenerative liquid metal cell," *J. Electrochem. Soc.*, 110, 1097-1103 (1963).
82. R. D. Weaver, S. W. Smith, and N. L. William, "The sodium/tin liquid metal cell," *J. Electrochem. Soc.*, 109, 653-657 (1962).  
S. W. Smith and R. D. Weaver, "A comparison of the system weight of the Na/Sn liquid metal cell for various applications," Report No. 4337-E, Delco-Remy Division, General Motors Corp. (March 1962).
83. B. Agruss, "Regenerative battery," U.S. Patent 3,245,836 (1966).

84. B. Agruss and H. Karas, "The thermally regenerative liquid metal concentration cell," in *Regenerative EMF Cells*, C. E. Crouthamel and H. L. Recht, eds., *Advances in Chemistry Series*, 64, 62-81, American Chemical Society, Washington, D.C. (1967).
85. R. E. Henderson, "Liquid metal cells," *Chem. Eng. Pr.*, 59, 56-7 (1963).  
R. E. Henderson and E. H. Hietbrink, "Mercury space power systems," in *Direct Conversion Proceedings*, Pacific Energy Conversion Conf., San Francisco, California, pp. 16-1 to 16-12 (1962).
86. R. E. Henderson, "Thermally regenerative fuel cells," *Proc. 6th AGARD Combustion and Propulsion Colloquium on Energy Sources and Energy Conversion*, Cannes, France, March 16, 1964; AGARDograph, No. 81, pp. 795-809.
87. R. B. Wright, "Diffusion of potassium in a liquid metal cell," Report No. N64-19798, the Allison Division of General Motors Corp., Indianapolis, Indiana, contract EDR-3814 (1964).
88. J. D. Mangus, "Research and development of an advanced laboratory liquid metal regenerative cell," Report No. AD-438519 (1964).
89. B. Agruss, E. H. Hietbrink, and T. F. Nagey, "Regenerating molten metal fuel cell," U.S. Patent 3,503,808 (1970).
90. M. F. Lantratov and E. V. Tsarenko, "Investigation of the thermodynamic properties of liquid metallic solutions in potassium-mercury system," *J. Appl. Chem. USSR*, 33, 7 (1960).
91. C. R. LaMantia and C. F. Bonilla, "Thermodynamics of the system potassium-mercury," *Proc. Symposium on Thermophysical Properties*, 4th, J. R. Mozynski, ed., American Society of Mechanical Engineers, New York, pp. 58-71 (1968).
92. V. T. Vorogushin, "Variation of the free-energy with the heat of evaporation in the thermodynamic cycle of a regenerative fuel cell," *Russ. J. Phys. Chem.*, 43(3), 435-6 (1969).
93. R. D. Oldenkamp, L. A. Heredy, and H. L. Recht, "The test program and performance analysis of the Atomics International thermally regenerative alloy cell (TRAC) system," *Proc. Intersociety Energy Conversion Engineering Conf.*, 1st, Los Angeles, California, pp. 324-331 (1966).
94. L. A. Heredy, M. L. Iverson, G. D. Ulrich, and H. L. Recht, "Development of a thermally regenerative sodium-mercury galvanic system. Part I. Electrochemical and chemical behavior of sodium-mercury galvanic cells," in *Regenerative EMF Cells*, C. E. Crouthamel and H. L. Recht, eds., *Advances in Chemistry Series*, 64, 30-42, American Chemical Society, Washington, D.C. (1967).

95. I. J. Groce and R. D. Oldenkamp, "Development of a thermally regenerative sodium-mercury galvanic system. Part II. Design, construction and testing of a thermally regenerative sodium-mercury galvanic system," in *Regenerative EMF Cells*, C. E. Crouthamel and H. L. Recht, eds., *Advances in Chemistry Series*, 64, 43-52, American Chemical Society, Washington, D.C. (1967).
96. R. D. Oldenkamp and H. L. Recht, "Development of a thermally regenerative sodium-mercury galvanic system. Part III. Performance analysis for a nuclear reactor-powered, thermally regenerative sodium mercury galvanic system," in *Regenerative EMF Cells*, C. E. Crouthamel and H. L. Recht, eds., *Advances in Chemistry Series*, 64, 53-61, American Chemical Society, Washington, D.C. (1967).
97. H. L. Recht and D.-E. McKenzie, "Energy conversion process and apparatus," U.S. Patent 3,419,435 (1968).
98. H. L. Recht and M. L. Iverson, "Porous matrix for galvanic cell," U.S. Patent 3,419,436 (1968).
99. M. L. Iverson, "Galvanic cell electrolyte," U.S. Patent 3,441,411 (1969).
100. L. A. Heredy, "High temperature galvanic cell," U.S. Patent 3,441,446 (1969).
101. M. L. Iverson and H. L. Recht, "The activity of sodium in sodium amalgams from measurement," *J. Chem. Eng. Data*, 12, 262-5 (1967).
102. K. Hauffe, "Determining the activities of metals in binary systems whose behavior is widely divergent from the ideal," *Z. Electrochem.*, 46, 348-50 (1940).
103. N. S. Kurnakow and N. A. Puschin, *Z. Anorg. Chem.*, 30, 87-101 (1902).
104. A. K. Fischer, "Phase diagram considerations for the regenerative bi-metallic cell," in *Regenerative EMF cells*, C. E. Crouthamel and H. L. Recht, eds., *Advances in Chemistry Series*, 64, 121-135, American Chemical Society, Washington, D.C. (1967).
105. For examples, see:  
S. M. Zivi, I. Pollack, H. Kacinkas, A. A. Chilenskias, and D. L. Barney, "Battery engineering problems in designing an electrical load leveling plant for lithium/iron-sulfide cells," *Proc. 14th Intersociety Energy Conversion Engineering Conference*, Boston, Massachusetts, American Chemical Society, Washington, D.C., pp. 722-729 (1979).  
F. J. Martino, T. W. Olszanski, L. G. Bartholme, E. C. Gay, and H. Shimotake, "Advances in the development of Li-Al/FeS cells for electric-automobile batteries," American Chemical Society, Washington, D.C., pp. 660-664 (1979).

106. C. E. Johnson and E. J. Hathaway, "Solid-liquid phase equilibria for the ternary systems Li(F,Cl,I) and Na(F,Cl,Br)," *J. Electrochem. Soc.*, 118, 631-4 (1971).
107. K. Hauffe and A. L. Griessback-Vierk, "Activity measurements on liquid-thallium alloys," *Z. Elektrochem.*, 53, 151 (1949).
108. M. F. Lantratov, "Thermodynamic properties of liquid-metal solutions in the Na-Pb system," *Russian J. Inorg. Chem. (transl.)*, 4, 2043-5 (1959).
109. B. Porter and M. Feinleib, "Determination of activity of sodium in Na-Pb alloys at high temperatures," *J. Electrochem. Soc.*, 103, 300-303 (1956).
110. E. J. Cairns, A. D. Tevebaugh, J. D. Bingle, C. E. Johnson, M. S. Foster, E. J. Hathaway, J. Peck, E. L. Gasner, T. F. Young, G. H. McCloud, A. K. Fischer, S. A. Johnson, S. E. Wood, H. Shimotake, G. Rogers, and J. Kargol, "Energy conversion," *Chemical Engineering Division Semiannual Report, July-December 1966, ANL-7325*, Argonne, Illinois: Argonne National Laboratory p. 179-196 (April 1967).
111. A. K. Fischer and S. A. Johnson, "Liquid-vapor equilibria in the sodium-lead system," *J. Chem. Eng. Data*, 15, 492-495 (1970).
112. H. Shimotake and E. J. Cairns, "Bimetallic cells with fused-salt electrolytes," in *Advances in Energy Conversion Engineering*, American Society of Mechanical Engineers, pp. 951-962 (1967).
113. J. C. Hesson, M. S. Foster, and H. Shimotake, "Self-discharge in alkali-metal-containing bimetallic cells," *J. Electrochem. Soc.*, 115, 787-790 (1968).
114. M. S. Foster, "Laboratory studies of intermetallic cells," in *Regenerative EMF cells*, C. E. Crouthamel and H. L. Recht, eds., *Advances in Chemistry Series*, 64, 136-148, American Chemical Society, Washington, D.C. (1967).
115. A. K. Fischer, S. A. Johnson, and S. E. Wood, "Liquid-vapor phase diagram and thermodynamics of the sodium-bismuth system," *J. Phys. Chem.*, 71, 1465-1472 (1967).
116. C. E. Johnson and A. K. Fischer, "New measurements for the sodium-bismuth phase diagram," *J. Less-Common Metals*, 20, 339-344 (1970).
117. M. S. Foster, S. E. Wood, and C. E. Crouthamel, "Thermodynamic of binary alloys. II. The lithium-tin system," *J. Phys. Chem.*, 70, 3042-45 (1964).
118. M. S. Foster, S. E. Wood, and C. E. Crouthamel, "Thermodynamic of binary alloys. I. The lithium-bismuth system," *Inorg. Chem.*, 3, 1428-1431 (1964).



119. M. S. Foster and C. C. Liu, "Thermodynamic of binary alloys. III. The lithium-tellurium system," J. Phys. Chem., 70, 950 (1966).
120. A. K. Fischer and S. A. Johnson, "Liquid-vapor equilibria and thermodynamics of the lithium-tin systems," J. Chem. Eng. Data, 17, 280-283 (1972).
121. A. J. deBethune, T. S. Licht, and N. Swendeman, "The temperature coefficients of electrode potentials," J. Electrochem. Soc., 106, 616-625 (1959).  
A. J. deBethune and H. O. Daley, Jr., "The thermal temperature coefficient of the calomel electrode between 0° and 70°C, II and III," J. Electrochem. Soc., 116, 1395-1401, 1401-1406 (1969).
122. A. J. deBethune, "Irreversible thermodynamics in electrochemistry," J. Electrochem. Soc., 107, 829-842 (1960).
123. J. N. Agar, "Thermogalvanic cells," in Advances in Electrochemistry and Electrochemical Engineering, P. Delahay and C. W. Tobias, eds., vol. 3, Interscience, pp. 31-121 (1963).
124. C. Wagner, "Thermoelectric power of cells with ionic compounds involving ionic and electronic conduction," Progr. Solid State Chem., 7, 1-37 (1972).
125. R. Zito, Jr., "Thermogalvanic energy conversion," AIAA J., 1, 2133-2138 (1963).
126. B. Sundheim, "Molten salts vs. thermoelectric materials," chapter 2 in Thermoelectric Materials and Devices, I. B. Cadoff and E. Miller, eds., Reinhold Publ. Corp., New York (1960).
127. R. W. Christy, "Ionic Materials," in Thermoelectric Materials and Devices, I. B. Cadoff and E. Miller, eds., Reinhold Publ. Corp., New York, pp. 173-183 (1960).
128. W. Vielstich, Fuel Cells, translated by O. J. G. Ives, Wiley-Interscience, New York, pp. 345-361 (1970).
129. N. Fuschillo, "Thermoelectric phenomena," in Thermoelectric Materials and Devices, I. B. Cadoff and E. Miller, eds. pp. 1-16 (1960) Reinhold Publ. Corp., New York.  
S. W. Angrist, "Direct Energy Conversion," 3rd ed., Allyn and Bacon, Inc., Boston, pp. 129-190 (1976).
130. Examples:  
L. Patrick and A. W. Lawson, "Thermoelectric power of pure and doped AgBr," J. Chem. Phys., 22, 1492-5 (1954).  
R. W. Christy, E. Fukushima, and H. T. Li, "Thermoelectric power of silver bromide containing cadmium bromide," J. Chem. Phys., 30, 136-8 (1959).

131. K. S. Pitzer, "Thermodynamics of thermocells with fused or solid electrolytes," *J. Phys. Chem.*, 65, 147-150 (1961).
132. J. N. Agar and W. G. Breck, "Thermal diffusion in nonisothermal cells. I. Theoretical relation and experiments on solutions of thalious salts," *Trans. Faraday Soc.*, 53, 167-78 (1957).
133. N. Fuschillo, "Thermoelectric figure of merit," in *Thermoelectric Materials and Devices*, I. B. Cadoff and E. Miller, eds., Reinhold Publishing Corp., New York, pp. 31-46 (1960).
134. M. Telkes, "Solar thermoelectric generators," *J. Appl. Phys.*, 25, 765-777 (1954).
135. T. Wartanowicz, "A theoretical analysis of a molten salt thermocell as a thermoelectric generator," *Advan. Energy Conversion*, 4, 149-158 (1964).
136. T. Wartanowicz, "Analysis performance and experimental investigations on a molten salt thermocell as a thermoelectrochemical energy converter," *Bull. Acad. Polon. Sci. Ser. Sci. Tech.*, 13, 911-16 (1965).
137. B. R. Sundheim and J. Rosenstreich, "Molten salt thermocells," *J. Phys. Chem.*, 63, 419-22 (1959).
138. R. H. Detig and D. H. Archer, "Thermoelectric effects in fused ionic materials," *J. Chem. Phys.*, 38, 661-666 (1963).
139. B. R. Sundheim and J. D. Kellner, "Thermoelectric properties of molten silver-silver nitrate-sodium nitrate system," *J. Phys. Chem.*, 69, 1204-8 (1965).
140. R. Haase, U. Prüser, and J. Richter, "Evaluation of measurements on thermocells containing molten salt mixtures," *Ber. Bunsenges. Phys. Chem.*, 81, 577-84 (1977). See also *ibidem*, 508-514.
141. M. Abraham and M. Gauthier, "Influence de la temperature sur le pouvoir thermoelectrique initial de quelques thermopiles a melanges fondus et surfondus de  $\text{AgNO}_3$  et  $\text{TiNO}_3$  avec electrodes de Ag," *Electrochim. Acta*, 15, 1399-1405 (1970).
142. M. Abraham and M. Gauthier, "Thermopiles a nitrates fondus: evolution du pouvoir thermoelectrique initial lors de la transition liquid-verre," *Electrochim. Acta*, 16, 953-9 (1971).
143. R. Haase, "Thermodynamics of Irreversible Processes," Reading, Massachusetts (1969).
144. R. Connan and J. Dupuy, "Perturbations dans les melanges  $\text{AgNO}_3$ - $\text{MNO}_3$  fondus par mesures de thermopiles - nouvelles possibilites d'exploitation," *Electrochim. Acta*, 15, 977-85 (1970).

145. M. Abraham and M. Gauthier, "La thermopotentiometrie appliquee a l'etude du comportement de certains liquides surfondus," *Electrochim. Acta*, 17, 279-84 (1972).
146. S. Senderoff and R. I. Bretz, "Ionic transport entropy in non-isothermal molten silver chloride cells," *J. Electrochem. Soc.*, 109, 56-61 (1972).
147. H. Holtan, Jr., "Thermocells with solid and fused electrolytes," *Koninkl. Ned. Akad. Wetenschap., Proc., Ser. B.*, 56, 498-509 (1953).  
H. Holtan, Jr. "Thermocells containing electrolytic solutions," *J. Electrochem. Soc.* 56, 510-14 (1953).
148. B. F. Markov, "Thermal electromotive forces with fused salts," *Doklad. Akad. Nauk. USSR*, 108, 115-17 (1956).
149. L. B. Anderson, S. A. Greenberg, and G. B. Adams, "Thermally and photochemically regenerative electrochemical systems," in *Regenerative EMF Cells*, C. E. Crouthamel and H. L. Recht, eds., *Advances in Chemistry Series*, vol. 64, American Chemical Society, Washington, D.C. pp. 213-276 (1967).
150. A. R. Nichols and C. T. Langford, "Entropy of the moving cuprous ion in molten cuprous chloride from thermogalvanic potentials," *J. Electrochem. Soc.*, 107, 842-7 (1960).
151. A. Kvist and A. Randsalie, "Thermoelectric power of molten and solid  $\text{Ag}_2\text{SO}_4$ ," *Z. Naturforsch.*, a 21, 278-81 (1966).
152. H. P. Meissner, D. C. White, and G. D. Uhlrich, "Thermocells: effect of pressure on voltage," *Advan. Energy Conversion*, 5, 205-16 (1965).
153. S. Senderoff, "Thermocell," U.S. Patent 3,294,585 (1966).  
S. Senderoff, "Thermocell battery," U.S. Patent 3,311,506 (1967).
154. W. Fischer, "Thermoelectric powers of cells of the type  $\text{Cl}_{2T}|\text{molten chloride}|_{T+\Delta T}\text{Cl}_2$ ," *Z. Naturforsch.*, a 21, 281-6 (1966).
155. R. J. Brood, "Thermocell," U.S. Patent 3,293,079 (1966).
156. H. Holtan, Jr., "Relation between temperature coefficient of isothermal cells and the thermopotentials of the corresponding thermocells," *Koninkl. Ned. Akad. Wetenschap., Proc.*, 57B, 138-41 (1954); *ibidem*, 592-5.  
H. Holtan, P. Mazur, and S. R. deGroot, *Physica*, XIX, 1109-18 (1953).
157. J. A. A. Ketelaar, "The unattainability of a unified EMF series for molten salts," *J. Electroanal. Chem.*, 65, 87-93 (1975).
158. H. E. Lawson, "Apparatus and method for thermal regeneration of electrical energy," U.S. Patent 3,374,120 (1968).

159. D. O. Raleigh and L. E. Topol, "Thermoelectric potentials in molten Bi-BiI<sub>3</sub> solutions," J. Chem. Phys., 41, 3179-84 (1964).
160. L. E. Topol and L. O. Ranson, "Magnetic susceptibilities of molten Bi-BiI<sub>3</sub> solutions," J. Chem. Phys., 38, 1633-70 (1963).
161. L. F. Grantham and S. J. Yosim, "Electrical conductivities of molten Bi-BiI<sub>3</sub> solutions," J. Chem. Phys., 38, 1671-76 (1963).
162. J. D. Kellner, "Thermal diffusion in an oxidation-reduction thermo-cell - the bismuth-bismuth iodide system," J. Phys. Chem., 70, 2341-47 (1966).
163. L. E. Topol, S. J. Yosim, and R. A. Osteryoung, "EMF measurements in molten bismuth-bismuth trichloride solutions," J. Phys. Chem., 65, 1511-19 (1961).  
L. E. Topol and R. A. Osteryoung, "EMF polarographic and chronopotentiometric studies in molten bismuth-bismuth tribromide solutions," J. Phys. Chem., 66, 1587-91 (1962).
164. "Solid electrolytes, general principles, characterization, materials applications," P. Hagenmuller and W. van Gool, eds., in Materials Science Series, Academic Press, New York (1978).
165. J. L. Weininger, "Halogen activated solid electrolyte cell," J. Electrochem. Soc., 105, 439-41 (1958).  
J. L. Weininger, "Iodine-activated solid electrolyte cell for use at high temperature," J. Electrochem. Soc., 106, 475-81 (1959).
166. J. L. Weininger, "Solid electrode battery," U.S. Patent 2,933,546 (1960).
167. J. L. Weininger and H. A. Liebafsky, "Solid electrolyte-gaseous cathode battery," U.S. Patent 2,987,568 (1961).
168. J. L. Weininger, "Thermogalvanic cells with silver iodide as a solid electrolyte," J. Electrochem. Soc., 111, 769-74 (1964).
169. J. L. Weininger, "Solid electrolyte thermocell," U.S. Patent 2,890,259 (1959).
170. J. L. Weininger, "Non-isothermal voltaic cell having iodine electrodes," U.S. Patent 3,297,486 (1967).
171. H. F. Hunger, "The silver|silver iodide|silver thermocell," J. Electrochem. Soc., 120, 1157-61 (1973).
172. A. Schiraldi, G. Chiodelli, and A. Magistris, "Thermoelectric power of AgI-Ag oxysalt ionic solids," J. Power Sources, 2, 257-64 (1977/1978).
173. G. Chiodelli, S. Magistris, and A. Schiraldi, "Solid electrolyte cells," Electrochim. Acta, 19, 655-6 (1974).

174. A. Schiraldi, G. Chiodelli, and A. Magistris, "Silver iodide-silver oxysalt electrolytes for solid-state cells," *J. Appl. Electrochem.*, 6, 251-5 (1976).
175. A. Schiraldi and E. Pizzati, "Thermoelectric powers of the systems silver iodide-silver molybdate(VI) or tungstate(VI)," *Z. Naturforsch.*, 31A, 1077-80 (1976).
176. R. E. Howard and A. B. Liddard, "Thermoelectric power of ionically conducting crystals," *Phyl. Mag.*, 2, 1462-1467 (1957).  
R. E. Howard and A. B. Liddard, "Thermoelectric power of ionic crystals," *Disc. Faraday Society*, 23, 113-21 (1957).
177. E. Haga, "Theory of thermoelectric power of ionic crystals. I-IV," *J. Phys. Soc. Japan*, 13, 1090-5 (1958) (cf. Ref. 130); 14, 992-6 (1969); 14, 1176-81 (1959); and 15, 1949-54 (1960).
178. A. R. Allnatt and P. W. M. Jacobs, "The thermoelectric power of ionic crystals. I. Theoretical," and "II. Results for potassium chloride," *Proc. Roy. Soc. (London)*, A260, 350-69 (1961); A267, 31-44 (1962).  
A. R. Allnatt and A. V. Chadwick, "Thermoelectric power of crystalline sodium chloride," *J. Chem. Phys.*, 47, 2372-8 (1967).  
A. R. Allnatt and M. H. Cohen, "Statistical mechanics of defect-containing solids. I. General formalism," and "II. Ionic crystals," *J. Chem. Phys.*, 40, 1860-70 and 1871-90 (1964).  
P. W. M. Jacobs and J. M. Maycock, "Polarization effects in the ionic conductivity of alkali halides crystals. I. Alternating current capacity," *J. Chem. Phys.*, 39, 757-62 (1963).  
A. R. Allnatt, P. W. M. Jacobs, and J. M. Maycock, "Polarization effects in the ionic conductivity of alkali halide crystals. II. Current-time dependence," *J. Chem. Phys.*, 43, 2526-32 (1965).
179. M. Shimoji and H. Hoshino, "Thermoelectric power of ionic crystals. I. General theory," *J. Phys. Chem. Solids*, 28, 1155-67 (1967).  
H. Hoshino and M. Shimoji, "Thermoelectric power of ionic crystals. III. Thermoelectric power and conductivity of potassium bromide containing barium bromide," *J. Phys. Chem.*, 29 1431-41 (1968); 31, 1553-63 (1970).
180. (a) A. Schiraldi, "Thermoelectric power of  $\beta$ - and  $\gamma$ -silver iodide," *Z. Phys. Chem. (Frankfurt/Main)*, 97, 285-93 (1974).  
(b) A. Magistris, E. P. Pezzati, and C. Sinistri, "Thermoelectric properties of high-conductivity solid electrolytes," *Z. Naturforsch.*, 27A, 1379-81 (1972).
181. P. D. Miller, A. B. Tripler, Jr., and J. J. Ward, "The application of irreversible thermodynamics to the thermogalvanic behavior of copper-copper sulfate systems," *J. Electrochem. Soc.*, 113, 746-9 (1966).
182. B. H. Clampitt and D. E. German, "Electrochemical cell for conversion of heat energy," U.S. Patent 3,253,955 (1966).

183. G. Hoffmann and A. David, "Investigations of some electrolyte thermopiles," *Acta Chim. (Budapest)*, 78, 373-85 (1973).
184. H. A. Liebhafsky, "Thermogalvanic cell," U.S. Patent 2,882,329 (1959).
185. B. W. Burrows, "Redox thermogalvanic cells for direct energy conversion," *Proc. 10th Intersociety Energy Conversion Engineering Conference*, pp. 821-7 (1975).
186. B. Burrows, "Discharge behavior of redox thermogalvanic cells," *J. Electrochem. Soc.*, 123, 154-9 (1976).
187. L. I. Bellchinskaya, S. A. Kaluzhina, and A. Y. Shatalov, "Temperature dependence of thermogalvanic current," *Elektrokhimiya*, 6, 228-30 (1970).
188. S. A. Kaluzhina, G. A. Mitroshkina, and A. Ya. Shatalov, "Electrochemical aspects of thermogalvanic cells. II. Thermogalvanic cells with iron in acidic sulfate electrolyte," *Elektrokhimiya*, 10, 924-7 (1974).
189. S. A. Kaluzhina and G. A. Mitroshkina, "Electrochemical aspects of thermogalvanic cells. III. Temperature dependence of the current of thermogalvanic cells on nickel, in an acid sulfate electrolyte," *Elektrokhimiya*, 12, 1013-5 (1976).
190. S. A. Kaluzhina and G. A. Mitroshkina, "Electrochemical aspects of thermogalvanic elements. V. Temperature dependence of the current of thermogalvanic elements in an acidified solution of proper ions," *Elektrokhimiya*, 14, 630-40 (1978).
191. F. A. Ludwig and J. J. Rowlette, "Continuous concentration cell," U.S. Patent 3,231,426 (1966).
192. R. H. Deysher, "Thermoelectric cell," U.S. Patent 2,310,354 (1943).
193. H. S. Harned and B. B. Owen, *Physical Chemistry of Electrolytic Solutions*, Reinhold, New York p. 436 (1950).
194. J. C. Angus, "Continuous gas concentration cells as thermally regenerative, galvanic cells," in *Regenerative EMF Cells*, C. E. Crouthamel and H. L. Recht, eds., *Advances in Chemistry Series*, 64, American Chemical Society, Washington, D.C. pp. 11-16 (1967).
195. J. C. Angus, "Method and apparatus for direct conversion of thermal energy to electrical energy," U.S. Patent 3,511,715 (1970).
196. J. T. Kummer and N. Weber, "Thermoelectric generators," U.S. Patent 3,458,356 (1968).
197. N. Weber, "A thermoelectric device based on beta-alumina solid electrolyte," *Energy Conversion*, 14, 1-8 (1974).

198. T. K. Hunt, N. Weber, and T. Cole, "Output power and efficiency for a sodium thermoelectric heat engine," Proc. 10th Intersociety Energy Conversion Engineering Conference, I, Newark, Delaware, pp.231-4 (1975).
199. T. K. Hunt, N. Weber, and T. Cole, "Research on the sodium heat engine," Proc. 13th Intersociety Energy Conversion Engineering Conf., San Diego, California, pp. 2011-7 (1978).
200. "Thermoelectric generator devices and methods, U.S. Patents 3,511,715 and 4,098,958 (1978).
201. Conversation with N. Weber, T. Cole, and T. K. Hunt (H. L. Chum), Dearborn, Michigan (May 1979).
202. G. J. May, "The development of beta-alumina for use in electrochemical cells: a survey," J. Power Sources, 3, 1-22 (1978).
203. R. Knodler and W. Baukal, "Determination of the life properties of beta-alumina tubes," J. Power Sources, 3, 23-8 (1978).
204. G. R. B. Elliott, "Electrochemical heat engine", LA-6632-MS (1976).
205. G. R. B. Elliott, W. J. Trela, and G. E. Dials, "Electrochemical heat engines for direct electric power generation and energy storage," Proc. A/AA/SAE 11th Propulsion Conference, Anaheim, California, AIAA Paper 75-1237 (1975).
206. G. R. B. Elliott, "Electricity and storage for residences using Li/I<sub>2</sub> electrochemical engines to augment photovoltaics," Proc. of the Electrochem. Soc. Meeting, 78, 428-35 (1978).
207. G. R. B. Elliott and N. E. Vanderborgh, "Electrochemical heat engines for power generation, load-leveling at site for underground coal conversion," Proceedings of the 13th Intersociety Energy Conversion Engineering Conf., San Diego, California, pp. 373-79 (1978).
208. G. R. B. Elliott and N. E. Vanderbargh, "Night storage and backup generation with electrochemical engines," LA-UR-78-606. Los Alamos, New Mexico: Los Alamos Scientific Laboratory (1978).
209. G. R. B. Elliott, "Electrochemical heat engine," U.S. Patent 4,090,012 (1978).
210. C. R. McCully, "Thermally regenerative galvanic cell employing the fluorides of arsenic, cerium and uranium," U.S. Patent 3,318,734 (1967).
211. Written correspondence between J. J. Lander (Director of Electrochemical Research, General Motors) and R. D. Weaver indicating that the concept of the Na-Cl<sub>2</sub> electrothermally regenerative transducer was proposed in September 1959 and that actual laboratory work started at that time.

212. J. J. Lander, S. W. Smith, and R. D. Weaver, "Electrothermal transducer," U.S. Patent 3,370,983 (1968).
213. R. D. Weaver, "Feasibility study of the electrothermally regenerative transducer," AD607 293 (1964).
214. D. A. J. Swinkels, "Lithium-chlorine battery," J. Electrochem. Soc., 113, 6-10 (1966).  
D. A. J. Swinkels and R. N. Seefurth, "Characterization of a porous graphite Cl<sub>2</sub> electrode," J. Electrochem. Soc., 115, 994-9 (1968).
215. D. A. J. Swinkels, "Electrolysis of fused alkali metal halides and alkali metal-alkali metal halide halogen fuel cells," Brit. Patent 1,144,388 (1969).  
D. A. J. Swinkels, "Electrochemical well with layered electrode of ceramic and carbon," U.S. Patent 3,544,373 (1970).
216. R. H. Hammond and W. M. Risen, Jr., "An electrochemical heat engine for direct solar energy conversion," Solar Energy, 23, 443-9 (1980).
217. M. S. S. Hsu and T. B. Reed, "Electrochemical power and hydrogen generation from high temperature electrolyte cells," Proceedings of the 11th Intersociety Energy Conversion Engineering Conference, State Line, Nevada, pp. 443-6 (1976).
218. M. S. S. Hsu, W. E. Morrow, Jr., and J. G. Goodenough, "High efficiency electrochemical plant," Proceedings of the 10th Intersociety Energy Conversion Engineering Conference, Newark, Delaware, pp. 555-63 (1975).
219. W. E. Morrow, Jr., and M. S. S. Hsu, "Electric power plant using electrolytic cell-fuel cell combination," U.S. Patent 4,087,976 (1978).
220. M. Steinberg, "Thermoelectrochemical power cycles," BNL-21323R, Brookhaven, New York: Brookhaven National Laboratory (1978).
221. F. J. Salzano and S. Srinivasan, Proceedings of the First International Energy Water Electrolysis Workshop, September 23-25, 1976, BNL 21165, Brookhaven, New York: Brookhaven National Laboratory.
222. S. Srinivasan, F. J. Salzano, and A. R. Landgrebe, eds., Proceedings of the Symposium on Industrial Water Electrolysis, 78-4, The Electrochemical Society, Inc., Seattle, Washington (1978).
223. National Fuel Cell Seminar Abstracts, coordinated by Courtesy Associates, Inc., Bethesda, Maryland, June 26-28, 1979.
224. W. E. O'Grady, S. Srinivasan, and R. F. Dudley, eds., Proceedings of the Workshop on the Electrocatalysts of Fuel Cell Reactions, Brookhaven National Laboratory, Brookhaven, New York, May 15-16, 1978, Vol. 79-2, The Electrochemical Society, Inc. (1979).



225. For example: H. S. Isaacs and L. J. Ohner, "The overpotential behavior of electrode materials at interfaces with  $ZrO_2$ - $Y_2O_3$  electrolytes," Proc. Electrochemical Society Meeting, Los Angeles, California, October 14-19, 1979, pp. 371-2.
226. For example: A. O. Isenberg, "Mass transport in solid oxides as relates to the fabrication of high temperature solid state fuel cells," Proc. Electrochemical Society Meeting, Los Angeles, California, October 14-19, 1979, pp. 364-5.
227. J. Greenberg, L. H. Thaller, and D. E. Weber, "A possible regenerative molten salt thermoelectric fuel cell," NASA Technical Note N64-27361 (1964).
228. J. Greenberg and L. H. Thaller, "Combined electrolysis device and fuel cell and method of operation," U.S. Patent 3,357,862 (1968).

<b>Document Control</b> <b>Page</b>	1. SERI Report No. TR-332-416 Vol. 2	2. NTIS Accession No.	3. Recipient's Accession No.
4. Title and Subtitle Review of Thermally Regenerative Electrochemical Systems Vol. 2		5. Publication Date April 1981 6.	
7. Author(s) Helena L. Chum; Robert A. Osteryoung		8. Performing Organization Rept. No.	
9. Performing Organization Name and Address Solar Energy Research Institute 1617 Cole Boulevard Golden, Colorado 80401		10. Project/Task/Work Unit No. 3356.50 11. Contract (C) or Grant (G) No. (C) (G)	
12. Sponsoring Organization Name and Address		13. Type of Report & Period Covered Technical Report 14.	
15. Supplementary Notes			
16. Abstract (Limit: 200 words) Thermally regenerative electrochemical systems (TRES) are closed systems that convert heat into electricity in an electrochemical heat engine that is Carnot cycle limited in efficiency. Past and present work on such systems is reviewed. Two broad classes of TRES are based on the types of energy inputs required for regeneration: thermal alone and coupled thermal and electrolytic. The thermal regeneration alone encompasses electrochemical systems (galvanic or fuel cells) in which one or more products are formed. The regeneration can be performed in single or multiple steps. The compounds include metal hydrides, halides, oxides, chalcogenides, and alloys or bimetallic systems. The coupled thermal and electrolytic regeneration encompasses electrochemical systems (galvanic or fuel cells) regenerated by electrolysis at a different temperature or different pressure. Examples include metal halides and water. Thermogalvanic or nonisothermal cells are included in this category. Also included are electrochemical engines in which the working electroactive fluid is isothermally expanded through an electrolyte. TRES cover temperature ranges from about 20°C to 1000°C. Engines with power outputs of 0.1 mW/cm <sup>2</sup> to 1 W/cm <sup>2</sup> have been demonstrated. Recommendations are made of areas of research in science and engineering that would have long-range benefit to a TRES program.			
17. Document Analysis a. Descriptors Thermal Regeneration; Electrochemical Cells; Regenerative Fuel Cells; Fuel Cells; Thermogalvanic Cells; Thermal Reactors; Distillation; Electrochemical Engines; Electrochemical Heat Engines; Hydrides; Halides; Chalcogenides; Oxides; Bimetallic Systems; Alloy Systems; Electrothermal Systems; Coupled Electrolytic Thermal Regeneration; Double Thermogalvanic System b. Identifiers/Open-Ended Terms Thermally Regenerative Electrochemical Systems (TRES) c. UC Categories 61			
18. Availability Statement National Technical Information Service U.S. Department of Commerce 5285 Port Royal Road Springfield, Virginia 22161		19. No. of Pages 227 20. Price \$9.50	